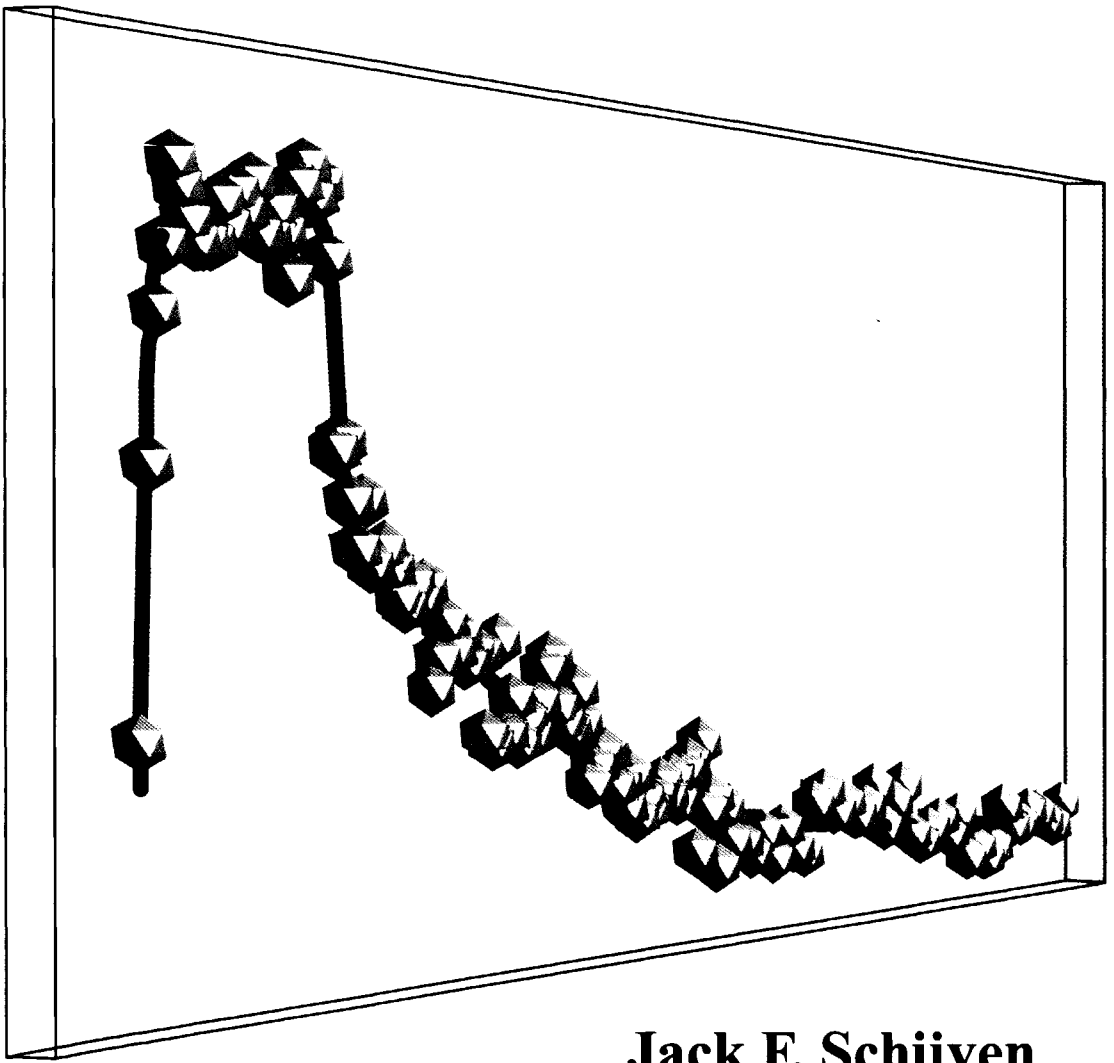


# **Virus Removal from Groundwater by Soil Passage**

**Modeling, Field and Laboratory Experiments**



**Jack F. Schijven**



## Stellingen behorende bij het proefschrift van Jack Schijven.

1. Virusverwijdering uit kunstmatig geïnfiltererd voorgezuiverd oppervlaktewater kan worden opgevat als een functie van botsingsefficiënties  $\alpha_\beta$  and  $\alpha_\lambda$ , afstervingscoëfficiënt  $\mu_1$ , parameter  $\gamma$ , poriewatersnelheid  $v$ , porositeit  $n$ , korrelgrootte  $d_c$  en de watertemperatuur. Initieel hoge verwijdering wordt bepaald door  $\alpha_\beta$ , welke exponentieel afneemt met een snelheid  $\gamma$  tot een constante basisverwijderingssnelheid, die wordt bepaald door  $\alpha_\lambda$  en  $\mu_1$ . Botsingsefficiënties  $\alpha_\beta$  en  $\alpha_\lambda$  hangen af van de fractie en de aard van heterogeen verdeelde plekken van gunstige hechtingsplaatsen.  
Dit proefschrift.
2. Een sterk negatief geladen virus zal minder hechten dan een minder sterk negatief geladen virus aan positief geladen hechtingsplaatsen op netto negatief geladen zandkorrels. Dit is omgekeerd, als er zodanig meer positief geladen hechtingsplaatsen zijn dat de nettolading van de zandkorrels positief is.
3. Zowel natuurlijk voorkomende F-specifieke RNA-bacteriofagen als humaan pathogene virussen in voorgezuiverd oppervlaktewater, dat wordt gebruikt voor kunstmatige aanvulling van grondwater, bestaan uit stabiele en slecht hechtende virussen. F-specifieke RNA-bacteriofagen zijn derhalve een uitstekend natuurlijk voorkomend surrogaat voor virusverwijdering door bodempassage. Bovendien is MS2, een sterk negatief geladen F-specifieke bacteriofaag, geen overdreven "worst case" model virus.
4. Een advection-dispersie model, dat reversibele hechting aan twee typen hechtingsplaatsen beschrijft, alsmede eerste orde afname door afsterving of afbraak van vrije en gehechte deeltjes, geeft een zeer goede beschrijving van het transport van micro-organismen en andere colloïdale deeltjes door verzadigd zand. Een model dat maar één type hechtingsplaatsen beschouwt kan de buiging van de staart van de doorbraakcurve niet volgen, hetgeen leidt tot een overschatting van de afstervingscoëfficiënt voor gehechte virussen. Echter, voor de voorspelling van virusverwijdering door bodempassage volstaat dit laatste model.  
Dit proefschrift.
5. Door middel van duin- en diepinfiltratie van voorgezuiverd oppervlaktewater worden virussen tenminste  $8 \log_{10}$  verwijderd binnen 25 dagen, respectievelijk 40 dagen, hetgeen zeer efficiënt is. Dit komt overeen met een afstand van 30 m, respectievelijk 38m. Echter, volgens een hypothetische "worst case" zijn grondwaterbeschermingsgebieden van drie tot zeven keer langere verblijftijden dan de huidige richtlijn van 60 dagen nodig om grondwater in zandige bodems afdoende te beschermen tegen virusbesmetting vanuit rioolwater.  
Dit proefschrift.
6. Als aggregaten van virussen voorkomen in waterige milieus, dan zijn ze waarschijnlijk reeds intracellulair gevormd en niet door virion-virion-coagulatie buiten de gastheercel.

7. Humaan pathogene virussen afkomstig uit ballastwater van vrachtschepen vormen een potentieel gezondheidsrisico.  
Ruiz et al., 2000. Nature 408, 49-50.
8. Zodra zoet recreatiewater de temperatuur van 20 °C overstijgt is er een sterk verhoogde kans bij zwemmers op het oplopen van een uitwendige oorinfectie.
9. Het aantal oöcysten van *Cryptosporidium* en cysten van *Giardia* in kalvergier kan met ongeveer 80% worden gereduceerd door indikking. Drogen van deze ingedikte mest geeft een nog zodanig doelmatige reductie, dat deze emissiebron van pathogene protozoa vele malen minder belangrijk wordt dan de emissie door de mens via huishoudelijk afvalwater.  
Schijven et al., 1999. RIVM rapport 289202 023; Robertson et al., 1992. Appl. Environ. Microbiol. 58, 3494-3500.
10. Negeren van het onderscheid in variabiliteit en onzekerheid in de kwantitatieve risico-analyse kan leiden tot een verkeerde schatting van risico's.  
Nauta, 2000. Int. J. Food Microbiol. 57, 9-18.
11. Piekconcentraties van pathogene micro-organismen in oppervlaktewater zijn het meest kritisch voor het daar aan gekoppelde infectierisico, maar de frequentie waarmee piekconcentraties optreden is heel onzeker.
12. Een "early warning" model dat een betrouwbare voorspelling doet over wel of niet voldoen aan de normen voor zwemwaterkwaliteit van een zwemstrand voor drie dagen is haalbaar en tevens onontbeerlijk voor de uitwerking van een adequaat bemonsteringsschema voor monitoring van de zwemwaterkwaliteit.
13. De Nederlandse overheid is verslaafd aan de accijnzen op genotmiddelen en brandstof.
14. Het fileprobleem in Nederland kan drastisch worden verkleind door een combinatie van de volgende maatregelen:
  - Beloning voor carpoolen.
  - Inzet van meer treinen (die op tijd rijden).
  - Beloning voor verhuizing tot binnen 20 km van het werk.
  - Afschaffing van de overdrachtsbelasting bij verkoop van de eigen woning.
  - Telewerken en flexibele werktijden.Financiëring hiervoor kan voor een belangrijk deel komen uit kostenbesparingen ten gevolge van het afschaffen van de Betuwelijn en het systeem voor rekeningrijden.
15. Een experiment moet worden gemodelleerd vóórdat het wordt uitgevoerd. Een experimentalist kan leren van een modelleur vóór het uitvoeren van een experiment. Een modelleur kan leren van een experimentalist na het uitvoeren van een experiment.
16. De toename in snelheid van nieuwe persoonlijke computers wordt tenietgedaan door de afname in kwaliteit van zowel hard- als software.

TR 3668

3668  
7535-11  
J. 06/01

# **Virus Removal from Groundwater by Soil Passage**

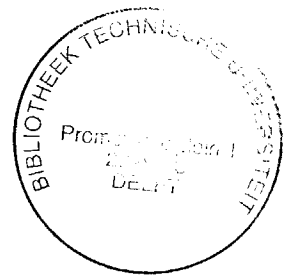
## **Modeling, Field and Laboratory Experiments**

### **Proefschrift**

ter verkrijging van de graad van doctor  
aan de Technische Universiteit Delft,  
op gezag van de Rector Magnificus prof. ir. K. F. Wakker,  
voorzitter van het College voor Promoties,

in het openbaar te verdedigen op maandag 2 april 2001 te 13:30 uur

door Jacobus Franciscus SCHIJVEN  
geboren te Heerle



Dit proefschrift is goedgekeurd door de promotor:  
Prof. dr. ir. C. van den Akker

Samenstelling promotiecommissie:

Rector Magnificus, voorzitter

Prof. dr. ir. C. van den Akker, Technische Universiteit Delft, promotor  
Dr. ir. S. M. Hassanizadeh, Technische Universiteit Delft, toegevoegd  
promotor

Prof. dr. ir. M. Th. van Genuchten, George E. Brown, Jr., Salinity  
Laboratory, USDA-ARS, Riverside, CA

Dr. ir. A. H. Havelaar, Rijksinstituut voor Volksgezondheid en Milieu

Prof. dr. ir. D. van der Kooij, Wageningen Universiteit

Prof. dr. ir. A. Leijnse, Wageningen Universiteit

Prof. dr. ir. M.C.M van Loosdrecht, Technische Universiteit Delft

Dit onderzoek werd uitgevoerd op het Microbiologisch Laboratorium voor  
Gezondheidsbescherming (MGB) van het Rijksinstituut voor  
Volksgezondheid en Milieu te Bilthoven, in het kader van project 289202,  
Watermicrobiologie, in opdracht en ten laste van het Ministerie van  
Volkshuisvesting, Ruimtelijke Ordening en Milieubeheer, Directoraat-  
Generaal Milieubeheer, Directie Bodem, Water en Landelijk Gebied.  
De financiële ondersteuning voor de uitgave van dit proefschrift door N. V.  
PWN Waterleidingbedrijf Noord-Holland, Gemeentewaterleidingen  
Amsterdam, N. V. Duinwaterbedrijf Zuid-Holland, het Rijksinstituut voor  
Volksgezondheid en Milieu en de Technische Universiteit Delft wordt zeer  
gewaardeerd.

ISBN 90-646-4046-7

Printed by Ponsen & Looijen B.V., Wageningen

**Aan Sylvia, Kevin en Dominic**

1



## Dankwoord

Allereerst bedank ik Sylvia voor de waardering die ze voor me had en de steun die ze me gaf tijdens dit promotieonderzoek. Nu heb ik dezelfde bewondering en waardering voor de uitdaging die zij voor zich heeft.

In de "LWL-periode" op het RIVM had ik een dubbele functie: onderzoek en automatisering. Vijf jaar geleden werd MGB geboren uit de fusie van LWL met LPM. Op dat moment koos ik geheel voor het onderzoek. Korte tijd later kwam de wens kwam bij me op om daarbij een echte wetenschappelijke uitdaging aan te gaan: een promotieonderzoek. De keuze van het onderwerp was niet moeilijk. Er lag reeds een vraag op het gebied van de kwetsbaarheid van Nederlandse grondwaterwinningen. Het onderwerp virusverwijdering tijdens transport door de bodem bood volop wetenschappelijke uitdagingen en is maatschappelijk relevant.

Grote dank aan Directie Bodem, Water en Landelijk Gebied van het Ministerie van Ruimtelijke Ordening en Milieubeheer, Directoraat-Generaal Milieubeheer, met name Wennemar Cramer voor hun instemming met dit promotieonderzoek.

Heel veel dank aan Arie Havelaar en André Henken voor het creëren van de ruimte binnen het RIVM om dit promotieonderzoek te kunnen doen en voor hun vertrouwen daarbij. Veel waardering heb ik voor Arie die vakinhoudelijk al vele jaren een uitstekend leermeester is. Dank aan Cees van den Akker om zijn waardering, interesse, begeleiding en aanmoediging voor dit onderzoek.

Grote waardering voor Gertjan Medema, die eveneens aan de basis van dit onderzoek heeft gestaan toen hij nog bij het RIVM werkte. Vanaf het moment dat hij bij het Kiwa is gaan werken, werd hij een onmisbare schakel in het veldonderzoek en is onze samenwerking op zeer prettige en collegiale wijze voortgezet, ook in andere onderzoeksprojecten.

Eindeloos veel dank aan Majid Hassanizadeh voor de vele leerzame en stimulerende discussies die we gevoerd hebben, voor de nauwgezette wijze waarmee hij alle manuscripten heeft gelezen en van commentaar voorzien. Ik kon me geen betere modelleermeester wensen.

Ook eindeloos veel dank aan Ria de Bruin voor haar inzet en enthousiasme, waarmee ze enorme bergen werk heeft verzet. Ik hoop dat ze als paranimf een beetje meepromoveert.

Het Kiwa en de betrokken waterleidingbedrijven (PWN, GWA, DZH, WML, WOB) ben ik eveneens veel dank verschuldigd. Zonder hun medewerking was dit promotieonderzoek niet mogelijk geweest. Speciaal mijn dank aan Wim Hoogenboezem voor zijn enthousiasme en grote mate van belangstelling. Dank aan Pieter Stuyfzand voor de leerzame kijk op hydrogeochemie en de waardevolle bijdrage daarvan aan het inzicht in adsorptieprocessen. Dank aan Ad Vogelaar voor de prettige samenwerking en veel waardering voor zijn creativiteit in het veld. En evenzo mijn grote dank aan Jos Peters en Marco van Baar, beiden toen nog Kiwanen, voor alle medewerking en hun ondersteuning in de duinen. Met plezier denk ik terug aan de mensen in het veld van PWN en WOB, met name Joost Bergsma en zijn medewerkers, Jos Thijs, en de laboratoriummedewerkers van

PWN, voor wie alle ik veel waardering heb voor hun hoge inzet bij nacht en ontij en hun hoge mate van enthousiasme.

Dank aan Theo Olsthoorn voor "het zeer gecharmeerd" zijn van dit werk. Door zijn proefschrift is het me ook gelukt doorbraakkrommen in een spreadsheet te berekenen.

I am grateful to Phil Berger (USEPA) for keeping me posted with so many publications and data from the US. I am sure that our contribution on bank filtration together with Ilkka Miettinen (National Public Health Institute, Kuopio, Finland) will find great appreciation.

Special thanks to Jirka Simunek and Rien van Genuchten from the US Salinity Laboratory, Riverside for their coöperation and support in writing the HYDRUS paper. It was very pleasant to work together with Jirka. The "Orange Sunday" in Bilthoven will stay in my mind forever. I feel honoured by Rien's interest in my work.

Special thanks also to Scot Dowd (USDA) and Suresh Pillai (Texas A&M University) for providing me their data and their support in writing the Texas paper.

Special thanks to Joe Ryan (University of Colorado, Boulder) for his thorough reviewing and stimulating discussions.

Toon Leijnse verdient ook veel dank voor zijn interesse in mijn werk, zijn aanmoediging en stimulerende discussies en zijn waardevolle aanwijzingen in het numerieke modelleren.

En dan niet te vergeten, mijn grote dank aan alle (ex)waterlabbers bij het ondersteunen en uitvoeren van de vele watermicrobiologische metingen: Mahdiah Bahar, Olaf Nijst, George Engels, Reina van der Heide, Agnes Holwerda, Willemijn Lodder en Ciska Schets. Imke Leenen en Ana Maria de Roda Husman ben ik vooral dankbaar voor hun nuttige commentaren op een aantal van mijn artikelen. Dank aan de RIVM-chauffeurs voor het plezier waarmee ze met je op pad gingen.

Veel waardering en dank heb ik voor het stimulerende enthousiasme en de vele wijze tips van Peter Teunis. Ook aan Eric Evers, Maarten Nauta en Katsuhisa Takumi ben ik veel dank verschuldigd, vanwege vele nuttige tips en voor de leerzame uurtjes risicomodellering op de maandagochtenden.

Tenslotte nog mijn speciale dank aan Jeannette Wouters van het secretariaat die altijd voor je klaar staat.

# Contents

Chapter 1	Introduction	1
Chapter 2	Removal of Viruses by Soil Passage: Overview of Modeling, Processes and Parameters	7
Chapter 3	Removal of F-specific RNA Bacteriophages and Fecal Indicator Bacteria by Dune Recharge and Estimation of Collision Efficiencies	69
Chapter 4	Model Removal of Bacteriophages MS2 and PRD1 by Dune Recharge at Castricum, The Netherlands	75
Chapter 5	Removal of Microorganisms by Deep well Injection	97
Chapter 6	Modeling Virus adsorption in Batch and Column Experiments	121
Chapter 7	Column Experiments for Evaluating Field Data on Virus Removal by Soil Passage through Saturated Dune Sand	135
Chapter 8	Kinetic Modeling of Virus Removal in Heterogeneous Porous Media	177
Chapter 9	Virus Removal by Soil Passage at Field scale and Groundwater protection	203
	Summary	219
	Samenvatting	229
	References	239
	Curriculum vitae	255
	Appendix EQ2KIN code	257



# Chapter 1

## Introduction

## 1.1 Drinking Water Production in The Netherlands

In The Netherlands, about 67% ( $794 \times 10^6 \text{ m}^3 \text{ yr}^{-1}$ ) of all drinking water is delivered from groundwater and 33% ( $399 \times 10^6 \text{ m}^3 \text{ yr}^{-1}$ ) from surface water (VEWIN, 1998). Due to government policy to limit desiccation – which affects agricultural production and especially nature reserves – groundwater withdrawal is not allowed to increase from the year 2000 onwards. During the last decade, the production of drinking water has not increased. To meet possible future increases in the demand for drinking water, surface water is becoming more important, especially in combination with treatment by soil passage (Mülschlegel and Kragt, 1998). Groundwater may become contaminated with viral, bacterial and protozoan pathogens from fecally contaminated water, e.g. from artificially recharged surface water, septic tanks or leaking sewage pipes. Surface water is contaminated with pathogenic microorganisms, mainly due to discharges of wastewater and by manure run-off from agricultural land.

Groundwater can be protected from contamination with pathogenic microorganisms by applying adequate setback distances between sources of contamination and production wells using the soil as a barrier. Likewise, surface water can be treated effectively to remove pathogens by means of passage through the subsurface, provided travel times and travel distances are adequate (e.g. Schijven and Rietveld, 1996). In The Netherlands, about 39% ( $186 \times 10^6 \text{ m}^3 \text{ yr}^{-1}$ ) of the surface water that is used for drinking water production, is treated by soil passage (artificial groundwater), like in riverbank filtration and in dune recharge with pretreated surface water (VEWIN, 1998). According to current guidelines (CBW, 1980), a travel time of 60 days is required at wellhead protection areas. For riverbank filtration in The Netherlands the travel time varies between 0.5 and 30 years and for artificial recharge of pretreated surface water between 35 and 135 days (Stuyfzand and Lüers, 1996). The travel time of 60 days is assumed to be adequate to inactivate pathogenic bacteria to the degree that no health risk exists (Knorr, 1937; CBW, 1980). A similar approach is followed in Germany (Dizer *et al.*, 1984, Matthess *et al.*, 1988). However, for decades, viruses and, more recently, protozoa have been recognized as pathogens of major health concern (e.g. Craun and Calderon, 1996; D'Antonio, 1985; Moore *et al.*, 1969; Rose, 1988). Due to their persistence in the environment and their infectivity, enteric viruses and the pathogenic protozoa *Cryptosporidium* and *Giardia* may be considered as the most critical waterborne pathogens for drinking water production (Medema and Havelaar, 1994). Because of this environmental persistence, a travel time of 60 days may be too short for sufficient inactivation of viruses and pathogenic protozoa. On the other hand, attachment to the soil grains may contribute significantly to their removal.

This raises the question to what extent the hygienic quality of drinking water is guaranteed. Clearly, there is a need to study the behavior of these pathogens in order to be able to evaluate the protection guideline of 60 days and to provide information for the evaluation of new and existing drinking water production systems from (artificial) groundwater.

## 1.2 Public Health Concerns Regarding Microbial Pathogens in (Artificial) Groundwater

Most of the waterborne viral, bacterial and protozoan pathogens are of fecal origin and are transmissible via a fecal-oral route of exposure. These pathogens can cause gastrointestinal illness, but severe illness as well. The impact of contaminated water on public health may range from asymptomatic infections to a few days of mild diarrhea, to severe disease requiring a doctor's care or hospitalization, to death, but acute gastroenteric illness is most common (Gerba, 1996). Certain individuals may be at greater risk of serious illness than the general population. In general, depending on the pathogen, individuals who are at increased risk of developing more severe outcomes from waterborne microorganisms are the very young, the elderly, pregnant women, the immunocompromised (e.g. organ transplants, cancer patients, AIDS patients), those predisposed with other illnesses (e.g. diabetes), and those with a chemical dependency (e.g. alcoholism) (Gerba, 1996).

Particularly in small communities and developing countries, the microbiological contamination of groundwater has profound and severe implications for public health. Contaminated groundwater can contribute to high morbidity and mortality rates from diarrheal diseases and sometimes lead to epidemics. The disposal of excreta using land-based systems is a key issue in groundwater quality and public health protection. The use of inappropriate water supply and sanitation technologies in peri-urban areas leads to severe and long-term public health risks. The use of poorly constructed sewage treatment works and land application of sewage can lead to groundwater contamination close to water supply sources (Pedley and Howard, 1997).

Although waterborne disease has largely been controlled in the USA, outbreaks continue to occur. To be considered a waterborne outbreak, acute illness must affect at least two persons and be epidemiologically associated with the ingestion of water (Craun and Calderon, 1996). In the period from 1971 to 1996, 643 outbreaks and over 570000 cases of illnesses were reported for all public surface water and groundwater systems (Craun and Calderon, 1996; EPA, 2000). Groundwater sources were associated with 58% of the total outbreaks and 16% of the associated illness. Surface water sources were associated with 33% of the total outbreaks and 82% of the associated illness. Contaminated source water was the cause of 86% of the outbreaks in groundwater systems. Of these outbreaks, 31% were associated with specific viral (enteric viruses), bacterial (*Shigella*, *Campylobacter*, *Salmonella*, *Yersinia*, *Escherichia coli*, *Plesiomonas shigelloides*), or protozoan pathogens (*Cryptosporidium* and *Giardia*), and 6% with chemicals. In 63% of cases, no causative disease agent was identified, but the majority of cases was probably viral (EPA, 2000). The number of individuals reported ill from these outbreaks is generally an underestimation of the actual levels of microbial diseases associated with drinking water, because endemic levels are not described and reporting of disease outbreaks is poor (Frost *et al.*, 1996). Also in Europe, consumption of drinking water has led to gastrointestinal illness, but information on illness that can be associated with fecal contamination of groundwater is scarce. For example, in the United Kingdom, 19 outbreaks were reported in the period of 1992 to 1996 that could be associated with the consumption of drinking water (Furtado *et al.*, 1998). In the United Kingdom, the share of groundwater in drinking water supplies is 35% (Pedley and Howard, 1997). In seven of the 19 outbreaks (37%), drinking water from groundwater supplies was concerned (Furtado *et al.*, 1998). The causative agent was *Cryptosporidium* in two of these outbreaks, *Giardia* in one outbreak and *Campylobacter* in

three outbreaks. In one outbreak no causative agent could be identified. With these seven outbreaks, 273 cases of illness were reported, of which 12 were hospitalized. In Finland, 24 waterborne outbreaks were reported in the period of 1980 – 1992 (Lahti and Hiivirta, 1995). About 40% of these outbreaks – affecting 7700 people - were due to contaminated water from community drinking water supplies from groundwater without disinfection. Four outbreaks were found to be caused by viruses, three by *Campylobacter*, and two by *Salmonella typhimurium*. In the period of 1998 – 1999, 14 outbreaks and 7400 cases of illness were reported in Finland, of which 13 outbreaks were associated with (artificial) groundwater (Miettinen *et al.*, 2000). Seven of these outbreaks were caused by caliciviruses, three by *Campylobacter*, and in three outbreaks the cause was unknown. In Germany, only rare information concerning waterborne disease and outbreaks is available. However, by means of geostatistical analysis, disease incidence could be positively associated with the use of groundwater for drinking water production, *i.e.* the districts with large surface water supplies were found to have a lower incidence of gastrointestinal infections (Dangendorf *et al.*, 2000).

For many decades, no data on waterborne disease outbreaks have been associated with fecal contamination of (artificial) groundwater in The Netherlands, probably primarily due to the application of multiple barriers in the treatment of surface water. However, enteric viruses and the pathogenic protozoa *Cryptosporidium* and *Giardia* are ubiquitously present in the Dutch surface waters (Medema *et al.*, 1996; Theunissen *et al.*, 1998; Schijven *et al.*, 1999; Hoogenboezem *et al.*, 2000). The emission and distribution of these pathogens to the Dutch surface waters has been modeled on a national scale (Schijven *et al.*, 1995, 1996; Medema *et al.*, 1997). Clearly, a high potential for waterborne transmission of microbial pathogens exists in The Netherlands, where surface water is used as the source for drinking water production, and adequate treatment must be guaranteed under all circumstances.

### **1.3 Safe Drinking Water from (Artificial) Groundwater Based on Maximum Allowable Concentrations of Pathogenic Microorganisms**

Currently, a different policy for production of safe drinking water in The Netherlands has been proposed (Medema and Havelaar, 1994; VROM, 1995) and incorporated into legislation in the beginning of the year 2001. This approach is based on a maximum acceptable infection risk of one per 10 000 persons per year associated with drinking water consumption and dose-response relationships for pathogens and has resulted in using maximum allowable concentrations in drinking water (Regli *et al.*, 1991). In the case of viruses, it is based on the dose response relationship of rotavirus and poliovirus 3, as a worst-case. The maximum allowable concentration is  $1.8 \times 10^{-7}$  viruses per liter. This implies that virus concentrations in surface water need to be reduced by 5 to 8  $\log_{10}$  in order to produce drinking water in which maximum allowable concentrations are not exceeded (Schijven *et al.*, 1996). This raises the question what travel times and travel distances are needed to achieve such reductions in the case of treatment by soil passage.

WHO has decided to base the coming edition of the Guidelines for Drinking Water Quality on a similar approach (J.Bartram, pers. comm.). Nevertheless, it may be clear from the foregoing that compliance with these maximum allowable concentrations can only be assessed by analysis of very large volumes of drinking water, *i.e.* in the order of  $10^5 - 10^7$  liter. This is considered to be impracticable and another approach for determining compliance must be followed. Concentrations of pathogenic microorganisms in treated

water can be calculated from the concentrations in source water and the effectiveness of the water treatment. The effectiveness of the water treatment can be determined by means of a computational model. In the case of soil passage as a water treatment, a model is needed that describes the fate and transport of the pathogenic microorganisms during soil passage.

#### 1.4 Scope and Objectives

This thesis is aimed at understanding, quantifying and modeling the processes that govern the removal of viruses by soil passage. The research comprises theoretical work, extensive field work, laboratory experiments and modeling. Although the focus is mainly on virus removal, some bacteria that serve as fecal indicators have been studied as well. Due to limitations, like permission to use in field situations, and limited sensitivity of virus assay-methods, bacteriophages were used as surrogates for pathogenic viruses.

First, an extensive literature review was carried out that covers a period of about twenty years of research on virus transport through the subsurface (Schijven and Hassanizadeh, 2000). The modeling that is used to describe and quantify adsorption and inactivation of viruses during subsurface transport is evaluated and the major factors that affect these processes are reviewed. Major model viruses, that are used as representatives of subsurface transport and behavior of pathogenic viruses, are evaluated.

Next, extensive field and laboratory studies were conducted that were aimed at measuring virus removal, quantifying the adsorption and inactivation processes and evaluating the role of bacteriophages as surrogates for viruses. The first field study was carried out at a dune recharge site at Heemskerk to measure removal of naturally present indicator organisms by passage through dune sand (Schijven *et al.*, 1998). Removal was studied only at short distance. To study removal at larger distances, high concentrations of bacteriophages were injected with the recharge water in a following field study on dune recharge at Castricum (Schijven *et al.*, 1999). A third field study concerned removal of microorganisms by deep well injection at Someren (Schijven *et al.*, 2000). The study was carried out at a pilot site and a cocktail of bacteriophages, bacteria and clostridium spores was injected.

Experimental work by Dowd *et al.* (1998), consisting of batch and column experiments was re-evaluated to analyze the adsorption behavior of five bacteriophages that differ in surface charge and to compare the results of different types of experiments (Schijven *et al.*, 2001d). A series of column experiments was designed to mimic the dune recharge field study and to study removal, removal processes and effects of soil heterogeneity in more detail (Schijven *et al.*, 2001a, 2001b). Also by means of these column experiments, the role of bacteriophages as model viruses was evaluated by comparing different bacteriophages and enteric viruses (Schijven *et al.*, 2001c).

In the field studies, analytical models were used to quantify adsorption and inactivation. A numerical model was developed to study two-site kinetic adsorption by fitting breakthrough curves from the column and field experiments (Schijven *et al.*, 2001b). A two-site kinetic model has also been implemented into existing software for simulating water flow and solute transport in one- and two-dimensional heterogeneous variably saturated porous media (Schijven and Simunek, 2001). This model was employed to analyze effects of dimensionality and heterogeneity on the bacteriophage removal that was observed in the field studies on dune recharge and deep well injection.

A transport model that adequately describes virus removal may be applied to design recharge systems like dune recharge, deep well injection, riverbank filtration, aquifer

storage recovery. Furthermore, it may be employed for the calculation of the travel times and distances that are needed for sufficient protection of groundwater well systems. The latter forms a scientific basis for a vulnerability analysis of the Dutch groundwater well systems. Moreover, a model that reliably predicts the vulnerability of groundwater wells from contamination with viruses will find worldwide application. A first step in the direction of a vulnerability analysis of Dutch groundwater well systems has been made in this thesis (Schijven and Hassanizadeh, 2001). A worst case situation with a leaking sewage pipe in an aquifer was simulated. Based on the knowledge about adsorption and inactivation from field studies, the travel times needed for adequate removal of virus were calculated.

To conclude, the objectives of this thesis were as follows:

1. Assess removal of model and pathogenic microorganisms by soil passage.
2. Study to what extent and in what manner the processes adsorption and inactivation contribute to this removal.
3. Develop a model that adequately describes removal of pathogenic microorganisms by soil passage.
4. Evaluate the role of model microorganisms as surrogates to pathogenic microorganisms.
5. Calculate a protection zone of a groundwater well system for adequate removal of viruses in a worst case scenario.

### **1.5 Outline of Thesis**

Chapter 2 gives a literature review on the removal of viruses by soil passage. Chapter 3 describes a field study on the removal of naturally present fecal indicator organisms by dune recharge. Removal of bacteriophages that were seeded in high numbers at a field site for dune recharge is presented in chapter 4. The third field study concerned removal of microorganisms by deep well injection, where a cocktail of bacteriophages, bacteria and clostridium spores was injected (chapter 5). Chapter 6 describes a laboratory study on adsorption of five different bacteriophages to Texas Brazos alluvium. Chapter 7 presents a series of column experiments on dune recharge. The data from the field studies (chapter 4 and 5) were re-analyzed by applying a one and two-site kinetic model in a one and two-dimensional fashion. This is presented in chapter 8. In chapter 9, data on virus removal in field studies are summarized and a protection for a groundwater well system in a worst case scenario is calculated.

## **Chapter 2**

# **Removal of viruses by soil passage: Overview of modeling, processes and parameters**

Schijven, J. F., Hassanizadeh, S. M. 2000. Removal of viruses by soil passage: overview of modeling, processes and parameters. *Crit. Rev. Environ. Sci. Tech.* 31, 49-125 (partially updated).

**Abstract.**

In this review, the modeling of subsurface virus transport under saturated conditions and the factors that affect adsorption and inactivation are evaluated. Both equilibrium and kinetic adsorption are considered. Equilibrium adsorption is found to be of little significance. Adsorption appears to be mainly kinetically limited. At pH 7 and higher, conditions are generally unfavorable for attachment, but viruses may preferentially attach to a minor surface fraction of soil grains that is positively charged. The relation of pH with surface charge and their effects on collision efficiencies are evaluated. Dissolved organic matter decreases virus attachment by competition for the same binding sites and thus reduces attachment. Bonded organic matter may provide hydrophobic binding sites for viruses and thus enhance attachment. Dissolved organic matter may disrupt hydrophobic bonds. The enhancing and attenuating effects of organic matter are very difficult to quantify and may be responsible for considerable uncertainty when predicting virus removal. Values of inactivation rate coefficients for attached viruses were calculated using data from some batch studies. Enhanced or reduced inactivation is found to be virus-specific and almost independent of adsorption. Temperature is the most important factor that influences virus inactivation. Probably, the inactivation rate coefficients of free and attached viruses change similarly with temperature.

Some frequently used bacteriophages are evaluated as model viruses. MS2 and PRD1 meet the requirements for worst-case model viruses, at water temperatures less than about 10° C, at pH 6 – 8 and if the soil does not contain too many hydrophobic sites and not too much multivalent cations. Bacteriophage  $\phi$ X174 may be a relatively conservative model virus, because of its low hydrophobicity and stability. Together in a cocktail, these three viruses span a range of properties, like size, surface charge and hydrophobicity. F-specific RNA bacteriophages may be very useful naturally occurring worst-case viruses. F-specific RNA bacteriophages that are present in surface water or treated wastewater that is used for recharging groundwater, consist of stable and poorly adsorbing viruses.

An inventory of parameter values from field studies is made. Attachment appears to be the major process that determines virus removal. Still, only very few data are available on attachment and detachment of viruses under field conditions. Removal of viruses by soil passage,  $\log_{10}(C/C_0)$ , appears to decline non-linearly with distance due to heterogeneities within the soil as well as within the population of transported virus-particles. Predictions of virus removal at larger distances are severely overestimated if they are based on removal data from column experiments or from short-distance field studies.

## **2.1 Introduction**

### **2.1.1 Safe Drinking Water Production**

Groundwater is a main source for drinking water production. Groundwater may become contaminated with pathogenic microorganisms from artificial recharge with wastewater or surface water, or from septic tanks or leaking sewage pipes. Therefore, to protect groundwater from contamination, adequate setback distances between these sources of contamination and production wells for drinking water are needed. Surface water is also a source for drinking water production and is becoming increasingly important. Surface water may be contaminated with pathogenic micro-organisms, mainly due to discharges of

wastewater and by manure run-off from agricultural land. To produce safe drinking water from surface water these pathogens need to be removed. One effective way is passage of surface water through soil, as is the case in bank filtration, dune recharge, and deep well injection. To assure production of safe drinking water from surface water, adequate travel times and travel distances are needed.

Pathogens of major threat to human health are viruses and the pathogenic protozoa *Cryptosporidium* and *Giardia*. Little is known about the fate of these pathogenic protozoa during soil passage (Hancock *et al.*, 1998), although new information is emerging (Brush *et al.*, 1999; Harter *et al.*, 1999). Much more information is available for viruses. It is believed that the processes that determine removal of viruses during soil passage also apply to protozoa, albeit to a different extent. Therefore, this review will be confined to the study of virus removal by soil passage. Viruses have been shown to be able to travel considerable distances through the subsurface depending on their size, their adsorption characteristics, and their degree of inactivation (Keswick and Gerba, 1980). Nevertheless, soil passage is considered as an important barrier against viruses (Schijven and Rietveld, 1996).

Currently, the extent of wellhead protection areas and bank filtration sites are based on the travel time of the groundwater or recharge water. For example, in Germany (Dizer *et al.*, 1984) and in The Netherlands a travel time of 50 – 60 days is required. This is based on the assumption that a groundwater travel time of 60 days is adequate to inactivate pathogenic micro-organisms, to the degree that no health risk exists (Knorr, 1937). However, due to the high persistence of *Cryptosporidium*, *Giardia* and viruses this may not be sufficient.

Current knowledge of infection risks of, as a consequence of drinking water consumption, has resulted in using maximum allowable concentrations for pathogenic micro-organisms in drinking water. These are based on a maximum acceptable infection risk of one per 10 000 persons per year and dose-response relationships for pathogens (Regli *et al.*, 1991). This approach has formed the basis for the Extended Surface Water Treatment Rule and it was under consideration for the Ground Water Disinfection Rule in the USA (Macler, 1996). Based on the maximum level of infection risk, a proposal for drinking water protection policy is being prepared in The Netherlands, that leads to similar maximum allowable concentrations (Schijven *et al.*, 1996). In case of viruses, it is based on the dose response relationship of rotaviruses, as a worst-case. This maximum allowable concentration is  $1.8 \times 10^{-7}$  viruses per liter. Obviously, such a very low concentration is not directly measurable. Therefore, the only way to evaluate the effectiveness of soil passage is to calculate virus concentrations at the production point from the concentrations in source water by means of a computational model.

### 2.1.2 Modeling Transport and Fate of Viruses during Soil Passage

After a certain travel time and travel distance through soil, viruses are removed. Virus removal is the disappearance of viruses from the water and is defined in this context as the logarithmic reduction of virus concentration,  $\log_{10}(C/C_0)$ . The processes of major importance for removal of viruses during soil passage are adsorption and inactivation (Keswick and Gerba 1980; Yates *et al.*, 1987). Advection and dispersion affect spreading of viruses and thereby attenuation of virus concentrations. Modeling is a way to quantify these processes. Adsorption of viruses to soil may be modeled as either irreversible or reversible. In the case of irreversible attachment, there is no detachment. In the case of reversible adsorption, one may have equilibrium and/or kinetic adsorption sites. In general, both kinds

of adsorption may occur in a given medium. In this review, when talking of adsorption, the effects of both attachment and detachment are meant. Thus, we consider a situation where viruses can adsorb to two different kinds of sites on solid grains. There are sites where attachment and detachment are fast relative to the flow velocity, allowing equilibrium to occur. For some other sites, adsorption is kinetically limited relative to flow velocity, with constant attachment and detachment rate coefficients. The governing equations of solute transport, including dispersion, advection and inactivation for three-dimensional saturated flow are as follows:

$$n \frac{\partial C}{\partial t} + \frac{\partial \rho_B S_{eq}}{\partial t} + \frac{\partial \rho_B S_{kin}}{\partial t} = \nabla \cdot (n \mathbf{D} \cdot \nabla C) - \nabla \cdot (n \mathbf{v} C) - Q \quad (1)$$

$$S_{eq} = k_{eq} C \quad (2)$$

$$\frac{\partial \rho_B S_{kin}}{\partial t} = n k_{att} C - k_{det} \rho_B S_{kin} - \mu_{s,kin} \rho_B S_{kin} \quad (3)$$

$$Q = n \mu_1 C + \mu_{s,eq} \rho_B S_{eq} + \mu_{s,kin} \rho_B S_{kin} \quad (4)$$

Here,  $C$  is the number of free viruses per unit volume in the aqueous phase,  $[L^{-3}]$ . In short, we refer to it as the free virus concentration. The adsorbed virus concentration is given in terms of number of viruses per unit mass of soil; we refer to it as the attached virus concentrations  $[M^{-1}]$ . The symbols  $S_{eq}$  and  $S_{kin}$  are used to denote the concentrations of viruses attached to equilibrium and kinetic sites, respectively. Further,  $\rho_B$  is the bulk density of the saturated soil,  $[M.L^{-3}]$  and  $n$  is the porosity,  $[-]$ ;  $\mathbf{D}$  is the hydrodynamic dispersion tensor,  $[L^2.T^{-1}]$ ;  $\mathbf{v}$  is the pore water velocity vector,  $[L.T^{-1}]$ ;  $k_{eq}$  is a distribution coefficient,  $[L^3.M^{-1}]$ ;  $k_{att}$  and  $k_{det}$  are the attachment and detachment rate coefficients, respectively  $[T^{-1}]$ ;  $\mu_1$  is the inactivation rate coefficients for the free viruses,  $[T^{-1}]$ ;  $\mu_{s,eq}$  and  $\mu_{s,kin}$  are the inactivation rate coefficients for attached viruses to equilibrium and kinetic sites, respectively  $[T^{-1}]$ .

### 2.1.3 Studying Virus Adsorption and Inactivation at Batch, Column and Field Scales

Adsorption of viruses to soil and concurrent inactivation can be studied at different scales: in batch, column and field experiments. In batch experiments almost always only equilibrium adsorption is studied. Advection and dispersion cannot be investigated in batch experiments. In columns, transport of viruses is studied often as a one-dimensional process. Columns can be made of packed soil material or undisturbed soil. In the latter case, as in the field, effects of dispersion should be considered. In uniformly packed columns, dispersion is usually small and may be neglected. In field studies, the actual situation is investigated. Depending on the hydrologic situation, transport may be modeled as 1-, 2- or 3-dimensional. The effect of dispersion can be very important in the field.

In batch and column studies, any combination of soil and virus may be considered, whereas in field studies many restrictions apply. Removal of pathogenic viruses under field

conditions can be studied only if contamination levels are high enough. Usually this is not the case. Only in exceptional situations, permission may be obtained to seed pathogenic viruses in the field. At a site that is in use for drinking water production, this will never be allowed. Therefore, model viruses that are not pathogenic but are still representative for the transport behavior of pathogenic viruses are needed. A model virus is suitable if its inactivation and adsorption are similar to that of pathogenic viruses under given conditions. This implies that it should be possible to predict removal of pathogenic viruses by passage through soil from the removal of the model virus.

Usually bacteriophages are used as model viruses. Bacteriophages offer the following advantages:

1. Bacteriophages are not pathogenic to human, but infect a specific host bacterium.
2. Bacteriophages can be prepared in large quantities ( $10^{10} - 10^{12}$  phages per ml), allowing seeding of high numbers. This makes it possible to show removal up to  $11 \log_{10}$ .
3. The assay of bacteriophages is relatively easy, whereas analysis of pathogenic viruses is much more complex, time consuming, and sometimes not possible at all.

#### 2.1.4 Purposes and Outline of the Review

Several reviews on the transport and fate of viruses through the subsurface have appeared. *E.g.*, Keswick and Gerba (1980) reviewed reports on virus isolation from groundwater sources for drinking water production and from recharged groundwater sites. Hydrogeological, biological and meteorological factors affecting the survival and transport of viruses in groundwater were identified. The following research needs were recommended: (1) investigation of virus-surface interactions and virus inactivation in groundwater; (2) development of experimental methods and predictive models; (3) development of criteria for adequate groundwater protection; (4) performing field studies at land treatment sites, septic tanks, and on disease outbreaks by groundwater contamination. Gerba (1984) presented a comprehensive review on the factors influencing virus adsorption and inactivation, which were studied mostly in batch experiments. Yates *et al.* (1987) also reviewed the factors affecting transport and inactivation of viruses through soils, including modeling of batch studies and of transport. They concluded that modeling of virus transport was constrained by a lack of quantitative information on virus behavior during transport. Yates and Yates (1992) presented an overview of the way inactivation, equilibrium adsorption, advection and dispersion determine transport of viruses. These factors were summarized in a quantitative manner by Gerba *et al.* (1992). Also of interest are the reviews on the transport of colloids in groundwater by Swanton (1995) and Ryan and Elimelech (1996).

The main purposes of this review are:

1. Evaluate the modeling that is used to describe and quantify adsorption and inactivation of viruses during subsurface transport ;
2. Review the major factors that affect these processes;
3. Evaluate model viruses as representatives of subsurface transport and behavior of pathogenic viruses,
4. Discuss the relative contributions of adsorption and inactivation to the removal of viruses during subsurface transport.

In section 2.2, modeling of equilibrium adsorption of viruses to soil in batch experiments and during transport through soil in column and field experiments is discussed. A similar study but for kinetic adsorption will be presented in section 2.3. Also, in section 2.3, colloid filtration theory, DLVO theory, hydrophobic interactions and blocking are discussed. In section 2.4, the factors that affect adsorption of viruses to soil are reviewed. In section 2.5, modeling of virus inactivation is reviewed and, the major factors that affect inactivation are discussed in section 2.6. This review will mainly focus on saturated flow conditions, however, because unsaturated conditions have a significant impact on inactivation, this will also be discussed. Section 2.7 discusses the effects of advection and dispersion on virus transport in the field. In section 2.8, some model viruses are evaluated. In section 2.9, the relative contribution of adsorption and inactivation to virus removal are evaluated, and removal of viruses with distance is discussed. Finally, a summary and conclusions are presented in section 2.10.

## 2.2 Equilibrium Adsorption

### 2.2.1 Equilibrium Adsorption in Batch Experiments

In batch experiments, a suspension of viruses is agitated with a quantity of the solid material of interest in a container. Concentration of viruses present in the water phase of the container is measured as a function of time. Concentration of viruses in a control container with water, but without soil is measured to calculate inactivation, but also to be able to compensate for possible losses due to attachment to the walls of the container. A typical semi-log plot of virus adsorption to soil in a batch suspension is given in Figure 1a. Initially, free virus concentrations decline with time, but after a short time, they remain almost constant. At that point, a distribution of viruses between solid and liquid phase is obtained, because of reversible adsorption. This apparent equilibrium is rapidly reached but is not instantaneous. It depends on the actual attachment and detachment rates. The time to equilibrium has been reported to vary from 30 minutes (*cf.* Gerba and Lance, 1978; Goyal

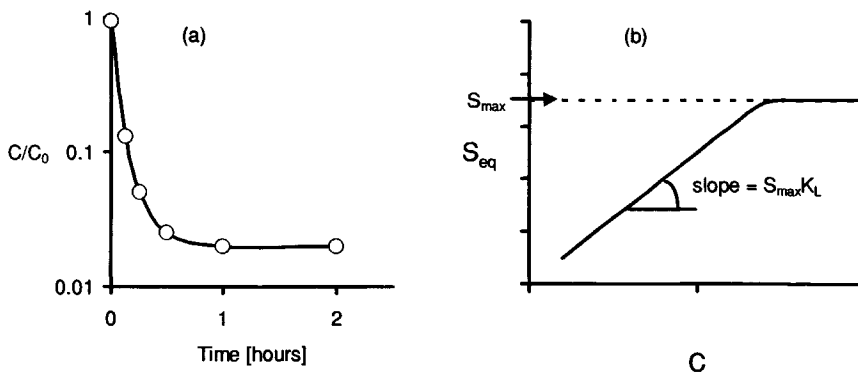


**Figure 1** Adsorption of a virus to soil in a batch suspension: (a) Decreasing concentration of free viruses with time; (b) Example of Langmuir isotherm.

and Gerba,1979; Taylor *et al.*, 1980; Gerba *et al.*, 1981; Singh *et al.*, 1986 and Gantzer *et al.*, 1994) to 60 – 90 minutes (*cf.* Moore *et al.*, 1981, 1982; Taylor *et al.*, 1981; Bales *et al.*, 1991 and Sakoda *et al.*,1997). In all these studies, inactivation was either neglected or found to be insignificant within the time scale of the experiment. At larger time scales, the free virus concentration continues to decrease at a steady rate due to inactivation. Commonly in batch experiments, the kinetic behavior, which is operative before steady state is reached, is not considered, and values of attachment and detachment rate coefficients are not determined. In batch studies, the apparent steady state concentrations are used to construct Langmuir or Freundlich isotherms (Yates *et al.*, 1987). The Langmuir model assumes that maximum attachment corresponds to a saturated monolayer of solute molecules on the adsorbent surface, that the active sites for attachment are all the same, and that there is no interaction between attached molecules. The Langmuir equation reads:

$$S_{eq} = \frac{S_{max} K_L C_{eq}}{1 + K_L C_{eq}} \quad (5)$$

Where  $S_{eq}$  is the concentration of adsorbed viruses and  $C_{eq}$  the concentration of free viruses after apparent equilibrium has been reached.  $S_{max}$  is the maximum adsorbed concentration when all active surface sites are occupied;  $K_L$  is a constant related to the bonding energy. A typical example of a Langmuir isotherm is plotted in Figure 1b. It shows that the slope of the increasing part of the curve equals  $S_{max}K_L$  and that the curve finally reaches  $S_{max}$ . When  $K_L C_{eq} \ll 1$ , the Langmuir equation may be linearized, to obtain a linear isotherm:

$$S_{eq} = S_{max} K_L C_{eq} \quad (6)$$

Freundlich isotherms have also been applied to describe attachment of viruses to soil (Gerba, 1984). Here, no assumption is made on homogeneity of active sites for attachment. The Freundlich formula reads:

$$S_{eq} = k_{eq} C_{eq}^m \quad (7)$$

Here,  $m$  is a constant. For many systems with low free virus concentrations,  $m$  is not significantly different from unity, whereby Equation 7 reduces to a linearized form similar to Equation 6 (Vilker and Burge 1980; Yates *et al.*, 1987).

Moore *et al.* (1981) showed that adsorption of poliovirus 2 to Ottawa sand could be described by the Langmuir equation:  $S_{max}$  appeared to be  $2.5 \times 10^{12}$  virus particles per kg of sand. At lower surface coverage, adsorption was successfully described by the Freundlich equation. Vilker and Burge (1980) summarized several examples where Freundlich and Langmuir isotherms were applied. In these examples,  $S_{max}K_L$  was shown to vary between 2 and  $6.4 \times 10^5$  liter/kg. In some of these examples,  $S_{max}$  was shown to be very large, *i.e.* in the order of  $10^{14} - 10^{15}$  sites per kg of soil, but  $K_L$  was shown to be very small, in the order of  $10^{-14} - 10^{-11}$  liter per virus. Vilker and Burge (1980) concluded that virus adsorption is saturation limited, that is to say, the number of adsorption sites is finite. They further concluded that the large values of  $S_{max}$  and the small values for  $K_L$  indicate that virus

adsorption is characterized by a large number of sites, but equilibrium strongly favors the liquid phase over the adsorbed phase. Other examples of application of Freundlich isotherms can be found in Gerba and Lance (1978), Taylor *et al.* (1980), Lipson and Stotzky (1983), Bales *et al.* (1991) and Sakoda *et al.* (1997).

In batch experiments, time to reach apparent equilibrium is not only dependent on the virus type and virus concentration, but it also depends on the particle size of the adsorbent and the degree of agitation (Vilker and Burge, 1980; Moore *et al.*, 1981). Adsorption of poliovirus 2 was relatively constant from one experiment to another, but adsorption to a few soils varied greatly. To organic muck 16 to 99% of the poliovirus was adsorbed, and to sandy loam 94% to 99.7% (Moore *et al.*, 1981). High variability in adsorption among different batch studies is thought to depend primarily on heterogeneity of soil preparations, like a wide range of particle sizes (Vilker and Burge, 1980). Jin *et al.* (1997) argued that results from batch experiments have neither been consistent, nor reproducible, largely due to the fact that there is no standard protocol. That is to say, different sizes and types of containers and different methods of agitation are used. Also, an air-water interface may be present in some, but absent in other experiments. All these differences may influence the equilibrium of a batch system. This makes it very difficult to compare values for adsorption between different batch studies. Nevertheless, batch tests have been used extensively to investigate the effects of various factors (*e.g.* pH, organic matter and soil type) and to compare adsorptive behavior of different viruses in combination with different solid materials under a given set of experimental conditions.

### 2.2.2 Equilibrium Adsorption of Viruses to Soil during Subsurface Transport

Equilibrium adsorption has been assumed in several column and field studies, neglecting kinetic adsorption (*e.g.* Park *et al.*, 1994; Powelson *et al.*, 1990; Powelson and Gerba, 1994; Tim and Mostaghimi, 1991). Under these assumptions and for a one-dimensional situation, Equations 1 and 4 are simplified to:

$$n \frac{\partial C}{\partial t} + \rho_B \frac{\partial S_{eq}}{\partial t} = nD \frac{\partial^2 C}{\partial x^2} - nv \frac{\partial C}{\partial x} - Q \quad (8)$$

$$Q = n\mu_1 C + \mu_s \rho_B S_{eq} \quad (9)$$

Equation 2 and 9 can be combined to:

$$R \frac{\partial C}{\partial t} = D \frac{\partial^2 C}{\partial x^2} - v \frac{\partial C}{\partial x} - Q/n \quad (10)$$

where, retardation coefficient  $R = 1 + \frac{\rho_B}{n} k_{eq}$ , which is evidently equal to or larger than 1.

Viruses are not removed by equilibrium adsorption. According to the equilibrium model description given by Equations 9 and 10, removal of viruses during subsurface transport is only due to virus inactivation. Sometimes an extra sink term for irreversible attachment is

also included to account for virus removal (Jin *et al.*, 1997; Matthess *et al.*, 1988; Yates and Ouyang, 1992):

$$R \frac{\partial C}{\partial t} = D \frac{\partial^2 C}{\partial x^2} - v \frac{\partial C}{\partial x} - k_{irr} C - Q/n \quad (11)$$

Here,  $k_{irr}$  is the irreversible attachment rate coefficient. It is usually denoted as filtration (see section 2.3.4).

For solute contaminants and proteins, temporal and spatial variability of the distribution coefficient has been observed, due to subsurface heterogeneities, like grain size, surface area, pH, temperature and redox potential (Chrysikopoulos and Sim, 1996). Assuming the same may be the case with viruses, Chrysikopoulos and Sim (1996) developed a transport model with a stochastic time-dependent distribution coefficient. Simulations with a time-dependent coefficient resulted in an enhanced spreading of the free virus concentration compared to the case with a constant  $k_{eq}$ .

In some cases, retardation coefficients of about 2 to 5 have been reported (Bales *et al.*, 1991, 1997; Powelson *et al.*, 1993; Powelson and Gerba, 1994). But in most experiments, little or no retardation was found (Bales *et al.*, 1991, 1993; Pieper *et al.*, 1997; Jin *et al.*, 1997; Schijven *et al.*, 1999). Apparently, retarded breakthrough by equilibrium adsorption is of little significance.

Values of the “retardation coefficient” of less than one have also been reported. That is to say, faster virus transport relative to that of a conservative salt tracer has been observed; most probably due to pore size exclusion of the virus (see section 2.7).

## 2.3 Kinetic Adsorption

### 2.3.1 Kinetic Analysis of Batch Experiments

In a batch suspension of viruses and soil, adsorption equilibrium is not reached instantaneously. Instead, virus adsorption at the micro-scale can be described as the result of two processes, each of which takes a certain time (see *e.g.* Gerba, 1984). In the first process, the viruses are transported close to the solid surface. Here, one speaks of mass transport. In the second process, the viruses are immobilized at the surface by physical and possibly chemical interactions. The overall rate of attachment depends on which of these two processes, mass transport or virus-surface interactions, is the rate-limiting step (Grant *et al.*, 1993). The kinetic behavior that is operative before apparent equilibrium is reached can be described by virus attachment to the soil, virus detachment from the soil, and inactivation of free and attached viruses. Thus, the kinetics of the system can be characterized by four parameters:  $k_{att}$ ,  $k_{det}$ ,  $\mu_i$ ,  $\mu_s$  (Figure 2). The governing equations are

$$n \frac{dC}{dt} = -nk_{att}C + k_{det}\rho_B S - n\mu_i C \quad (12)$$

$$\rho_B \frac{dS}{dt} = nk_{att}C - k_{det}\rho_B S - \mu_s \rho_B S \quad (13)$$

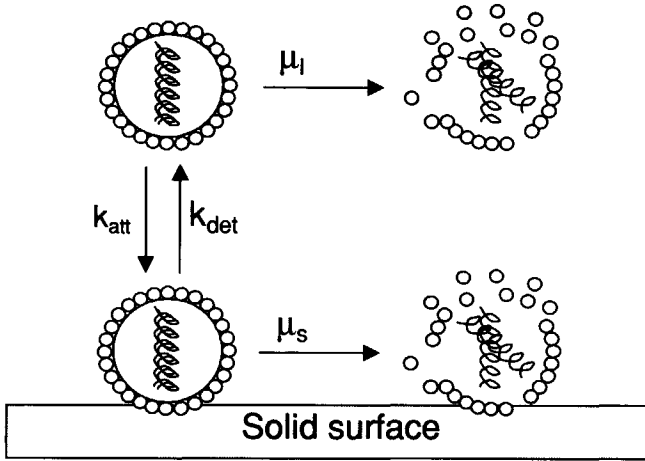


**Figure 2** Attachment and inactivation of virus in bulk fluid and at the solid-liquid interface (Grant et al., 1993). Here,  $k_{att}$  is the attachment rate coefficient;  $k_{det}$  is the detachment rate coefficient;  $\mu_i$  is the inactivation rate coefficient of viruses in the aqueous phase and  $\mu_s$  that of viruses attached to the solid surface.

As we have seen in section 2.2.1, on a time scale of a few hours, inactivation of viruses in a batch system is commonly negligible. In that case, Equations 12 and 13 have the following analytical solution:

$$C/C_0 = \frac{k_{det} + k_{att} \exp[-(k_{att} + k_{det}) t]}{k_{att} + k_{det}} \quad (14)$$

The slope of the C-t curve at t=0, assuming negligible inactivation, is approximately equal to  $-k_{att}$  (Figure 1a). This is evident from Taylor series expansion of Equation 14, which yields:

$$C/C_0 = 1 - k_{att} t + \frac{t^2}{2} k_{att} (k_{att} + k_{det}) - \frac{t^3}{6} (k_{att} + k_{det})^2 + \dots \quad (15)$$

Thus,  $k_{att}$  may be evaluated from early measurements of a batch experiment. Once an apparent steady state is reached (*i.e.* negligible dC/dt) and neglecting inactivation, from Equations 12 and 13 it also follows:

$$\frac{\rho_B}{n} S_{eq} = \frac{k_{att}}{k_{det}} C_{eq} = \frac{\rho_B}{n} k_{eq} C_{eq} = (R-1) C_{eq} \quad (16)$$

Thus, from equilibrium results,  $k_{det}$  can be obtained. Therefore, it is possible to determine both  $k_{att}$  and  $k_{det}$  from batch experiments.

Often, adsorption of viruses to soil in batch experiments is expressed as the fraction of viruses that is adsorbed at equilibrium. The relation between the ratio  $k_{att}/k_{det}$  and the adsorbed fraction  $f$ , at equilibrium, is as follows:

$$\frac{k_{att}}{k_{det}} = \frac{C_0}{C_{eq}} - 1 = \frac{f}{1-f} \quad (17)$$

On longer time scales, *e.g.* days, virus inactivation will be significant and causes disappearance of viruses from the system. The interplay of kinetic effects and virus inactivation in a batch system will be discussed in section 2.5.3.

### 2.3.2 Kinetic Adsorption of Viruses to Soil during Subsurface Transport

Under transport conditions, adsorption of viruses to soil may be kinetically limited relative to advection. In field studies (*e.g.* Bales *et al.*, 1997; Schijven *et al.*, 1999), it appeared that attachment rates were relatively fast compared to advection, whereas detachment rates were much slower. Bales *et al.* (1997) expressed this in terms of time scales for attachment or detachment relative to advection over a characteristic travel distance  $L$  by  $v/(k_{att}L)$  and  $v/(k_{det}L)$ , respectively. It was found that the former term was about two orders of magnitude smaller than one, whereas the latter was about three orders of magnitude greater than one. At very low flow rates, *e.g.* under some natural gradient conditions, kinetically-limited adsorption may successfully be described by equilibrium adsorption. The attachment and detachment rates determine the shape of virus breakthrough curves. To show the differences and similarities between equilibrium and kinetically-limited adsorption, various breakthrough curves for a column were simulated using the CXTFIT-code (Toride *et al.*, 1995). This code is based on analytical solutions of equilibrium and kinetic transport models, including governing Equations 1 to 4 for a one-dimensional situation. The breakthrough of virus seeded at a constant concentration on top of a column for a duration of 10 days was calculated and is displayed in Figures 3a and 3b. The parameter values that were used for these simulations are given in Table 1. Dispersion is mainly determined by the characteristics of the porous medium, provided that no size and/or charge effects are present. A virus entering a soil will, therefore, experience the same dispersion as a conservative salt tracer. This is the case when considering curves A and B. A conservative salt tracer will not be retarded and  $C/C_0$  reaches a plateau of 1 shortly after breakthrough (curve A). A virus that does not attach to the soil will show the same breakthrough as the salt tracer, but the plateau is lower due to inactivation of the virus (curve B). If a virus is also retarded due to equilibrium adsorption, it will show the same curve as B, but shifted to the right (curve C). In addition, the plateau is lower, because more time is available for inactivation to occur. If this virus is subject to a higher dispersion, the shape of the curve becomes flatter as is illustrated by curve D. Here, a fraction of the virus breaks through earlier, but the time to peak breakthrough is concurrent with the middle of the plateau of curve C.

Curve E simulates breakthrough of a virus, with the same dispersion as the salt, but now exhibiting kinetically-limited adsorption, where the attachment and detachment rate coefficients are of the same order of magnitude. The time to peak breakthrough is retarded.

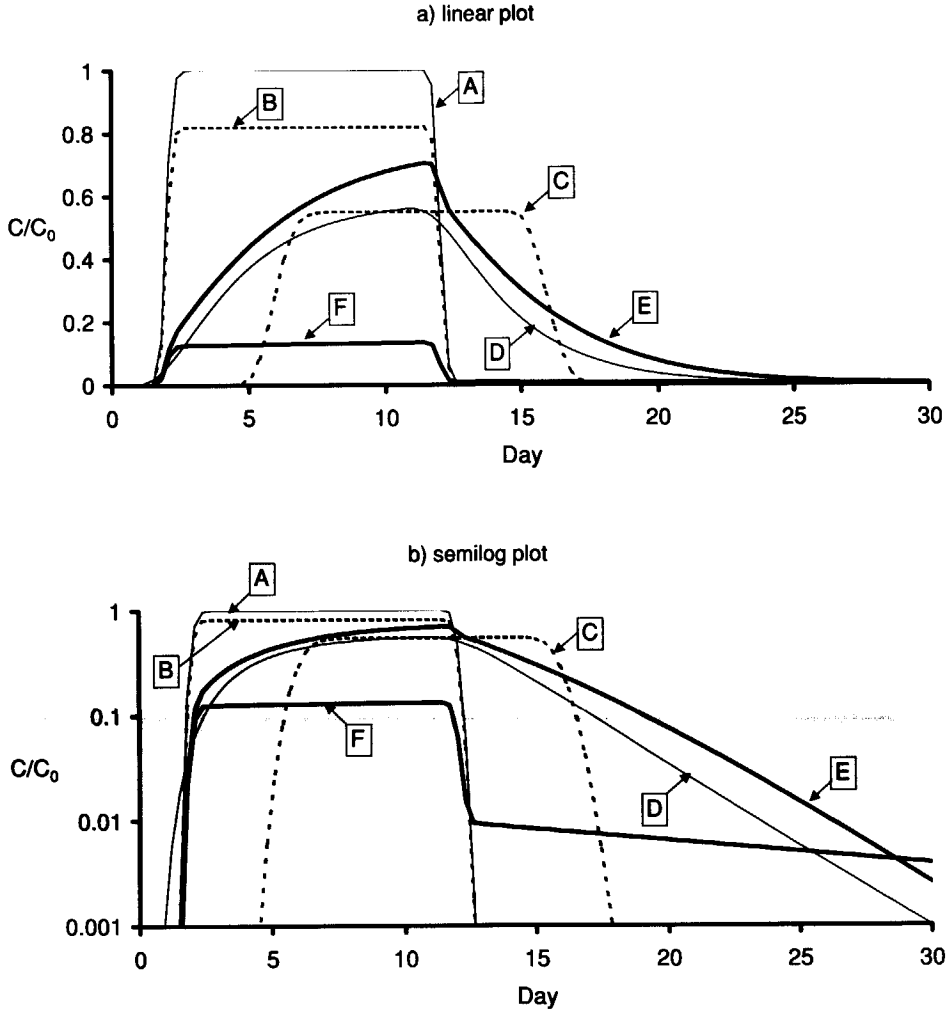


**Figure 3a and b** Simulated breakthrough curves of (A) a conservative salt tracer, (B) a virus that does not adsorb, but that is inactivated, (C) a virus that is retarded due to equilibrium adsorption, and that is inactivated, (D) like (C) with higher dispersion, (E) a virus that adsorbs to kinetically limited sites, and that is inactivated, (F) like (E) but now detachment is much slower. See Table 1 for corresponding parameter values.

**Table 1** Parameter values used to simulate breakthrough curves for (A) a conservative salt tracer and (B) – (F) for a virus exhibiting different types of adsorptive behavior. Resulting breakthrough curves are shown in Figure 3a and 3b. Pore water velocity = 1.5 m/day and distance = 3 m.

Parameter	A Salt tracer	B Virus - adsorption + inactivation	C Virus as B + equilibrium adsorption	D Virus as C + high dispersion	E Virus as B +kinetic adsorption	F Virus as E slow detachment
D	0.02	0.02	0.02	1	0.02	0.02
R	1	1	3	3	-	-
$k_{att}$	-	-	-	-	1	1
$k_{det}$	-	-	-	-	0.5	0.005
$\mu_l = \mu_s$	0	0.05	0.05	0.05	0.05	0.05

Dimension of D is [ $m^2 \cdot day^{-1}$ ], that of  $k_{att}$ ,  $k_{det}$ ,  $\mu_l$  and  $\mu_s$  is [ $day^{-1}$ ].

In fact, curve D and E in Figure 3a and 3b are very similar. Curve F simulates the virus, now exhibiting slow detachment. The shape of this curve on linear concentration-scale is now the same as A and B, only the maximum concentration is lower due to attachment. However, when plotted on a semi-log scale a tail becomes visible which makes it distinct from the other curves (Figure 3b). Now, if one stops measurements before the end of the plateau is reached, or if only linear plots are made, one may conclude that there is no reversible adsorption but a very high rate of irreversible adsorption (see *e.g.* Jin *et al.*, 1997).

These simulations show that description of virus transport by an equilibrium model and a kinetic model may lead to similar results, and that investigation of tailing on a semi-log plot is needed to tell the difference. A shortcoming of many virus transport experiments is that the tail of the breakthrough curve is not measured, so that the kinetic behavior cannot be observed (see *e.g.* Powelson *et al.*, 1990; Powelson and Gerba, 1994; Jin *et al.*, 1997). Modeling of both equilibrium and kinetic adsorption was carried out by Bales *et al.* (1991, 1997). Adsorption of bacteriophages MS2 and PRD1 was shown to be reversible and kinetically limited (Bales *et al.*, 1991, 1993, 1997; Kinoshita *et al.*, 1993). The kinetic effect was evidenced from the slow rising limbs and the long tails of the breakthrough curves. Bales *et al.* (1991) showed that in order to fit an equilibrium model to MS2-breakthrough curves, apparent dispersion values of up to 150 times higher than for the salt tracer had to be used to fit the rising limbs of the breakthrough curve. Furthermore, to fit the declining limbs of the breakthrough curve, a small dispersion value and an apparent R of less than 1 were needed. This is physically unacceptable and it indicates that the adsorption must be modeled as a kinetic process. Bales *et al.* (1991, 1997) found that the contribution of equilibrium adsorption to the total adsorption was negligible, and that kinetic adsorption controlled virus attenuation.

In the study of Bales *et al.* (1993), breakthrough curves of MS2 in silica showed a gradual increase in free virus concentrations towards maximum breakthrough concentration, similar to curve E. This means that the detachment rate coefficient is in the order of the attachment rate coefficient. However, the breakthrough curves of MS2 in columns with hydrophobic

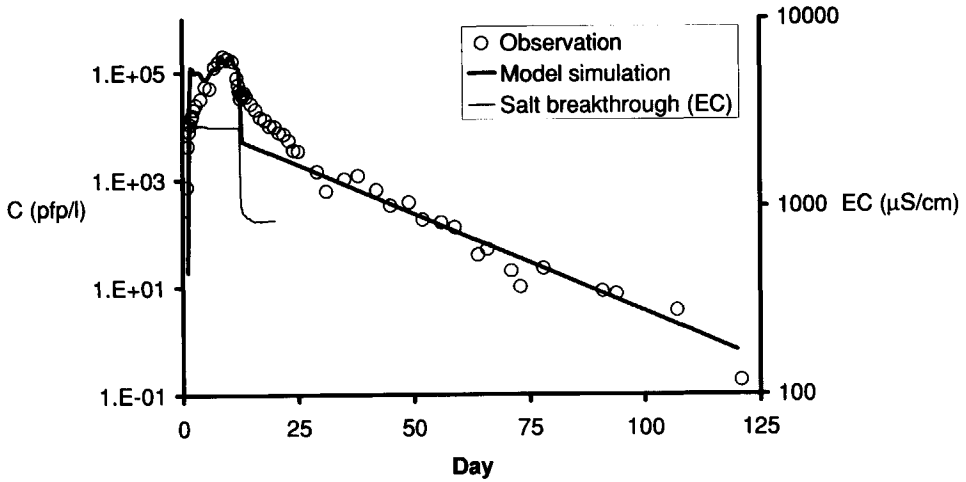


**Figure 4** Breakthrough curve of MS2 after 2.4 m of passage through dune sand (Schijven *et al.*, 1999). Observed and simulated concentrations are shown. EC is the electrical conductivity that was measured during breakthrough of the sodium chloride tracer.

bonded silica reached a steady state value much sooner, similar to curve F. In this case, detachment is much slower than attachment.

Other clear examples of kinetic behavior are shown for bacteriophages MS2, PRD1,  $\phi$ X174, Q $\beta$  and PM2 in a column study by Dowd *et al.* (1998), for MS2, PRD1,  $\phi$ X174 and poliovirus 1 in field studies by DeBorde *et al.* (1999), for MS2 and  $\phi$ X174 by DeBorde *et al.* (1998), and for MS2 and PRD1 by Schijven *et al.* (1999). In these field studies, phage transport was not retarded by equilibrium adsorption. Figure 4 shows a typical breakthrough curve of MS2 from the field study by Schijven *et al.* (1999). It was found that the value of  $k_{att}$  mainly determined the maximum breakthrough concentrations. It was also found that the tail slope was mainly determined by the value of  $\mu_s$ , whereas its intercept was mainly affected by the value of  $k_{det}$ . The end of the rising limb and the start of the declining limb of the breakthrough curves could not be simulated completely, due to an as yet unknown process. Possibly, there is more than one type of kinetic sites involved.

There is growing evidence from column and field experiments that removal of viruses during transport is mainly governed by kinetic adsorption. Neglect of kinetic effects and use of equilibrium adsorption models may lead to an estimation of an artificially large dispersion coefficient. If detachment is slow compared to attachment, tailing may be observed only if measurements are carried out for long enough time and when concentrations are plotted on a semi-log scale.

### 2.3.3 Batch versus Column Experiments

Estimates of adsorption parameters from batch experiments appear to be of limited use in the prediction of virus adsorption in column or field experiments. As already pointed out in previous sections, apparent equilibrium distribution is commonly assumed in batch systems, whereas kinetic attachment/detachment is needed to describe adsorption under

transport conditions. Also, due to the stirring in a batch experiment, the number of accessible sites for attachment is much higher than in a column. In a column, attachment rates may thus be so low that attachment rates of various viruses are relatively close to each other. Detachment is limited by diffusion over an energy barrier resulting from virus-soil interactions and by diffusion across a boundary layer near the solid surface (Ryan and Elimelech, 1996). The diffusion coefficient of the virus and the thickness of the boundary layer control the rate of transport across the diffusion boundary layer. The latter is controlled primarily by the velocity of the advecting fluid. If this velocity increases, the thickness of the diffusion boundary layer will decrease. Therefore, the detachment rate coefficient in a batch system is presumably smaller than under transport conditions, where there is advective flow. This implies that the observed ratio  $k_{att}/k_{det}$  from a batch experiment is expected to be larger than that obtained from a column or field experiment.

Bales *et al.* (1991) found that adsorption of MS2 in columns with silica-beads was kinetically limited. They found ratio a value of 0.36 l/kg for  $k_{att}/k_{det}$  in the column experiment, but in the batch experiment  $k_{att}/k_{det}$  was found to be 700 times higher. The 270-times higher specific surface area of the silica-sorbent that was used in the batch experiment may only partly explain this difference. Therefore, these findings suggest that  $k_{att}/k_{det}$  from a batch experiment is indeed larger than that from a column or field experiment. Powelson and Gerba (1994) estimated the retardation coefficient R from column experiments with MS2 (R=1.4), PRD1 (R=2.2) and poliovirus 1 (R=5.2), using the equilibrium model as described by Equation 11. These estimates were 12-130 times smaller than those determined from batch studies.

Contrary to expectations, in some batch experiments, values for the ratio  $k_{att}/k_{det}$  are found to be smaller than in corresponding column experiments. Goyal and Gerba (1979) carried out a number of batch experiments where the percentage of adsorption was determined after 30 minutes. Their results are converted to the ratio  $k_{att}/k_{det}$  using Equation 17, and are reported in Table 2. This ratio is generally found to be less than one at pH 7 – 8. But as discussed in the previous section,  $k_{att}/k_{det}$  was found to be much larger than one in column studies (Bales *et al.*, 1991, 1993) and field studies (Bales *et al.*, 1997; Pieper *et al.*, 1997, DeBorde *et al.*, 1999; Schijven *et al.*, 1999). This is perhaps an artifact due to the duration of batch experiments being too short. The following comparison between column experiments of Wang *et al.* (1981) and Lance *et al.* (1982) and the batch experiments of Goyal and Gerba (1979) also seems to support this. Wang *et al.* (1981) and Lance *et al.* (1982) studied removal of poliovirus 1 and echoviruses 1 and 29 in columns with the same soils. Residence time of the viruses in the columns was about 3 days. It was found that poliovirus 1 and both echoviruses were all removed very well (99% - 99.9%). Lance *et al.* (1982) suggested that poliovirus 1 does not behave significantly different from other enteroviruses under transport conditions in long soil columns that approximate field conditions. However, in the batch experiments of Goyal and Gerba (1979), poliovirus 1 adsorbed very well to different soils, whereas echovirus 1 and 29 were the least adsorbing viruses (Table 2). Thus, the difference in adsorption that was found in batch experiments was not found in column experiments. An explanation for this difference may be that echoviruses attach much slower than poliovirus 1, and thus may not have reached equilibrium after 30 minutes in the batch tests, whereas in the columns, these viruses had sufficient time to attach to a similar extent. The following analysis from a field study by

**Table 2** Values of the ratio  $k_{att}/k_{det}$  from batch experiments with viruses from group I, II and III and nine different soils. Data derived from Goyal and Gerba (1979).

PH	4.5	4.9	5.5	7.1	7.1	7.8	8	8	8.2	pI <sup>a</sup>
<i>Group I</i>										
CB4 V216	142	2.0	0.79	0.14	0.020	0.43	0.52	0.47	0.52	
CB4 V240	76	12	2.7	1.3	0	0	0.32	0.35	0.54	
Echo 1 Farouk	332	9	3.5	0.39	0.27	1.2	0.14	0.12	0.15	5.1
Echo 1 V212	332	2.3	3.8	0.79	0.30	0.85	0.61	0.23	0.010	6.4
Echo 1 V239	49	1.9	2.1	0.053	0.11	0	0.96	1.1	1.1	5.3
Echo 1 V248	499	999	4.6	0	0.33	0.43	0.33	0.49	0.49	5.0
$\phi$ X174	4999	32	4.9	0.22	0.0050	0	0.14	0	0	6.7
MS2	999	0.89	0.52	2.2	0.20	0.20	1.3	0.64	0.43	3.5 <sup>b</sup>
<i>Average</i>	929	132	2.9	0.64	0.15	0.39	0.54	0.43	0.40	
<i>Group I</i>										
CB3 Nancy	9.0	4.9	2.7	1.3	12	24	32	32	0.54	
Echo 7 Wallace	99	2.1	0.087	0.25	49	999	199	99	0.28	
Polio 1 LSc 2ab	999	16	1.3	0.72	19	999	249	99	4.6	6.6
T2	9999	249	1.8	0.087	9.0	0.56	19	6.1	2.3	4.2
T4	332	332	6.1	0	49	2.6	124	332	16	4-5
<i>Average</i>	2288	121	2.4	0.47	28	405	125	114	4.7	
<i>Group III</i>										
f2	99	0.064	0	0	0.35	0	0	0.19	0.0030	
<b>Soil characteristics</b>										
$f_{oc}$ %	0.3	1.4	0.4	3.6	4.2	0.88	0.78	1.7	0.27	
Clay (%)	39	53	4	3	54	3	36	28	13	
Silt (%)	13	16	4	8	20	8	24	13	10	
Sand (%)	48	13	92	89	26	89	40	59	77	

<sup>a</sup>pI-values taken from Gerba (1984). <sup>b</sup>pI for MS2 from Penrod *et al.* (1995)

Schijven *et al.* (1999) also illustrates that a much longer time may be needed to reach equilibrium in a batch experiment. In this study, a value for  $k_{att}/k_{det}$  of about 5000 was found (see also Table 8). Using Equation 14 and the values from this field study, it can be shown that apparent equilibrium would be reached after 40 hours in a batch experiment. Now, if one stops this batch experiment after, say, only one hour, a ratio  $k_{att}/k_{det}$  of only 0.18 would be found. Thus, it is believed that in many cases, batch experiments may have been stopped far too soon, thereby causing a strong underestimation of  $k_{att}/k_{det}$ . Also, this would mean that a low value of  $k_{att}/k_{det}$  that is found in a batch experiment after a short period of time, is rather a consequence of slow adsorption than of equilibrium.

Nevertheless, it may not always be the case that  $k_{att}$  in batch experiments is larger than in column experiments. An example is reported in Jin *et al.* (1997). They stopped a batch experiment of  $\phi$ X174 and sand after 3 hours and estimated a retardation coefficient R of 4.5. This means they assumed equilibrium adsorption was reached. Then, based on this value, they predicted a retarded breakthrough curve for their column experiments. However, breakthrough of  $\phi$ X174 was not found to be retarded in any of the column experiments (R = 1), implying that the removal process was not due to equilibrium

adsorption. As already pointed out in the previous section, measurements in the column experiment were stopped before the end of the plateau of the breakthrough curve was reached. Detachment in the column experiments was, therefore, not investigated. Thus, the authors interpreted the removal process as a first order irreversible attachment in both column and batch experiments. This interpretation then indicated that  $k_{att}$  of  $\phi X174$  obtained from the column experiment was found to be about twice as high as that from the batch experiment. At this point there is no clear explanation for these observations.

### 2.3.4 Colloid Filtration

Analogous to attachment of viruses to solid surfaces in a batch system, attachment of viruses in flowing water to the surfaces of solid particles in a porous medium involves two processes: mass transport to the surface and virus-surface interactions (see section 2.3.1). Therefore, the attachment rate coefficient  $k_{att}$  depends on microscale flow and diffusion characteristics as well as surface properties of viruses and soil grains. These processes are also described by colloid filtration theory, which allows exclusion of the effects of flow and diffusion by expressing the attachment rate of viruses in terms of single collector efficiency  $\eta$  and collision efficiency  $\alpha$ . According to this theory, a suspended particle may come into contact with a particle of the solid medium, the collector, either by interception, sedimentation or diffusion (Yao *et al.*, 1971). The attachment rate coefficient is related to the single collector efficiency  $\eta$  and the collision efficiency  $\alpha$  as follows (Yao *et al.*, 1971):

$$k_{att} = \frac{3}{2} \frac{(1-n)}{d_c} \alpha \eta v \quad (18)$$

Here,  $d_c$  is the average diameter of collision (grain size), [L]. The fraction of particles that collide with the collector, is given by  $\eta$ , the single collector efficiency. Viruses can be regarded as colloidal particles, because of their size and surface charge. Viruses are small in size and their transport in the immediate vicinity of the collector surface is dominated by Brownian diffusion, whereas effects of interception and gravitation are negligible. In this case the single collector efficiency is given by the Smoluchowski-Levich approximation (Penrod *et al.*, 1996):

$$\eta = 4A_s^{1/3} N_{pe}^{-2/3} \quad (19)$$

Here,  $N_{pe} = d_c n v / D_{BM}$ , a Péclet number, that accounts for diffusion;

$D_{BM} = K_B (T + 273) / (3\pi d_p \mu)$  is the diffusion coefficient, [ $L^2 T^{-1}$ ];  $K_B = 1.38 \times 10^{-23}$  is the Boltzmann constant [J/K]; T is temperature;  $d_p$  is the virus particle size;  $\mu$  is the dynamic viscosity [ $ML^{-1} T^{-1}$ ];  $A_s = 2(1 - \gamma^5) / (2 - 3\gamma + 3\gamma^5 - 2\gamma^6)$  is Happel's porosity dependent parameter, with  $\gamma = (1 - n)^{1/3}$ .

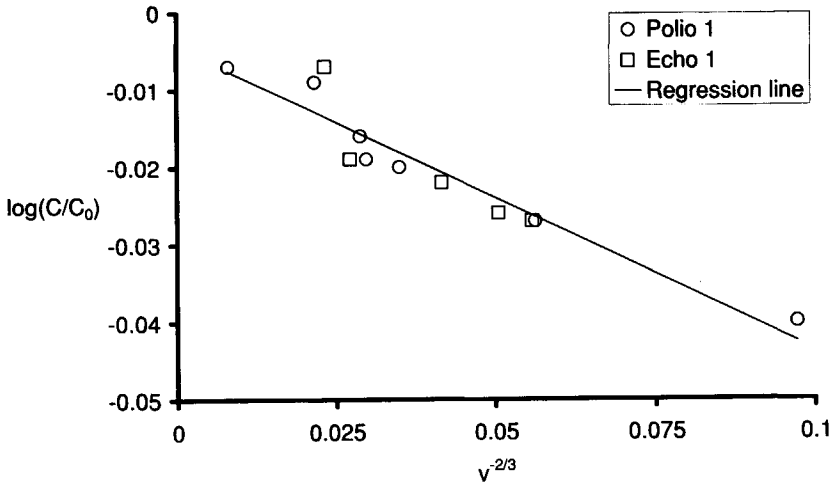


**Figure 5** Removal,  $\log_{10}(C/C_0)$  of poliovirus 1 and echovirus 1 versus  $v^{-2/3}$  (data from Wang *et al.*, 1981).

Funderburg *et al.* (1981), Wang *et al.* (1981) and Lance *et al.* (1982) found that virus removal in columns was inversely related to the flow velocity. Data on removal of poliovirus 1 and echovirus 1 in the upper 17 cm of the columns in the study by Wang *et al.* (1981) offer the possibility to investigate the relation between virus removal and flow rate. In a column with characteristic length L, assuming steady state conditions, neglecting dispersion, virus inactivation and detachment, the solution of Equation 1 is:

$$\log\left(\frac{C}{C_0}\right) = -\frac{k_{att}}{v} \frac{L}{2.3} = -\frac{\psi}{2.3} v^{-2/3} \quad \text{where } \psi = \alpha L \frac{3(1-n)}{2 d_c} 4A_s^{1/3} \left(\frac{DBM}{d_c n}\right)^{2/3} \quad (20)$$

Thus, colloid filtration theory predicts that virus removal,  $\log_{10}(C/C_0)$ , is proportional to  $v^{-2/3}$  (Yao *et al.*, 1971). In the study by Wang *et al.* (1981), it was found that poliovirus 1 and echovirus 1 were removed to a similar extent at different flow rates. Figure 5 shows removal of both viruses versus  $v^{-2/3}$ . This relation appears to be linear with a correlation coefficient of 90%. Also, Jin *et al.* (1997) observed less removal of  $\phi$ X174 when flow velocity was increased. The ratio of virus removal at the different flow velocities was approximately equal to the ratio of the two flow velocities to the power of  $-2/3$ . This suggests that the relation between virus removal and flow velocity, as described by colloid filtration theory, is valid.

The collision efficiency,  $\alpha$ , represents the fraction of the particles colliding with the solid grains which remain attached to the collector (Martin *et al.*, 1992). The collision efficiency reflects the net effect of repulsive and attractive forces between the surfaces of the particles and the collector and depends on the surface characteristics of the virus and soil particles. Therefore, it depends on pH, organic carbon content, and ionic strength. It is believed that  $\alpha$  is independent of hydrodynamic effects (velocity and dispersion). So, if for a given set of

conditions, like type of virus, type of soil, pH, organic carbon content and ionic strength  $\alpha$  is known, it is possible to calculate the value of  $k_{att}$  for a different set of physical conditions using Equation 18. This emphasizes the importance of knowing the value of  $\alpha$  under a given set of conditions.

Commonly,  $\alpha$  is derived from experimental values of  $k_{att}$  and calculated values of the single collector efficiency  $\eta$  using Equation 18 (Bales *et al.*, 1991, 1993; Kinoshita *et al.*, 1993; Penrod *et al.*, 1996; Redman *et al.*, 1997 and Schijven *et al.*, 1998, 1999). Alternatively,  $\alpha$  has been estimated from relative breakthrough (RB) of the mass of viruses relative to that of a conservative salt tracer (Pieper *et al.*, 1997; DeBorde *et al.*, 1999; Ryan *et al.*, 1999) and assuming irreversible adsorption using the following equations:

$$\alpha = \frac{d_c \left[ \left[ 1 - 2(\alpha_L/x) \ln(RB) \right]^2 - 1 \right]}{6(1-n)\eta\alpha_L}, \text{ where } RB = \left[ \frac{\int_{t_0}^{t_f} \frac{C_{virus}}{C_{0,virus}} dt}{\int_{t_0}^{t_f} \frac{C_{salt}}{C_{0,salt}} dt} \right] \quad (21)$$

The collision efficiency can also be calculated according to the so-called IFBL (Interaction Force Boundary Layer) approximation (Swanton, 1995; Ryan and Elimelech, 1996):

$$\alpha = \left( \frac{\beta}{1+\beta} \right) S(\beta) \text{ where } \beta = \frac{1}{3} (2)^{-1/3} \Gamma \left( \frac{1}{3} \right) A_s^{-1/3} \left( \frac{D_{BM}}{U d_c} \right)^{1/3} \left( \frac{k_F d_c}{D_{BM}} \right) \quad (22)$$

Here,  $k_F$  is a pseudo-first-order coefficient that accounts for the retarding effect of double layer repulsion on the attachment rate, [L<sup>-2</sup>T].  $S(\beta)$  is a slowly varying function of  $\beta$  with tabulated numerical values, and  $U$  is the superficial flow velocity, [LT<sup>-1</sup>] (Ryan and Elimelech, 1996). As will be described in the next section, theoretical values of the collision efficiency, and thus also of the attachment rate coefficient, considerably underestimate experimental values.

### 2.3.5 DLVO Theory

The attractive and repulsive forces that exist between colloids (e.g. viruses) and grain surfaces determine the interactions between them. These forces can be described in profiles of the intersurface potential energy by DLVO theory (Derjaguin-Landau-Verwey-Overbeek). Such profiles are constructed by summing the potential energies of double layer repulsion or attraction, London-van der Waals attraction, and poorly characterized short-range “non DLVO” forces such as hydration and steric repulsion (Ryan and Elimelech, 1996). An example of a DLVO-energy profile is shown in Figure 6. The total potential energy curve is characterized by an attractive energy well at a very small separation distance ( $\delta$ ), with the primary minimum ( $\phi_{min1}$ ), a repulsive energy barrier ( $\phi_{max}$ ), and a shallow attractive energy well at a larger separation distance, with the secondary minimum ( $\phi_{min2}$ ).

The van der Waals attraction is an electrical force between instantaneous dipole moments within the different molecules (Gerba, 1984). It is linearly dependent on the value of the Hamaker constant. The Hamaker constant depends on the nature of the interacting materials (Swanton, 1995). The Hamaker constants of most forms of organic matter are similar to

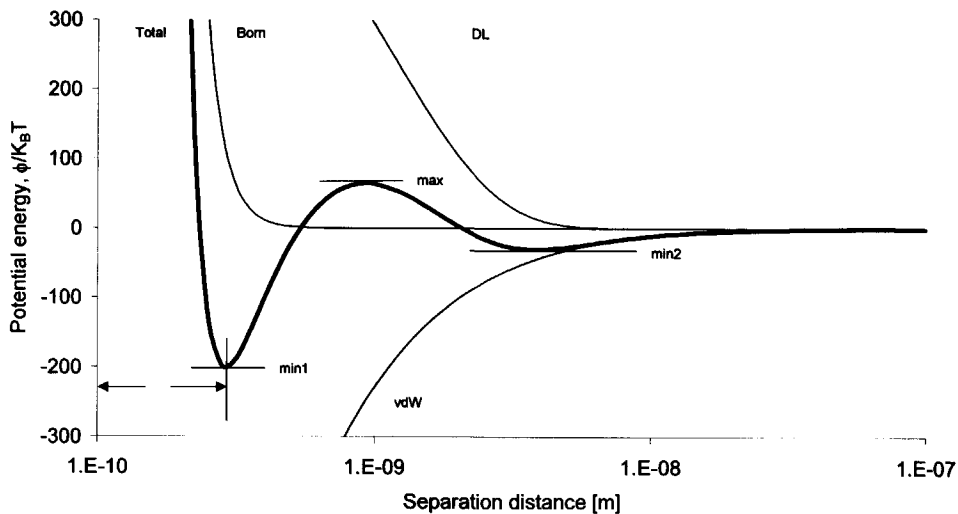


**Figure 6** DLVO energy as a function of separation distance between a colloid and a collector. The total potential energy ( $\phi^{Total}$ ) is the sum of the double layer potential energy ( $\phi^{DL}$ ), the van der Waals potential energy ( $\phi^{vdW}$ ) and the Born potential energy ( $\phi^{Born}$ ). The total potential energy curve is characterized by an attractive well at a very small separation distance ( $\delta$ ), the primary minimum ( $\phi_{min1}$ ), a repulsive energy barrier ( $\phi_{max}$ ) and a shallow attractive well at a larger separation distance ( $\phi_{min2}$ ). The potential energy is normalized by  $k_B T$  (Ryan and Elimelech, 1996).

those of water, hence the van der Waals interactions between organic colloids are weak. Inorganic matter tends to have large Hamaker constants and thus a stronger inherent attraction for virus (Moore *et al.*, 1981).

A double layer potential energy arises from the overlap of diffuse clouds of ions (double layers) that accumulate near charged surfaces to balance the surface charge. If the interacting surfaces are like-charged, the double layer potential energy will be repulsive (Ryan and Elimelech, 1996). If the surfaces are oppositely charged, the double layer potential energy will be attractive. In formulations of the double layer theory, potential energy is considered to be sensitive to variations in the surface potentials of the colloid and the collector, ionic strength of the solution and colloid size. The dependence on colloid size has not been verified (Ryan and Elimelech, 1996).

It has been shown that the rate coefficients for attachment ( $k_{att}$ ) and detachment ( $k_{det}$ ) should increase exponentially as the height of the corresponding energy barriers increases (Ryan and Elimelech, 1996):

$$k_{att} \propto \exp\left(-\frac{|\phi_{max}|}{k_B T}\right) \quad (23)$$

$$k_{det} \propto \exp\left(-\frac{|\phi_{max} - \phi_{min1}|}{k_B T}\right) \quad (24)$$

DLVO theory provides a conceptual framework to understand interactions of virus particles and solid surfaces under different conditions, such as pH, ionic strength and colloid size. The effects of these conditions are discussed more in detail in section 2.4.

DLVO theory has, however, several shortcomings in predicting attachment and detachment rates. It has generally been shown that under unfavorable conditions for attachment, DLVO theory underestimates attachment by many orders of magnitude. At pH 7 – 8, as in many aquifers, the net surface charge of most viruses and soils is negative, and thus conditions for attachment are generally unfavorable. Under such conditions, colloid-surface interactions are the rate-limiting process for attachment (Ryan and Elimelech, 1996). Experimentally determined collision efficiencies are sensitive to the ionic strength of the solution and to the electrokinetic (zeta) potentials of particles and collectors but not to the degree predicted by theory. Experimentally determined collision efficiencies and attachment are virtually independent of colloid particle size, in contrast with DLVO theory predictions. Also, it has been shown that the sensitivity of attachment rates to ionic strength decreases markedly as the degree of surface charge heterogeneity increases (Ryan and Elimelech, 1996). Furthermore, DLVO theory was formulated for smooth bodies with ideal geometries (*e.g.* spheres interacting with flat surfaces) and uniform properties. In practice, real particles are irregular, the surface of the bodies are rough and are likely to be heterogeneous in composition and charge (Swanton, 1995).

Under favorable conditions, *i.e.* in the absence of repulsive energy barriers or in the presence of attractive double layer interactions, colloidal transport to the vicinity of the soil surfaces is the rate-limiting step. In this case, particle attachment models within the framework of the DLVO-theory are satisfactory in predicting the effect of solution ionic strength, fluid velocity and particle size. Favorable chemical conditions for attachment may develop in groundwaters with high levels of water hardness and ionic strength. Attachment will also be favorable for solid surfaces (or patches on solid surfaces) which are positively charged due to iron, aluminium, or manganese oxide coatings (Ryan and Elimelech, 1996). Because of the electrostatic attractive forces, it is reasonable to assume that attachment to such favorable patches is irreversible (Ryan and Elimelech, 1996).

Bales *et al.* (1991) suggested that attachment to kinetically limited sites would occur in the primary minimum, and to fast equilibrium sites in the secondary minimum. But as was shown in their and other studies (Bales *et al.*, 1993, 1997; Kinoshita *et al.*, 1993; Schijven *et al.*, 1999), kinetically limited attachment prevails. Loveland *et al.* (1996) calculated DLVO-profiles for PRD1 and quartz with or without ferric oxyhydroxide coatings and showed that secondary minima were extremely small. So, probably, attachment of a virus in the secondary minimum of a site is not significant. Loveland *et al.* (1996) suggested that a secondary minimum does need to be deep to affect virus transport. Under strongly repulsive conditions, viruses will not attach in the primary minimum. Instead, viruses may accumulate in the boundary layer in front of the energy barrier. In time, diffusion and advection will carry them out of the boundary layer and back to the advective flow. Regardless of the depth of the secondary minimum, the transport of these viruses has been retarded by reversible attachment.

### 2.3.6 Hydrophobic Interactions

As reviewed by Gerba (1984), hydrophobic interactions between viruses and solid surfaces may also contribute significantly to adsorption. Hydrophobic interactions may be seen as a consequence of the thermodynamically unfavorable interaction of hydrophobic substances with water molecules and is not due to interactions among hydrophobic particles themselves (Wait and Sobsey, 1983). Hydrophobic interactions are not described by DLVO-theory (Swanton, 1995). Interactions between hydrophobic groups on the surfaces of the virus and the solid may cause an increase in virus attachment. At high pH, when both the surfaces are negatively charged, hydrophobic interactions may be the major factor maintaining virus attachment (Shields and Farrah, 1983; Gerba, 1984; Bales *et al.*, 1991). Bales *et al.* (1991) showed that MS2 attached much less to silica beads in a batch experiment at pH 7 than at pH 5, but when the silica beads were coated with C<sub>18</sub>-trichlorosilane, 400 times more attachment took place, independent of pH. Bales *et al.* (1991) concluded, that hydrophobic effects are important for adsorption of even relatively hydrophilic viruses. Loveland *et al.* (1996) argued that the addition of hydrocarbon chains to a silica surface decreases the negative surface charge of the silica surface in addition to providing hydrophobic attachment sites for viruses. According to Loveland *et al.* (1996), increased virus attachment may, therefore, be more reasonably attributed to a decreased double layer repulsion rather than to hydrophobic expulsion from solution. Hydrophobic interactions of viruses with solid surfaces have been suggested to play a role in the interaction between poliovirus 1 and Millipore and Zeta plus filters (Farrah *et al.*, 1981). Also, between poliovirus 1, echovirus 1 and rotavirus SA 11 and highly organic estuarine sediments (Wait and Sobsey, 1983) and between poliovirus 1 and nitrocellulose membrane filters (Shields and Farrah, 1983). Bales *et al.* (1991, 1993) suggested hydrophobic interactions of MS2, and PRD1 with octadecyltrichlorosilane coated silica. It was also suggested for MS2,  $\phi$ X174, T7, PRD1 and  $\phi$ 6 with nitrocellulose and cationic polysulfone membranes (Lytle and Routson, 1995).

### 2.3.7 Blocking

When particles attach to a solid surface, the attachment rate may decrease with time if particle-particle interactions are repulsive; the solid surface becomes progressively occluded as particles accumulate. This surface exclusion phenomenon is termed blocking. Ryan and Elimelech (1996) have reviewed the blocking process of colloids and how it is modeled. Blocking may prevail in groundwater having low ionic strength and low levels of hardness. Because the majority of the available surface area of solids in groundwater has chemical characteristics unfavorable for particle deposition, colloidal attachment in groundwater is thought to be largely restricted to a minor patch-wise distributed fraction having energetically favorable charge characteristics (Ryan and Elimelech, 1996). The same restrictions apply to attachment of viruses. Jin *et al.* (1997) observed blocking of  $\phi$ X174 in a sand column. Initially, significant removal of  $\phi$ X174 took place, but with increasing amounts of attached phages, the attachment rate dropped and an increase of C/C<sub>0</sub> up to one was observed. However, under field conditions, virus concentrations in recharging water are so low that blocking of binding sites with viruses is not likely to occur. In case of contamination of an aquifer with wastewater, viruses represent only a very minor

fraction of the wastewater organic matter. In that case, organic matter will probably block binding sites and a progressive blocking effect of viruses will not be the case.

## 2.4 Factors affecting Adsorption of Viruses to Soil

### 2.4.1 Introduction

The interactions that take place between viruses and soil particles are determined by their surface characteristics. Virus-soil interactions are electrostatic and hydrophobic in nature. Surface characteristics may be altered by changes in pH, ionic strength, multivalent ions and organic matter (Gerba, 1984). Changes in these interactions are quantified by changes in attachment and detachment rate coefficients. As we have seen in section 2.3.5, DLVO theory provides a conceptual framework to understand many of these changes. In the following sections, the effect of virus and soil type, pH, ionic strength, multivalent cations, and organic matter on attachment and detachment of viruses to solid surfaces will be discussed in more detail.

### 2.4.2 Effect of Virus Type

The behavior of different viruses in their interactions with solids is believed to be the result of differences in the electrical charge and the hydrophobicity of the virus surface (Shields and Farrah, 1987). Most viruses have a size in the range of 20 – 200 nm and consist of nucleic acid encapsulated in a protein capsid. The amino acids in this protein coat contain weakly acidic and basic groups, like carboxyl and amino groups, that determine the amphoteric nature of the virus particle. The isoelectric point (pI) of a virus particle is the pH value at which it has a zero net charge. However, localized pockets of positive and negative charges may still exist across the virus surface. The isoelectric point of a virus may vary not only by the type of the virus but also by the strain (Gerba, 1984). At pH-values above 5, the electrophoretic mobility of MS2, a measure of its surface charge, remains constant (Penrod *et al.*, 1995). At pH-values above 6, electrophoretic mobilities of vaccinia virus, reovirus and  $\lambda$  are also relatively insensitive to changes in pH (Penrod *et al.*, 1995). At higher pH's, PRD1 (Loveland *et al.*, 1996) and recombinant Norwalk-like virus particles (Redman *et al.*, 1997), however, show a further decrease in their negative charge.

The coat proteins of a virus may contain spans of amino acids that are hydrophobic. Dependent on the way these proteins are folded, such hydrophobic parts may either be on the inside or the outside of the virus coat (Gerba, 1984). Viruses differ in hydrophobicity, as was shown by Shields and Farrah (1987), who determined the hydrophobic nature of 15 viruses by means of octyl-sepharose chromatography. Echovirus 5 and MS2 were found to be the most hydrophobic of the viruses tested, while echovirus 7 and  $\phi$ X174 were found to exhibit little if any hydrophobic character. According to Lytle and Routson (1995) in a study on the retention of viruses by nitrocellulose and cationic polysulfone membranes,  $\phi$ X174 was the least hydrophobic of the viruses studied, but hydrophobicity of MS2, T7, PRD1 and  $\phi$ 6 was not much different. A detailed description of the coat proteins of MS2, including its hydrophobic outer regions, is presented by Penrod *et al.* (1996).

Adsorption behavior of viruses is very complex and even under relatively well-defined conditions of batch experiments, a non-unique behavior is observed. Several studies (Burge

and Enkiri, 1978; Goyal and Gerba, 1979; Singh *et al.*, 1986) have clearly shown that most viruses, even strains of the same type, may behave differently under similar conditions. Goyal and Gerba (1979) compared attachment of a large number of different types and strains of human enteroviruses, bacteriophages and a simian rotavirus to nine different soil types. From these data, it was possible to distinguish two groups of viruses according to their mean percentage of adsorption at equilibrium (Gerba *et al.*, 1981). It was remarked that this grouping depended on the choice of viruses and soils that were studied. Viruses of group II adsorb very well to most soils, sludges and marine sediments, while those of group I adsorb to a lesser degree. Mean percentage of adsorption of viruses of group I was 44% and that of group II 78%. Bacteriophage f2 is probably a special case as its mean adsorption of 16% was significantly lower than that of all the other viruses. Table 2 summarizes the batch experiments of Goyal and Gerba (1979). Recall that, instead of giving percentages of adsorption at equilibrium, the ratio  $k_{at}/k_{det}$  is calculated using Equation 17. Adsorption of group I viruses is most affected by pH, exchangeable iron content and organic carbon content of the soil. Adsorption is inversely correlated with pH, which explained 83% of the variation in the mean attachment. Adsorption of group I viruses is also inversely correlated with the organic matter content of the soil, but positively correlated with exchangeable iron. Adsorption of group II viruses was not found to be significantly affected over the range of soil characteristics studied here. Gerba *et al.* (1981) suggested that the net charge of group I viruses was influenced more over the range of pH values and organic matter concentrations found in nature than that of group II viruses.

Several studies indicate that knowledge of the pI of a virus makes it possible to predict the likelihood of its attachment to a charged surface (Gerba, 1984). Also, Gerba (1984) suggested that group I viruses might have lower isoelectric points (pI) than group II viruses. However, the data in Table 2 are not in agreement with that suggestion. Dowd *et al.* (1998) observed a linear relationship between amount of adsorption to soil and the isoelectric point of five different phages, MS2, PRD1, Q $\beta$ ,  $\phi$ X174 and PM2 in circulating flow columns, *i.e.* in these columns the outflow is connected to the inflow. The amount of adsorption was the least for the phages with the higher pI. This is contradictory to the expectation that a virus with higher pI is less electronegatively charged and thus adsorbs better because of weaker repulsion. Besides, in flow-through columns this relation with pI was not found. Possibly, the presence of multivalent cations was the cause that more negatively charged viruses attach more.

The isoelectric point is only an indication of what the net surface charge of a virus may be at a given pH. Penrod *et al.*, (1996) and Redman *et al.* (1997) showed that  $\lambda$  and Norwalk virus-like particles have a stronger negative zeta-potential than MS2 at pH 5 – 7, although MS2 has a lower pI than the other two. Penrod *et al.* (1996) found strong evidence that the surface charge of MS2 originates from the charge of the amino acid residues that are present on the exterior of the virus particle, by calculating pI of MS2 correctly from the ionization of these exteriorly located amino acid residues. They also suggested that the attachment rate of MS2 is not only determined by electrostatic repulsion, but also by steric repulsion of hydrophilic loops that protrude from the surface of MS2. In this study, it was also shown that the attachment rate of phage  $\lambda$  was determined primarily by the surface charge on the capsid of this virus but the tail of  $\lambda$  contributes relatively little to the overall charge of the virus.

Due to the differences in electrical charge and hydrophobicity that exists between different types of viruses, and even between different strains of the same virus type, virus-soil interactions will differ, and thus virus removal by soil passage will be virus type dependent. Therefore, to predict removal of viruses by soil passage, a combination of viruses may be considered which represent a range of adsorption characteristics. Alternatively, a virus, which adsorbs less than other viruses under certain conditions, may be considered as a worst-case model virus. Viruses with a strong negative surface charge and little hydrophobicity meet these requirements.

### 2.4.3 Effect of Soil Type

Ryan and Elimelech (1996) described that most of the surface area of soil grains has chemical characteristics unfavorable for particle deposition. Therefore, colloidal attachment in groundwater is thought to be largely restricted to a minor fraction of the grain surface having energetically favorable charge characteristics. These favorable sites, resulting from surface charge heterogeneity, are often manifested as positively-charged patches on the surface of negatively-charged mineral grains. Such patch-wise charge heterogeneities are general to all aqueous geologic settings, originating from inherent differences in the surface properties of adjacent crystal faces on mineral grains, and from minerals having bulk- or surface-bound chemical impurities. Oxides of iron, aluminium and manganese are the most common source of surface charge heterogeneity in the groundwater environment. These oxides carry a positive charge at near neutral pH and are generally present in minor amounts as surface coatings on mineral grains. It has been shown that minor degrees of charge heterogeneity on collector surfaces result in attachment rates that are orders of magnitude larger than similar surfaces having no charge heterogeneity.

Several studies appear to support this concept that viruses preferably attach to a surface fraction of the soil having favorable charge characteristics. Solids that have high isoelectric points are better virus adsorbents than those with low isoelectric points (Gerba, 1984). Also, favorable for attachment of viruses are a higher cation exchange capacity (Burge and Enkiri, 1978), exchangeable iron (Gerba *et al.*, 1981) and iron oxides (Moore, *et al.*, 1981; Lipson and Stotzky, 1983; Grant *et al.*, 1993; Loveland *et al.*, 1996). Attachment of viruses has been shown to be better to soils with higher specific surface areas (Moore *et al.*, 1982). Generally, granular soils are weaker adsorbents than clays and minerals (Sobsey *et al.*, 1980; Moore *et al.*, 1981). Clays may have surfaces that have a very heterogeneous charge distribution. *E.g.* Vilker *et al.* (1983) suggested that poliovirus 1 adsorbed to the edges of montmorillonite particles, where regions of positive charges are located due to the presence of aluminium ions. Farrah and Preston (1993) modified sand by precipitation of metallic salts. Columns of this modified sand removed significantly more viruses (poliovirus 1, coxsackievirus B5, echovirus 5 and MS2) than columns of unmodified sand. In batch experiments, Moore *et al.* (1981) showed an apparent surface saturation of poliovirus 2 (about 30 nm in size) to Ottawa sand at pH 7.5 of  $2.5 \times 10^{12}$  virus particles/kg. It was thus concluded, that granular materials, like Ottawa sand (surface area  $0.018 \text{ m}^2/\text{g}$ ), have an enormous capacity for viruses and are unlikely to become saturated in natural systems. Nevertheless, at this maximum concentration of attached virus particles, only approximately 1% of the total sand surface was covered. Jin *et al.* (1997) demonstrated blocking of  $\phi$ X174 in columns with Ottawa sand. Ottawa sand contains detectable levels of

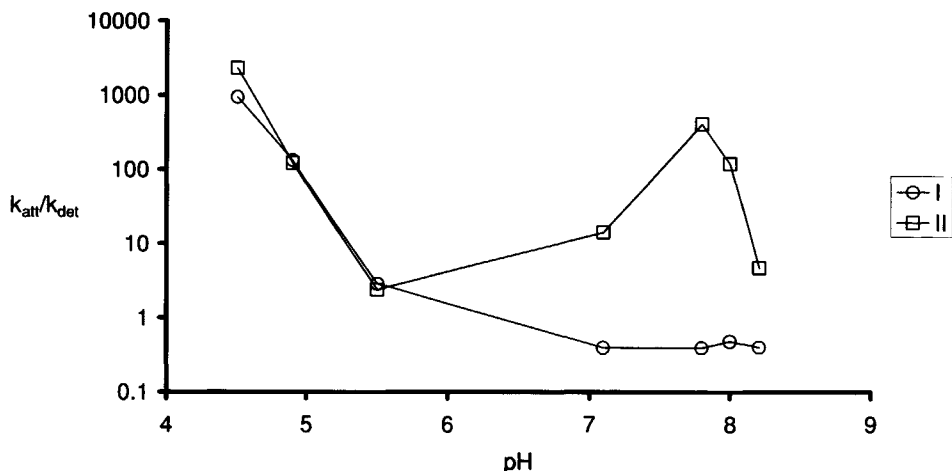


**Figure 7** Average values of ratio  $k_{att}/k_{det}$  versus pH of viruses of group I and II to soil in a batch suspensions (Goyal and Gerba, 1979). See also values in Table 2.

iron, probably in the form of goethite. By calculation of the surface area that is occupied by a monolayer of  $\phi X174$ -particles, they also showed that the apparent saturation of the sorption sites was far less than the total surface area of the sand. Therefore, they suggested that the active surface for virus attachment was limited to patches of positive charges on the sand particles formed by goethite.

#### 2.4.4 Effect of pH

In many batch studies, it has been shown that, generally, viruses attach to a lesser extent at higher pH (Burge and Enkiri, 1978; Goyal and Gerba, 1979; Sobsey *et al.*, 1980; Taylor *et al.*, 1980, 1981; Gerba *et al.*, 1981, Grant *et al.*, 1993). According to DVLO-theory, this can be explained by an increased electrostatic repulsion at higher pH. Figure 7 shows a plot of the average values of the ratio  $k_{att}/k_{det}$  versus pH for viruses of group I and II from the study of Goyal and Gerba (1979). In the range of pH 4.5 to 5.5 there is little difference between viruses of group I and II. Goyal and Gerba remarked that the naturally isolated viruses used in their study were all isolated from field samples by adsorption to membranes at low pH. Thus, viruses that did not have this characteristic would not have been isolated. Within the pH-range of 4.5 to 5.5, the ratio  $k_{att}/k_{det}$  declines with increasing pH. The ratio for group I viruses continues to decrease, but at a lower rate, as pH increases. It appears that the ratio  $k_{att}/k_{det}$  of group I viruses becomes less than 1 at a pH equal to or higher than their pI. However, the ratio  $k_{att}/k_{det}$  of a group II virus show an increase for pH-values of up to 8, at which point it also decreases with increasing pH. (see also Table 2).

Tables 3 and 4 are an inventory of collision efficiencies of viruses in column and field studies, at different pH-values, respectively. In figure 8, the collision efficiency of MS2 is plotted versus pH within the range of 4 – 9 and at different ionic strengths, using the data from Table 3. The pI of MS2 is 3.5, it is therefore negatively charged within this pH-range. The different column studies appear to show a coherent pattern. The value of  $\alpha$  decreases

**Table 3** Collision efficiency  $\alpha$  for viruses from column studies (6-35 cm).

Virus	Soil	pH	NaCl [M]	$f_{oc}$	$\alpha$	Reference
MS2	Glass beads	5.0	0.01	-	0.0015	Bales <i>et al.</i> (1991) <sup>a</sup>
		5.0	0.08	-	0.0015-0.0028	
	Silica beads	5.0	0.05	$2 \times 10^{-7}$	0.018	Bales <i>et al.</i> (1993)
		7.0	0.05	$2 \times 10^{-7}$	0.0022	
	Sand Cape Cod	5.7	0.1	$<1 \times 10^{-4}$	0.007	Kinoshita <i>et al.</i> (1993)
		7.0	0.1	$<1 \times 10^{-4}$	0.01	
		8.2	0.1	$<1 \times 10^{-4}$	0 <sup>b</sup>	
	Quartz	3.5	0.01	-	0.12	Penrod <i>et al.</i> (1996)
		3.5	0.3	-	0.16	
		5.0	0.01	-	0.009	
5.0		0.1	-	0.09		
5.0		0.3	-	0.04		
PRD1	Glass beads	5.5	0.01	-	0.0015-0.0033	Bales <i>et al.</i> (1991) <sup>a</sup>
	Sand Borden	6.5	0.1	$3 \times 10^{-4}$	0.17	Kinoshita <i>et al.</i> (1993)
		7.0	0.1	$3 \times 10^{-4}$	0.14	
		7.6	0.1	$3 \times 10^{-4}$	0.15	
	Sand Cambridge	7.0	0.1	$5 \times 10^{-4}$	1.11	
	Sand Cape Cod	5.7	0.1	$<1 \times 10^{-4}$	0.62- $\geq$ 0.94	
		7.0	0.1	$<1 \times 10^{-4}$	0.63-0.82	
		8.2	0.1	$<1 \times 10^{-4}$	0.58	
Polio 1	Silica beads	5.5	0.05	$2 \times 10^{-7}$	0.014	Bales <i>et al.</i> (1993)
		7.0	0.05	$2 \times 10^{-7}$	0.0040	
		7.0	0.05	$2 \times 10^{-7}$	0.0072	
$\lambda$	Quartz	3.9	0.01	-	1.25	Penrod <i>et al.</i> (1996)
		5.0	0.01	-	0.045	
		5.0	0.1	-	0.53	
		5.0	0.3	-	0.65	

<sup>a</sup>Corrected for the factor  $A_s^{1/3}$ , which was not applied in the original publication.

<sup>b</sup>set to 0, because no removal was found.

by a factor of approximately 0.9 for every increase in pH by one tenth. A similar pattern of electrophoretic mobility of MS2 versus pH has been shown by Penrod *et al.* (1995), and strongly indicated that surface charge of the virus particles as a function of pH determines attachment. This pattern also strongly resembles that of the ratio  $k_{att}/k_{det}$  of group I viruses with pH (Figure 7). It also resembles that of the zeta-potential of quartz as a function of pH (Loveland *et al.*, 1996). The negative charge of quartz decreases from pH 2.3 – 6, and remains minimal at pH values above 6.

MS2 did not adsorb or only poorly in columns with sandy soils at pH 5 – 8 (Bales *et al.*, 1991, 1993; Kinoshita *et al.*, 1993). Detachment was slow, but was enhanced when pH increased. This effect was moderate, because few MS2-particles had attached (Kinoshita *et al.*, 1993). Bales *et al.* (1993) showed that removal of MS2 by attachment to silica beads in columns was much greater at pH 5 than at pH 7. Also, poliovirus 1 attached much more at pH 5.5 than at pH 7. Both viruses detached only slowly. At pH 7, the collision efficiency of

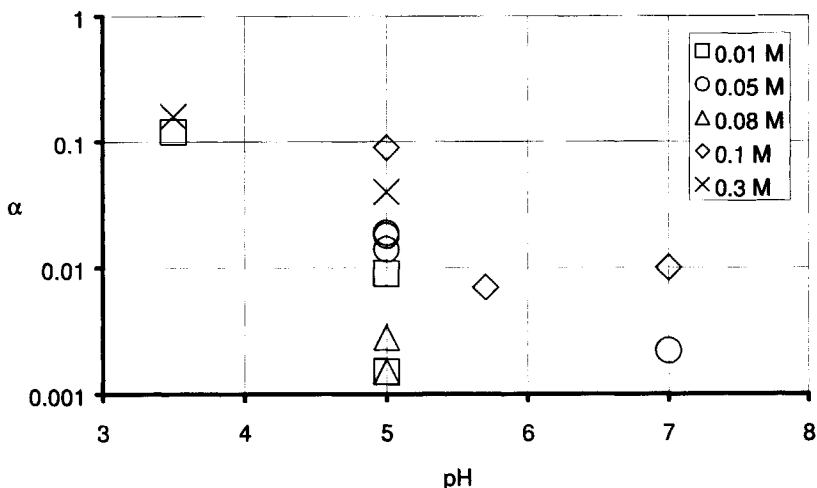


**Figure 8** Collision efficiency  $\alpha$  versus pH of MS2 at different ionic strengths. See also values in Table 3.

poliovirus 1 was 2 – 3 times higher than that of MS2, but almost the same at pH 5 – 5.5. In the study of Penrod *et al.* (1996) removal of bacteriophages MS2 and  $\lambda$  was compared. Although the net surface charge of  $\lambda$  was stronger negative than that of MS2, attachment of  $\lambda$  was more than that of MS2. It was suggested by Penrod *et al.* (1996) that a steric repulsive force exists in case of MS2. This steric repulsive force arises from the hydrophilic polypeptide loops, which extend a maximum of 1 nm off of the MS2 surface. A similar difference in attachment between MS2 and recombinant Norwalk virus particles in quartz bed columns was found by Redman *et al.* (1997). MS2 has a significantly lower pI but a less negative zeta potential at pH  $\geq 7$  than the Norwalk virus particles. Still, MS2 attached less than the Norwalk virus particles at both pH's 5 and 7.

The collision efficiency of PRD1 has also been shown to be pH-dependent. In columns with silica beads at pH 5.5 (Bales *et al.*, 1991),  $\alpha$  for PRD1 was between 0.006 and 0.013, and at pH 7, PRD1 did not adsorb at all (Table 3). Detachment was very slow compared to attachment, but increased strongly at pH 8. In the same study, MS2 attached even less than PRD1. In a sandy aquifer under natural gradient conditions, attached PRD1-phages released rapidly when pH was increased from 5.7 to pH 6 – 8 (Bales *et al.*, 1995). Also, injection with high pH-water in a sandy aquifer, which elevated pH from 7.4 to 8.4, resulted in significant remobilization of attached PRD1-phages (Bales *et al.*, 1997). At pH 8.4, attachment rates decreased by a factor of 2 – 3. Concurrently, the detachment rate coefficient increased by a factor  $10^4$  –  $10^5$  to a value higher than the attachment rate coefficient. In a field study by Ryan *et al.* (1999), it was also shown that an increased pH induced extra detachment of PRD1. This effect was less in a sewage-contaminated zone, where a pH of 8.5 was reached, than in an uncontaminated zone, where a pH of 10 was reached. According to Ryan *et al.* (1999) an increase to pH 8.5 may not exceed the isoelectric point of some ferric oxyhydroxides. It is likely that in the study by Bales *et al.* (1997) phosphate adsorbed to the ferric oxyhydroxides thereby augmenting the charge reversal caused by the pH increase.

**Table 4** Collision efficiencies  $\alpha$  for viruses from field studies.

Virus	Soil	Distance [m]	pH	EC [ $\mu\text{S}/\text{cm}$ ] <sup>a</sup>	$f_{oc}$	$\alpha \times 10^{-3}$	Reference
MS2	Sand / gravel	7.5	7.2	288	-	4-182 <sup>b</sup>	DeBorde
	(Missoula)	19.4	7.2	288	-	4-202 <sup>b</sup>	<i>et al.</i> (1998a)
	Dune sand	2.4	7.3-8.3	900	$1 \times 10^{-3}$	1.4	Schijven
		30	7.3- 8.3	900	$1 \times 10^{-3}$	0.27	<i>et al.</i> (1999)
PRD1	Sand	0.94	7.4	311	$3 \times 10^{-4}$	2.8-3.0	Bales
	(Borden)	0.94	8.4	311	$3 \times 10^{-4}$	0.85-1.6	<i>et al.</i> , 1997
	Sand	1.0	5.0-5.7	60-100	$<1 \times 10^{-4}$	9-13	Pieper
	(Cape Cod)	1.0	6.0-6.7	350-450	$1 \times 10^{-2}$	1.4-2.6	<i>et al.</i> , 1997
	Sand	0.9 – 1.0	5.4-5.6	30-40	$<1 \times 10^{-4}$	$32 \pm 16$	Ryan
	(Cape Cod)	0.9 – 1.0	5.8-6.0	250-330	$1 \times 10^{-2}$	$16 \pm 5$	<i>et al.</i> , 1999
	Sand / gravel	7.5	7.2	288	-	14- 632 <sup>b</sup>	DeBorde
	(Missoula)	19.4	7.2	288	-	5-385 <sup>b</sup>	<i>et al.</i> (1998a)
Dune sand	2.4	7.3-8.3	900	$1 \times 10^{-3}$	2.4	Schijven)	
	30	7.3-8.3	900	$1 \times 10^{-3}$	0.43	<i>et al.</i> (1999)	
$\phi\text{X174}$	Sand / gravel	7.5	7.2	288	-	6-311 <sup>b</sup>	DeBorde
	(Missoula)	19.4	7.2	288	-	7-319 <sup>b</sup>	<i>et al.</i> (1998a)
Polio 1 (CHAT)	Sand / gravel	7.5	7.2	288	-	47-2108 <sup>b</sup>	DeBorde
	(Missoula)	19.4	7.2	288	-	19-866 <sup>b</sup>	<i>et al.</i> (1998a)
FRNAPH's	Dune sand	2	7.3-8.3	900	-	20	Schijven
						(1.5-2.9) <sup>c</sup>	<i>et al.</i> (1998)
		4	7.3- 8.3	900	-	0.78 (0.040- 4.) <sup>c</sup>	

<sup>a</sup>Electrical conductivity as a measure of ionic strength. <sup>b</sup>Corresponding to a range in grain size from 0.00125 – 0.012 m. <sup>c</sup>95% confidence interval.

Also, Loveland *et al.* (1996) clearly showed that at higher pH, attachment of PRD1 is slower and detachment is faster. In this study, in equilibrium non-flowing columns, PRD1 was attached to quartz and ferric oxyhydroxide-coated quartz surfaces over a wide range of pH values. At a pH value of about 2.5 – 3.5 pH units above the isoelectric point of the mineral surfaces, a so-called attachment edge existed. Viruses attached at a pH below this edge were irreversibly attached but were reversibly attached at a pH above this edge. DLVO potential energy calculations showed that the attachment edge occurred at the pH at which the potential energy of the primary minimum was near zero, implying that the position of the primary minimum (attractive or repulsive) controlled the equilibrium distribution of the viruses. Virus attachment to a homogeneous mineral surface is either irreversible or reversible depending on the pH of attachment, but not both (Loveland *et al.*, 1996). But in a heterogeneous medium, minerals may exist to which attachment is irreversible, *e.g.* ferric oxyhydroxide, and minerals to which attachment is reversible, *e.g.*

quartz. This is the case when pH lies between that of the isoelectric points of the two types of sites (Loveland *et al.*, 1996).

From batch studies it has become clear that high pH generally favors free virus and low pH favors attached virus (Gerba, 1984). This has been confirmed in column and field studies for viruses, like MS2 and PRD1 that have low pI's, but also for poliovirus 1 (pI of 6.6), and phage  $\lambda$  (pI of 5). At higher pH, electrostatic repulsion increases, reflected in a higher maximum and a higher primary minimum in the DVLO-profile. This results in a decreased attachment rate and an increased detachment rate. In most aquifers, surface characteristics of the soil are much more heterogeneous than that of the quartz sand in the columns of Loveland *et al.* (1996), and also different viruses may be present that have different pI's. Therefore, dependent on pH and thus on the charge of the virus and soil particles, adsorption of some of these viruses may be irreversible, whereas that of others may be reversible.

### 2.4.5 Effect of Ionic Strength and Multivalent Cations

According to DLVO theory, a higher ionic strength compresses double layers, thereby increasing attachment rates. In batch studies, it was shown that viruses tend to adsorb strongly to various materials at high ionic strength (*e.g.* Lipson and Stotzky, 1983; Grant *et al.*, 1993). In a column study by Penrod *et al.* (1996), it was found that the collision efficiencies of bacteriophages MS2 and  $\lambda$  increase with ionic strength in the range of 0.01 – 0.1 M NaCl at pH 5 (Table 3). A similar increase of  $\alpha$  for MS2 is the case at pH 3.5 (see also Figure 8). A further increase of salt concentration to 0.3 M NaCl has little impact on the collision efficiency of phage  $\lambda$ , but causes a decrease in the value of  $\alpha$  for MS2. The findings of Dowd *et al.* (1998) suggest that more negatively charged viruses attach more than less negatively charged viruses in the case of high concentrations of multivalent cations. Redman *et al.* (1999) studied adsorption of a filamentous bacteriophage, SJC3, in quartz columns at different ionic strengths and cation-valence. SJC3 is a bacteriophage that has been isolated from highly treated wastewater. Experiments were carried out at pH 7, where surface charge of the bacteriophage and the quartz are negative. SJC3 attached more to the quartz when the ionic strength was increased by increasing the concentration of a particular salt from 1 to 100 mM. One exception was observed when using 1 mM NaCl. Contrary to the expectation, removal of the bacteriophage was higher in this case. The authors suggested that at this low concentration of NaCl the filamentous bacteriophage has stiffened. Due to this stiffness, SJC3 may be retained in the column by straining. If DLVO-profiles are repulsive at all separation distances, DLVO-theory predicts increased detachment rates at lower ionic strength (Ryan and Elimelech, 1996). In agreement with this prediction, Gerba and Lance (1978) found that detachment of poliovirus 1 was enhanced by deionized water that was applied to simulate heavy rainfall. Redman *et al.* (1999) also showed that attached particles of bacteriophage SJC3 easily detach when the salt concentration was changed from 1 mM  $\text{CaCl}_2$  to 1 mM NaCl. However, if the DVLO-profile is attractive near the solid surface, DLVO-theory will predict an increasing detachment rate at higher ionic strength (Ryan and Elimelech, 1996). Penrod *et al.* (1996) found that with increasing ionic strength there was a similar increase of both the attachment and detachment rate coefficients. This suggests that in case of the experiments of Penrod *et*

*al.* (1996) forces between the virus and the solid surface were attractive at a very short separation distance.

Multivalent cations can link virus and adsorbents of like charge by forming salt bridges between them (Sobsey *et al.*, 1980; Moore *et al.*, 1982, Lipson and Stotzky, 1983) or by charge reversal (Grant *et al.*, 1993). Bales *et al.* (1991) showed in a batch experiment at pH 5 that attachment of MS2 to silica beads was at least 10 times higher in the presence of  $\text{Ca}^{2+}$  than without  $\text{Ca}^{2+}$ . These effects of multivalent ions are of electrostatic nature. Redman *et al.* (1999) also showed that bacteriophage SJC3 attached more to quartz when the ionic strength was increased by using a multivalent ( $\text{Ca}^{2+}$  or  $\text{Mg}^{2+}$ ), instead of a monovalent ( $\text{Na}^+$ ) cation. In a field study by Bales *et al.* (1997) with the same soil type, pH and velocity as in the column study of Kinoshita *et al.* (1993), PRD1 attached much less than in the column study. Pieper *et al.* (1997) suggested that a possible explanation for the difference might have been the presence of calcium phosphate affecting surface charge in the column study of Kinoshita *et al.* (1993) by cation-bridging or charge reversal. But, as Farrah (1982) showed, calcium phosphate, which is an antichaotropic agent, may also promote hydrophobic interactions.

#### 2.4.6 Effect of Organic Matter

The major occurrence of dissolved and/or suspended organic matter is in the form of humic substances (Shimizu *et al.*, 1998). Commonly, humic substances are, similar to viruses, negatively charged, and hence they compete with viruses for the same binding sites (Gerba, 1984). Among dissolved and/or solid organic matter in the aquifer matrix, humic substances have the highest affinity to non-ionic hydrophobic organic compounds (Ouyang *et al.*, 1996; Shimizu *et al.*, 1998). Other forms of dissolved organic matter consist of proteins, polypeptides and amino acids. From equilibrium batch experiments, it has become clear that dissolved and/or suspended organic matter tends to compete with viruses for attachment sites on the soil surface and thereby reduce virus attachment (Gerba, 1984). Dissolved or suspended organic matter can also be used to elute previously attached viruses (Sobsey *et al.*, 1980). Thus, detachment of viruses may be strongly increased by dissolved or suspended organic matter.

Dizer *et al.* (1984) showed that in sand columns at pH 7, attachment rates of poliovirus 1, coxsackieviruses A9 and B1, echovirus 7 and rotavirus SA11 were the lowest in secondary effluent as compared with groundwater, tertiary effluent and distilled water. Dizer *et al.* (1984) also found that virus attachment to sand in a batch test was reduced by dissolved surfactants. It was suggested that these surfactants disrupted hydrophobic bonds between the sand and the viruses. Such surfactants may also have been present in the secondary effluent, which decreased virus attachment in the columns.

The effect of dissolved organic matter may not always be apparent, *e.g.* if the nature of the soil is more important for adsorption. Gerba and Lance (1978) found that adsorption of poliovirus 1 and its movement through a loamy sand soil was not affected by the high organic matter content of primary sewage effluent (70 mg/l) compared to that of secondary sewage effluent (10 mg/l). According to the authors, the sewage effluent did not saturate adsorption sites, even after 9 days of flooding. Thus, dissolved organic matter has not influenced adsorption of poliovirus 1 because an excess of adsorption sites was available.

Under unsaturated flow conditions, the effect of dissolved organic matter is even more complex. Powelson *et al.* (1991) found that natural humic material and sewage sludge organic matter decreased removal of MS2 in unsaturated columns with loamy sand. On the contrary, in a field study, Powelson *et al.* (1993) found that the effluent type did not affect removal of MS2, whereas PRD1 was removed three times more in secondary treated effluent compared to tertiary treated effluent, which has lower concentrations of dissolved organic matter. Powelson and Gerba (1994) compared behavior of poliovirus 1 and bacteriophages MS2 and PRD1 in columns with a sandy soil under unsaturated conditions with secondary and tertiary effluent, but found no significant influence of the effluent type on removal of any of these viruses.

Similarly, the effect of solid and/or bonded organic carbon content ( $f_{oc}$ ) of the soil is found to be ambiguous. On one hand, a soil with bonded organic carbon has fewer sites for virus adsorption. On the other hand, the bonded and/or solid organic matter may provide hydrophobic adsorption sites in a soil where virus adsorption is otherwise very low. So, the effect depends on the combination of soil type, virus type and nature of organic matter. Gerba *et al.* (1981) carried out a statistical analysis on the batch adsorption data from Goyal and Gerba (1979). Adsorption of group-I viruses (Table 2) was inversely related with pH and with  $f_{oc}$ . Variation in adsorption was explained for 83% by pH and for 12% by  $f_{oc}$ . In batch experiments, Moore *et al.* (1982) observed that adsorption of reovirus 3 to 30 different types of soils and minerals was found to decrease significantly with increasing  $f_{oc}$ . However, when the soil with the highest organic content was omitted from the analysis, there was no significant correlation with  $f_{oc}$ . The authors concluded that  $f_{oc}$  has a significant effect only at high values. The value of  $f_{oc}$  of the organic muck was 3.4%. So, probably, at low  $f_{oc}$ , organic matter does not occupy all adsorption sites for viruses. In another batch study, Moore *et al.* (1981) found a strong negative correlation between  $f_{oc}$  and adsorption of poliovirus 2 to 34 different types of soils and minerals. The authors described that soil organic matter is a weak adsorbent for poliovirus because of its low pI, and therefore, negative charge, and because organic matter exhibits weak van der Waals attraction. They further reasoned that some of the soil organic matter, particularly lower-molecular-weight fractions, is soluble and may pass into solution. The dissolved organic matter may be adsorbed onto other surfaces, and thereby compete for the same binding sites as viruses. On the other hand, in batch studies reported by Burge and Enkiri (1978), adsorption of  $\phi$ X174 to four different kinds of soil was found to increase with increasing  $f_{oc}$ . Nevertheless, adsorption of  $\phi$ X174 to a fifth soil with a much higher  $f_{oc}$  was found to be much lower. According to the authors, this was due to blocking of adsorption sites by organic matter. They did not explain the positive correlation of adsorption with  $f_{oc}$  when considering only the four soils. However,  $f_{oc}$  of these four soils was also negatively correlated with pH. Since the effect of pH on virus adsorption may be expected to be stronger than that of  $f_{oc}$  (Gerba *et al.*, 1981), pH probably acted as a confounder. That is to say, the observed effect on adsorption was rather an effect of increasing pH, than of decreasing  $f_{oc}$ .

An example of cases, where bonded organic material may provide hydrophobic adsorption sites for viruses, is clearly shown by Bales *et al.* (1993). They used columns with negatively charged silica beads at pH 7, which were artificially coated with very small amounts of hydrophobic C<sub>18</sub>-chlorosilane. Attachment of MS2 could be increased considerably by even very small amounts of this bonded hydrophobic organic carbon material (Table 4 and Figure 9). Bales *et al.* (1993) also showed that the binding sites in a

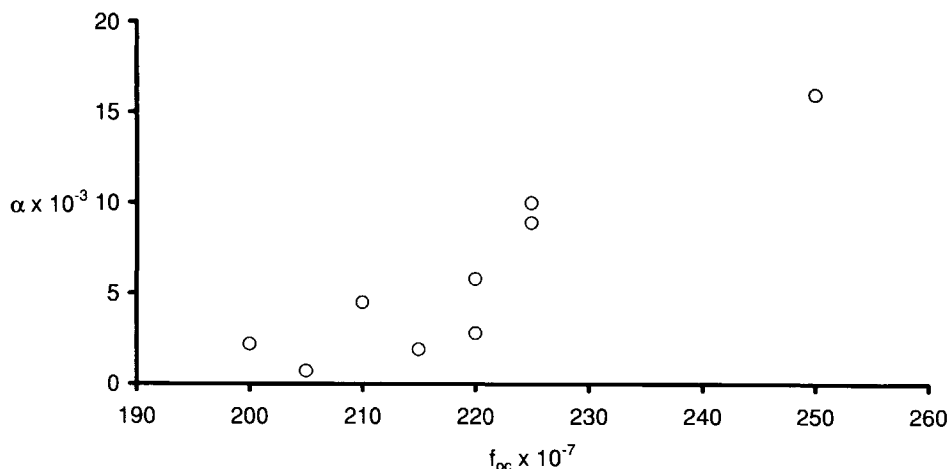


**Figure 9** Collision efficiency  $\alpha$  of MS2 in 15-cm columns of silica beads (pH 7) with an increasing fraction bonded organic matter,  $f_{oc}$  ( $C_{18}$ -chlorosilane). Data from Bales *et al.* (1993). The highest value of  $\alpha$  is actually  $> 0.016$ .

column of silica beads with only 0.00215% bonded  $C_{18}$ -chlorosilane could not be saturated with even 70 pore volumes of  $10^5$  MS2 particles per ml. The concentration of bonded MS2-particles was approximately  $10^7$  pfu/g.

Yet, an opposite effect was observed in a field study by Pieper *et al.* (1997) in a sand and gravel aquifer with positively charged iron-oxide coating. They showed that attachment of PRD1 was less in soil with higher  $f_{oc}$ . They injected  $^{32}P$ -labeled PRD1 into sewage-contaminated ( $f_{oc}$  of 1%) and uncontaminated zones ( $f_{oc} < 0.01\%$ ) of the aquifer (see also data in Table 4). In the contaminated zone, only 42% of PRD1 attached over the first meter whereas in the uncontaminated zone 83% removal was found. Corresponding estimates of collision efficiencies were found to be about 6 times smaller in the contaminated zone than in the uncontaminated zone. Injection of Linear Alkylbenzene Sulfonates (LAS) remobilized 87% of attached PRD1 in the contaminated zone, but only 2.2 % in the uncontaminated zone. The authors suggested that LAS caused charge reversal of ferric oxyhydroxide coatings on the soil surface to which PRD1 was attached. They reasoned that the injected amount of LAS was insufficient to cause this charge reversal in the uncontaminated zone. However, removal of LAS itself in both zones was similar (12 – 14%), which implies that this explanation is probably not correct. In another study at the same field site, Ryan *et al.* (1999) showed that anionic surfactant dodecylbenzenesulfonate (DBS) was also much more effective at mobilizing PRD1 in the contaminated zone than in the uncontaminated zone. They argued that abundant organic matter in the contaminated zone reduced the amount of DBS needed to reverse the charge of ferric oxyhydroxides. Their results suggested that PRD1 attached strongly attached in the uncontaminated zone. Another explanation is that PRD1 in the uncontaminated zone primarily attached to sites with ferric oxyhydroxide coatings, whereas these sites were already taken by organic matter in the contaminated zone. Therefore, attachment of PRD1 in the contaminated zone may have been mainly through hydrophobic interactions with bonded organic matter. This kind of attachment is weaker than attachment to sites of positively-charged iron oxides (Moore

*et al.*, 1981). Thus, it may be reasoned that in the study by Pieper *et al.* (1997) and Ryan *et al.* (1999), injected LAS and DBS, respectively, increases detachment of PRD1 in the contaminated zone much more than in the uncontaminated zone by disrupting hydrophobic bonds between the soil and PRD1. This mechanism is consistent with the suggestion of Dizer *et al.* (1984), that surfactants can disrupt hydrophobic bonds (see also Gerba, 1984). In the vicinity of a hydrophobic site, one may expect less electrostatic repulsion, especially if that site consists of bonded polymeric organic matter. Such polymers may interact in two ways: by steric hindrance or by forming bridges between surfaces. According to Ryan and Elimelech (1996), surfactant attachment may cause colloid release by some "non-DLVO" force like steric repulsion.

To summarize this section on the effect of organic matter, dissolved organic matter may compete for the same binding sites as viruses and because they are usually present in higher concentrations than viruses, they can decrease virus attachment. Dissolved organic matter, like surfactants, may also disrupt hydrophobic bonds between soil and virus, resulting in an increased detachment rate. At the same time, viruses and many organic materials contain hydrophobic groups on their surfaces. Therefore, once adsorbed, organic matter may provide hydrophobic binding sites for viruses. Also, the presence of solid organic matter may result in an increased attachment rate through hydrophobic binding. The hydrophobic adsorption effect will be most pronounced in soil with negatively charged grain surfaces. The enhancing and attenuating effects of organic matter on adsorption of viruses and their dependence on soil and virus properties makes their quantification very difficult, especially under field conditions. Effects of organic matter are, probably, responsible for considerable uncertainty in predicting virus removal.

## 2.5 Virus Inactivation

### 2.5.1 Introduction

In Equations 3 and 4 virus inactivation was described by the inactivation rate coefficients  $\mu_f$  and  $\mu_s$  of respectively free and attached viruses. Modeling of the inactivation of free viruses is described in section 2.5.2. Section 2.5.3 discusses the modeling of  $\mu_s$  in a batch suspension with soil. In section 2.5.4, modeling of virus inactivation during subsurface transport is discussed.

### 2.5.2 Virus Inactivation in Water

Virus inactivation is usually assumed to follow first-order kinetics, as in Equations 3 and 4. But non-linear inactivation curves, resulting from external and internal factors, have also been found. External factors that influence virus inactivation are the environmental factors that will be discussed in section 2.6 and affect the population of viruses as a whole. Hurst *et al.* (1992) analyzed the effects of different environmental factors on virus inactivation by means of different regression equation formats and evaluated these formats. Hurst *et al.* (1992) considered environmental factors such as temperature, conductivity and turbidity of the water, ability to support bacterial growth. According to Hurst *et al.* (1992), virus inactivation is not first-order, but a time-dependent process.

Internal factors that influence virus inactivation may be the presence of virus aggregates or the existence of significant variations in sensitivities among the virus population to the factors that cause inactivation (Yates *et al.*, 1987). Grant (1994) presented a mathematical model for first order inactivation of total infectious units of viruses, including Brownian coagulation of virions. This model predicted that virion-virion coagulation is negligible in most aquatic environments because virus concentrations are too low or because inactivation occurs too quickly. The predicted coagulation in highly concentrated laboratory suspensions was too high also, because laboratory studies had indicated that at neutral or alkaline pH coagulation of poliovirus was minimal. Grant (1994) reasoned that to the extent that viral aggregates actually exist in aquatic environments, they are probably formed intracellularly and not by coagulation outside the host cell. Furthermore, in aquatic environments, virus aggregates may be dispersed by changes in solution chemistry. Grant (1995) also developed a kinetic model for the inactivation of viruses that exhibit a range of initial aggregate sizes. Aggregates of viruses are assumed to be more resistant to inactivation because all virus-particles within an aggregate must be inactivated before the aggregate as a whole is considered inactive. Also, undamaged components of inactive virus-particles within an aggregate may recombine by a process called multiplicity reactivation (MR). Grant's kinetic model successfully fitted experimental data from a study on inactivation of vaccinia virus. Usually data on inactivation of individual virus particles, as well as the level of initial aggregation and the number of active components per virus particle needed for MR are not available, but in this study on the inactivation of vaccinia virus they were. The model correctly predicted the relatively slow inactivation that was observed for the aggregated suspension. None of the models of Grant (1994; 1995) address higher order inactivation, due to variation in individual viruses within a population of viruses, association with other types of viruses, or association with other non-viral organic or inorganic material. These associations, however, are known to be important (see section 2.6.3).

Grant *et al.* (1993) showed a biphasic decline of the logarithmic concentration with time of phage  $\lambda$ , indicating that a population of phage  $\lambda$  consists of two subpopulations with different sensitivity towards inactivation. Rossi (1994) argued that such a biphasic course of inactivation was possibly caused by interaction of virus particles with the walls of the synthetic vials that were used. He showed that this was the case for phage T7, but in a glass vial its inactivation was first order. He also mentioned the existence of very fine colloidal clay particles, to which the viruses were attached, as a possibility that may have caused non-linear inactivation.

### 2.5.3 Virus Inactivation in Water with Soil

According to Grant *et al.* (1993) batch experiments involving viruses and soil are fundamentally non-equilibrium systems, because viruses will also disappear from the liquid phase by inactivation. Inactivation of viruses that are attached to soil may proceed at a different rate than that of free viruses. Grant *et al.* (1993) developed a numerical model that enables estimation of  $k_{att}$ ,  $k_{det}$ ,  $\mu_1$  and  $\mu_s$  for viruses in a batch suspension with soil and demonstrated this for phage  $\lambda$ . No other study has been reported where values of each of  $k_{att}$ ,  $k_{det}$ ,  $\mu_1$  and  $\mu_s$  were estimated by kinetic analysis of batch experiments. In a batch system, viruses are subject to adsorption and inactivation, simultaneously. Depending on

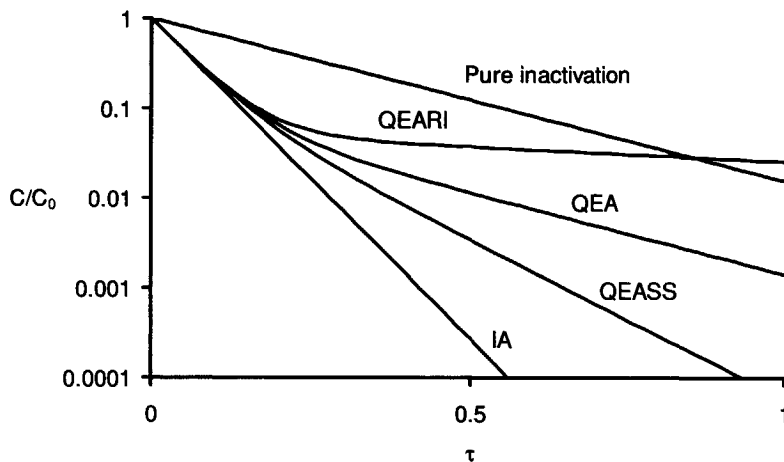


**Figure 10** Semilog-plot showing four possible kinetic behaviors in a batch suspension of viruses with soil compared to pure inactivation of viruses in a suspension without soil (Grant *et al.*, 1993).  $C/C_0$  is reduced concentration of viruses in aqueous phase;  $\tau$  is nondimensional time. See section 2.5.3 for explanation of behaviors. QEA:  $\mu_s = \mu_i$ ; QEARI:  $\mu_s < \mu_i$ ; QEASS:  $\mu_s > \mu_i$ ; IA:  $k_{det} = 0$ .

the relative strength of these processes, Grant *et al.* (1993) distinguished the following four possible behaviors (Fig 10):

1. Quasi-equilibrium adsorption (QEA) is the case, when virus inactivation is not influenced by the presence of a solid, thus the inactivation rate coefficient of detached viruses equals that of attached viruses ( $\mu_i = \mu_s$ ).
2. Quasi-equilibrium adsorption and reduced inactivation (QEARI) is observed when virus particles that are attached to solid materials inactivate slower than those in the aqueous phase ( $\mu_s < \mu_i$ ).
3. Quasi equilibrium adsorption and surface sink (QEASS) is the case when the solid surface acts like a sink for virus particles if virus inactivation is either accelerated in the presence of the surface ( $\mu_s > \mu_i$ ), or a portion of reversibly attached viruses become irreversibly attached with time. These two possibilities are indistinguishable.
4. Irreversible attachment (IA) is observed when viruses are attached irreversibly directly from solution ( $k_{det} = 0$ ). The curves for IA and pure inactivation have the same intercepts, but the slope of the IA-curve is steeper (Figure 10).

There is another way of examining inactivation rate coefficients from batch experiments, as demonstrated by Rossi (1994) and Formentin *et al.* (1997). Viruses that are attached to clay particles, are still capable of infecting their host, and thus can still be enumerated. In such batch experiments with clay particles, it is thus possible to count the total number of viruses, *i.e.* the number of attached and free viruses together from samples taken at different times. By subtracting the counted number of free virus particles from that of the total number, the number of attached infectious virus particles is obtained. In this way, inactivation of free and attached viruses can be followed and compared directly.

Commonly in batch studies, only the free virus concentration is measured with time. Several of such studies exist that have compared inactivation of viruses in a batch suspension with and without soil added (Sobsey *et al.*, 1980, 1986; Nasser *et al.*, 1993; Gantzer *et al.*, 1994; Blanc and Nasser, 1996; Sakoda *et al.* 1997). From the data of these studies it is still possible to calculate a value of  $\mu_s$ . In these studies, percentage of adsorption and the decay rate of the free virus concentration in the suspension with soil,  $\mu_{eff}$ , were measured. The value of this decay rate lies between that of  $\mu_l$  and  $\mu_s$ . In these studies, an apparent equilibrium was reached within a short period of time, whereas inactivation was measured over a much longer period of time. Therefore, it is possible to calculate  $\mu_s$  from the ratio  $k_{att}/k_{det}$ ,  $\mu_l$  and  $\mu_{eff}$ . Applying Equation 10, but eliminating the terms for dispersion and advection, and substituting Equations 9, 2 and Equation 16 gives:

$$R \frac{dC}{dt} = -(\mu_l + (R-1)\mu_s) C \quad (25)$$

This equation has the following solution:

$$C = C_0 \exp\left[-\frac{\mu_l + (R-1)\mu_s}{R} t\right] \quad (26)$$

Now,  $\mu_s$  can be calculated as follows:

$$\mu_s = (R\mu_{eff} - \mu_l)/(R-1), \text{ where } \mu_{eff} = -\frac{1}{t} \ln\left(\frac{C}{C_0}\right) \quad (27)$$

Values of  $\mu_s$ , calculated using Equation 27 from the batch studies of Sobsey *et al.* (1980, 1986) and Blanc and Nasser (1996), are presented and evaluated in section 2.6.

#### 2.5.4 Virus Inactivation under Transport Conditions

Several virus transport models have been developed that incorporate constant first-order inactivation of free ( $\mu_l$ ) and attached ( $\mu_s$ ) viruses (Chrysikopoulos and Sim, 1996; Sim and Chrysikopoulos 1995, 1996, 1998; Toride *et al.*, 1995). Also, models exist that do not distinguish between inactivation of free and attached viruses (Park *et al.*, 1994, 1995; Tim and Mostaghimi, 1991; Yates *et al.*, 1986; Yates and Ouyang, 1992; Yates and Yates, 1987; 1988). Based on the existence of two or more subpopulations of viruses in a suspension with different inactivation rate coefficients, Sim and Chrysikopoulos (1996) also developed a transport model, incorporating kinetic reversible adsorption and different time-dependent inactivation rate coefficients for suspended and attached viruses. The multiphasic sequential inactivation was approximated by a pseudo first-order expression with a time-dependent inactivation rate coefficient. This way, inactivation of viruses in some batch studies was simulated better. Model simulations showed that this approximation of virus inactivation implies extended survival of viruses, and consequently more distant migration. This, more sophisticated way of modeling virus inactivation during subsurface transport under

saturated conditions may also be useful when considering heterogeneous populations of different viruses that exhibit multiphase inactivation.

The contribution of virus inactivation to the removal of virus under unsaturated conditions is much greater. Furthermore, daily fluctuations in temperature in the upper unsaturated soil layers are considerable. Therefore, Yates and Ouyang (1992) developed a model (VIRTUS) that simultaneously describes the transport of water, heat and viruses through the unsaturated zone of the soil. VIRTUS was only tested with data from one unsaturated column experiment (Powelson *et al.*, 1990), where model predictions were close to measured breakthrough concentrations. The temperature-dependent inactivation rate capabilities of the model were not tested, simply because experiments were carried out at constant temperature.

In experiments with saturated columns, inactivation of viruses is usually insignificant, and therefore, neglected within the time scale of the experiment (Bales *et al.*, 1989, 1991, 1993; Dowd *et al.*, 1998; Jin *et al.*, 1997; Penrod *et al.*, 1996; Redman *et al.*, 1997). At field-scale, virus inactivation may be significant because of much longer timescales. To date, the field study by Schijven *et al.* (1999), is the only field study where both  $\mu_1$  and  $\mu_s$  were estimated (Table 8). The inactivation rate coefficient  $\mu_1$  for MS2 and PRD1 was estimated from inactivation rates in suspensions with recharge water from the field. The inactivation rate coefficient  $\mu_s$  for each of these phages could be estimated from the slope of the tails of the breakthrough curves (Figure 3).

## 2.6 Factors affecting Virus Inactivation in the Subsurface

### 2.6.1 Introduction

Viruses lose their ability to infect host cells with time by inactivation. Viruses are inactivated because of disruption of coat proteins and degradation of nucleic acids (Gerba, 1984). The factors that influence inactivation of viruses have already been reviewed by Yates *et al.* (1987). They mention three reports on inactivation rates for viruses in groundwater (Keswick *et al.*, 1982; Bitton *et al.*, 1983; Yates *et al.*, 1985). Since then a number of new studies have been carried out. Table 5 shows an inventory of the values of  $\mu_1$  for viruses in groundwater and sewage water from several studies. Table 6 gives an inventory of  $\mu_s$ -values that were calculated using Equation 27 and data from the studies of Sobsey *et al.* (1980, 1986) and Blanc and Nasser (1996). In some cases, the value of  $R\mu_{\text{eff}}$  was less than that of  $\mu_1$ . This would result in an estimate for  $\mu_s$  of less than zero, which is unrealistic. These estimates were, therefore, omitted. Possibly, the value of the ratio  $k_{\text{air}}/k_{\text{det}}$  was higher than measured. This implies that equilibrium was not reached in these cases, because adsorption was too slow. As already pointed out in section 3.3, this leads to an underestimation of the ratio  $k_{\text{air}}/k_{\text{det}}$ , and thus of R.

Inactivation is usually regarded as a first order process (see section 2.5). The most important factors that influence virus inactivation rates are temperature, adsorption to particulate matter and soil, unsaturated conditions and microbial activity. These factors are discussed in the following sections.

Effects of other factors are found to be of insignificant importance, although some exceptions are reported. Yates *et al.* (1985) found that pH, ammonia, calcium hardness, magnesium hardness, total hardness, nitrate, total dissolved solids and turbidity did not

**Table 5** Inactivation rate coefficient  $\mu_i$  [ $\text{day}^{-1}$ ] of viruses in groundwater and wastewater.

°C	Water	MS2	FRNAPH	PRD1	Polio 1	Echo 1	HAV	Reference
4	GRW	0.063						<i>Yates et al. (1985)<sup>b</sup></i>
7	GRW	0.0058		0.01				<i>Yahya et al. (1993)</i>
7	GRW	0.10		0.10				
10	GRW	0.11		0.025	0.11		0.19	<i>Blanc and Nasser (1996)</i>
10	GRW <sup>a</sup>				0.010			<i>Matthess et al. (1988)</i>
10	GRW-deionized				0.032			
10	GRW				0.013			
10	GRW		0		0		0.10	<i>Nasser et al. (1993)</i>
10	PE <sup>a</sup>		0		0.046		0.17	
10	PE		0.031		0.0077		0.12	
10	SE	0.077		0.054	0.03			<i>Blanc and Nasser (1996)</i>
10	TE	0.091		0.051	0.11		0.17	
12	GRW	0.16			0.18	0.24		<i>Yates et al. (1985)<sup>b</sup></i>
13	GRW	0.22			0.20	0.25		<i>Yates et al. (1985)<sup>b</sup></i>
16	GRW (5.4 mg/l O <sub>2</sub> )				0.21			<i>Jansons et al. (1989b)</i>
16	GRW (0.2 mg/l O <sub>2</sub> )				0.069			
17	GRW	0.18			0.31	0.28		<i>Yates et al. (1985)<sup>b</sup></i>
20	GRW		0.0077		0.038		0	<i>Nasser et al. (1993)</i>
20	PE <sup>a</sup>		0.038		0.077		0.15	
20	PE		0.084		0.14		0.15	
20	SE <sup>a</sup>				0.054			<i>Sobsey et al. (1980)</i>
20	SE				0.14			
22	GRW (0.06 mg/l O <sub>2</sub> )				0.16			<i>Jansons et al. (1989)</i>
22	GRW				0.10			<i>Bitton et al. (1983)</i>
23	GRW	0.36		0.035	0.17		0.18	<i>Blanc and Nasser (1996)</i>
23	GRW	1.3		0.12				<i>Yahya et al. (1993)</i>
23	GRW	0.58		0.30				
23	GRW	0.73			1.2	0.92		<i>Yates et al. (1985)<sup>b</sup></i>
23	SE	0.38		0.18	0.23		0.025	<i>Blanc and Nasser (1996)</i>
23	TE	0.28		0.069	0.15			
25	GRW <sup>a</sup>						0.082	<i>Sobsey et al. (1986)</i>
25	GRW						0.33	
25	PE <sup>a</sup>				0.10	0.10	>	
							0.055	
25	PE				0.33	0.33	0.055	
25	SE <sup>a</sup>				0.13	0.082	0.055	
25	SE				0.13	0.13	0.073	
30	GRW		0.031		0.12		0.054	<i>Nasser et al. (1993)</i>
30	PE*		0.038		0.12		0.20	
30	PE		0.015		0.21		0.18	

**Table 5 (continued)** Inactivation rate coefficient  $\mu$  [ $\text{day}^{-1}$ ] of viruses in groundwater and wastewater.

°C	Water	Reo 3	CA9	CB1	Echo 5	Echo 6	Echo 7	Echo 11	Echo 24	Reference.
10	GRW <sup>a</sup>	0.019	0.012			0.032				<i>Matthess et al. (1988)</i>
10	GRW	0.027	0.019			0.019				
10	GRW-deionized	0.031	0.040			0.038				
16	GRW (2.3 mg/l O <sub>2</sub> )						0.23			<i>Jansons et al. (1989b)</i>
16	GRW (1.6 mg/l O <sub>2</sub> )							0.12		
19	GRW (1.2 mg/l O <sub>2</sub> )				0.12					
20	SE <sup>a</sup>	0.12								<i>Sobsey et al. (1980)</i>
20	SE	0.51								
22	GRW (0.2 mg/l O <sub>2</sub> )							0.25		<i>Jansons et al. (1989b)</i>

°C = temperature; GRW = groundwater; PE, SE, TE = primary, secondary and tertiary effluent; <sup>a</sup>sterilized. <sup>b</sup>Average values

**Table 6** Inactivation rate coefficient  $\mu_s$  of viruses in water with soil.

		Water °C	$k_{att}/k_{det}$	$\mu_s$	$\mu_s$	$k_{att}/k_{det}$	$\mu_s$	$\mu_s$	$k_{att}/k_{det}$	$\mu_s$	$\mu_s$
<i>Sobsey et al. (1980)</i>			<i>Polio 1</i>			<i>Reo 3</i>					
			<u>nst</u>		<u>st</u>	<u>nst</u>		<u>st</u>			
Lakeland sand	SE	20	3.2	0.086	0.022	1.2	-	0.037			
Ponzer muck	SE	20	0.5	1.2	0.65	12	0.25	0.024			
Bentonite	SE	20	2.3	0.12	0.056						
Kaolinite	SE	20	99	0.093	0.048						
<i>Sobsey et al. (1986)</i>			<i>Polio 1</i>			<i>Echo 1</i>			<i>HAV</i>		
			<u>nst</u>		<u>st</u>	<u>nst</u>		<u>st</u>	<u>nst</u>		<u>st</u>
FM sand	GRW	25							0.47	0.38	0.18
	SE	25	5.7	0.23	0.063	0.042	0.95	-	0.39		
	PE	25	99	0.13	0.16	0.064	-	0.29	3.0		
Corolla sand	GRW	25							0.064	1.0	0.51
	SE	25	0.52	0.71	0.021	0.031	0.13	0.082	0.064		
	PE	25	0.72	0.068	0.39	0.042	-	0.39	0.12		
Ponzer muck	GRW	25	0.11	2.2	1.6	0.087	2.1	1.6	0.69		
	SE	25	0.075			0.075			0.30		
	PE	25	0.16	-	0.96	0.12	-	0.20	0.22	0.21	
Bentonite	GRW	25							0.39		
	SE	25	0.087	-	-	0.15	0.38	-	0.56		
	PE	25	0.32	-	0.15	1.5	-	0.15	0.72		
Kaolinite	GRW	25							99		
	SE	25	99	0.33	0.065	99	0.13	0.060	99	0.066	0.066
	PE	25	99	0.22	0.094	0.087	0.33	-	0.56		
Cecil sandy clay	GRW	25	99	0.074	0.083	99	0.17	0.13	99		
	SE	25	99			99			99		
	PE	25	99	0.092	0.064	99	0.16	0.22	99		
<i>Blanc and Nasser, 1996</i>			<i>Polio 1</i>			<i>MS2</i>			<i>PRD1</i>		
			<u>nst</u>		<u>st</u>	<u>nst</u>		<u>st</u>	<u>nst</u>		<u>st</u>
Loamy sand	GRW	10	199	0.03		0.18	0.17		4.8	0.07	
		23		0.16			0.46			0.15	
	SE	10	142	0.03		0.18	0.27		15	0.09	
		23		0.17			1.34			0.12	
Sand	GRW	10	3.5	0.019		11	0.30		37	0.030	
		23		0.022			0.44			0.081	
	SE	10	0.38	0.013		3.3	0.16		199	0.088	
		23		0.014			0.64			0.13	

GRW = groundwater; SE = secondary effluent; PE = primary effluent, nst = not sterilized, st = sterilized.

significantly affect inactivation of MS2, poliovirus 1 and echovirus 1. Inactivation of MS2, however, increased significantly with calcium hardness. Mathess *et al.* (1988) reported that the inactivation rates of coxsackievirus A9 and B1, echovirus 7 and poliovirus 1 were larger in deionized than untreated groundwater. The type of water (groundwater, secondary and primary effluent) was not found to significantly affect inactivation rates of poliovirus 1, echovirus 1, HAV, MS2 and PRD1 (Sobsey *et al.*, 1986; Blanc and Nasser, 1996). But Nasser *et al.* (1993) found a greater value of  $\mu_1$  of poliovirus 1, HAV and F-specific RNA bacteriophages (FRNAPH's) in primary effluent than in groundwater.

### 2.6.2 Effect of Particulate Matter and Soil on Virus Inactivation

Viruses in the environment are often associated with particulate matter or other surfaces and this has a major effect on their inactivation and transport in the environment (Gerba, 1984). Adsorption to organic matter or clays, like kaolinite and montmorillonite, or aggregation in the environment has been demonstrated for bacteriophages T2 (Gerba and Schaiberger, 1975), T7 (Bitton and Mitchell, 1974) and f2 (Armon and Cabelli, 1988) and for poliovirus 1 (Landry *et al.*, 1983; Metcalf *et al.*, 1984) and poliovirus 2 (Moore *et al.*, 1981). Natural colloids, which are usually defined by their size of 1 – 1000 nm, are present in relatively large concentrations (ranging from  $10^8$  –  $10^{17}$  particles per liter) in waters of diverse geological environments (Swanton, 1995). Gerba *et al.* (1978) found that in treated sewage effluent, the largest quantity of solid-associated coliphages are attached to particles greater than 8.0  $\mu\text{m}$  and less than 0.65  $\mu\text{m}$ . But, Hejkal *et al.* (1981) indicated that in treated wastewater the majority of enteric viruses are free or attached to particles smaller than 0.3  $\mu\text{m}$ . Metcalf *et al.* (1984) also showed that enteroviruses and rotaviruses in estuarine water adsorb preferentially to particles smaller than 0.3  $\mu\text{m}$  in diameter. Particles less than 0.3  $\mu\text{m}$  include clays, cell fragments, waste products and other miscellaneous debris (Levine *et al.*, 1985). Furthermore, Payment *et al.* (1988) showed that in river water 77% of indigenous enteric viruses and 66% of coliphages were probably free or associated with particles with a diameter of less than 0.25  $\mu\text{m}$ . Thus, a substantial fraction of viruses is attached to wastewater effluent solids and other colloidal particles with a size of less than 0.3  $\mu\text{m}$ .

Virus association with solids in natural waters has been observed to generally reduce virus inactivation, but some exceptions have been reported, too (Gerba, 1984). Reduced inactivation due to adsorption to suspended matter or marine sediment in sewerage or estuarine water has been reported for poliovirus 1, echovirus 1, coxsackieviruses A9 and B3, rotavirus SA11, HAV, F-specific bacteriophages and phages of *Bacterioides fragilis* (Smith *et al.*, 1978; Liew and Gerba, 1980; Metcalf *et al.*, 1984; Rao *et al.*, 1984; Chung and Sobsey, 1992; Gantzer *et al.*, 1994). Mathess *et al.* (1988) showed that addition of sand to groundwater at 10 °C reduced the inactivation rate of coxsackievirus B1, but the inactivation rates of coxsackievirus A9 and echovirus 7 were not affected by the addition of sand. Grant *et al.* (1993) showed a reduced inactivation of phage  $\lambda$  in a batch suspension with Ottawa sand at pH 10, but not at pH 5 or 7. Sakoda *et al.* (1997) also reported significantly reduced inactivation of bacteriophages MS2 and Q $\beta$  in PBS (pH 7.2) by addition of cellulose, DEAE-cellulose, cellulose phosphate, kaolin, carbon, suspended solids and sediment from a river.

In some studies increased inactivation in the presence of soil was reported. Sobsey *et al.* (1980) found this for poliovirus 1 in Ponzer muck. Blanc and Nasser (1996) reported this

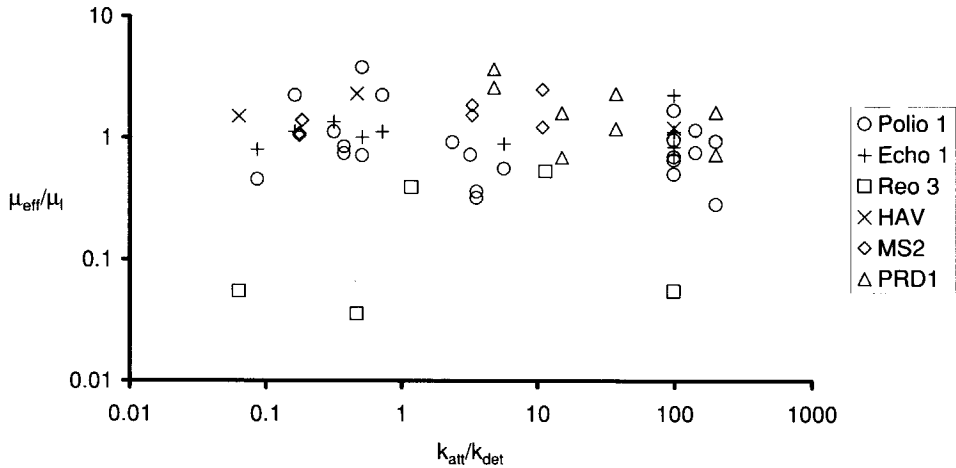


**Figure 11.** Reduction factor for inactivation rate  $\mu_{eff}/\mu_i$  versus  $k_{att}/k_{det}$  for viruses in a batch system with soil.

for MS2 and PRD1 in sand and loamy sand. In the study of Formentin *et al.* (1997), it was observed that bacteriophage  $\phi 1$ , a filamentous phage with a length of 100 nm, attached massively to attapulgite and was subsequently inactivated more rapidly. In this study, it was found that concentrations of free and attached MS2 particles increased after the addition of attapulgite. Possibly, existing aggregates of MS2 disintegrated when attachment to attapulgite took place.

Reduced inactivation was found to be more pronounced in case of stronger attachment, especially to clays (Hurst *et al.*, 1980). Babich and Stotzky (1980) found that in the presence of clay minerals the inactivation rate of phage  $\phi 11M15$  in natural lake water was greatly reduced, with the sequence of protection being attapulgite > vermiculite > montmorillonite > kaolinite. Whether reduced inactivation in the presence of clay will be observed or not may also depend on its concentration. Gerba and Schaiberger (1975) did not find any increase in the survival duration of phage T2 in the presence of low kaolinite concentrations in natural seawater. Also, Gantzer *et al.* (1994) showed that the inactivation rate of poliovirus 1 in seawater was not significantly reduced in the presence of low concentrations of montmorillonite (3 and 15 mg/l) compared to that without this clay. These low concentrations of montmorillonite represent the density of suspended matter in a natural seawater. However, with 500 mg/l of clay, virus inactivation was significantly less. In Figure 11, the ratio  $\mu_{eff}/\mu_s$  is plotted as a function of the ratio  $k_{att}/k_{det}$  using the data from the studies that are summarized in Table 6. Within this context, a value of  $\mu_{eff}/\mu_i$  of less than one defines reduced inactivation (see Equation 27). It appears that inactivation of poliovirus 1, echovirus 1 and HAV is usually reduced but in some cases enhanced, independent of  $k_{att}/k_{det}$ . Inactivation of reovirus 3 is reduced in all cases, but that of MS2 is enhanced in all cases, and that PRD1 is enhanced in most cases. In Figure 12,  $\mu_s$  is plotted as a function of the ratio  $k_{att}/k_{det}$  using the data from Table 6. It also seems that  $\mu_s$  is independent of  $k_{att}/k_{det}$ . But at values of  $k_{att}/k_{det} < 1$ ,  $\mu_s$  for poliovirus 1, echovirus 1 and MS2 shows more variation and can be relatively high. For values of  $k_{att}/k_{det} > 1$ ,  $\mu_s$  is generally less than about 0.25 day<sup>-1</sup> for all viruses that are shown here. The data from Figures 11 and

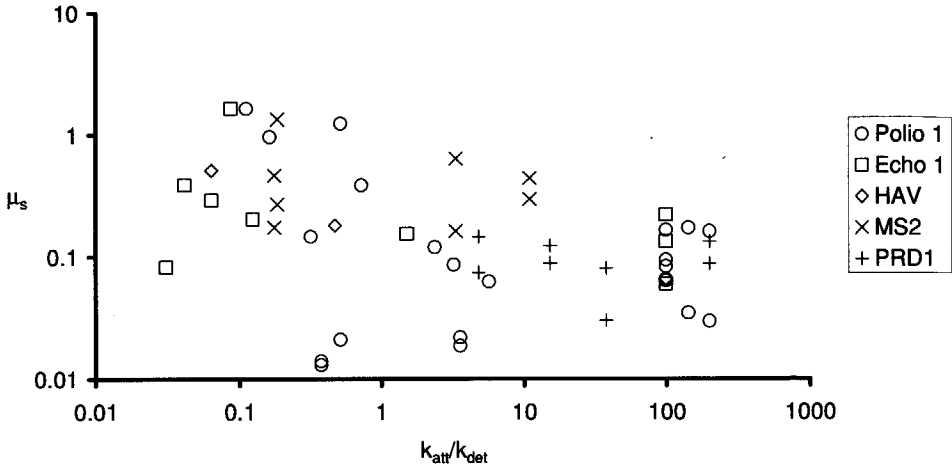


**Figure 12** Inactivation rate coefficient  $\mu_s$  versus  $k_{att}/k_{det}$  for viruses in a batch system with soil.

12 suggest that reduced or enhanced inactivation is very much virus-type specific, and almost independent of  $k_{att}/k_{det}$ . Gerba (1884) mentioned that reduced inactivation may be the result of protection from proteolytic enzymes or other virus-inactivating substances, increased stability of the virus capsid when attached, prevention from aggregate formation, and blocking from ultraviolet radiation. The latter is of importance in surface waters. Sakoda *et al.* (1997) suggested that attachment of viruses onto a solid surface prevents them from swelling, and subsequent activity loss.

In the studies analyzed above, the batch suspension was not agitated continuously. Therefore, a protection against forces along the air-water interface probably does not play a role. This may, however, play a significant role, depending on the degree of agitation (see section 2.6.5). In the cases where virus inactivation in the presence of soil was enhanced, presumably this may have been caused by the attachment and detachment processes. Viruses may be degraded because of attachment to sites with metal oxides (Gerba, 1984).

Two field studies exist where virus inactivation was investigated during subsurface transport under saturated conditions. In a field study by Schijven *et al.* (1999),  $\mu_1$  for free MS2-particles ( $0.03 \text{ day}^{-1}$ ) was found to be three times less than  $\mu_s$  for attached MS2-particles ( $0.09 \text{ day}^{-1}$ ), whereby attachment was very low. This observation is consistent with the analysis from batch experiments with MS2 (Figure 11), that generally showed enhanced inactivation of MS2 in the presence of soil. In case of PRD1, the estimate of  $\mu_1$  was not clear, but was likely less than that of  $\mu_s$  ( $0.07 \text{ day}^{-1}$ ). On the other hand, DeBorde *et al.* (1998) found indications for reduced inactivation of MS2 and  $\phi$ X174 during subsurface transport at field scale. Inactivation was followed for about one half year ( $6 - 12 \text{ }^\circ\text{C}$ ). In enclosed tubes,  $\mu_1$  for MS2 and  $\phi$ X174 were about  $0.06$  and  $0.03 \text{ day}^{-1}$ , respectively. The tails of the breakthrough curves declined slower in time, *i.e.*  $0.016 \text{ day}^{-1}$  for MS2 and negligible for  $\phi$ X174. There is no clear explanation for the difference between the two field studies, where both enhanced and decreased inactivation of attached viruses under transport conditions were observed.

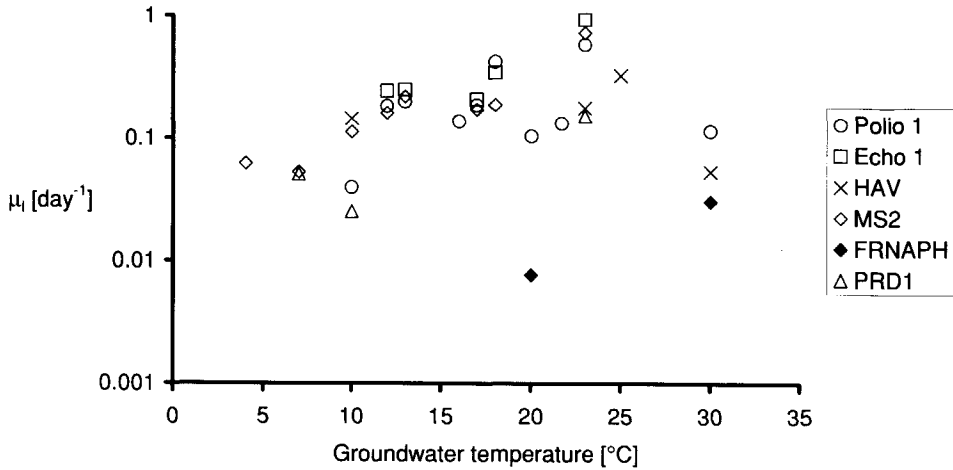


**Figure 13** Inactivation rate coefficient  $\mu_1$  versus temperature for viruses in non-sterilized groundwater from different studies. See values in Table 5 and parameters of regression analysis in Table 7.

**Table 7** Regression analysis of  $\ln(\mu_1)$  for viruses with groundwater temperature ( $T$ , °C).

Equation:  $\ln(\mu_1) = aT + b$

	Polio 1	Echo 1	HAV	MS2	FRNAPH's	PRD1
Number of observations	10	5	4	8	2	3
Slope $a$	0.033	0.12	-0.024	0.12	0.14	0.09
Intercept $b$	-2.4	-3.0	-1.4	-3.5	-7.6	-4.0
Correlation coefficient	7%	71%	8%	85%	100%	71%

### 2.6.3 Effect of Temperature

Temperature is the most important factor that influences virus inactivation (Hurst *et al.*, 1980; Yates *et al.*, 1985, 1987). Inactivation rates increase with temperature (Hurst *et al.*, 1980; Yates *et al.*, 1985; Jansons *et al.*, 1989b; Nasser *et al.*, 1993; Yahya *et al.*, 1993; Blanc and Nasser, 1996). Figure 13 shows how  $\mu_1$  for MS2, F-specific RNA bacteriophages, PRD1, poliovirus 1, echovirus 1 and HAV changes with temperature in non-sterilized groundwater. This figure was constructed using the data from Table 5. Regression analysis suggest an exponential dependence of  $\mu_1$  on temperature in the form:

$$\ln \mu_1 = aT + b \quad (28)$$

Values of coefficients  $a$  and  $b$  for six different viruses are given in Table 7. Here, it should be noted that this analysis was based on only a few data for FRNAPH's and PRD1, therefore the values for these viruses are only indicative. Clearly, the temperature sensitivity of  $\mu_1$  depends on the type of virus. Yates *et al.* (1985) found no significant differences between inactivation rates of poliovirus 1, MS2 and echovirus 1 at different

temperatures in groundwater samples from different sites. However, Sobsey *et al.* (1986) found lower values of  $\mu_1$  for poliovirus 1 and echovirus 1 at 25 and 30°C. Therefore, the data in Table 7 indicate that inactivation of poliovirus 1 is much less sensitive to temperature than MS2 or echovirus 1 (see values of slope  $a$ ). Table 7 further shows that HAV may be regarded as insensitive to changes in temperature. FRNAPH's appear to be very stable as compared with other viruses, but are very sensitive to changes in temperature, as is MS2. In seawater, inactivation rate coefficients for FRNAPH's and HAV were 0.08 and 0.07 day<sup>-1</sup> at 5°C, respectively, and 1.0 and 0.3 day<sup>-1</sup> at 25 °C, respectively (Chung and Sobsey, 1992). So, possibly, FRNAPH's are not that stable as the data of Nasser *et al.* (1993) suggest.

The values of  $\mu_s$  that were derived from Blanc and Nasser (1996) allow evaluation of  $\mu_s$ -variation with temperature. It appears that  $\mu_s$ -values for MS2, PRD1 and poliovirus 1 that are attached to loamy sand significantly increase with temperature. The same is the case with  $\mu_s$ -values for MS2, PRD1 that are attached to sand, but not for poliovirus 1. Probably,  $\mu_s$ -values change similarly with temperature as  $\mu_1$ -values.

### 2.6.4 Effect of Microbial Activity

Inactivation of viruses may be enhanced because of microbial activity (Yates *et al.*, 1987). Hurst *et al.* (1980) found that the concentration of sewage effluent in distilled water under sterile aerobic and anaerobic, as well as under non-sterile anaerobic incubation conditions did not significantly affect virus inactivation. But under non-sterile aerobic conditions, inactivation of poliovirus 1 proceeded faster. This indicates a deleterious effect of aerobic micro-organisms on the survival of poliovirus 1. Also, inactivation of poliovirus 1 and reovirus 3 in settled sewage (Sobsey *et al.*, 1980) and of poliovirus 1, echovirus 1 and HAV in groundwater, secondary and primary effluent (Sobsey *et al.*, 1986) was slower under sterile conditions than under non-sterile conditions in most cases (Table 5). The same can be said for inactivation of attached viruses (Table 6). Jansons *et al.* (1989b) measured inactivation of poliovirus 1 in dialysis bags in different boreholes at a field site. The dissolved oxygen concentration in groundwater was different between boreholes. They found that the inactivation rate of poliovirus 1 was 3 times higher at a mean dissolved oxygen concentration of 5.4 mg/l compared to 0.2 mg/l. Also, *Pseudomonas maltophilia* was found in large numbers only in the borehole with the higher dissolved oxygen concentration. Inactivation of poliovirus 1 may have been directly affected by a higher dissolved oxygen concentration, or by microbiological activity due the higher dissolved oxygen concentration.

Seemingly, inactivation rates of viruses are not always affected by the activity of micro-organisms. Babich and Stotzky (1980) did not find a significant difference in inactivation rate of bacteriophage  $\phi$ 11M15 between natural, autoclaved, or filtered lake waters. Also, Mathess *et al.* (1988) found no significant difference between the inactivation rates of coxsackievirus A9 and B1, echovirus 7 and poliovirus 1 in sterile and non-sterile groundwater.

### 2.6.5 Effect of Unsaturated Conditions

In the calculation of attachment to soil in saturated columns, inactivation of viruses is usually neglected within the time scale of the experiment. However, under unsaturated conditions, the contribution of the effect of inactivation on virus transport is much more important. Powelson *et al.* (1990) showed that MS2 was neither adsorbed nor inactivated in a saturated 1-m column with a loamy fine sand (pH 8), because after less than two pore volumes the effluent concentration reached that of the influent concentration. But in a column under unsaturated conditions, the effluent concentration was significantly reduced. By analysis of soil samples from the unsaturated column, it appeared that MS2 adsorbed only poorly, but was removed by enhanced inactivation. Powelson and Gerba (1994) showed that in columns under unsaturated conditions, removal of the MS2, PRD1 and poliovirus 1 was more than three times higher as under saturated conditions. Poletika *et al.* (1995) showed in a lysimeter with undisturbed unsaturated soil, that MS2 was attached stronger and inactivated faster. These results suggested that the air-water interface may be retaining and/or inactivating viruses during transport through unsaturated soil.

Hurst *et al.* (1980) showed that the inactivation rate of poliovirus 1 increased as the soil moisture content of a sandy soil increased from 5 to 15% and then decreased when the soil moisture content increased from 15 to 25%. Apparently, inactivation was at its maximum near the soil moisture saturation point. Possible explanations for this observation would include soil moisture-level-dependent differences in the extent of virus attachment to the soil and the mechanisms of attachment. Rossi (1994) showed that, in a batch test, inactivation of bacteriophage T7 increased due to the action of strong agitation. During this strong agitation, virus particles have a higher probability to come into contact with the air-water interface. Addition of organic matter (tryptone, humic acid) saturated the air-water interface with organic matter. This lowered the chance of a virus particle entering the air-water interface and resulted in a reduced inactivation rate. Addition of attapulgite-clay resulted in very fast attachment of the virus particles to the clay particles, lowering the chance of entering the air-water interface even more and an even stronger reduction of the inactivation rate was observed. Therefore, it was believed that contact with the air-water interface increases inactivation. Also, by addition of attapulgite, H40/1 and H6/1 were very effectively protected against strong agitation (Formentin *et al.*, 1997). Thompson *et al.* (1998) showed that bacteriophage MS2 was protected against the air-water-solid contact line when attached to soil particles. In this case, the solid was the hydrophobic polypropylene wall of the tube containing the suspension. At the air-water-polypropylene contact line surface tensions are much higher than at an air-water-glass contact line. A similar effect of a synthetic tube wall on inactivation was also observed by Rossi (1994) for phage T7 (see section 2.5.1). These findings suggest that physical forces associated with the air-water-solid contact line may be responsible for enhanced inactivation.

The effect of unsaturated conditions on virus removal is highly dependent on the type of virus (Jin *et al.*, 2000). MS2 is inactivated more in a container with synthetic walls than in glass container, but this is not the case for  $\phi$ X174 (Thompson *et al.*, 1998). MS2 is more hydrophobic than  $\phi$ X174 (Shields and Farrah, 1987; Lytle and Routson, 1995) and will, therefore, enter more easily an air-water-interface, and attach more to hydrophobic solid surfaces, and is subsequently inactivated due to unfolding of coat proteins at the interface (Jin *et al.*, 2000). Under unsaturated conditions in soil, removal of both MS2 and  $\phi$ X174 is

increased, but that of MS2 the most. The increased removal of MS2 is due to increased inactivation, but that of  $\phi$ X174 is due to increased adsorption (Jin *et al.*, 2000).

### 2.7 Advection and Dispersion of Viruses

It has been shown in both laboratory and field studies that physical heterogeneities of the soil increases the dissimilarities between the transport behavior of microorganisms and conservative solute tracers (Harvey, 1997). Harvey (1997) described movement of microorganisms and solute tracers in relatively uniform granular material, like sand, fractured media, and stratified granular material that consists of adjacent layers of finer and coarser sand. In relatively homogeneous sand, viruses are transported at the same velocity as a conservative salt tracer (*e.g.* Pieper *et al.*, 1997; Schijven *et al.*, 1999). However, in fractured media the kinetically or spatially available flow path can be considerably smaller for microorganisms than for a solute tracer (Harvey, 1997). Many studies of bacterial movement exist that generally show a rapid movement of bacteria due to preferential flow through macropores, cracks, worm holes, and channels formed by plant roots (Abu-Ashour *et al.*, 1994). Even more generally, colloids have been shown to be most mobile in soils with relatively large pores (Ouyang *et al.*, 1996). In fractured or stratified soils, tracers like chloride or bromide are small enough to advect or diffuse into fine fractures that are connected to preferential flow paths that are inaccessible to microorganisms (Harvey, 1997). Breakthrough of a solute in such heterogeneous soils will, therefore, be partially retarded and much more dispersed than a colloidal particle such as a virus. In addition, the solute tracer will fail to reach a steady state value for  $C/C_0$  of 1 as was shown by Bales *et al.* (1989). Breakthrough curves of solute tracers in heterogeneous soils will typically have the shape of curve E in Figure 3a. Diffusion into a matrix with small pores has the same retarding effect as kinetically-limited adsorption. Therefore, time to peak breakthrough of the solute will be later than that of the virus. In these cases, where the average flow velocity of viruses is higher than that of water,  $v$  in Equation 1 should be interpreted as the flow velocity of the viruses. Rehmann *et al.* (1999) developed a stochastic model for virus transport that accounts for effects of spatial variability in aquifer hydraulic conductivity. They could simulate that a high degree of aquifer heterogeneity can lead to virus breakthrough preceding that of a conservative tracer.

Bales *et al.* (1989) found that 35 – 40% of MS2 was excluded from the pore volume in a column with sandy soil. Bales *et al.* (1989) also studied transport of phage f2 and two solute tracers, isothiocyanate and pentafluorobenzoic acid in columns with non-sorbing fractured rock. The breakthrough curve of f2 showed little dispersion, whereas the solute tracers were dispersed, because of diffusion into the porous matrix. The authors concluded that bacteriophages are better tracers for transport of colloidal contaminants than solutes, because they were not subject to matrix diffusion. McKay *et al.* (1993) showed that MS2 and PRD1 traveled at rates of 2 to more than 5 m/d in a fractured clay-rich till, whereas bromide and  $^{18}\text{O}$  were transported at rates of only 0.01 to 0.07 m/d. Also, in a clay-rich till, Hinsby *et al.* (1996) showed that MS2 and PRD1 were transported at high rates of 4 – 360 m/day. These high rates were similar to water flow rates in the fractures. The chloride concentration took more than 43 hours to approach steady state, because of diffusion into the small pores of the matrix between the fractures. The phages reached steady state in less

than 3 hours, because of pore size exclusion. Rossi (1994) showed that bacteriophages H40/1 and H6/1 were transported in karst faster than uranine and naphthionate due to preferential flow. Rossi *et al.* (1994) showed that bacteriophages T7 and f1 migrated about 3 times faster than naphthionate, based on time to peak breakthrough. Migration rates of the tracers could be correlated with permeability distribution obtained by Radio-Magneto Tellury measurements. This showed that the tracers followed the more permeable pathways. The same was found with phages H40/1, H6/1, T7 and Psf2 compared to uranine by Rossi (1994) in a karstic aquifer.

Paul *et al.* (1995) used bacteriophages PRD1 and  $\phi$ HSIC1 as tracers to investigate fate and transport of sewage through a highly porous limestone matrix to marine waters (Key Largo). Bacteriophage  $\phi$ HSIC was seeded into a septic tank and PRD1 at an injection point for disposal of domestic wastewater. Estimated rates of migration of the two bacteriophages ranged from 14 – 580 m/day, which is over 500-fold greater than the water velocity, which was measured by subsurface flow meters. The phages traveled at least a distance of 800 m. Concentrations of the viruses varied with the falling tides. However, in this study, it was not clear, whether the phages really traveled faster than the water because measurement of water flow was not carried out at the same time and place. Heavy rainfall preceded this study and may have caused unusually high flow rates. It was not clear, whether PRD1 could reach surface marine waters from the injection point. In a subsequent study, Paul *et al.* (1997) repeated seeding with bacteriophages MS2, PRD1 and  $\phi$ HSIC1 at Key Largo, but also at another disposal well (Middle Keys). The different phages traveled at similar rates and made their way rapidly to surface marine waters from both injection wells, but transport rates were much greater in Key Largo than in the Middle Keys, respectively 460 m/day and 24 m/day. This difference in flow rates could be ascribed to differences in tidal pumping, and also to the fact that there exist man-made channels through the limestone at the Key Largo-site, but not at the Middle Keys.

Sinton *et al.* (1997) studied the movement of somatic coliphages, FRNAPH's and faecal coliforms through an alluvial gravel aquifer where effluent was irrigated. Breakthrough was followed at 60 m and about 400 m. In a second experiment, MS2, *E. coli* J6-2 and rhodamine WT dye were injected and could also be detected at 400 m. In both experiments, the phages exhibited the shortest times to peak concentration, followed by the bacteria, and then the dye. Sinton *et al.* (1997) interpreted these data by suggesting that the bacteria were transported faster than the dye because of pore-size exclusion; the phages were transported even faster than the bacteria, because the electrostatic repulsion of the phages is supposedly stronger than that of the bacteria, or that the phages are more often attached to other particles of a size that are transported faster than bacteria. Sinton *et al.* (1997) based transport velocity of the dye, the phages and the bacteria on the arrival time of peak concentrations. As was explained in section 2.3.2, differences in time to peak concentration can also be an effect of different values of kinetic attachment and detachment rate coefficients (curves E and F in Figure 3a). Thus, it may be reasoned that the difference between  $k_{att}$  and  $k_{det}$  was much less for the bacteria than for the phages, which is a more plausible explanation for the observed difference in time to peak concentration between the bacteria and the phages. In addition, kinetic effects may have played some role in the breakthrough of the rhodamine WT dye. A study exists where it was shown that rhodamine WT does not behave conservatively, but exhibited nonequilibrium adsorption (Di Fazio and Vurro, 1994).

To conclude, advection and dispersion are properties of the soil and water, and are commonly determined by means of solute (*e.g.* salt) transport experiments. However, viruses may travel faster than the average water flow and show a smaller dispersion than a solute. Several studies have shown that viruses are transported faster than classic solute tracers, because they can be excluded from small pores and, therefore, preferentially follow more permeable pathways. This shows that for movement of colloids, bacteriophages are better tracers than solutes.

## 2.8 Model Viruses

### 2.8.1 Introduction

As pointed out in section 2.1.4, model viruses are needed to represent the behavior of pathogenic viruses during subsurface transport and to predict their removal. Bacteriophages MS2, PRD1,  $\phi$ X174 and naturally occurring FRNAPH's have been used extensively to study virus transport under various column and field conditions. In this section, the role of these bacteriophages as model viruses is evaluated.

### 2.8.2 MS2

MS2 is an icosahedral virus with a diameter of 27 nm and a low isoelectric point of 3.5. The three-dimensional structure of its capsid is known at the atomic level (Penrod *et al.*, 1996). MS2 may be considered as a relatively conservative tracer for virus transport in saturated sandy soils at pH 6 – 8 and with a low organic carbon content, because under those conditions it showed little or no adsorption (Bales *et al.*, 1989; Powelson *et al.*, 1990; Herbold-Paschke *et al.*, 1991; Kinoshita *et al.*, 1993; Jin *et al.*, 1997; Schijven *et al.*, 1999). A low organic content would imply low hydrophobicity of the soil.

In most soils, attachment of MS2 is also relatively low compared to most other viruses (Goyal and Gerba, 1979). Herbold-Paschke *et al.* (1991) showed that only a few percent of bacteriophages T4, MS2 and  $\phi$ X174 attached in 1-m columns filled with coarse or medium-grade quartz sand. MS2 removal was less than or equal to that of T4 and  $\phi$ X174, and much less than that of simian rotavirus SA11. In columns with a sandy soil (pH 7.5), Bradford *et al.* (1993) showed that MS2 was removed less (0 to 68%) than poliovirus 1 (99%) and simian rotavirus SA-11 (90%). Farrah and Preston (1993) showed less or equal removal of MS2 compared to poliovirus 1, coxsackievirus B5 and echovirus 5 in column with sand that was or was not modified by precipitation of metallic salts. Bales *et al.* (1993) showed that the collision efficiency of MS2 in columns with silica beads was 2 – 3 times lower than that of poliovirus 1 at pH 7, but about the same at pH 5 – 5.5 (Table 2). Sobsey *et al.* (1995) observed that removal of MS2 in 10-cm columns with clay loam (52% clay) at pH 6 – 8 was similar to that of hepatitis A virus (HAV), poliovirus 1 and echovirus 1. Removal of MS2 in columns with organic muck was less than or equal to that of these viruses. Penrod *et al.* (1996) and Redman *et al.* (1997) showed that due to steric repulsion, attachment of MS2 to silica was less than that of bacteriophage  $\lambda$  and recombinant Norwalk virus particles to quartz sand at pH 5 – 7, although both had a stronger negative surface charge than MS2. Jin *et al.* (1997) compared transport of MS2 and  $\phi$ X174 in short sand columns (10 or 20 cm). MS2 did not adsorb but  $\phi$ X174 was retained significantly. In the field studies of DeBorde *et al.* (1999) and Schijven *et al.* (1999) removal of MS2 and PRD1 was similar.

In the same study of DeBorde *et al.* (1999) removal of  $\phi$ X174 was slightly more efficient and that of poliovirus 1 (CHAT) even more.

However, possibly due to its hydrophobicity, MS2 may attach more than other viruses to some soils, *e.g.* to soil K in the batch study of Goyal and Gerba (1979). Using continuously circulating columns of a sandy soil (95% sand, 7% silt, 2% clay, pH 7.1), Dowd *et al.* (1998) found that the attached fraction of MS2 was greater than that of four other bacteriophages, PRD1, Q $\beta$ ,  $\phi$ X174 and PM2, possibly due to the presence of multivalent cations. In the same study of Dowd *et al.* (1998), attachment of MS2 to the sandy soil in a flow-through column was intermediate.

With regard to inactivation, MS2 is less stable than several pathogenic viruses (Table 5). MS2 is inactivated faster at higher temperatures, but at temperatures lower than 7 °C, its inactivation rate is very low and similar to that of PRD1 (Yates *et al.*, 1985; Yahya *et al.*, 1993; Blanc and Nasser, 1996, Schijven *et al.*, 1999).

To conclude, MS2 meets the requirements for a worst case model virus, provided the water temperature is less than about 10° C and the soil does not contain too many hydrophobic sites and the concentration of multivalent cations is low.

### 2.8.3 PRD1

PRD1 is an icosahedral bacteriophage with a diameter of 62 nm with an inner lipid membrane (Bales *et al.*, 1991; Caldentey *et al.*, 1990). Its pI lies between 3 and 4 (Loveland *et al.*, 1997). PRD1 may be considered as a worst-case model virus because of its low inactivation rate between 10-23 °C (Yahya *et al.*, 1993; Blanc and Nasser, 1996, see also Table 5). Because of its larger size, PRD1 is of interest as a representative of rotaviruses and adenoviruses (Sinton *et al.*, 1997). Although, adenovirus and PRD1 may differ in surface charge, it is worth mentioning that PRD1 is much closer in structural design to adenovirus than any other known bacteriophage, and vice versa. The major capsid protein (P3) of PRD1 has the same double “jellyroll” fold as the human adenovirus type 2 hexon, despite their very different sequences and sizes. This implies that the basic structure as well as the assembly pathways of complex viruses were perfected very early in evolution and have been retained despite the high mutability of viruses (Belnap and Stevens, 2000). This observation further strengthens the validity of using bacteriophages as model viruses for the less-tractable animal viruses that cause human diseases.

With regard to attachment characteristics, PRD1 seems to behave less conservative than MS2 (Bales *et al.*, 1991; Kinoshita *et al.*, 1993; Powelson *et al.*, 1993, Dowd *et al.*, 1998), possibly because it is more hydrophobic than MS2 (Shields and Farrah, 1987; Bales *et al.*, 1991; Kinoshita *et al.*, 1993; Lytle and Routson, 1995). However, in a sandy aquifer (Bales *et al.*, 1997) PRD1 attached at a much lower rate than compared to the column studies (using the same soil) by Kinoshita *et al.* (1993). Detachment was much slower than attachment, but the detachment rate increased  $10^4 - 10^5$  times by a high pH-pulse (Bales *et al.*, 1997). In the field studies by DeBorde *et al.* (1999) and Schijven *et al.* (1999) removal of PRD1 was similar to that of MS2. Apparently, PRD1 may also be considered as a relatively conservative model virus, similar to MS2, under field conditions in sandy soils at pH 6 – 8 and with low organic carbon content and low concentration of multivalent cations. In addition, PRD1 is more stable at higher temperatures (12° – 23° C).

### 2.8.4 Bacteriophage $\phi$ X174

Bacteriophage  $\phi$ X174 is less hydrophobic than MS2 (Shield and Farrach, 1987). In studies on the retention of viruses by barrier materials, like membranes, condoms, testing gloves,  $\phi$ X174 is regarded as the best model virus, because it exhibits the least electrostatic and hydrophobic interaction (Shields and Farrach, 1987; Lytle and Routson, 1995; Fujito and Lytle, 1996).  $\phi$ X174 has essentially no charge at neutral pH ( $pI = 6.6 - 6.8$ ) and a size of 27 nm (Fujito and Lytle, 1996; Dowd *et al.*, 1998).

Jin *et al.* (1997) found that breakthrough of  $\phi$ X174 in columns with Ottawa sand attached significantly, whilst MS2 did not. It was suggested that this difference in adsorption behavior was a reflection of the difference in the isoelectric points of the two viruses. The authors suggested that because the  $pI$  of  $\phi$ X174 is same as that of poliovirus 1 it should have similar attachment behavior. However, Funderberg *et al.* (1981) already showed that these viruses behave differently. They studied removal of poliovirus 1, reovirus 3, bacteriophage  $\phi$ X174 in columns of eight different soils. The strongest positive correlation was found between removal of poliovirus 1 and reovirus 3, and soil cation exchange capacity. Whereas removal of these enteroviruses was correlated more with soil properties, removal of  $\phi$ X174 was affected most by the residence time in the column. Removal of  $\phi$ X174 was usually less than that of poliovirus 1. In columns with quartz sand, removal of  $\phi$ X174 was less than that of bacteriophage T4, and more than or equal to that of MS2. However, removal of all these phages was quite low (Herbold-Paschke *et al.*, 1991). Dowd *et al.* (1998) showed that in a sandy soil in circulating-flow columns and in flow-through columns removal of  $\phi$ X174 was less than that of MS2, PRD1, PM2 and Q $\beta$ .

In field studies of DeBorde *et al.* (1998, 1999),  $\phi$ X174 appeared to be very stable, *i.e.* its inactivation was negligible over a period of about one half year.

To conclude,  $\phi$ X174 may be a relatively conservative model virus, because of its low hydrophobicity (Shields and Farrach, 1987) and stability (DeBorde *et al.*, 1998, 1999). In soils, where hydrophobic interactions would significantly increase virus removal,  $\phi$ X174 would be a better choice as a model virus than *e.g.* MS2 or PRD1. However, the value of pH will strongly determine whether  $\phi$ X174 will behave conservative. A pH range of 6 – 8 is very common for most soils, and at pH 6 the net surface charge of  $\phi$ X174 will be positive, but at pH 8 it will be negative.

### 2.8.5 F-specific RNA Bacteriophages

F-specific bacteriophages have similar physical properties as enteroviruses, especially with respect to size (Bitton, 1980; Havelaar, 1993). MS2 belongs to group I of FRNAPH's (Havelaar, 1986). As naturally present model viruses they are of high interest to represent enteroviruses in various treatment processes of surface water, including soil passage. Before entering a treatment like soil passage, enteroviruses and FRNAPH largely have followed the same path, *i.e.* both have passed the sewerage system, followed by sewage treatment, discharge into surface water and some kind of pre-treatment before recharge into soil. It may be reasoned that along this path from the sewerage system to the point of recharge into an aquifer, viruses that are less stable, or that adsorb readily to solid surfaces, have disappeared already. This suggests that a selection has taken place of very stable and

poorly adsorbing viruses, *i.e.* worst-case viruses. This selection has been the same for FRNAPH's and enteroviruses.

In surface water, FRNAPH's occur in numbers of  $10^2$ - $10^4$  times higher than enteroviruses (Havelaar *et al.*, 1993). Therefore, it has been possible to show 4 to 6  $\log_{10}$  removal of FRNAPH's by riverbank filtration (Havelaar *et al.*, 1995).

In an alluvial gravel aquifer where effluent was irrigated, Sinton *et al.* (1997) studied transport of somatic coliphages, FRNAPH's and faecal coliforms in one experiment and of MS2 and *E. coli* J6-2 in a second experiment. Concentrations of all these micro-organisms were similarly reduced, about 9  $\log_{10}$  after 400 m of transport. Concentration of the rhodamine WT dye was reduced about 7  $\log_{10}$  over this distance. This shows that removal of FRNAPH's and MS2, also an F-specific RNA bacteriophage, is similar. Low collision efficiencies of naturally present FRNAPH have been found by Schijven *et al.* (1998) under field conditions (Table 3). DeBorde *et al.* (1998) found a removal rate of naturally present FRNAPH's and somatic coliphages that was half that of bacteriophages MS2 and  $\phi$ X174. However, the latter two bacteriophages were seeded as slug-injections, whereas F-specific bacteriophages were continuously introduced with sewage effluent.

In the study of Nasser *et al.* (1993), FRNAPH appeared to be very persistent at 10 – 30 °C, and not affected by the type of water. They were even more persistent than HAV, which can be regarded as a very persistent virus (Sobsey *et al.*, 1986; Nasser *et al.*, 1993; Blanc and Nasser, 1996). However, Chung and Sobsey (1992) observed that FRNAPH's are less stable in seawater than HAV.

To conclude, FRNAPH's as a group of naturally occurring viruses are very useful model viruses for the behavior of viruses during subsurface transport. FRNAPH's behave relatively conservative, like MS2 and they have been shown to be very persistent. Moreover, naturally present FRNAPH's may consist of stable and poorly adsorbing viruses prior to treatment by soil passage.

## 2.9 Virus Removal by Soil Passage

### 2.9.1 Relative contributions of adsorption and inactivation to virus removal

Thus far, in this review, adsorption and inactivation were evaluated separately. This section will focus on the relative contributions of these processes to virus removal by soil passage. Virus adsorption to soil is the most important process for attenuation. But actual removal, *i.e.* disappearance of viruses, is due to inactivation, and also of irreversible attachment, if it exists. Under steady state conditions, the relative contributions of inactivation and adsorption to the removal of viruses by soil passage can be compared easily. A steady state situation occurs when input of virus is continuous. This usually is the case, *e.g.* during bank filtration, dune recharge, deep well injection, or continuously leaking sewage pipes and may be seen as a worst-case situation. Considering a one-dimensional steady state situation, Equation 1 may be simplified to:

$$\alpha_L \frac{\partial^2 C}{\partial x^2} - \frac{\partial C}{\partial x} = \frac{Q}{mv} \quad (29)$$

Here,  $\alpha_L$  is the longitudinal dispersivity, [L].

Under steady state conditions, it follows from Equation 3 that

$$\mu_{s,kin} \rho_B S_{kin} = nk_{att} C - k_{det} \rho_B S_{kin} \quad (30)$$

Substitution of Equations 2 and 30 into 4 gives

$$Q = \lambda n C \quad \text{where,} \quad \lambda = \mu_l + \mu_{s,eq} \frac{\rho_B}{n} k_{eq} + \frac{k_{att}}{1 + k_{det}/\mu_{s,kin}} \quad (31)$$

Now, the solution of Equation 29 can be written as

$$\log \left( \frac{C}{C_0} \right) = \frac{x}{2.3} \left( \frac{1 - \sqrt{1 + 4\alpha_L \frac{\lambda}{v}}}{2\alpha_L} \right) \quad (32)$$

where  $C_0$  is the concentration at  $x = 0$ , and  $\log_{10}(C/C_0)$  is defined as virus removal. From Equations 31 and 32, the relative contributions of adsorption and inactivation to virus removal can be deduced. Because equilibrium adsorption has been shown to be of little importance in several studies (Bales *et al.*, 1991, 1993, 1997; Pieper *et al.*, 1997; Jin *et al.*, 1997; Schijven *et al.*, 1999), the second term in Equation 31 may be neglected. From Equation 31 it can be seen that if there is no inactivation at all, there will be no removal ( $\lambda = 0$ ) under steady state conditions. If there is no detachment, removal will be determined by inactivation and irreversible attachment of free viruses ( $\lambda = \mu_l + k_{att}$ ).

In the field study by Schijven *et al.* (1999), it appeared that  $k_{det} \ll \mu_{s,kin}$  and  $k_{att} > \mu_l$ , therefore  $\lambda \approx k_{att}$ . In that case, virus removal is mainly determined by attachment, which appears to work as irreversible attachment. In a field study of Bales *et al.* (1997), virus inactivation was considered to be insignificant. The authors concluded that virus removal could be described primarily by  $k_{att}$  and  $k_{det}$ , and that simply knowing a retardation factor is not sufficient. This is justified only if  $k_{det}$  is much smaller than  $\mu_s$ . Also, Pieper *et al.* (1997) and DeBorde *et al.* (1999) regarded virus inactivation as negligible during their field experiments, and considered virus removal to be solely determined by attachment.

Although detachment rates were not calculated in these studies, the shapes of their breakthrough curves suggest that detachment rates were much lower than attachment rates.

Table 8 summarizes values of  $k_{att}$ ,  $k_{det}$ ,  $\mu_l$  and  $\mu_s$  for MS2 and PRD1 calculated from observed virus removal in a few field studies. Values for  $k_{att}$  and  $k_{det}$  have been reported in only two field studies. Bales *et al.* (1997) reported two values for each (Table 8). During a high pH-pulse,  $k_{att}$  was only a factor 2 lower, whereas  $k_{det}$  increased by a factor of  $5 \times 10^4$ .

In that case  $k_{det}$  was larger than  $k_{att}$  and probably much larger than  $\mu_s$  implying that the kinetic term in Equation 31 took the form of the adsorption equilibrium. Schijven *et al.*

(1999) found different  $k_{att}$ - and  $k_{det}$ -values for different travel distances (see next section).

All in all, it appears that only very few data are available on attachment and detachment of viruses under field conditions. In order to be able to predict virus removal, more values of attachment, detachment and inactivation rate coefficients for viruses under various conditions are needed. Comparison of the  $\alpha$ -values from Tables 2 and 3 give the impression

**Table 8** Values of  $\alpha$ ,  $k_{att}$ ,  $k_{det}$ ,  $\mu_1$  and  $\mu_s$ , [ $day^{-1}$ ], for MS2 and PRD1 from field studies.

Parameter	MS2	PRD1	References
$k_{att}$		6.1 – 11	Bales <i>et al.</i> (1997)
	0.8 – 4.1	0.7 – 4.0	Schijven <i>et al.</i> (1999)
$k_{det}$		0.0003 – 15	Bales <i>et al.</i> (1997)
	0.00087 – 0.0030	0.00077 – 0.0034	Schijven <i>et al.</i> (1999)
$\mu_1$ (5 ± 3 °C)	0.03	0.12	Schijven <i>et al.</i> (1999)
$\mu_s$ (2 – 5 °C)	0.09	0.07	Schijven <i>et al.</i> (1999)

that, at least for short travel distances, these values are similar for column and field situations. However, this needs verification. Except during perturbations like a high pH, it seems that  $k_{det}$  is generally much smaller than  $k_{att}$ , which is consistent with observations from several column studies (e.g. Bales *et al.*, 1991, 1993; Kinoshita *et al.*, 1993; Penrod *et al.*, 1996; Dowd *et al.*, 1998). Possibly, the ratio of  $k_{att}/k_{det}$  from column-scale may be extrapolated to field-scale under similar conditions. However, this needs to be verified too. The inactivation rate coefficients that were found in a field study by Schijven *et al.* (1999) are similar in value to those from the batch studies which are summarized in Table 5 and 6. This suggests that the values for inactivation rate coefficients as found in batch experiments may be used for prediction of virus transport at field scale. But more information is needed to verify this.

Yates *et al.* (1986) calculated safe setback distances, solely based on inactivation rates of MS2. To that purpose, they sampled groundwater from 71 sites within a certain area and determined inactivation rates of MS2 in these samples at the corresponding in-situ temperatures (20 to 30.5 °C). Virus inactivation rates of other nearby sites in the area were calculated by means of kriging, a geostatistical technique. A contour map could be made that showed the variation in separation distances assuring 7- $\log_{10}$  reduction in virus concentrations by inactivation. This approach was extended by combining kriging with a linear relation for  $\mu_1$  of MS2 with temperature. This eliminated the need of having to measure virus inactivation rates in the laboratory (Yates and Yates, 1987). This way, similar maps of setback distances could be constructed. Yates and Yates (1988) extended this model even further to account for alterations in the flow field by pumping. This geostatistical model may, however, underestimate setback distances, because at higher temperatures, the inactivation rate of MS2 is higher than that of other viruses, such as HAV (Yates *et al.*, 1986; see also section 2.6.2). On the other hand, setback distances may grossly be overestimated this way, because the contribution of inactivation of attached viruses was not included (see Equation 31).

### 2.9.2 Removal of Viruses with Distance

From Equation 32 with constant rate coefficients for attachment, detachment and inactivation, it can be deduced that in a saturated soil under steady state conditions, virus removal ( $\log_{10}(C/C_0)$ ) should decline in a linear fashion with travel distance. In several field studies (Bales *et al.*, 1995; Pieper *et al.*, 1997; DeBorde *et al.*, 1998, 1999) viruses were seeded as slug-injections, thus no steady state was achieved. In that case, apparent removal

rates are expected to increase with distance due to dispersion. However, several column and field studies have shown that the removal rate appears to be initially higher.

Gerba and Lance (1978) have shown that approximately one  $\log_{10}$  of poliovirus 1 was removed ( $C/C_0 = 0.1$ ) from primary sewage during passage through the first 5 cm of a column with loamy sand. An additional 35-cm travel distance was necessary to reduce the virus concentration another  $\log_{10}$ . Similar results were obtained when the column was flooded with secondary sewage. Wang *et al.* (1981) analyzed removal of poliovirus 1 and echovirus 1 after continuous application to columns with three different sands and a sandy loam for 3-4 days at constant flow rates. Removal of both viruses appeared to be very similar. Statistical analysis indicated that the rate of virus removal in the upper 17-cm depth of the soil column was significantly greater than in the lower depths of the soil column. In a field study of Bales *et al.* (1995), concentration of PRD1 was attenuated about 5  $\log_{10}$  after the first 2 m of passage in a sandy aquifer. Attenuation of PRD1 was estimated relative to that of bromide to account for dilution effects. However, an additional attenuation of only one  $\log_{10}$  during the following 9 m was observed. In another field study of Bales *et al.* (1997), bacteriophages PRD1 and M1 both were removed about 4  $\log_{10}$  after 0.94 m of passage through a sandy aquifer, but only another one  $\log_{10}$  after the following 1.6 m. A conservative tracer did not decrease similarly and, therefore, dispersion was ruled out as a possible cause. Pieper *et al.* (1997) presented relative breakthrough of PRD1 with distance at a field site with a sewage-contaminated and an uncontaminated zone. They found that the strongest attenuation occurred during the first 1.8 m, but concentrations of PRD1 remained nearly constant during the next 1.8 m. Plotting relative breakthrough of PRD1 on a log-scale showed that the removal rate of PRD1 was initially higher. Similar results were obtained by Schijven *et al.* (1998). They measured efficient reduction of FRNAPH's by 3.8  $\log_{10}$  after 2 m of dune infiltration. But at 4 m, an additional reduction of only 0.83  $\log_{10}$  was found, albeit with a large uncertainty. Consequently, the corresponding estimated value of the collision efficiency is much lower at 4 m than 2 m (See Table 3). Schijven *et al.* (1999) seeded bacteriophages MS2 and PRD1 during 11 days at a field site for dune recharge. Removal of MS2 and PRD1 was very similar. Bacteriophage concentrations were reduced about 3  $\log_{10}$  within the first 2.4 m and another 5  $\log_{10}$  in a linear fashion within the following 27 m. DeBorde *et al.* (1999) reported removal with distance of MS2, PRD1,  $\phi$ X174 and poliovirus 1 (CHAT) under field conditions. Maximum breakthrough concentrations of MS2, PRD1 and  $\phi$ X174 decreased about 2.5  $\log_{10}$  with 8 m and an additional 3.5 - 5  $\log_{10}$  within the next 32 m. Concentrations of poliovirus 1 decreased 4  $\log_{10}$  within the first 8 m and about 1  $\log_{10}$  in the following 12 m. In another field study by DeBorde *et al.* (1998) removal rates of MS2 and  $\phi$ X174 seemed to decrease with distance, but not significantly. MS2 and  $\phi$ X174 were seeded as slug-injections. In other words, if the viruses had been seeded for a longer period of time, such that semi-steady state conditions could have been assumed, the removal rate would likely have declined with distance. However, removal rates of somatic and F-specific bacteriophages were found to be linear over a distance of 18 m. These naturally occurring bacteriophages were present due to continuous infiltration of sewage effluent.

With the exception of FRNAPH's and somatic coliphages in the study by DeBorde *et al.* (1998), these studies all suggest that initial higher removal of viruses with distance is typical. This phenomenon may be explained by soil and/or virus heterogeneity.

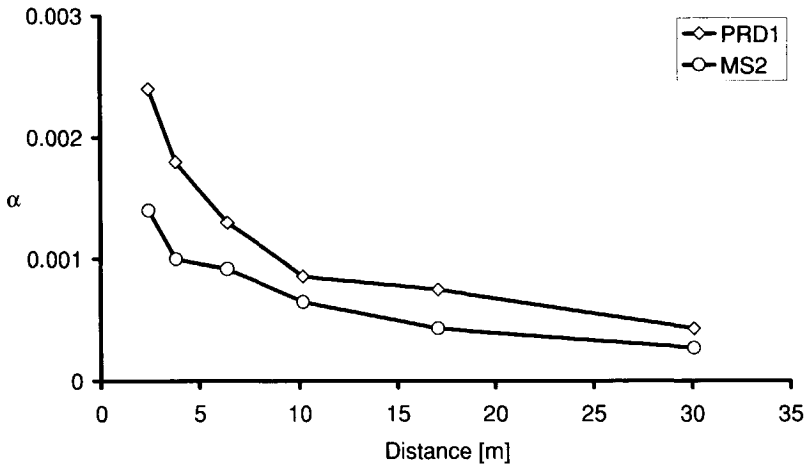


**Figure 14** Collision efficiency  $\alpha$  for MS2 and PRD1 with travel distance (Schijven *et al.*, 1999).

Soil heterogeneity may be a cause, *e.g.* if more sites of attachment are available in the first centimeters of passage through a column or in the first meter at a field location. Although this may be the case in field studies, in the column studies that are referred to here, the columns were filled in small increments to obtain uniform packing of the soil. Therefore, it seems unlikely that the first centimeters contained a larger proportion of silt and clays, or smaller grains that could cause more efficient attachment. The field studies of Bales *et al.* (1995) and Pieper *et al.* (1997) were performed in the same aquifer that was contaminated by sewage disposal. The soil consisted of stratified, well-sorted, medium to coarse sand with some gravel, and groundwater velocity ranged from 0.2 – 0.7 m/day and porosity from 20 – 40% (Bales *et al.*, 1995). From these studies, it is not clear if injection of the studied bacteriophages took place in finer soil material. Furthermore, non-linear removal with distance appeared to be independent of the extent of sewage contamination (Pieper *et al.*, 1997). From the field study by Bales *et al.* (1997), it is not clear whether PRD1 and M1 were injected at a point with finer soil material. Extensive soil analysis in the study by Schijven *et al.* (1999) showed that the average grain size of the soil was even larger in soil samples from the first 5 and 10 – 15 cm than in soil samples taken at the monitoring wells. Therefore, the possibility that fine-grained sediments at the bottom of the compartment were the cause of high early attachment could be ruled out. On the other hand, higher concentrations of bonded organic matter were found in the soil samples at shorter distance. This suggests that the bacteriophages may have been removed more efficiently during the first meters of soil passage by hydrophobic interactions. However, from the above, it appears that soil heterogeneity does not satisfactorily explain initial higher virus removal.

Viral heterogeneity may be a cause for the greater initial removal, *i.e.* the viruses in the suspensions that were used for seeding a column or a field site may have different affinities for attachment sites, as was suggested by Pieper *et al.* (1997) and Schijven *et al.* (1999). Figure 14 shows how collision efficiency  $\alpha$  for MS2 and PRD1 gradually decrease with distance, as was observed in a field study by Schijven *et al.* (1999). Albinger *et al.* (1994)

reported a range of collision efficiencies for bacteria, even in the extreme case of a uniform collector surface and a monoclonal bacterial population. These variations in  $\alpha$  could neither be explained by preferential retention of larger cells nor by intra-population genetic variation. Although, the outer surface of a virus particle is less complex than that of a bacterial cell, virus particles that are released from their host cell may be still attached to cell debris, which would account for differences in adsorption between virus particles. Furthermore, Goyal and Gerba (1979) have shown that virus adsorption to soil not only depends on the type and strain of virus under consideration, but may also vary between isolates of the same virus type. Viruses may be present as aggregates (see section 2.5.1) and it has been shown that viruses attach readily to other colloidal particles, like clays that are ubiquitously present in sewage water and surface water (see section 2.6.3). It may be reasoned that combinations of viruses and other colloidal particles thus behave as particles with different size and density and therefore, different collision efficiencies, but also with different collision efficiencies. In addition, different types of viruses that are attached to the same type of colloidal particles may show the same behavior during subsurface transport. Possibly, transport of a fraction of virus particles may be enhanced, due to their attachment to inorganic colloids such as silicate clays and iron or aluminium oxide clays. Such colloidal particles are *e.g.* released in an anoxic environment and can migrate considerable distances (Ouyang *et al.*, 1996).

Viral heterogeneity is the most likely explanation for the non-linear removal of FRNAPH's by dune recharge (Schijven *et al.*, 1998). Although FRNAPH's form a rather homogeneous group, they consist of different virus-types, that differ in size and surface charge. Therefore, they are likely to differ in collision efficiencies. It can be argued that FRNAPH's with higher  $\alpha$ 's attach faster, thereby lowering the average  $\alpha$  of the population of free phages, as they are transported further.

Rehman *et al.* (1999) developed a large-scale model of virus transport in aquifers using spectral perturbation analysis. A sensitivity analysis showed that aquifer heterogeneity can lead to virus breakthrough actually preceding that of a conservative tracer. Also, use of a heterogeneous colloid filtration term results in higher predicted concentrations than the use of a simple first-order constant attachment rate. It was pointed out that measurements of the spatial variability of the collision efficiency would be extremely important in predicting virus transport.

To conclude, removal of viruses by soil passage apparently declines with distance. This has important consequences for prediction of their removal, thus also for the calculation of setback distances to adequately protect groundwater sources and to assure adequate treatment of infiltrated surface water. From the above, it is clear that predictions of virus removal at larger distances are severely overestimated if they are based on removal data from column experiments or from field studies where transport was studied over short distances.

To improve predictions on the removal of viruses by soil passage, knowledge of the soil heterogeneities at the location of interest is clearly needed. Also, heterogeneity of the transported virus-particles, *i.e.* the distribution of collision efficiencies within the population of virus-particles, including its cause should be investigated further.

## 2.10 Summary and Conclusions

### 2.10.1 Adsorption

Many batch experiments with suspensions of viruses and soil have been carried out to investigate the effects of various factors on virus-soil interactions. Commonly, on a time scale of only a few hours, virus inactivation is negligible and equilibrium adsorption has been reported to be reached, or has been assumed to be reached. Also, in many column and field studies, adsorption of viruses during transport was assumed to reach equilibrium. This is described by retardation coefficient  $R$ , whereby a value of  $R$  greater than one reflects retarded breakthrough due to equilibrium adsorption. However, only in some cases, retardation coefficients of about 2 – 5 have been reported. Usually little or no retardation is found. Therefore, retarded breakthrough by equilibrium adsorption is believed to be of little significance. Kinetically-limited attachment and detachment mainly govern removal of viruses during transport and determine the shape of breakthrough curves. In field studies, it appeared that attachment rates were relatively fast, whereas detachment rates may be much slower. Dependent on soil heterogeneity, viruses may travel faster than the average water flow and show a smaller dispersion than a solute, because they can be excluded from small pores and, therefore, preferentially follow more permeable pathways.

In a batch suspension of viruses and soil, adsorption equilibrium is not reached instantaneously. Instead, virus attachment at the micro-scale can be described as the result of mass transport, within a pore, to the solid surface and subsequent immobilization at the surface by physical and possibly chemical interactions. The overall rate of attachment depends on which of these two processes is the rate-limiting step. At pH 7 – 8, as in many aquifers, the net surface charge of most viruses and soils is negative, and thus conditions for attachment are generally unfavorable. Under such conditions, virus-surface interaction is the rate-limiting process for attachment. In the absence of repulsive energy barriers, or in the presence of attractive double layer interactions, conditions for attachment are favorable. In that case, mass transport to the vicinity of the soil surfaces is the rate-limiting step. Favorable chemical conditions for attachment may develop in groundwater with high levels of water hardness and ionic strength. Attachment will also be favorable for solid surfaces (or patches on solid surfaces) which are positively charged due to iron, aluminium, or manganese oxide coatings. Attachment to such favorable patches may be irreversible. Several studies support the concept that viruses preferably attach only to a fraction of the soil surface having favorable charge characteristics.

Unfortunately, estimates of adsorption parameters from batch experiments appear to be of little use to predict adsorption of viruses in column or field experiments. Values for adsorption obtained from different batch studies are even difficult to compare because there is no standard protocol. They are highly variable due to heterogeneity of soil preparations, different sizes and types of containers, different methods of agitation, and differences in the air-water interface. Most batch studies were carried out to measure equilibrium adsorption, whereby attachment and detachment rate coefficients are not determined. Only one batch study exists where the kinetic part (that is operative before equilibrium is reached) was analyzed (Grant *et al.*, 1993). Therefore, values of attachment and detachment rate coefficients from batch studies are not available, but even if they were, they are not applicable for predicting virus removal in transport situations. Due to the stirring in a batch

experiment the number of accessible sites for attachment is much higher than in a column. In a column, attachment rates are, therefore, much lower. The opposite is probably true for the detachment rate. The detachment rate coefficient for a virus in a batch system is probably smaller than under transport conditions, where there is advective flow. This implies that the observed ratio  $k_{att}/k_{det}$  from a batch experiment is expected to be much larger than that from a column or field experiment. This difference between batch and column experiments has been found in several studies, where equilibrium adsorption was assumed.

A problem with many batch experiments reported in the literature is that the measurements are probably stopped too early. Almost all batch experiments are used to evaluate equilibrium adsorption coefficients. However, in most cases, it is not clear if equilibrium has been reached. The ratio of  $k_{att}/k_{det}$  may, therefore, have been strongly underestimated. In several column and field studies at pH 7–8, where kinetically-limited adsorption was considered, the ratio  $k_{att}/k_{det}$  was found to be very large. This is totally opposite to the expectation that  $k_{att}/k_{det}$  from a batch experiment is expected to be larger than that from a column or field experiment. Calculations predicted that equilibrium in a batch system would be reached only after about 40 hours. Also, this would mean that a low percentage of adsorption that is found in a batch experiment after a short period of time, is rather a consequence of slow adsorption than of equilibrium.

The major factor that affects adsorption is pH. At higher pH, electrostatic repulsion increases, resulting in a decreased attachment rate and an increased detachment rate. In most aquifers, surface characteristics of the soil are heterogeneous and also different viruses with different pI's may be present. Therefore, dependent on pH and thus on the charge of the virus and soil particles, adsorption of some of these viruses may be irreversible, whereas that of others may be reversible. At pH 7–8, adsorption will mainly be reversible. Dissolved organic matter may decrease virus attachment to soil because of competition for the same binding sites. Dissolved organic matter, like surfactants may disrupt hydrophobic bonds between soil and virus, resulting in an increased detachment rate. At the same time, viruses and many organic materials contain hydrophobic groups on their surfaces. Therefore, once adsorbed, bonded organic matter may provide hydrophobic binding sites for viruses. Also, the presence of solid organic matter may result in an increased attachment rate through hydrophobic binding. The enhancing and attenuating effects of organic matter on adsorption of viruses and their dependence on soil and virus properties makes their quantification very difficult, especially under field conditions. Effects of organic matter will therefore be responsible for considerable uncertainty in predicting virus removal.

### 2.10.2 Inactivation

Commonly, virus inactivation is considered as a first-order rate process. Inactivation rates of viruses that are attached to solids may be reduced or enhanced. In this review values of the inactivation rate coefficient  $\mu_s$  for attached viruses were calculated using data from some batch studies. It appeared that enhanced or reduced inactivation is very much virus-specific and almost independent of the ratio  $k_{att}/k_{det}$ . Reduced inactivation may be the result of protection from proteolytic enzymes or other virus-inactivating substances, increased stability of the virus capsid when attached, prevention from aggregate formation, and blocking from ultraviolet radiation. Attachment of viruses to solids may also significantly

reduce inactivation by preventing them from entering into the air-water interface, or the air-water-solid contact line. Enhanced virus inactivation in the presence of soil may also occur in some cases, probably due to repeated attachment and detachment cycles.

Temperature is the most important factor that influences virus inactivation. Inactivation rates increase with temperature. The temperature sensitivity of  $\mu_1$  depends on the type of virus. Probably,  $\mu_s$ -values change similarly with temperature as  $\mu_1$ -values. Inactivation of some pathogenic viruses, such as HAV, is very insensitive to temperature changes.

Microbial activity may increase inactivation rates of viruses under aerobic conditions.

### 2.10.3 Model Viruses

Adsorption and inactivation are strongly virus dependent. One way to model the removal of pathogenic viruses by soil passage is to use a cocktail of viruses that represent a range of these characteristics. Alternatively, a virus that adsorbs less and is more stable than other viruses under certain conditions, may be considered as a worst-case model virus.

MS2 meets the requirements of a worst case model virus, provided the water temperature is less than about 10° C and the soil does not contain too many hydrophobic sites. PRD1 may also be considered as a relatively conservative model virus under field conditions in sandy soils at pH 6–8 and with low organic carbon content. In addition, PRD1 is more stable than MS2 at higher temperatures.

Bacteriophage  $\phi$ X174 may be a relatively conservative model virus, because of its low hydrophobicity and stability. Thus in soils with a high organic carbon content,  $\phi$ X174 would be a better choice as a model virus than for example MS2 or PRD1. However, the value of pH will strongly determine whether  $\phi$ X174 will behave conservatively. There is a significant change in its adsorption behavior when pH varies from 6 to 8, a very common pH range for most soils. At pH 6 the net surface charge of  $\phi$ X174 will be positive (high attachment), but at pH 8 it will be negative (low attachment).

FRNAPH's, as a group of naturally occurring viruses, are very useful model viruses. They behave relatively conservative, like MS2, also an FRNAPH, and they have been shown to be very persistent. Moreover, F-specific RNA bacteriophages that are present in surface water or treated wastewater that is used for recharging groundwater, consist of stable and poorly adsorbing viruses.

In practice, only few viruses have been used as model viruses. Among them, MS2 seems to meet the requirements for a model virus very well. Nevertheless, when carrying out a field experiment, it is advisable to make use of two or three model viruses that span a range of properties, like size, surface charge and hydrophobicity. In that regard MS2, PRD1 and  $\phi$ X174 make a promising cocktail.

### 2.10.4 Virus Removal

In a recent field study, it was found that virus removal was mainly determined by attachment (Schijven *et al.*, 1999). Similarly, in other field studies, virus inactivation was considered to be insignificant, and therefore virus removal was considered to be solely determined by attachment (Bales *et al.*, 1995, 1997; Pieper *et al.*, 1997; DeBorde *et al.*, 1998, 1999). Although detachment rates were not calculated in these studies, the shapes of their breakthrough curves suggest that detachment rates were much lower than attachment

rates. Although large numbers of laboratory studies have been performed to investigate the factors affecting virus transport through the subsurface, only few well-defined field studies have been carried out. Therefore, only very few data are available on attachment and detachment of viruses under field conditions. In order to be able to quantify virus removal under various field conditions, more values of attachment, detachment and inactivation rate coefficients are needed. DeBorde *et al.* (1998) proposed to generate a database of a limited number of field studies that span the range of hydrogeological settings, conditions and viruses. This review may be considered as a first step towards such a database as it provides an inventory of field studies and parameter values obtained from these studies, even though these data are incomplete. Also, in this review, an inventory has been made of collision efficiencies, values of attachment, detachment and inactivation rate coefficients for attached and free viruses both at laboratory and field scale.

Field experiments are costly, complex and often raise more questions. Thus, it may still be useful and desirable to carry out column and batch experiments to obtain parameters that can be extrapolated to the field situation. Possibly, values for collision efficiencies as found in column experiments are similar to those from field experiments, at least for short travel distances. Possibly, the ratio of  $k_{att}/k_{det}$  from column-scale may be extrapolated to field-scale under similar conditions. The values for inactivation rate coefficients as found in batch experiments may be used for prediction of virus transport at field scale. The possibility of extrapolating parameter values from laboratory scale to field scale needs to be verified. Furthermore, laboratory scale experiments are needed to compare removal of model viruses with that of pathogenic viruses.

Removal of viruses by soil passage appears to decline with distance. Possible causes for this non-linear removal may be heterogeneities within the soil as well as within the population of transported virus particles. In the aqueous environment, viruses appear to be partially attached to other colloidal particles. This may explain heterogeneity of the adsorptive characteristics of transported virus particles. The non-linearity of removal with distance has important consequences for prediction of virus removal, thus also for the calculation of setback distances that are needed to adequately protect groundwater sources and to insure adequate treatment of infiltrated surface water. Predictions of virus removal at larger distances are severely overestimated if they are based on removal data from column experiments or from small-scale field studies. To improve predictions on the removal of viruses by soil passage, knowledge of the soil heterogeneities at the location of interest is needed. Also, heterogeneity of the transported virus particles, *i.e.* the distribution of collision efficiencies within the population of virus-particles, including its cause should be investigated further.

### Acknowledgments

A.H. Havelaar, A.M. de Roda Husman, and E.J.T.M. Leenen from the National Institute of Public Health and the Environment, Bilthoven, The Netherlands are greatly acknowledged for their stimulating and expert comments.

## **Chapter 3**

# **Removal of F-specific RNA Bacteriophages and Fecal Indicator Bacteria by Dune Recharge and Estimation of Collision Efficiencies**

Schijven, J. F., Hoogenboezem, W., Nobel, P. J., Medema, G. J. and Stakelbeek, A. 1998. Reduction of FRNA-bacteriophages and faecal indicator bacteria by dune infiltration and estimation of sticking efficiencies. *Water Sci. Technol.* 38, 127-131.

### Abstract

A field study was performed to investigate removal by dune recharge and to estimate collision efficiencies of F-specific RNA bacteriophages, total and thermotolerant coliforms, fecal streptococci and spores of sulfite reducing clostridia. Removal was considered as a betabinomially distributed process and a Monte Carlo simulation was applied for estimating collision efficiencies. Removal of F-specific RNA bacteriophages within the first 2 m was  $3.8 \log_{10}$  and the collision efficiency was about 0.002. The fecal indicator bacteria were removed only  $0.9 \log_{10}$  within 2 m and the collision efficiency was 0.007. Concentrations of spores of sulfite reducing clostridia were reduced  $1.9 \log_{10}$  and their collision efficiency was about 0.009.

### 3.1 Introduction

In the Netherlands about 14 % of the total drinking water production relies on artificial recharge of pre-treated surface water in dune areas. Soil passage is considered as an important barrier to pathogenic micro-organisms but little is known in quantitative terms. To obtain more data, removal of F-specific RNA bacteriophages (FRNAPH) and fecal indicator bacteria by dune recharge was investigated at a production site near Heemskerk, at the West Coast of The Netherlands. The infiltrating water originated from the river Rhine and was pre-treated by chlorine disinfection, flocculation/sedimentation, rapid sand filtration and activated carbon filtration. This reduces enterovirus concentrations in the source water (0.02-10 viruses/l) about  $1 - 2 \log_{10}$  (Havelaar *et al.*, 1995). Due to detection limit problems, it would not be possible to show more than  $2 \log_{10}$  removal of enteroviruses by dune recharge. Instead, the present study aimed to investigate removal of FRNAPH, as a model for enteroviruses. In surface water, FRNAPH occur in 100 – 10 000 times higher numbers than enteroviruses (Havelaar *et al.*, 1993). FRNAPH have similar physical properties as enteroviruses, especially size is similar (Goyal and Gerba, 1979; Havelaar, 1993). Removal of the concentrations of total and thermotolerant coliforms (TOTCOL and THCOL), fecal streptococci (FSTR) and spores of sulfite reducing clostridia (SSRC) was also studied to evaluate their behavior compared to FRNAPH.

### 3.2 Methods

#### 3.2.1 Site Description

At the Heemskerk site, production wells were located at 15 m intervals and between two parallel recharge basins at a distance of 40 m from the banks of each of these basins, thereby creating a two-dimensional flow field. Perpendicular to the bank of one of these basins, two monitoring wells were located at a distance (L) of 2 and 4 m from the bank. Interstitial velocity ( $v$ ) of the infiltrating water was about 2 m/day. The soil consists of fine aeolic dune sand with geometric mean grain size ( $d_c$ ) of 0.2 mm and a porosity ( $n$ ) of 0.35. Two weeks before the start of the sampling about 5-10 cm of sediment was scraped off from the bottom of the basin to prevent possible effects of clogging. The pH of the water before and after recharge was between 7.5 and 7.8.

### 3.2.2 Microbiological Analyses

The recharge basin and the wells were monitored during a three-month period. Samples of 6 – 90 l from the recharge pond and of 850 – 1200 l at the observation wells were concentrated by filtration (Havelaar *et al.*, 1993) and assayed for FRNAPH as described in ISO 10705-1 (1995). TOTCOL, THCOL, FSTR and SSRC were assayed from samples of 1 l as described by Havelaar *et al.* (1993).

### 3.2.3 Calculation of Removal

It was assumed that the counted number of microorganisms in a sample at the monitoring wells followed a betabinomial distribution (Stuart and Ord, 1987). This implies that the probability  $p$  of not being removed by dune recharge is constant within a sample for each individual of a population of a certain group of microorganisms, but  $p$  is beta distributed between samples. Also, measurements before and after dune recharge were paired, which implied that variation in concentrations within a few days was neglected. Using the method of maximum likelihood, mean and percentile values for  $p$  were determined. Removal is given as  $-\log_{10}(p)$ .

### 3.2.4 Estimation of Collision Efficiencies

Dispersion of the transported microorganisms was neglected because the monitoring wells were located at only 2 and 4 m distance and the fine dune sand was rather homogeneous. It was also assumed that removal of FRNAPH and bacteria is mainly determined by attachment, detachment was neglected. Inactivation of FRNAPH and the bacteria can be neglected, because the temperature of the infiltrating water was 0.2 °C to 3 °C and travel times were only 1 – 2 days. Bacterial growth was not considered to occur under these conditions, either. Bacterial straining was also neglected. Consequently, collision efficiencies ( $\alpha$ ) were calculated from the removal data using the following equation (Martin *et al.*, 1992):

$$\alpha = -\log_{10}(p) \frac{2}{3} \frac{2.3d_c}{(1-n)\eta L} \quad (1)$$

The single collector efficiency  $\eta$  was calculated according to:

$$\eta = 1.0A_s N_{Lo}^{1/8} N_R^{15/8} + 0.00388A_s N_G^{1.2} N_R^{0.4} + 4A_s^{1/3} N_{Pe}^{-2/3} \quad (2)$$

where,  $N_R = d_p / d_c$  accounts for interception;  $N_G = d_p^2(\rho_p - \rho)g / (18\mu\nu n)$  for gravity effects;  $N_{Lo} = 4H / (9\mu d_p^2 \nu n)$  for van der Waals interactions; and  $N_{Pe} = d_p \nu n / D_{BM}$  for diffusion. In these definitions,  $d_p$  and  $d_c$  represent the particle and collector size [m], respectively;  $g = 9.8806$  [m/s<sup>2</sup>] is the gravitational acceleration;  $\rho = 999.703$  [kg/m<sup>3</sup>] and  $\rho_p$  are the density of water and the transported particle, respectively;  $\mu = \rho * 0.000947 / (T + 42.5)^{1.5}$  is the dynamic viscosity [kg/m.s] with T the water temperature [°C];  $H = 6.2 \times 10^{-21}$  is the Hamaker constant [J] for the bacterium-glass-water interface (Rijnaarts *et al.*, 1995);

$D_{BM} = K_B(T + 273)/(3\pi d_p \mu)$  is the diffusion coefficient [ $\text{m}^2/\text{s}$ ] with Boltzmann-constant  $K_B = 1.38 \times 10^{-23}$  (J/K);  $A_s = 2(1 - \gamma^5)/(2 - 3\gamma + 3\gamma^5 - 2\gamma^6)$  is Happel's porosity-dependent parameter, with  $\gamma = (1 - n)^{1/3}$ .

FRNAPH are small,  $d_p = 21 - 30$  nm (Havelaar, 1993) and their transport in the immediate vicinity of the collector surface is dominated by Brownian diffusion. In this case  $\eta$  is restricted to the last term in Equation 2. TOTCOL, THCOL and FSTR have sizes in the range of 0.3 - 1.1 by 0.6 - 6  $\mu\text{m}$ . From these sizes a geometric mean range of the bacterial diameter  $d_p = (\text{length} \times \text{width})^{1/2}$  was estimated: 0.4 - 2.6  $\mu\text{m}$ . Bacterial density  $\rho_p$  was in the range of 1040 - 1130 ( $\text{kg}/\text{m}^3$ ) as suggested by Bouwer and Rittman (1992). SSRC have an assumed size of 1  $\mu\text{m}$  and a buoyant density of 1270  $\text{kg}/\text{m}^3$  (Tisa *et al.*, 1982).

Median and percentile values of the distribution of  $\alpha$  were determined by applying the Monte Carlo approach to Equation 1. The fitted beta distribution for  $p$  was used together with uniform distributions for  $d_p$  and  $\rho_p$  within the ranges mentioned above. Monte Carlo runs comprised of 40 000 drawings and were repeated for each measured temperature.

### 3.3 Results

Concentrations of FRNAPH and the fecal indicator bacteria are shown in Table 1. After 2 m of dune recharge, efficient removal of FRNAPH of 3.8  $\log_{10}$  could be shown (Table 2). At 4 m, a removal of only an additional 0.83  $\log_{10}$  was found, but with a large uncertainty. Removal of TOTCOL and THCOL at well 1 was the lowest, but also with a large uncertainty. SSRC were reduced more efficiently than TOTCOL and THCOL. Removal of FSTR could not be estimated by the aforementioned approach, because no FSTR were detected in the samples at well 1. Only one sample of each of the fecal indicator bacteria was investigated at well 2. A colony count of TOTCOL of 10 in 1 l was found; the other indicator bacteria were not detected. Removal of the indicator bacteria at well 2 could therefore not be calculated.

The effect of temperature within the range of 0.2 - 3.0  $^{\circ}\text{C}$  had a minor effect on the estimates of the collision efficiencies (Table 2). Estimates of  $\alpha$  of FRNAPH at well 1 were about 0.002, which is low and indicates unfavorable conditions for attachment. The estimate of  $\alpha$  at well 2 is even lower, but more uncertain. Mean collision efficiencies of the faecal indicator bacteria are also low: 0.007 for TOTCOL and THCOL and 0.009 for SSRC.

Removal of Fecal Indicator Organisms by Dune Recharge

**Table 1** Concentrations of FRNAPH and fecal indicator bacteria.

	Date of sampling	Temp. °C	FRNAPH			TOTCOL	THCOL	FSTR	SSRC
			N <sup>a</sup>	l <sup>b</sup>	N/l	N/l	N/l	N/l	N/l
Infiltrating	11-12-95	1.0	738	92	8.0				
Water	22-01-96	0.5	1065	25	43	26	22	8	39
	29-01-96					49	14	1	4
	19-02-96	0.5	474	20	24	102	41	2	104
	26-02-96	4.1	1005	6.5	155	179	36	4	219
Monitoring	22-01-96	0.2	1	850	0.001	1	0	0	0
Well 1 (2 m)	29-01-96	1.5	52	1200	0.043	18	5	0	8
	19-02-96	2.1	12	1070	0.011	22	12	0	3
	26-02-96	3.0	13	1190	0.011	0	0	0	1
Monitoring	29-01-96	1.2	0	1200	< 0.0025				
Well 2 (4 m)	26-02-96	3	5	1200	0.0042	10	0	0	0

<sup>a</sup>N = Number of plaque-or colony-forming particles; <sup>b</sup>Sample volume.

**Table 2** Removal [ $-\log_{10}(p)$ ] and collision efficiencies ( $\alpha$ ) of FRNAPH and fecal indicator bacteria.

	FRNAPH <sup>a</sup>	FRNAPH <sup>b</sup>	TOTCOL <sup>a</sup>	THCOL <sup>a</sup>	SSRC <sup>a</sup>
Removal	3.8	0.83	0.85	0.86	1.9
95% CI	3.2 – 5.6	0.083 – 8.0	0.19 – 4.6	0.15 – 6.0	1.6 – 2.6
$\alpha \times 10^{-3}$ (0.2 °C)	2.0		6.8	7.7	9.7
95% CI	1.5 – 2.9		1.0 – 27	0.82 – 35	7.7 – 13
$\alpha \times 10^{-3}$ (1.5 °C)		0.78	6.6	7.5	
95% CI		0.040 – 4.0	1.0 – 26	0.78 – 34	
$\alpha \times 10^{-3}$ (2.1 °C)	1.9		6.4	7.3	9.2
95% CI	1.5 – 2.7		1.0 – 25	0.74 – 34	7.3 – 12
$\alpha \times 10^{-3}$ (3.0 °C)	1.9	0.75	6.3	7.1	9.0
95% CI	1.4 – 2.7	0.040 – 3.8	0.94 – 25	0.72 – 33	7.2 – 12

<sup>a</sup>From recharge basin to well 1; <sup>b</sup>From well 1 to well 2.

### 3.4 Discussion and Conclusions

Estimates of  $\alpha$  of FRNAPH were low, indicating unfavorable conditions for attachment. Nevertheless, FRNAPH concentrations were reduced efficiently within the first 2 m of dune recharge, which can be contributed to the small grain size of the sand and a relatively high collision efficiency. From the data it cannot be concluded, if removal of FRNAPH by dune recharge increases linearly with distance or not. Although uncertain, the estimate of  $\alpha$  of FRNAPH at well 2 was lower than at well 1. FRNAPH form a rather homogeneous group, but they likely differ in collision efficiencies, because virus adsorption to soil depends on the type and strain of virus under consideration, and may also vary between isolates of the same virus type (Goyal and Gerba, 1979). It can be reasoned that FRNAPH with higher  $\alpha$ 's attach faster, thereby lowering the average  $\alpha$  of the population of free phages, as they are transported further. This may be the case with enteroviruses too. Similar low collision efficiencies were found for MS2 in a column with silica at pH 7 (Bales *et al.*, 1993). MS2 is considered as a good conservative tracer for virus transport in sandy soils with low organic carbon content (Bales *et al.*, 1989). Thus, FRNAPH may also be considered as valuable indicators of virus transport through the subsurface.

The fecal indicator bacteria were removed to a lesser extent. Although estimated collision efficiencies were higher than that of FRNAPH, single collector efficiencies were much lower. The low collision efficiency of SSRC combined with their high persistence makes it interesting to further investigate their potential as an indicator for removal of *Cryptosporidium* by soil passage.

### Acknowledgements

Arie Havelaar is acknowledged for stimulating and expert comments on the significance of fecal indicators and Eric Evers and Peter Teunis for their expert support in data analysis.

## **Chapter 4**

# **Modeling Removal of Bacteriophages MS2 and PRD1 by Dune Recharge at Castricum, The Netherlands**

Schijven, J. F., Hoogenboezem, W., Hassanizadeh, S. M., Peters, J. H. 1999. Modelling removal of bacteriophages MS2 and PRD1 by dune recharge at Castricum, Netherlands. *Water Resour. Res.* 35, 1101-1111.

### Abstract

Removal of model viruses by dune recharge was studied at a field site in the dune area of Castricum, The Netherlands. Recharge water was dosed with bacteriophages MS2 and PRD1 for eleven days at a constant concentration in a 10-by-15-m compartment that was isolated in a recharge basin. Breakthrough was monitored for 120 days at six wells with their screens along a flow line. Concentrations of both phages were reduced about  $3 \log_{10}$  within the first 2.4 m and another  $5 \log_{10}$  in a linear fashion within the following 27 m. A model accounting for one-site kinetic attachment as well as first order inactivation was employed to simulate the bacteriophage breakthrough curves. The major removal process was found to be attachment of the bacteriophages. Detachment was very slow. After passage of the pulse of dosed bacteriophages, there was a long tail whose slope corresponds to the inactivation rate coefficient of  $0.07 - 0.09 \text{ day}^{-1}$  for attached bacteriophages. The end of the rising and the start of the declining limbs of the breakthrough curves could not be simulated completely, probably due to an as yet unknown process.

### 4.1 Introduction

In this paper, results of a field study, aimed at investigating virus removal processes during dune recharge, are presented. In the Netherlands about 14 % of the total drinking water production relies on pre-treated surface water that is artificially recharged in dune areas. When renovating or designing recharge systems, drinking water companies want to minimize side effects of artificial recharge and keep the land claim for recharge projects within limits (Peters, 1996). This may conflict with travel time and travel distance that are required for the production of safe drinking water. Drinking water is considered to be safe if certain maximum allowable concentrations of pathogenic micro-organisms are not exceeded. Maximum allowable concentrations of pathogens in drinking water can be calculated from a maximum acceptable risk of infection of one per 10 000 persons per year, drinking water consumption and dose response relations of pathogens (Regli *et al.*, 1991). For viruses, this maximum allowable concentration is  $1.8 \times 10^{-7} \text{ pfp.l}^{-1}$  (plaque forming particles/l). This approach has formed the basis for the Extended Surface Water Treatment Rule (ESWTR) and is under consideration for the Ground Water Disinfection Rule (GWDR) in the USA (Macler, 1996). In The Netherlands, a proposal for drinking water protection policy is being prepared, which leads to similar maximum allowable concentrations. Concentrations of enteroviruses in the source surface water are in the range of 0.02-10  $\text{pfp.l}^{-1}$ , but may be considerably higher due to incidental storm water overflow (Schijven *et al.*, 1996). Prior to recharge in the dune sand, the surface water is pre-treated by flocculation/sedimentation, rapid sand filtration and activated carbon filtration, thereby reducing virus concentrations by about  $1 - 2 \log_{10}$  (that is a reduction by a factor of 10 to 100). Thus, a reduction of at least  $8 \log_{10}$  may still be required by dune recharge to comply with the maximum allowable concentration of  $1.8 \times 10^{-7} \text{ pfp.l}^{-1}$ .

A field study was carried out at a location for dune recharge at Castricum, The Netherlands, in order to show that a reduction of at least  $8 \log_{10}$  is possible during the passage of water from the recharge basins to the production wells. This could not be established with the aid of pathogenic viruses because of their very low concentrations. Instead, highly concentrated suspensions of bacteriophages MS2 and PRD1 were added to the recharge water. These bacteriophages impose no health threats and their enumeration at such high concentrations

is not affected by naturally present bacteriophages. MS2 and PRD1 are considered to be good model viruses because they attach less than most pathogenic viruses and are relatively persistent during transport through the subsurface, as evidenced in the literature. Bacteriophages MS2 and PRD1 have relatively low isoelectric points (Bales *et al.*, 1991) and are therefore expected to attach poorly to most soils (Gerba, 1984). At the field site studied here, the soil mainly consists of calcareous, fine dune sand with an organic carbon content of about 0.1 – 0.2% and a pH of 7 – 8 (Stuyfzand, 1993). Under such conditions, MS2 and PRD1 have been observed to attach poorly (Bales *et al.*, 1989, 1991, 1997; Powelson *et al.*, 1990; Herbold-Paschke *et al.*, 1991; Kinoshita *et al.*, 1993; Jin *et al.*, 1997). Moreover, to minimize virus inactivation, the study was performed during the winter period. At temperatures less than 7 °C the inactivation rate of MS2 in groundwater is very low and similar to that of PRD1 (Yahya *et al.*, 1993).

The goals of this field study were as follows:

1. To measure reduction in concentrations of bacteriophages MS2 and PRD1 as a function of time and distance.
2. To gain insight into the extent and the manner with which attachment and inactivation contribute to the removal of the bacteriophages in relation to travel time and distance.
3. To evaluate the applicability of the employed transport model by comparing measured with calculated breakthrough values.

## 4.2 Site Description

The Castricum artificial recharge system was constructed in the mid-1950s, in old dune reclamation areas near the village of Castricum, about 30 km to the west of Amsterdam. The system was last expanded in 1972. Technical renovations were carried out between 1990 and 1993 together with nature conservation and development (Peters *et al.*, 1992). The system now covers around 150 hectares and has a drinking water production capacity of  $25 \times 10^6 \text{ m}^3 \cdot \text{y}^{-1}$ . Pre-treatment of the surface water is carried out near the intake points at the River Rhine and Lake IJssel. The pre-treatment consists of coagulation, sedimentation, rapid sand filtration and partially active carbon filtration. The open water area of the recharge basins is approximately 22 ha. The recharge basins are on average 0.8 m deep and have a fairly constant water level of 2.85 m above mean sea level. The water is retrieved using around 600 shallow wells, each approximately 9 m deep, distributed over 12 separate suction lines. The phreatic aquifer is around 10 m thick and consists of fine aeolian dune sands. Hydraulic conductivity is about  $12 \text{ m} \cdot \text{day}^{-1}$  (at a water temperature of 5 °C). Effective porosity with respect to flow is approximately 0.35. Below the phreatic layer is about 15 m of silt-containing sand with a lower hydraulic permeability.

Basin V was selected as the test site because its flow pattern was known and could be kept constant throughout the test period (Figure 1). The pumping rate was  $330 \text{ m}^3 \cdot \text{h}^{-1}$  from a series of 55 wells, each 10 m apart. Within basin V, a  $150\text{-m}^2$  compartment was constructed using PVC sheeting along wooden poles. The water level in the compartment was kept the same as that of the basin. The distance from this compartment to the extraction well PCQ414 was 63 m with a water travel time of approximately 40 days.

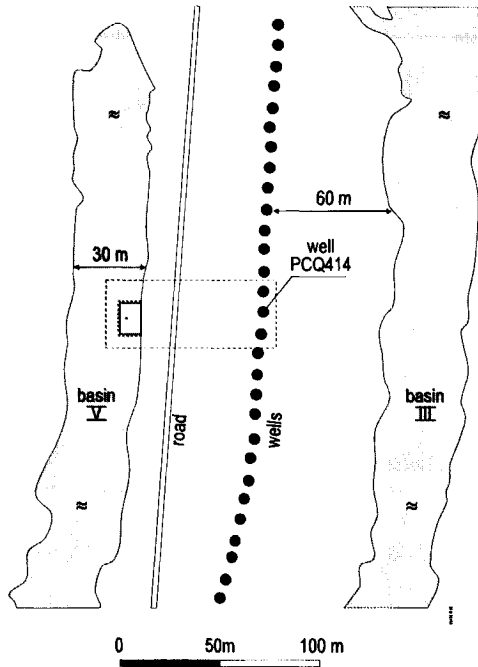


**Figure 1** Top view of field site, Castricum, The Netherlands. Isolated compartment of 150  $m^2$  is situated in basin V, opposite to abstraction well PCQ414.

Along a line almost perpendicular to the bank of basin V, six monitoring wells (W1 to W6) were installed at distances of 2.4 m, 3.8 m, 6.4 m, 10 m, 17 m and 30 m. The well screens were 0.25 m long and were positioned at different depths so as to be along a calculated flow line. A schematic representation of the groundwater situation is shown in Figure 2.

### 4.3 Experimental and Modeling Methods

#### 4.3.1 Soil Analysis

Soil samples were taken very near to the screens of the monitoring wells. Also, soil was collected from the first few centimeters of the bottom of the compartment and from the subsurface between the compartment and the first monitoring well. The samples were analyzed for grain size by laser grain size analysis (Konert and Vandenberghe, 1997) and for organic carbon content, cation exchange capacity, metal ions (Si, Ti, Al, Fe, Mg, Mn, Ca, K, Na, P) and Al-, Fe- and Mn-oxalate as described in Stuyfzand and van der Jagt (1997).

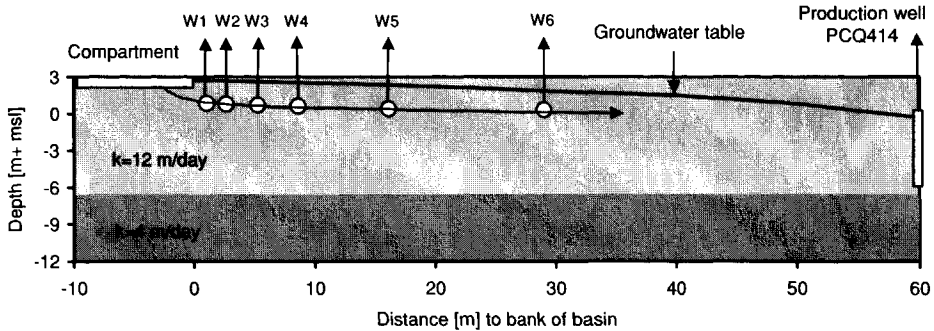


**Figure 2.** Schematic cross section of field site with compartment and monitoring wells W1 to W6. Curved arrow indicates flow path;  $k$  is the hydraulic conductivity [m/day]; depth is given in meters above sea level (msl).

#### 4.3.2 Salt Tracing

Prior to the dosage of the water with bacteriophages, sodium chloride was added to the compartment as a conservative salt tracer to estimate interstitial flow velocity and medium dispersivity. The chloride concentration of the water in the compartment was increased in one step from  $150 \text{ mg.l}^{-1}$  to  $750 \text{ mg.l}^{-1}$  and kept at this level for exactly 7 days. During 35 days electrical conductivity (EC) was measured at 10 minutes intervals in the six monitoring wells by means of fixed EC-sensors with a data logger. Water was continuously pumped from the wells at a rate of  $4 \text{ l.h}^{-1}$  to prevent distortion of the measurements by stagnant water in the borehole pipes above the screens.

#### 4.3.3 Bacteriophages Preparation and Dosage

Suspensions of 2 l with  $3 \times 10^{14}$  pfp of MS2 and 2 l with  $3 \times 10^{13}$  pfp of PRD1 were prepared as described in ISO 10705-1 (1995) using hosts *E. coli* HfrH (WG21) for MS2 and *S. typhimurium* LT2 for PRD1. Phage suspensions were pre-diluted, distributed in bottles and kept at  $5 \pm 3 \text{ }^\circ\text{C}$ .

In preparation for the dosage in the compartment,  $2.5 \times 10^{13}$  pfp of MS2 and  $2.5 \times 10^{12}$  pfp of PRD1 were added to 200 l of cold water from the recharge basin in a 1000-l PVC container. Then, uniform dilution was obtained by filling the container up to 1000 l with basin water. No stirring was applied to avoid enhancing inactivation of the phages. Dosage of the water with phages started by emptying bottles with  $2.2 \times 10^{13}$  pfp of MS2 and  $2.2 \times 10^{12}$  pfp of PRD1 at the center of the compartment. This was done in order to raise the concentrations of MS2 and PRD1 in the compartment immediately to about  $10^8$  and  $10^7$  pfp.l<sup>-1</sup>, respectively. The concentrations were kept constant by pumping phages from the 1000-l container at a rate of  $30 \text{ l.h}^{-1}$  into the compartment. When a container was empty it was replaced by another freshly prepared 1000-l container with the same concentrations of MS2 and PRD1 as before. The water in the compartment was continuously circulated with a pump to promote mixing and achieving a uniform concentration. Dosage of the phages was carried out for a period of exactly eleven days.

### 4.3.4 Bacteriophages Sampling

To avoid cross-contamination, all activities related to the dosage were kept strictly separated from sampling and were performed by different crew. Samples of 100 ml were taken from two central locations in the compartment every day at 9:00 A.M. Temperature and pH of the water in the compartment were also measured at the same time.

At the surface, the monitoring wells were covered with polyester covers. In these covers, water was constantly pumped up at a rate of  $4 \text{ l.h}^{-1}$ . This water was led through PVC pipes to a place downstream the recharge compartment to avoid its contamination. A heating cable was placed in the covers and in the PVC-pipes to avoid freezing of water. Samples were also taken at  $4 \text{ l.h}^{-1}$  by disconnecting the tubing to fill a bottle. The volume of water samples varied depending on the expected concentration. The scheme for taking samples from the monitoring wells was based on the assumption that the phages traveled equally fast as the salt tracer. Preliminary calculations were made to predict the breakthrough curves at the six monitoring wells. Starting two days before the expected breakthrough time at a given well, samples were taken every 6 hours so as to capture the rising limb of the breakthrough curve. After breakthrough was observed, samples were taken every 24 hours. Nine days later, before a decrease in phage concentration was anticipated, sampling frequency was increased to every 6 hours for about two days so as to capture the declining limb of the breakthrough curve. Then, samples were taken every 24 hours and later in the experiment once or twice a week. At wells W1 to W4, sample size was 250 ml as long as concentrations were above 10 pfu per 100 ml, then samples of 10 l were taken. At well W5 only 10-l samples were taken during breakthrough. At well W6, three samples of 1000 l were taken every 48 hours during maximum expected breakthrough. To that aim, a PVC container of 1000 l was filled at a rate of 1000 l/day. These samples of 1000 l were concentrated in the field by the filtration method as described by van Olphen *et al.* (1984). If more than one well needed to be sampled at the same time, the well with the lowest breakthrough concentration, usually farthest away from the compartment, was sampled first. Temperature and pH were immediately measured in an additional (small) sample. All samples were collected in separate cooling-boxes and processed for phage-enumeration within 18 hours.

### 4.3.5 Inactivation Rate of Free Bacteriophages in Water

The field study was performed in the wintertime, when water temperature is low and thus inactivation is minimal. Nevertheless, in contrast to column studies inactivation is not negligible because of longer time scales and larger distances. To measure inactivation of the phages in the water phase during the experiment, both field and laboratory experiments were carried out. In the field, a sample of 2 l was taken from well W1 at a rate of  $4 \text{ l.h}^{-1}$  on the third day of maximum breakthrough. This sample was distributed over 20 bottles of 100 ml, which were kept in a dark plastic bag hanging in the basin outside the compartment. Once a day, a bottle was taken from this bag for phage counting. In the laboratory, 2 l of three different waters (peptone saline, water from the recharge basin, and water from well W1 after breakthrough when phage concentrations were less than 1 pfu-l) were dosed with MS2 and PRD1 at about the same concentration as the maximum breakthrough concentration at well W1. These suspensions were also distributed over 20 bottles of 100 ml, stored in the dark at  $5 \pm 3 \text{ }^\circ\text{C}$  and analyzed regularly for a period of about one month. In

this manner, inactivation rates under four different conditions were determined: under field conditions in well water and under laboratory conditions in peptone saline, compartment water and well water.

#### 4.3.6 Bacteriophage Enumeration

All samples were split in halves. MS2 was assayed as described in ISO 10705-1 (1995) using host strain WG49 (Havelaar *et al.*, 1984). PRD1 was assayed according to ISO 10705-1 using *S. typhimurium* LT2 as the host, omitting nalidixic acid in the top agar layer. If concentrations in the 100-ml samples were expected to be higher than  $10^4$  pfpl<sup>-1</sup>, 1 ml of the appropriate dilutions was applied to 9-cm petri-dishes with Tryptone Yeast Glucose Agar (TYGA). Samples of 100 ml with expected concentrations in the range of  $10$  to  $10^4$  pfp.l<sup>-1</sup> were divided in 20 portions of 5 ml and applied separately to 15-cm petri-dishes with TYGA. Samples of 10 l were concentrated by ultra-filtration as described by van Olphen *et al.* (1984) to about 20 ml. Samples of 1000 l were filtrated with Milligard 1.2  $\mu$ m cartridge filters (Millipore) in the field. These filters were eluted with beef extract, pH 9 and concentrated further by ultra-filtration to a final volume of about 20 ml. All concentrated samples were applied in aliquots of about 5 ml to 15-cm petri-dishes with TYGA.

#### 4.3.7 Elution Experiments

A soil sample of about 5 kg was taken from a location next to the screen of W1 at day 45 of the field experiment. This was done in order to measure the amount of attached bacteriophages that are still viable and to investigate detachment as a function of pH. The sample was kept saturated by an excess of water from the same location. Five 6-cm columns were made with soil from this sample in glass cylinders with a diameter of 9 cm. At  $5 \pm 3$  °C, bacteriophages were eluted from a column with 400 ml of water from the recharge basin (no phages added) and from columns using the same water but with pH adjusted to 8, 9 and 10. One column was eluted with 600 ml of beef extract at pH 9. The pore-water velocity was adjusted to  $1.5 \text{ m.day}^{-1}$  to approximate field conditions. Fractions of 11 ml were analyzed for pH and for MS2 and PRD1 concentrations.

#### 4.3.8 Conceptual Model

The major transport processes included in the mathematical model of our field experiments are advection, hydrodynamic dispersion, attachment, detachment and inactivation. The water flow at the field site has a predominantly one-dimensional direction: from the recharge basin towards the line of wells. The temporal changes in flow velocity are negligible. Therefore, it was assumed that the water flow is steady state and one-dimensional. This allowed the use of analytical solutions. In one dimension, dispersion is equal to the dispersivity times flow velocity:  $\alpha_L v$ .

Attachment of MS2 and PRD1 has been shown to be reversible and kinetically limited (Bales *et al.*, 1991, 1993, 1997; Kinoshita *et al.*, 1993). In columns with sandy soil (Bales *et al.*, 1989) and silica beads (Bales *et al.*, 1991) dispersion of both MS2 and PRD1 and the salt tracer have been shown to be similar. In field studies where preferential flow was absent, PRD1 was transported at about the same rate as a conservative salt tracer (Bales *et*

*al.*, 1995; Pieper *et al.*, 1997). Therefore, phage transport may be simulated using a one-site kinetic model (Bales *et al.*, 1991; McCaulou *et al.*, 1994; Toride *et al.* 1995). Inactivation is modelled as first-order decay with different rate coefficients for free and attached phages. The governing equations read:

$$\frac{\partial C}{\partial t} = \alpha_L \nu \frac{\partial^2 C}{\partial x^2} - \nu \frac{\partial C}{\partial x} - k_{att} C - \mu_f C + k_{det} \frac{\rho_B}{n} S \quad (1)$$

$$\frac{\rho_B}{n} \frac{\partial S}{\partial t} = k_{att} C - k_{det} \frac{\rho_B}{n} S - \mu_s \frac{\rho_B}{n} S \quad (2)$$

Subject to boundary conditions  $C = C_0$  at  $x = 0$  and  $\frac{\partial C}{\partial x} = 0$  at  $x = \infty$ . Here,  $C$  is the concentration of free phages [pfp.m<sup>-3</sup>];  $S$  is the concentration of attached phages [pfp.kg<sup>-1</sup>];  $t$  is the time [days];  $x$  is the distance [m];  $\alpha_L$  is the dispersivity [m];  $\nu$  is the average interstitial water velocity [m/day];  $\rho_B$  is the dry bulk density [kg.m<sup>-3</sup>];  $\theta$  is the porosity [-];  $k_{att}$  and  $k_{det}$  are the attachment and detachment rate coefficients, respectively [day<sup>-1</sup>];  $\mu_f$  and  $\mu_s$  are the inactivation rate coefficients of the free and attached phages, respectively [day<sup>-1</sup>]. For our model computations, a modified version of the computer code CXTFIT (Toride *et al.*, 1995) has been used. This code is based on analytical solutions of equilibrium and nonequilibrium transport models, including governing Equations 1 and 2.

## 4.4 Evaluation of Results and Parameter Estimation

### 4.4.1 Soil Analysis and Water Chemistry

Results of chemical and physical analysis of soil samples are given in Table 1. The samples taken near wells W1, W4 and W6 show no differences in composition. However, the samples that were taken between the compartment and well W1 show that the organic carbon content is higher near the compartment (0.4%) and then decreases to 0.1 – 0.2%

**Table 1.** Chemical and physical analysis of soil samples

	A <sup>a</sup>	B <sup>a</sup>	C <sup>a</sup>	D <sup>a</sup>	E <sup>a</sup>	W1	W4	W6
Distance <sup>b</sup>	0	-	-	-	2.4	2.4	10	30
Depth <sup>b</sup>	0-0.05	0.1-0.15	0.3-1.5	1-1.5	2-2.3	2-2.3	3.2-3.3	6-6.5
Grain size <sup>c</sup>	235	240	240	203	209	209	209	203
Clay <sup>d</sup> (≤2 μm)	0.55	0.49	0.49	0.70	0.50	0.85	0.77	0.86
Silt <sup>d</sup> (>2, ≤53 μm)	1.19	2.55	0.98	1.52	1.07	3.42	2.14	4.28
Sand <sup>d</sup> (>53 μm)	98.26	97.26	98.53	97.78	98.43	95.70	96.87	94.84
f <sub>oc</sub> <sup>d</sup>	0.37	0.25	0.15	2.7	0.088	0.10	0.20	0.079
CEC <sup>e</sup>	16	13	8.6	102	6.5	14	15	14
Al-oxalate <sup>f</sup>	0.20	0.18	0.23	0.23	0.19	0.32	0.27	0.41
Fe-oxalate <sup>f</sup>	1.0	1.1	1.1	0.56	0.73	1.2	1.1	1.7
Mn-oxalate <sup>f</sup>	0.026	0.022	0.012	0.021	0.0047	0.019	0.020	0.020

<sup>a</sup>A: sample taken from bottom of compartment. B-E: samples taken between bottom of compartment and W1; <sup>b</sup>[m]; <sup>c</sup>Geometric mean [μm]; <sup>d</sup>[%]; <sup>e</sup>[meq.kg<sup>-1</sup>]; <sup>f</sup>[g.kg<sup>-1</sup> d.w.].

**Table 2.** Chemistry of recharge and production well water during field experiment.

	Recharge water		Production well water	
	Average	Standard deviation	Average	Standard deviation
Electric conductivity <sup>a</sup>	822	57	914	11
Dissolved oxygen <sup>b</sup>	9.7	1.9	1.1	0.38
Ca <sup>2+</sup> <sup>c</sup>	2200	220	2300	52
Mg <sup>2+</sup> <sup>c</sup>	520	38	630	19
Fe (dissolved) <sup>c</sup>	1.9	1.7	8.8	3.2
HCO <sup>3-</sup> <sup>c</sup>	2400	220	2800	41
Cl <sup>-</sup> <sup>c</sup>	4000	37	4500	220

<sup>a</sup>[ $\mu\text{S}\cdot\text{cm}^{-1}$ ]; <sup>b</sup>[ $\text{mg}\cdot\text{l}^{-1}$ ]; <sup>c</sup>[ $\mu\text{M}$ ].

towards W1. The very high organic carbon content (2.7%) at 1 – 1.5 m (sample D) is most probably only a local feature. Related to the organic carbon content is the cation exchange capacity, which indeed shows a similar spatial pattern. The geometric mean grain size of samples A – C is higher in combination with a lower percentage of clay and silt than the other samples. The values of the metal-ions and metal-oxalates show some variability with distance, but no significant trends. In Table 2, the chemistry of the water in the recharge basin and at the production well are given (data from drinking water company). EC is twice as high as in the water of the contaminated zone reported by Pieper *et al.* (1997), because concentrations of chlorine, bicarbonate and bivalent cations are much higher. During soil passage, dissolved oxygen concentrations decrease, whereas the dissolved iron concentrations increase, due to oxidation of iron sulfides (Stuyfzand, 1993).

#### 4.4.2 Description of the Breakthrough Curves of the Salt Tracer and the Phages

The concentration of MS2 measured in the recharge compartment was on the average  $1.1 \times 10^8$  pfp.l<sup>-1</sup> and varied between  $5.4 \times 10^7$  and  $2.1 \times 10^8$  pfp.l<sup>-1</sup>. The concentration of PRD1 was on the average  $1.0 \times 10^7$  pfp.l<sup>-1</sup> and varied between  $5.4 \times 10^6$  and  $2.4 \times 10^7$  pfp.l<sup>-1</sup>. This may be ascribed to variations in power supply to the dosage pump, but not to mixing problems in the compartment. This can be deduced from the fact that EC-measurements showed complete mixing of the salt in the compartment within 30 minutes. The temperature of the recharge water increased gradually from 2 to 7 °C during the first 52 days and that of the monitoring wells from 3 to 9 °C during the first 93 days. Temperature of the recharge water fluctuated  $\pm 1$  °C during the day. The pH of the water varied between 7.3 and 8.3. At wells W1 to W4, complete breakthrough was monitored but at W5 and W6 only maximum breakthrough concentrations were measured (68 and 2.2 pfp.l<sup>-1</sup> at W5 and 0.83 and 0.060 pfp.l<sup>-1</sup> at W6, of MS2 and PRD1 respectively). The breakthrough curves of phages and salt tracer for wells W1 to W4 are shown in Figures 3 and 4 with the salt breakthrough curve projected over a period of 11 days for the sake of comparison. Maximum EC-levels were about 2700  $\mu\text{S}\cdot\text{cm}^{-1}$  at all wells. This implies that there was no dilution. As expected, breakthrough times of MS2 and PRD1 at wells W1 to W4 were the same as that of the salt tracer.

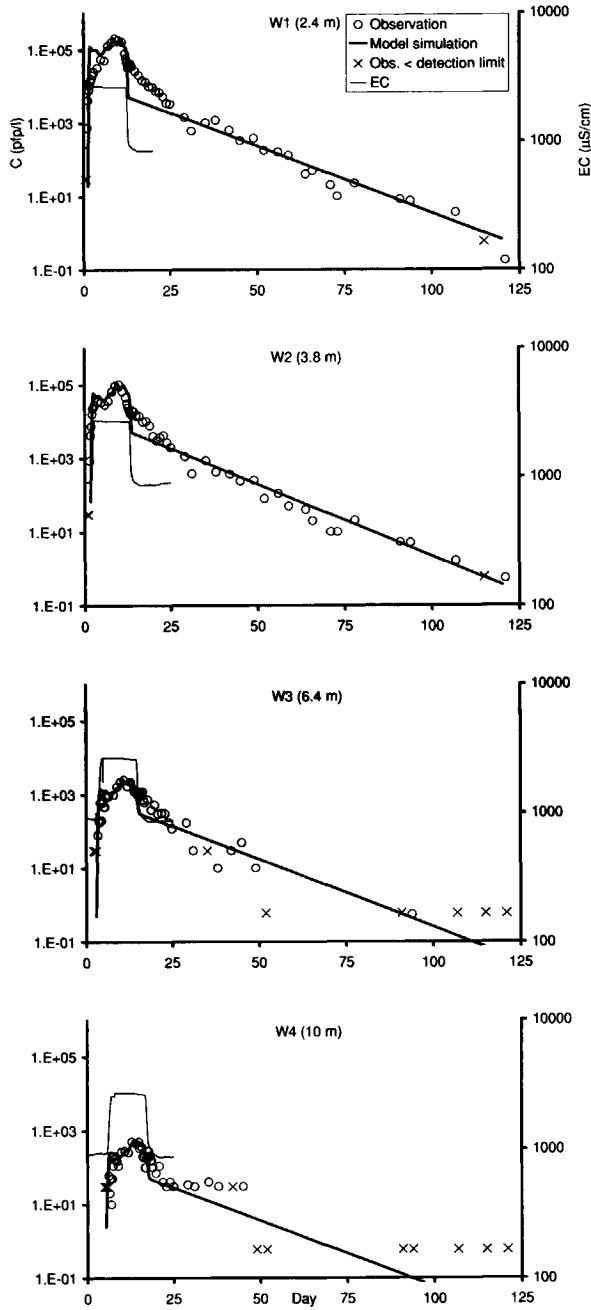


**Figure 3** Breakthrough curves of sodium chloride (measured as electrical conductivity = EC) and MS2 at wells W1 to W4. Detection limit depends on sample volume.

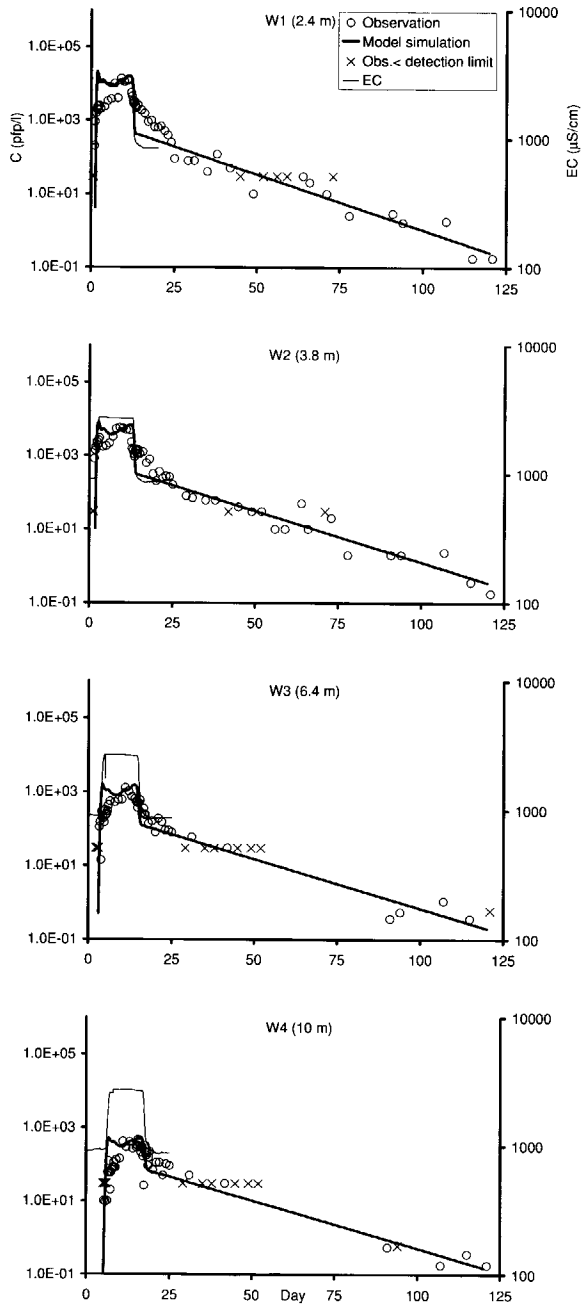


**Figure 4** Breakthrough curves of sodium chloride (measured as electrical conductivity = EC) and PRD1 at wells W1 to W4. Detection limit depends on sample volume.

**Table 3** *Estimated values of model parameters*

			W1	W2	W3	W4	W5	W6
NaCl	x	m	2.4	3.8	6.4	10.2	17.1	30.1
	v	m.day <sup>-1</sup>	1.41	1.56	1.59	1.57	1.52	1.19
	$\alpha_L^a$	m	0.008	0.012	0.017	0.017	0.0096	0.08
MS2	$\mu_s$	day <sup>-1</sup>	0.085	0.092	0.092			
	$k_{att}$	day <sup>-1</sup>	4.1	3.2	2.8	2.0	1.3	0.8
	$\eta^b$		0.61	0.60	0.56	0.57	0.58	0.69
	$\alpha^c$		0.0014	0.0010	0.00092	0.00065	0.00043	0.00027
	$k_{det}$	day <sup>-1</sup>	0.00087	0.0016	0.0026	0.0018	0.00052	0.0030
PRD1	$\mu_s$	day <sup>-1</sup>	0.071	0.067	0.067	0.067		
	$k_{att}$	day <sup>-1</sup>	4.0	3.1	2.2	1.5	1.3	0.7
	$\eta^a$		0.34	0.32	0.31	0.32	0.32	0.38
	$\alpha^c$		0.0024	0.0018	0.0013	0.00086	0.00075	0.00043
	$k_{det}$	day <sup>-1</sup>	0.00077	0.0011	0.0018	0.0025	0.0021	0.0034

<sup>a</sup>Dispersivity, <sup>b</sup>single collector efficiency, <sup>c</sup>collision efficiency.

#### 4.4.3 Parameter Estimation and Sensitivity Analysis

Model parameters that needed to be evaluated were  $v$ ,  $\alpha_L$ ,  $k_{att}$ ,  $k_{det}$ ,  $\mu_1$  and  $\mu_s$ . The quantities  $v$  and  $\alpha_L$  were found from fitting the salt breakthrough curves using CXTFIT with the values of  $k_{att}$ ,  $k_{det}$ ,  $\mu_1$  and  $\mu_s$  set to zero. The resulting values are shown in Table 3. The flow velocity variations were relatively small between wells W1 and W5. The values for dispersivity ( $\alpha_L$ ) were very low, confirming that the soil was rather homogeneous.

The inactivation rates of free phages were determined directly from laboratory measurements as described in section 4.4.4. The remaining parameters,  $k_{att}$ ,  $k_{det}$  and  $\mu_s$ , can in principle be determined with the aid of CXTFIT in inverse simulation mode. However, our computations and sensitivity analysis have shown that CXTFIT is not suitable for fitting the phages breakthrough curves. The fitted breakthrough curve obtained with CXTFIT in inverse mode is shown in Figure 5a (semi-log scale) and Figure 5b (linear scale). The corresponding values for parameters  $k_{att}$ ,  $k_{det}$  and  $\mu_s$  are given in column A of Table 4. The fitted breakthrough curve deviates significantly from the observed breakthrough curve both at high concentrations (curve A in Figure 5b) and at the tail section (curve A in Figure 5a). This is due to the fitting procedure used in CXTFIT, where model parameters are estimated by minimizing the sum of squared residuals. Because the tail concentrations are orders of magnitude smaller than the maximum breakthrough concentration, their weight in the fitting procedure will be negligible. This procedure does not account properly for the processes that affect the tail section. Therefore, a different approach was chosen to estimate the parameter values of  $k_{att}$ ,  $k_{det}$  and  $\mu_s$ . This is described in detail in the following sections.

In order to show the effects of various parameters on the shape of the breakthrough curve and to aid our parameter estimation strategy, the following limited sensitivity analysis was carried out. Starting with the set of parameter values suggested by CXTFIT (column A in

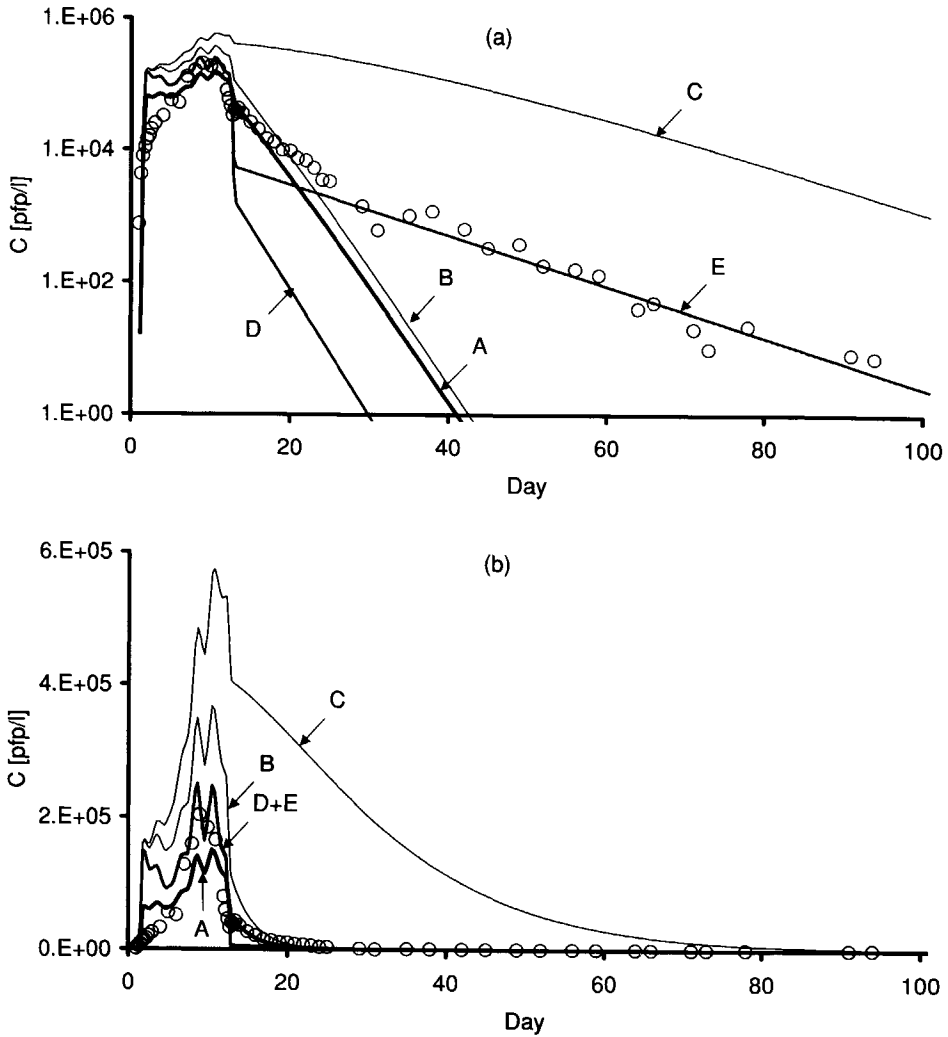


**Figure 5** Breakthrough curves of MS2 at well W1 with concentrations on a logarithmic scale (a) and a linear scale (b). A : Fitted curve using CXTFIT in inverse mode. B, C, D and E: Simulated curves. For corresponding parameter values see Table 4.

**Table 4** Sensitivity analysis: Parameter values used to calculate the breakthrough curves in Figure 3a and b.

	A	B	C	D	E
$k_{att}$ [day <sup>-1</sup> ]	4.6	4.0	4.0	4.0	4.0
$k_{det}$ [day <sup>-1</sup> ]	0.041	0.041	0.041	0.0008	0.0008
$\mu_s$ [day <sup>-1</sup> ]	0.44	0.44	0.09	0.44	0.09

Table 4),  $k_{att}$  was decreased from 4.6 to 4.0 and the other parameter values were kept constant (column B of Table 4). This resulted in curve B of Figure 5a and 5b with higher maximum concentrations than observed. Next, the values of  $\mu_s$  and  $k_{det}$  were varied over a wide range. We found that the tail slope is mainly determined by the value of  $\mu_s$ , whereas its intercept is mainly affected by the value of  $k_{det}$ . Some typical values are given in Table 4. Keeping  $k_{det}$  constant, variation of  $\mu_s$  results in the change of the tail slope with little effect on the intercept (compare curves A, B and C or D and E). However, variation of  $k_{det}$  at a constant  $\mu_s$  changes the intercept significantly but has a small effect on the slope (compare curves B and D or C and E). Curve E comes closest to the observed breakthrough curve. In all cases,  $k_{det}$  is much smaller than  $k_{att}$ . In none of the simulations it was possible to fit the rising and declining limbs of the observed breakthrough curve completely. One of the major assumptions in our model is that the transport is one-dimensional. This is justified by the fact that the flow is almost everywhere horizontal and the dispersion is very small. The influence of dispersion on the calculated breakthrough curves has been investigated by varying the value of dispersivity from 0.008 to 0.024 m. The corresponding values of  $k_{att}$  that were needed to obtain the same breakthrough curves were found to be 4.0 and 4.1, respectively. This shows that variability of  $\alpha_L$  does not significantly affect the estimation of  $k_{att}$ . The effect of lateral dispersion is expected to be even smaller as transversal dispersivity is about ten times less than longitudinal dispersivity. Therefore, a one-dimensional modeling approach is valid.

#### 4.4.4 Inactivation Rates of Free Bacteriophages

Results of the inactivation experiments for free phages are shown in Figure 6. It is evident that the inactivation rate is first order under all conditions. MS2 was stable in peptone/saline. Rate coefficients calculated from these curves are given in Table 5. Inactivation of MS2 in the field test was less than in the laboratory test in water from either the compartment or the well; this could be due to temperature effects. PRD1 was very stable under all conditions in the laboratory, which is consistent with the reported stability of this phage (Yahya *et al.*, 1993). Surprisingly, however, PRD1 was found to inactivate at a rate of  $0.12 \text{ day}^{-1}$  in the field test, four times faster than MS2 ( $0.030 \text{ day}^{-1}$ ). Both phages were enumerated from exactly the same bottles; thus, conditions were exactly the same for both phages. Naturally, for the simulation of the breakthrough curves of MS2 and PRD1, the values of  $\mu_i$  obtained from the field inactivation experiment were used. These values are well within the range of values reported by others. The inactivation rate coefficient of MS2 in groundwater at  $4 \text{ }^\circ\text{C}$  has been reported to be  $0.028 - 0.15 \text{ day}^{-1}$  by Yates *et al.* (1985) and  $0.041 \text{ day}^{-1}$  by Powelson *et al.* (1990). Also, according to Yahya *et al.* (1993) the inactivation rate coefficients of both MS2 and PRD1 at  $7 \text{ }^\circ\text{C}$  are  $0 - 0.092 \text{ day}^{-1}$ . It should be noted that values of inactivation rate coefficients presented in this paper (in  $\text{day}^{-1}$  units) are a factor of 2.3 higher than found in many other works. This is because inactivation rate coefficients are often expressed in units of  $\ln 10$  per day (see *e.g.* Yates *et al.*, 1985); this unit is equivalent to the value in  $\text{day}^{-1}$  divided by 2.3 ( $\ln 10$ ).

**Table 5** Inactivation rate coefficient  $\mu_i$  [ $\text{day}^{-1}$ ] for MS2 and PRD1

Experimental conditions		MS2	PRD1
At laboratory ( $5 \pm 3$ °C)	Peptone/saline	0.0019	0.0060
	Recharge water	0.044	0.0074
	Water from W1	0.064	0.0094
At field site ( $2 - 5$ °C)	Water from W1	0.030	0.12

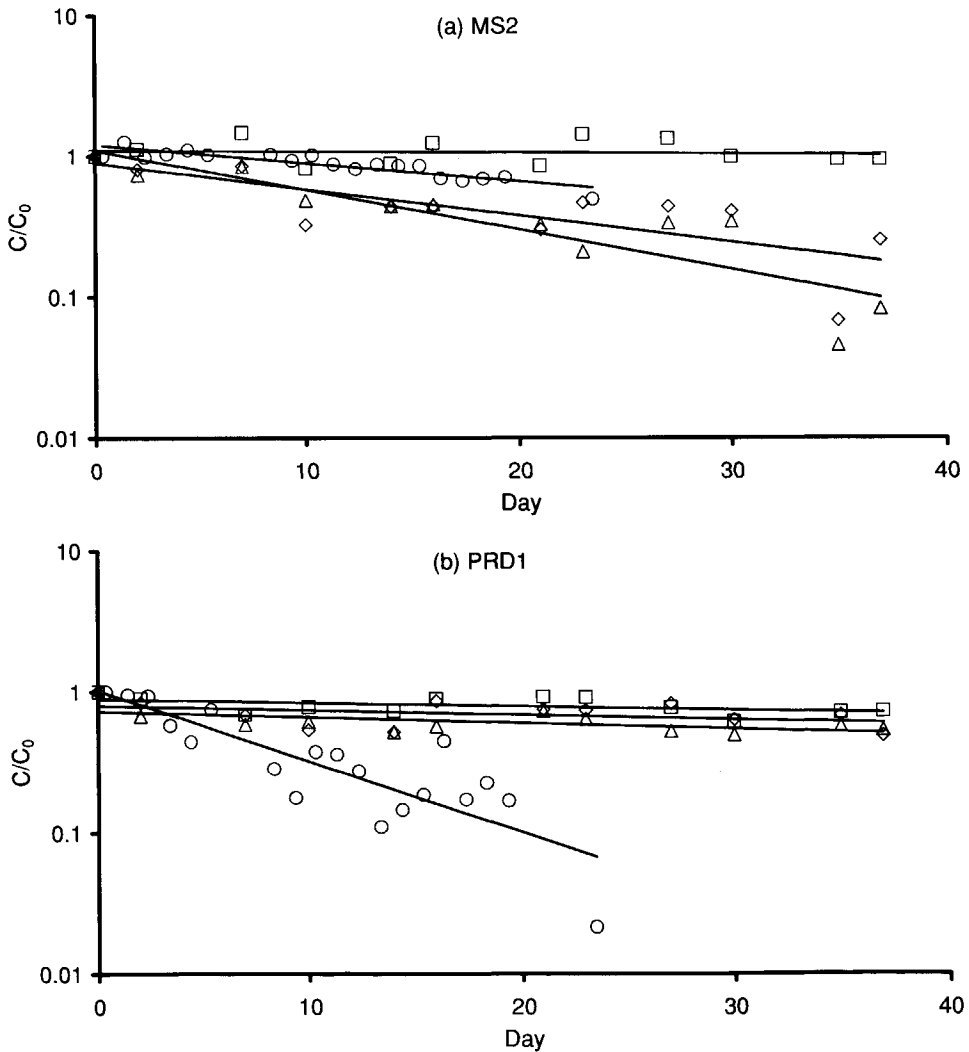


**Figure 6** Inactivation of MS2 (a) and PRD1 (b) at the laboratory in peptone/saline (squares), in compartment water (diamonds), in W1 well water (triangles) and at the field site in W1 well water (circles). Lines are the corresponding linear regression lines.

#### 4.4.5 Inactivation Rates of Attached Bacteriophages

As pointed out earlier, the slope of the tail of the breakthrough curves is mainly determined by the value of  $\mu_s$ . Here, an approximate solution for the tail is obtained and then measured breakthrough tails are used to evaluate  $\mu_s$ . When a pulse of dosed phages has passed a position  $x$ , the attachment starts to decrease. Assuming that dispersion is negligible and rewriting Equations 1 and 2 in a Lagrangian reference frame (i.e. following the water motion), we obtain:

$$\frac{\partial C}{\partial t} = -(k_{att} + \mu_l)C + k_{det} \frac{\rho_B}{n} S \quad (3)$$

$$\frac{\rho_B}{n} \frac{\partial S}{\partial t} = -(k_{det} + \mu_s) \frac{\rho_B}{n} S + k_{att} C \quad (4)$$

Elimination of  $S$  between these two equations yields:

$$\frac{\partial^2 C}{\partial t^2} + \lambda_1 \frac{\partial C}{\partial t} + \lambda_2 C = 0 \quad (5)$$

where  $\lambda_1 = k_{att} + \mu_l + k_{det} + \mu_s$  and  $\lambda_2 = k_{att}\mu_s + k_{det}\mu_l + \mu_l\mu_s$ .

The solution of Equation 5 is

$$C = C_0 \exp(-\xi t) \quad (6)$$

$$\text{with, } \xi = \frac{1}{2} \lambda_1 \left[ 1 - \sqrt{1 - \frac{4\lambda_2}{\lambda_1^2}} \right] \quad (7)$$

Taylor series expansion of the term inside the brackets and neglecting second and higher order terms yields:

$$\xi = \frac{1}{2} \lambda_1 \left[ 1 - \left( 1 - 2 \frac{\lambda_2}{\lambda_1^2} + \frac{1}{2} \left( \frac{\lambda_2}{\lambda_1^2} \right)^2 + \dots \right) \right] \cong \frac{\lambda_2}{\lambda_1} = \left( \mu_s + \frac{k_{det}\mu_l + \mu_l\mu_s}{k_{att}} \right) \left( 1 + \frac{\mu_l + k_{det} + \mu_s}{k_{att}} \right)^{-1} \quad (8)$$

Now, because  $k_{att}$  is orders of magnitude higher than the other rate coefficients,  $\xi$  may be approximated with  $\mu_s$  so that the solution (6) becomes:

$$C = C_0 e^{-\mu_s t} \quad (9)$$

Equation 9 shows that the slope of the tail of the breakthrough curve in a semi-log graph is mainly determined by  $\mu_s$ . Based on this, the values of  $\mu_s$  from the breakthrough curves were estimated, and the results are given in Table 3.

At wells W1 to W3,  $\mu_s$  for MS2 varied only slightly, from 0.085 to 0.092 day<sup>-1</sup>. The value of 0.092 day<sup>-1</sup> was also employed in simulation of breakthrough at W4. Likewise,  $\mu_s$  for PRD1 at wells W1 to W5 was fairly constant: 0.067 – 0.071 day<sup>-1</sup>. It is evident that the inactivation rate of attached MS2 was higher than that of free MS2. The same can be said for attached PRD1 compared to free PRD1 in the laboratory test but not compared to PRD1 in the field test. An increase in inactivation rate of MS2 and PRD1, by a factor 2 to 3, due to attachment to soil has also been reported by Blanc and Nasser (1996).

#### 4.4.6 Attachment Rate Coefficients

For the evaluation of  $k_{att}$  an approximate solution of Equation 1 was developed for the duration of the experiment where maximum breakthrough concentrations ( $C_{max}$ ) were observed. In this period, a steady state situation was assumed to have been reached. Neglecting detachment, Equation 1 then reads:

$$\alpha_l v \frac{\partial^2 C_{max}}{\partial x^2} - v \frac{\partial C_{max}}{\partial x} - (k_{att} + \mu_l) C_{max} = 0 \quad (10)$$

The solution of this equation is

$$C_{max} = C_0 \exp(-\psi x) \text{ where, } \psi = \frac{\left[ \sqrt{1 + \frac{4\alpha_l}{v} (k_{att} + \mu_l)} \right] - 1}{2\alpha_l} \quad (11)$$

Here,  $C_0$  is the maximum concentration of dosed bacteriophages. This solution can be rearranged to:

$$k_{att} = v \frac{\left[ 1 - 2\alpha_l \frac{2.3}{x} \log_{10} \left( \frac{C_{max}}{C_0} \right) \right]^2 - 1}{4\alpha_l} - \mu_l \quad (12)$$

With  $\mu_l$  already determined from inactivation experiments, this equation can be used to estimate the value of  $k_{att}$ . The results are reported in Table 3. Apparently,  $k_{att}$  decreases with distance from about 4 to 0.8 day<sup>-1</sup> for both phages.

Attachment rate coefficient  $k_{att}$  is known to depend on microscale flow and diffusion characteristics as well as surface properties of viruses and soil grains. It is possible to exclude the effects of flow and diffusion by expressing the attachment rate of viruses in terms of collision efficiency  $\alpha$ , defined by (Yao *et al.*, 1971; Bales *et al.*, 1991, 1993; McCaulou *et al.*, 1994; Penrod *et al.*, 1996):

$$\alpha = \frac{2}{3} \frac{d_c}{(1-\theta)} \frac{k_{att}}{v \eta} \quad (13)$$

Here,  $d_c$  is the average diameter of the collector (grains) [m]. MS2 and PRD1 are small in size (26 en 62 nm, respectively) and their transport in the immediate vicinity of the soil grains is dominated by Brownian diffusion (Penrod *et al.*, 1996). Thus, the single collector efficiency  $\eta$  was calculated as given by Penrod *et al.* (1996).

Values for  $\alpha$  are also given in Table 3. Similar to  $k_{att}$ ,  $\alpha$  decreases with distance from 0.0014 to 0.00027 for MS2 and from 0.0024 to 0.00043 for PRD1. These very low values of  $\alpha$  reflect unfavorable conditions for attachment, mainly because of the relatively high pH of 7.3 – 8.3.

#### 4.4.7 Detachment Rate Coefficients

Given the values of  $k_{att}$ ,  $\mu_1$  and  $\mu_s$  as described above, the value of  $k_{det}$  was adjusted so as to obtain a best fit to the measured breakthrough curve. These values are given in Table 3. It is apparent that, compared to attachment, detachment is very slow.

#### 4.4.8 Removal versus Distance

Figure 7 shows reduction of the maximum concentrations of both phages versus distance. Removal of both phages appeared to be very similar. It can be seen that removal is not linear with distance. However, linear regression analysis of the removal data with distance from wells W1 to W6 revealed high correlation coefficients of 93% and 97% for MS2 and PRD1, respectively. This suggests that removal was linear with distance between the monitoring wells and that the first 3.1 and 2.6  $\log_{10}$ -removal in concentrations of MS2 and PRD1, respectively, occurred somewhere before the first well at a higher attachment rate.

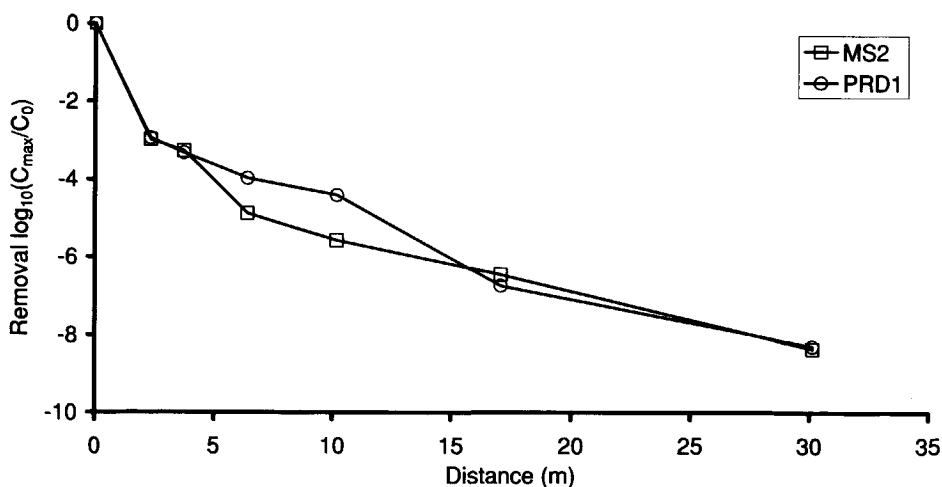


Figure 7 Removal ( $\log_{10}(C_{max}/C_0)$ ) of MS2 and PRD1 versus distance (m).

**Table 6** Elution of MS2 and PRD1 from soil columns at different pH

Influent pH	7.5	8	9	10	9 + beef-extract
Effluent pH	7.5 - 7.9	7.7 - 8.0	8.1 - 8.5	7.8 - 8.9	8.2 - 8.7
*Column dry weight [g]	576	572	615	572	607
<i>Number of MS2-phages:</i>					
Eluted	129	117	191	339	430
†Simulated (CXTFIT)	33000	33000	36000	33000	35000
<i>Number of PRD1-phages:</i>					
Eluted	0	0	2	30	18
‡Simulated (CXTFIT)	4600	4600	4900	4600	4900

\*24 hours 105 °C; †MS2: C(measured) = 330 pfp.l<sup>-1</sup>; C(simulated) = 358 pfp.l<sup>-1</sup>; S(simulated) = 58 pfp.g<sup>-1</sup>; ‡PRD1: C(measured) = 33 pfp.l<sup>-1</sup>; C(simulated) = 48 pfp.l<sup>-1</sup>; S(simulated) = 8 pfp.g<sup>-1</sup>.

#### 4.4.9 Elution Experiments

The results of the elution experiments described in section 4.3.7 are shown in Table 6. Total numbers of bacteriophages eluted at different pH are given. With increasing pH, more phages were eluted. This effect seems stronger for PRD1 than for MS2. Nevertheless, the amount of phages that detached is much smaller than predicted by the model. According to the simulation with CXTFIT (Toride *et al.*, 1995), the number of phages that should have been eluted by beef-extract is about 35000 for MS2 and 4900 for PRD1. These values are 80 times higher for MS2 and 270 times higher for PRD1 than actually was eluted with beef-extract. Assuming that elution with beef-extract at pH 9 released all attached phages, it seems that phages were removed already at a much higher attachment rate prior to well W1. This is in agreement with the high removal rate between the compartment and W1.

#### 4.5 Discussion and Conclusions

Removal of model viruses by dune recharge was studied at a field site in the dune area of Castricum, The Netherlands. After dosage of the recharge water with bacteriophages MS2 and PRD1, their breakthrough was followed at different monitoring wells along a flow line. A one-site kinetic model was employed to estimate parameter values for attachment, detachment and inactivation rate coefficients. Comparison of calculated and measured breakthrough curves shows that maximum breakthrough concentrations and the tail sections are modeled satisfactorily. Noticeable discrepancies are found at the end of the rising limbs and the onset of the declining limbs. This effect, however, becomes less and less pronounced, as we get farther away from the recharge basin. This indicates that:

1. There is an unknown removal/release process, which is not being modeled here.
2. This process seems to be present mainly in the section before W1.
3. The extra attachment process seems to be reversible, as we can find a higher measured concentration at the declining limb than calculated.

At this stage we can only speculate on the nature of this extra process. One explanation may be that the attachment rate coefficient is proportional to the concentration of free phages and the detachment rate coefficient is proportional to the concentration of attached phages. Another possibility is that due to heterogeneities of the soil or within the phage population,

attachment and detachment rate coefficients are much higher in the section before W1 (see below).

This field study has shown that at least 8 log<sub>10</sub> reduction of phage concentration can be achieved within 30 m of passage in sandy dunes for both MS2 and PRD1. This corresponds to a travel time of about 25 days. Within the first 2.4 m, reduction was about 3 log<sub>10</sub> and an additional 5 log<sub>10</sub> was removed within 30 m. Thus, the reduction in concentrations of MS2 and PRD1 was not linear with distance. The removal of the bacteriophages before reaching W1 is much higher than thereafter. After W1, the reduction increased linear with distance, whereby the maximum breakthrough concentrations were mainly determined by attachment. The following observations indicate the existence of an extra removal process before well W1:

1. Linear regression of the reduction between wells W1 and W6 shows a correlation coefficient of 93% and 97% with distance for MS2 and PRD1, respectively. Deviations from the regression line probably reflect subsurface heterogeneities and measurement errors.
2. The calculated amount of attached phages was found to be 100 times higher than the amount that could actually be eluted by beef extract from a soil sample taken near the screen of W1. This suggests that the bacteriophages were removed before reaching W1 by processes unaccounted for in the model.
3. Soil analysis showed a higher of organic carbon content in the soil samples from the first 5 cm and 10 – 15 cm, as well as in soil from 1 – 1.5 m. Bales *et al.* (1993) showed that with increasing small amounts of hydrophobic organic material bonded to silica beads, the attachment rate coefficient of MS2 increased. The initial higher removal of the bacteriophages may thus be explained by hydrophobic interactions with organic matter.

Yet another possibility that could explain the initially higher removal of the bacteriophages may be variations in the surface properties of the phage population. Phages that are stickier are removed faster. This possibility has been posed before by Pieper *et al.* (1997), who also showed initial higher removal of PRD1.

One may contemplate that the existence of fine-grained sediments at the bottom of the compartment may be the cause of high early attachment. This possibility can be ruled out. It was shown that the average grain size of the soil was larger in the samples from the first 5 and 10 – 15 cm than in soil samples taken at the monitoring wells.

Although attachment was found to be the major process in removing the phages, the corresponding very low estimated values of the collision efficiencies show that conditions for attachment were highly unfavorable. This is consistent with the concept that in sandy soils with relatively high pH, electrostatic repulsion is important (Bales *et al.*, 1991, 1993). However, it must be mentioned that we had expected higher values for phages collision efficiencies because of two reasons. First, in our case, the concentrations of oxalate-extractable iron were found to be 3 – 10 times higher than in the sewage contaminated soil reported by Pieper *et al.* (1997). Furthermore, their soil contained about 1 % bonded organic matter, which is considerably higher than in our case. This would imply that in our case, there is a higher amount of available iron oxide coatings, which promotes attachment. Secondly, concentrations of bivalent cations were rather high in our case (Table 2). Bales *et al.* (1991) showed that Ca<sup>2+</sup>-concentrations of 1 – 100 μM at pH 7 are already sufficient to promote attachment of viruses. However, in our case, pH was still the major factor in

suppressing the attachment rate of the bacteriophages. According to Loveland *et al.* (1996) electrostatic forces between PRD1 and quartz sand or ferric oxyhydroxide are repulsive at all separation distances at a pH above 7.3. The pH values in our field study were found to be 7.3 – 8.3 and this is clearly higher than the pH values in the study by Pieper *et al.* (1997), which were reported to lie between 6 – 6.7.

The removal rates of MS2 and PRD1 were almost equal. The very low collision efficiencies found in this study reflect relatively conservative behavior of both MS2 and PRD1 and suggest they are suitable indicators for virus transport. In other words, these low collision efficiencies indicate that the soil conditions are unfavorable to attachment of other viruses too.

Attachment was shown to be reversible, with a very small detachment rate. The elution experiment at different pH's and with beef extract confirm the finding of Bales *et al.* (1993) that large chemical perturbations are needed to enhance detachment, at least for MS2. In the present field study, pH varied from 7.3 – 8.3. The elution experiment indicated that within this range release of MS2 and PRD1 was not enhanced dramatically. This is in agreement with the observations of the field study.

This study has increased our understanding of the removal processes for bacteriophages MS2 and PRD1 at field scale. A number of important properties, in particular attachment characteristics, have been quantified. Reasonably good simulation results have been obtained with a simple one-dimensional analytical model. However, a number of important questions have remained open. The role of heterogeneities in medium properties and possible variation of attachment and detachment coefficients with concentrations have to be investigated. These will be subjects of future numerical modeling and laboratory experiments.

### Acknowledgements

The contribution of Kiwa to the study was conducted as part of the research program of the Dutch drinking water companies and received financial support from the European Union, within the scope of the 'Environment and Climate Research Program' (contract ENV4-CT95-0071). This work was partly funded by the Ministry of Housing, Physical planning and the Environment under project 289202, Water Microbiology.

Bacteriophage PRD1 and its host *S. typhimurium* LT2 were kindly provided by C.P. Gerba. The improvements of CXTFIT made by N. Toride are gratefully acknowledged. J. Bergsma, A. Stakelbeek, M.J.C. van Baar, P.J. Nobel are acknowledged for their contribution in setting up this study and their support in the field. The PWN biological laboratory and the co-workers at the production plant at Castricum are greatly acknowledged for all the fieldwork sometimes performed under harsh conditions. H.A.M. de Bruin is thanked for taking care of logistics and conducting phage analysis. G. B. Engels, M. Bahar, R. v.d. Heide and F.M. Schets are thanked for conducting phage analysis. A.H. Havelaar and E.J.T.M. Leenen are acknowledged for their stimulating and expert comments.



## **Chapter 5**

# **Removal of Microorganisms by Deep Well Injection**

Schijven, J. F., Medema, G. J., Vogelaar, A. J. and Hassanizadeh, S. M. 2000 Removal of microorganisms by deep well injection. *J. Contam. Hydrol.* 44, 301-327.

### Abstract

The removal of bacteriophages MS2 and PRD1, spores of *Clostridium bifermentans* (R5) and *Escherichia coli* (WR1) by deep well injection into a sandy aquifer was studied at a pilot field site in the southeast of The Netherlands. Injection water was seeded with the microorganisms for five days. Breakthrough was monitored for 93 days at four monitoring wells with their screens at a depth of about 310 meters below surface. Within the first 8 meters of soil passage, concentrations of MS2- and PRD1 were reduced by  $6 \log_{10}$ , that of R5-spores by  $5 \log_{10}$  and that of WR1 by  $7.5 \log_{10}$ . Breakthrough of MS2 and R5 could also be followed at greater distances from the injection well. Concentrations of MS2 were reduced only about  $2 \log_{10}$  in the following 30 m, and reduction of concentrations of R5 was negligible. Apparently, attachment was greater during the first 8 meters of aquifer passage.

At the point of injection, the inactivation rate coefficient of free MS2 was found to be  $0.10 \text{ day}^{-1}$ , that of free PRD1  $0.054 \text{ day}^{-1}$ , and that of *E. coli* strain WR1  $0.083 \text{ day}^{-1}$ . In injection water that had passed 8 m of soil, inactivation of MS2-phages was found to be less than in water from the injection well:  $0.024 \text{ day}^{-1}$ . Probably, the higher inactivation rate of MS2 in water from the injection well may be ascribed to the activity of aerobic bacteria.

Inactivation of the R5-spores was not significant.

From geochemical mass balances it could be deduced that within the first 8 meters distance from the injection well ferric oxyhydroxides precipitated as a consequence of pyrite oxidation, but not at larger distances. Ferric oxyhydroxides provide positively charged patches on to which fast attachment of the negatively charged microorganisms may take place. The non-linear logarithmic reduction of concentrations with distance may therefore be ascribed to preferable attachment of microorganisms to patches of ferric oxyhydroxides that are present within 8 meters distance from the injection point, but not thereafter. Declogging of the injection well introduced hydrodynamic shear that remobilized MS2, which were then transported farther downstream.

### 5.1 Introduction

In this paper, results of a field study, aimed at investigating removal of viruses and bacteria from pretreated surface water by deep well injection are presented. In the Netherlands, about a third of the total drinking water production relies on surface water. Surface water is contaminated with pathogenic microorganisms, mainly because of discharges of domestic wastewater and manure run-off from agricultural land. To produce drinking water from surface water these pathogens need to be removed. One effective way is found to be passage of surface water through soil, as has been shown in the case of bank filtration (Havelaar *et al.*, 1995; Schijven and Rietveld, 1996) and dune recharge (Schijven *et al.*, 1998, 1999). Removal of microorganisms for drinking water production by deep well injection is another effective option. When renovating or designing recharge systems, drinking water companies want to minimize ecological side effects of artificial recharge and keep the land claim for recharge projects within limits (Peters, 1996). Deep well injection offers the added advantage that the use of land as well as effects on surface ecosystems are kept to a minimum. Knowledge about the removal of microorganisms is important for the design of deep well injection systems. Therefore, a field study was carried out at a pilot location for deep well injection to investigate removal processes of

bacteriophages, bacterial spores and bacteria. Highly concentrated suspensions of bacteriophages MS2 and PRD1, spores of *Clostridium bifermentans* (R5) and *Escherichia coli* (WR1) were added to the injection water for a period of five days. Their transport was followed in monitoring wells at different distances from the injection well. MS2 and PRD1 are considered to be relatively conservative tracer viruses because they attach less than most pathogenic viruses and are relatively persistent during transport through the subsurface, as evidenced in the literature (see Schijven and Hassanizadeh, 2000, for an extensive review). Spores of *Clostridium bifermentans* were chosen as surrogates for removal of oocysts of *Cryptosporidium parvum*. Although these spores are about 5 times smaller in diameter (1  $\mu\text{m}$ ), they resemble *Cryptosporidium parvum*-oocysts in being highly persistent in the aquatic environment. According to colloid filtration theory (Yao *et al.*, 1971), the 1- $\mu\text{m}$  spores will collide less frequently with the soil grains than the 5- $\mu\text{m}$  oocysts which is a conservative approach. Strain WR1 of *Escherichia coli* was selected as a representative of fecal bacteria. Although MS2 was co-injected with an *Escherichia coli* strain, it will not replicate by using this strain as a host, because the water temperature (12  $^{\circ}\text{C}$ ) was too low for any *E.coli* strain to produce F-pili (Woody and Cliver, 1995). Together, the injected microorganisms span a size range of about 26 – 2600 nm.

The goals of this field study were the following:

1. Measuring reduction in concentrations of microorganisms by deep well injection as a function of distance.
2. Gaining insight into the contribution of attachment and inactivation to the removal of microorganisms.
3. Investigating effects of declogging of the injection well on the removal of microorganisms.

## 5.2 Site Description

The deep well injection site is located near the village of Someren in the southeast of The Netherlands. It has been constructed to investigate the feasibility of deep well injection for storage and treatment of pre-treated surface water for drinking water production. The deep well injection project started in July 1996. Surface water is taken in from a nearby canal, the Zuid-Willemsvaart, at a distance of 95 m from the pilot site. Surface water is primarily taken in during nighttime, when concentrations of suspended solids are lower due to the absence of shipping traffic, and stored in a pond. Pre-treatment consists of micro-straining, coagulation, rapid sand filtration and active carbon filtration. Figure 1 shows a schematic vertical cross-section of the aquifer. The pre-treated surface water is injected at well IP2 through a screen at a depth of 280 – 310 m below the surface. The borehole of the injection well has a diameter of 80 cm. The standing pipe has an inner diameter of 46 cm for the first 36 m and an inner diameter of 23 cm for the next 272 m. The standing pipe is surrounded by a gravel pack of 15 – 28 cm. A 50-m thick layer of clay overlies this aquifer. The aquifer itself lies on top of another clay layer which is 2 – 3 meters thick. The aquifer consists of several sandy layers (fluvial sediments) that differ in permeability. Water is pumped up at production well PP1 at a distance of 98 m from the injection point and at a depth of 278 – 298 m below the surface. Monitoring wells were located at distances of 8 m (WP3), 12 m

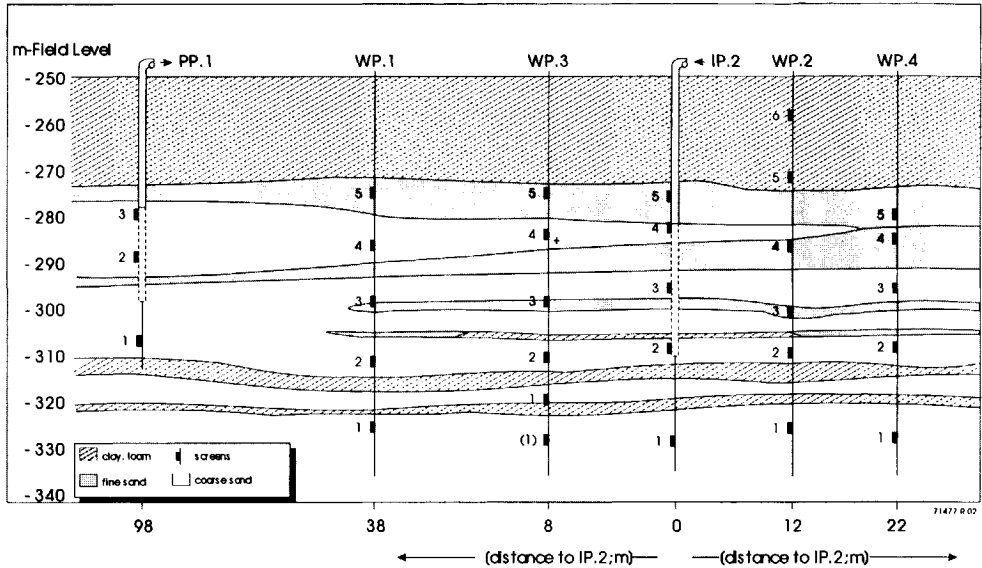


**Figure 1** Schematic cross section of field site with injection well IP2, monitoring wells WP1 to WP4 and production well PP1. Samples were taken from the number-2 screens

(WP2), 22 m (WP4) and 38 m (WP1) from the injection well along the line of flow symmetry connecting IP2 and PP1. They are screened with 2-m long polyvinylchloride (PVC) screens at depths of 275 m, 285 m, 297 m, 310 m and 330 m below the surface, respectively. Such monitoring screens were also installed in the gravel pack surrounding the screen in the borehole of injection well IP2.

During the first two years of its performance, the deep well injection site was studied extensively in order to assess its injection capacity and to investigate factors that affect this capacity. In particular, travel times and quality changes of the injected water (Stuyfzand, 1999) and frequency and causes of clogging have been studied (Vogelaar, 1999). The study on the removal of microorganisms started in October 1998. During this study, the injection rate of recharge water was kept constant at  $960 \text{ m}^3 \cdot \text{day}^{-1}$ . Samples from all the wells were taken from the number-2 screens at 310 m below the surface. These screens are all situated within the same layer of sand. This sand layer has the highest permeability as compared to the other sand layers within this aquifer. Its permeability is  $25 \text{ m} \cdot \text{day}^{-1}$  (Stuyfzand, 1999). Table 1 shows the results of granular and chemical analyses of soil core samples from this sand at a depth of 295 m. The groundwater in this sand is anoxic (oxygen-, nitrate- and sulfate-free) and alkaline. The sand has low calcium content ( $\text{Ca} \leq 0.3\%$ ). Cation exchange capacity (CEC) is moderate. More than 80% of the adsorbed cations are calcium-ions. The sulfide content is high (655 - 4600 mg S per kg) and is largely present as  $\text{FeS}_2$  (pyrite) (Stuyfzand, 1999).

**Table 1** Granular and chemical analysis of soil from production well PP1 at the time of construction (Stuyfzand, 1999).

Depth	m	295
Grain size <sup>a</sup>	$\mu\text{m}$	272
Clay ( $\leq 2 \mu\text{m}$ )	%	0.9
Silt ( $> 2$ and $\leq 53 \mu\text{m}$ )	%	1.1
Sand ( $> 53 \mu\text{m}$ )	%	98
Porosity		0.32
$f_{oc}$	%	0.17
CEC	$\text{meq.kg}^{-1}$ dry weight	10
Fe-(hydr)oxides	$\text{mg.kg}^{-1}$ dry weight	< 1
Mn-(hydr)oxides	$\text{mg.kg}^{-1}$ dry weight	< 1

<sup>a</sup>Grain size is geometric mean.

### 5.3 Experimental and Modeling Methods

#### 5.3.1 Salt Tracing

Prior to the injection of water with microorganisms, sodium chloride was injected as a conservative salt tracer to estimate interstitial flow velocity of the injected water and dispersivity of the porous medium. For a period of exactly five days, 265 kg NaCl in 880 liter was injected each day into the main injection pipeline through which pretreated surface water was injected at a rate of  $960 \text{ m}^3.\text{day}^{-1}$ . This resulted in a salt concentration of  $0.275 \text{ kg.m}^{-3}$  in injection water and the electrical conductivity (EC) of the injection water increased in one step from  $450 \mu\text{S/cm}$  to about  $1000 \mu\text{S/cm}$ .

In each monitoring well, 300 meters of polyethylene (PE) tubing with an inner diameter of 10 mm was installed. The end of the tubing was one meter above the bottom of the screens. Three submersed pumps were connected in series along the tubing. During the first 2 weeks of the salt tracing, EC was measured automatically from the number-2 screens of IP2, WP3 (8 m) and WP2 (12 m). Water was pumped up continuously at a rate of  $0.1 \text{ l.min}^{-1}$  from the top of the water column in the monitoring wells in order to refresh stagnant water at the level of the screens. EC-measurements at the level of the number-2 screens were carried out at 4-hour intervals. To that aim, water was pumped up at a rate of  $1.51 \text{ l.min}^{-1}$  for 30 minutes and EC was measured at the end of this pumping period by means of fixed EC-sensors with a data logger.

EC-measurements in samples from the number-2 screens of WP1 (38 m) and WP4 (22 m) were carried out manually at daily and weekly intervals. Prior to the manual sampling for EC-measurements, a mobile pump was used to pump up 25 liters of water from the top of the water column in order to refresh stagnant water at the level of the screens, and the content of the tubing was refreshed first with twice its volume (50 l) at a pumping rate of  $1.5 \text{ l.min}^{-1}$ .

### 5.3.2 Microorganisms, Preparation and Dosage

Highly concentrated bacteriophage suspensions were prepared as described in Schijven *et al.* (1999). A highly concentrated suspension of spores of *C. bifermentans* R5 was prepared by culturing R5 on Perfringens agar base medium (Oxoid) for 18 hours at 37°C. One to two ml of sterile water was pipetted onto the plates after cultivation and the colony material was suspended by swabbing the colonies with a sterile swab. The colony material from several plates was combined. To prevent alteration of the surface properties of the spores, the suspension was not pasteurized and contained vegetative cells. These vegetative cells were not included in the analysis, since the samples were pasteurized before analysis. *E. coli* WR1 was grown in buffered peptone water for 18 hours at 37°C. Cells were harvested by centrifugation and washed in sterile water. All suspensions were pre-diluted, distributed over five 1-liter bottles, and kept at  $5 \pm 3$  °C. All microorganisms were kept in separate bottles to prevent interaction. Concentrations were  $7 \times 10^{13}$  plaque-forming particles per liter (pfp.l<sup>-1</sup>) of MS2,  $5 \times 10^{11}$  pfp.l<sup>-1</sup> of PRD1,  $2 \times 10^{10}$  colony-forming particles per liter (cfp.l<sup>-1</sup>) of R5 and  $10^{12}$  pfp.l<sup>-1</sup> of WR1.

At the pilot site, 1-liter bottles with suspensions of the microorganisms were emptied into 96 liters of fresh injection water in a PVC container that was stirred gently. The seeding of the aquifer with microorganisms started by pumping the contents of the 100-liter container into the main injection pipeline at constant rate within 24 hours. Just before the container was empty, it was filled again with 96 liter of fresh injection water and one liter of each of the highly concentrated suspensions of the microorganisms. Microorganisms were injected in this fashion for a period of exactly five days.

### 5.3.3 Sampling

To avoid cross contamination, seeding activities were kept strictly separated from sampling activities and were performed by different persons. Samples of 100 ml were taken from each 100-liter container just after filling of the container and after 24 hours, when the container was almost empty.

The scheme for taking samples from the monitoring wells was based on the assumption that the microorganisms traveled equally fast as the salt tracer. Prior to each sampling, 40 liters was pumped out from the top of the water column in the monitoring well at a rate of about 2 l.min<sup>-1</sup> in order to refresh stagnant water at the screen-level. Also, prior to each sampling, 40 liter of water was pumped out from the level of the number-2 screen in order to rinse the content of the sampling tubing and pumps with about twice their volume. Depending on the expected breakthrough concentrations, 4-liter or 400-liter samples were taken by filling 20-liter PVC-containers at a rate of 2 l.min<sup>-1</sup>. Temperature and pH were immediately measured on site in an additional (small) sample. All samples were kept under refrigeration and analyzed for tracer microorganisms within 18 hours.

To account for possible loss of injected microorganisms by attachment to the 300-m long sampling tubing, the following experiment was carried out. At the end of the transport experiment with microorganisms, the PE-tubing, including the three small, submersed pumps at monitoring well WP1 (38 m) was taken out. First, the tubing was emptied. Next, a 20-liter suspension containing about  $10^6$  MS2 and  $10^6$  R5 was pumped through the tubing and recollected. Subsequently, the tubing was rinsed with three portions of 10 liter of tap

water, which were also collected. Finally, 20 liter of a beef-extract, with pH 9, was pumped through the tubing and recollected at the end. All samples were analyzed for MS2- and R5-concentrations.

These analyses showed that no significant loss of MS2 and R5 occurred during the passage of microorganisms through 300 m of sample tubing. Therefore, the measured concentrations may be considered to represent those in the water at 300 m below surface.

### 5.3.4 Microorganism Enumeration

All samples were split into four parts. MS2 was assayed as described in ISO 10705-1 (1995) using host strain WG49 (Havelaar *et al.*, 1984). PRD1 was assayed according to ISO 10705-1 using *S. typhimurium* LT2 as the host, omitting nalidixic acid in the top agar layer. For enumeration of spores of *C. bifermentans*, samples of up to one liter were pasteurized for 15 minutes at 75°C and filtered through a 47 mm 0.45µm nitrocellulose filter. Larger samples were filtered through 143 mm 0.45 µm filters, and then these filters were pasteurized in a humid chamber for 15 minutes at 75°C (Hijnen *et al.*, 2000). The filters were placed in the lid of a 9-cm or 15-cm petri dish and embedded in Perfringens Agar Base medium (Oxoid) of 45°C. The medium was sealed with the base of the petri dish and incubated at 44°C. After 24 and 48 hours the number of black colonies was recorded. Both large and small colonies were observed in the samples from the observation wells. Between 0% and 93% of the colonies were small colonies (average 36%). Small and large colonies were typed using API20A (Biomérieux). Only the larger colonies were found to be *C. bifermentans*. Hence, only the counts of the large colonies were used in this study. The smaller colonies could not be classified by API20A.

For enumeration of *E.coli* WR1, samples of up to one liter were filtered through a 47 mm 0.45µm nitrocellulose filter, but larger samples were filtered through 143 mm 0.45 µm filters. Filters were placed onto Lauryl Sulphate agar and incubated for 5 hours at 25°C and 14 hours at 44°C. Yellow colonies were counted and all colonies from the observation well samples were confirmed by incubation at 44°C in brilliant green bile lactose broth.

### 5.3.5 Declogging

Clogging is one of the most troublesome phenomena when applying artificial recharge. Clogging may be caused by accumulation of suspended particles, bacterial growth, chemical precipitation, gas generation, and compaction of the clogging layer (Pyne, 1995). Because the injection rate was kept constant, an increased hydraulic head was measured at the injection well due to the clogging that took place. In the course of this field study, declogging of the injection well was carried out twice. The first declogging was carried out 31 days after the start of the injection with microorganisms. At day 93, pumping was stopped and the site was left undisturbed to simulate Aquifer Storage Recovery (ASR). ASR is a cost-effective technology that is widely used for underground storage of large volumes of water (Pyne, 1995). After a period of four months, a second declogging was carried out.

The declogging was carried out as follows. First, injection of water was stopped. Then, the hydraulic head was lowered 20 meters by air pressure, followed by immediate release of air pressure. This induced a high rate of flow of water towards the injection well for a few seconds. The aim was to cause the release of clogged material in the vicinity of the

injection well. This procedure was carried out 25 times. Next, water was pumped up from the injection well at a flow rate of  $200 \text{ m}^3 \cdot \text{hour}^{-1}$ . During the first declogging  $68 \text{ m}^3$  of water was pumped up and during the second declogging  $1100 \text{ m}^3$  of water. The volume of the standing pipe is  $17 \text{ m}^3$ . Samples were taken to analyze the suspended sediment content. The sediment was investigated for its iron, manganese and aluminum content by shaking  $2.5 \text{ g}$  of the sediment in  $0.1$  liter of ammonium oxalate/ oxalic acid, pH 3, for a period of 2 hours. Subsequently, the extract was analyzed for iron, manganese and aluminum by atomic adsorption spectrometry as described in Houba *et al.* (1989) and Stuyfzand and van der Jagt (1997). To analyze the chemical processes that have taken place during ASR, water samples were also analyzed for turbidity, iron, and total organic carbon (TOC). This was also an opportunity to investigate where most of the injected microorganisms were retained. Therefore, during back-pumping samples of 1 liter (first declogging) and 200-liter (second declogging) were taken to analyze for MS2 and R5.

### 5.3.6 Conceptual Model

Major transport processes included in the mathematical model of our field experiments are advection, hydrodynamic dispersion, attachment, detachment and inactivation. The flow field is assumed to be at steady state. The monitoring wells WP1 – WP4 lie along the line of flow symmetry connecting IP2 and PP1. The number-2 screens of all wells are located at the same depth within a 30-m thick high-permeable sand layer. Therefore, the flow is assumed to be one-dimensional. Furthermore, calculations of the actual flow velocity profile shows that after a distance of about 8 meters, the variations in velocity magnitude remain limited. Thus, for our modeling purposes the velocity is assumed to be constant. Transverse dispersivity was neglected. Attachment and detachment are modeled as first order processes. Inactivation is modeled as first-order decay with different rate coefficients for free and attached microorganisms. With these assumptions, the governing equations of a one-dimensional, one-site kinetic transport model apply:

$$\frac{\partial C}{\partial t} = \alpha_L v \frac{\partial^2 C}{\partial x^2} - v \frac{\partial C}{\partial x} - k_{att} C - \mu_f C + k_{det} \frac{\rho_B}{n} S \quad (1)$$

$$\frac{\rho_B}{n} \frac{\partial S}{\partial t} = k_{att} C - k_{det} \frac{\rho_B}{n} S - \mu_s \frac{\rho_B}{n} S \quad (2)$$

Subject to boundary conditions  $C = C_0$  at  $x = 0$  and  $\frac{\partial C}{\partial x} = 0$  at  $x = \infty$ . Here,  $C$  is the

concentration of free microorganisms, *i.e.* microorganisms in the aqueous phase [number. $\text{m}^{-3}$ ];  $S$  is the concentration of attached microorganisms [number. $\text{kg}^{-1}$ ];  $t$  is the time [days];  $x$  is the distance from the injection well towards the production well [m];  $\alpha_L$  is the longitudinal dispersivity [m];  $v$  is the average interstitial water velocity [ $\text{m} \cdot \text{day}^{-1}$ ];  $\rho_B$  is the aquifer bulk density [ $\text{kg} \cdot \text{m}^{-3}$ ];  $n$  is the porosity [-];  $k_{att}$  and  $k_{det}$  are the attachment and detachment rate coefficients, respectively [ $\text{day}^{-1}$ ];  $\mu_f$  and  $\mu_s$  are the inactivation rate coefficients of the free and attached microorganisms, respectively [ $\text{day}^{-1}$ ]. The computer code CXTFIT (Toride *et al.*, 1995) contains the analytical solution of these equations, including the code for inverse parameter estimation.

Dispersion of both MS2 and PRD1 and the salt tracer have been shown to be similar in columns with sandy soil (Bales *et al.*, 1989) and silica beads (Bales *et al.*, 1991). In field studies where preferential flow was absent, PRD1 was transported at about the same rate as a conservative salt tracer (Bales *et al.*, 1995; Pieper *et al.*, 1997; Schijven *et al.*, 1999). Therefore, the quantities  $v$  and  $\alpha_L$  that were found from fitting the salt breakthrough curves using CXTFIT (Toride *et al.*, 1995) were assumed to apply to the microorganisms too. Attachment of MS2 and PRD1 has been shown to be reversible and kinetically limited (Bales *et al.*, 1991, 1993, 1997; Kinoshita *et al.*, 1993; Schijven *et al.*, 1999). Therefore, phage transport may be simulated using a one-site kinetic model. Moreover, in many field studies (see *e.g.* Bales *et al.*, 1991; McCaulou *et al.*, 1994; Schijven *et al.*, 1999), the level of breakthrough was found to be mainly determined by attachment, with detachment being much slower. The same applies for bacterial transport. In several column studies (Hornberger *et al.*, 1992; Camper *et al.*, 1993; McCaulou *et al.*, 1994, 1995; Rijnaarts *et al.*, 1995; Hendry *et al.*, 1997) and a field study (Harvey and Garabedian, 1991), it has been shown that the level of breakthrough of bacteria is mainly determined by attachment, and that detachment is much slower. The temperature of the water in the aquifer was about 12 °C and, therefore, bacterial growth was not considered. The average grain size diameter of the aquifer sand of the present field study, was 0.27 mm. The size of the studied bacteria is less than 5% of the average grain size and, therefore, straining can be neglected (Harvey and Garabedian, 1991).

We found that the tails of the breakthrough curves of the microorganisms could not be fitted satisfactorily using CXTFIT. This was ascribed to the limited number of measurements and considerable variations in the concentrations along the tails of the breakthrough curves. As an approximate alternative, it is assumed that the detachment rate is much smaller than the inactivation rate of attached microorganisms. Therefore, under steady state conditions (reached during maximum breakthrough concentration) Equation 1 reduces to:

$$\alpha_L v \frac{\partial^2 C}{\partial x^2} - v \frac{\partial C}{\partial x} - (k_{att} + \mu_l) C = 0 \quad (3)$$

Equation 3 has the following solution:

$$\log\left(\frac{C_{max}}{C_0}\right) = \frac{x}{2.3} \frac{\left(1 - \sqrt{1 + 4\alpha_L \frac{k_{att} + \mu_l}{v}}\right)}{2\alpha_L} \quad (4)$$

where  $\log(C_{max}/C_0)$  is the logarithmic reduction in concentration. By rearranging Equation 4 the value of  $k_{att}$  can be calculated (Schijven *et al.*, 1999):

$$k_{att} = \frac{\left[1 - 2\alpha_L \frac{2.3}{x} \log\left(\frac{C_{max}}{C_0}\right)\right]^2 - 1}{4\alpha_L} v - \mu_l \quad (5)$$

The value of  $\mu_1$  was obtained measuring the inactivation rate in water from IP2 and WP3 (8 m) at the laboratory as described below.

### 5.3.7 Inactivation rate of Free Microorganisms in Water

To measure inactivation of the microorganisms in the water phase during the experiment, a 4-liter sample was taken from well IP2 on the third day of injection of the microorganisms. A 4-liter sample was also taken from monitoring well WP3 (8 m) during maximum breakthrough. The bottles with these samples were stored in a cold room at  $11.8 \pm 0.5$  °C and analyzed regularly for a period of about four months. In this manner, inactivation rates of free microorganisms just before and after 8 meters of aquifer passage were determined.

### 5.3.8 Estimates of Collision Efficiencies

From the values of  $k_{at}$ , collision efficiencies,  $\alpha$ , were calculated. The collision efficiency is an empirical constant that accounts for electrostatic interactions, in this case, between microorganisms and the porous medium. Collision efficiencies were calculated using the following equation (Yao *et al.*, 1971):

$$\alpha = \frac{2}{3} \frac{d_c}{(1-n)} \frac{k_{at}}{v} \frac{1}{\eta} \quad (6)$$

where  $\alpha$  is the collision efficiency and  $\eta$  is the single collector efficiency. The single collector efficiency  $\eta$  was calculated using the following relationship due to Martin *et al.* (1992):

$$\eta = 1.0 A_s N_{Lo}^{1/8} N_R^{15/8} + 0.00388 A_s N_G^{1.2} N_R^{0.4} + 4 A_s^{1/3} N_{Pe}^{-2/3} \quad (7)$$

Here,  $N_R = d_p / d_c$  accounts for interception,  $N_G = d_p^2 (\rho_p - \rho) g / (18 \mu v n)$  for gravity effects,  $N_{Lo} = 4H / (9 \mu d_p^2 v n)$  for van der Waals interactions, and  $N_{Pe} = d_p v n / D_{BM}$  for diffusion. In these definitions,  $d_p$  and  $d_c$  represent the microorganism particle and grain sizes [m], respectively,  $g$  is the gravitational acceleration,  $\rho$  and  $\rho_p$  are the density of water and the microorganism particle, respectively,  $\mu = \rho * 0.000947 / (T + 42.5)^{1.5}$  is the dynamic viscosity [kg/m.s] with  $T$  the water temperature [°C],  $H = 6.2 \times 10^{-21}$  is the Hamaker constant [J] for the bacterium-glass-water interface (Rijnaarts *et al.*, 1995),  $D_{BM} = K_B (T + 273) / (3 \pi d_p \mu)$  is the diffusion coefficient [m<sup>2</sup>/s] with Boltzmann-constant  $K_B = 1.38 \times 10^{-23}$  (J/K), and  $A_s = 2(1 - \gamma^5) / (2 - 3\gamma + 3\gamma^5 - 2\gamma^6)$  is Happel's porosity-dependent parameter, with  $\gamma = (1 - n)^{1/3}$ . R5-spores have an assumed size of 1  $\mu$ m and a buoyant density of 1270 kg/m<sup>3</sup> (Tisa *et al.*, 1982). Because MS2 is small ( $d_p = 26$  nm, Bales *et al.*, 1991) its transport in the immediate vicinity of the collector surface is dominated by Brownian diffusion. In this case,  $\eta$  is given approximately by the last term in Equation 7.

**Table 2** Initial and maximum concentrations and removal of the injected microorganisms.

		MS2	PRD1	R5	WR1
$C_0^a$	[N.l <sup>-1</sup> ]	$7.1 \times 10^7$ $\pm 1.4 \times 10^7$	$4.3 \times 10^5$ $\pm 1.4 \times 10^5$	$1.6 \times 10^4$ $\pm 5.7 \times 10^3$	$1.1 \times 10^6$ $\pm 2.6 \times 10^5$
$C_{IP2}^b$	[N.l <sup>-1</sup> ]	IP2 $6.1 \times 10^7$ $\pm 1.2 \times 10^7$	$5.1 \times 10^5$ $\pm 2.8 \times 10^5$	$3.0 \times 10^4$ $\pm 1.7 \times 10^4$	$1.2 \times 10^6$ $\pm 5.6 \times 10^5$
$C_{well}^0$	[N.l <sup>-1</sup> ]	WP3 (8 m)	0.89 $\pm$ 0.42	0.29 $\pm$ 0.10	0.03
		WP1 (38 m)	0.26 $\pm$ 0.13	0.16 $\pm$ 0.18	-
		WP2 (12 m)	4.6 $\pm$ 2.0	0.70 $\pm$ 0.60	-
		WP4 (22 m)	0.73	0.097 $\pm$ 0.016	-
$-\log_{10}(C_{well}^0/C_0)$		WP3 (8 m)	5.9	5.7	4.7
		WP1 (38 m)	8.4	-	5.0
		WP2 (12 m)	7.2	7.1	4.4
		WP4 (22 m)	8.0	-	5.2

<sup>a</sup> $C_0$  was calculated from the concentration in the 100-l container and the volume of injected water. <sup>b</sup> $C_{IP2}$  concentration was measured in the gravel pack surrounding the standing pipe in the injection well IP2; <sup>c</sup> $C_{well}^0$  concentration was calculated from average breakthrough concentration over the period of maximum breakthrough of salt.  $\pm$  standard deviations.

## 5.4 Results

### 5.4.1 Description of the Breakthrough Curves

Table 2 shows the injected concentrations of the microorganisms,  $C_0$ , as calculated from the concentration in the 100-l container and the injection rate of surface water.  $C_0$  was not found to be significantly different from the concentration,  $C_{IP2}$ , that was measured in the gravel pack of the injection well. At the end of five days of the injection with microorganisms,  $C_{IP2}$  did not go to zero immediately but showed a considerable tailing (Figure 2). This tailing is most probably caused by gradual release of microorganisms retained in the borehole of the injection well by attachment. Compared to the number of injected microorganisms, the number of microorganisms that formed the tail part at IP2, *i.e.* that were slowly released, were 2.4% for MS2, 1.7% for PRD1, 12% for R5 and 1.5% for WR1.

PRD1 could only be detected at well WP3 (8 m) and WP2 (12 m), and *E. coli* strain WR1 only in one sample at WP3. Transport of MS2 and R5 could be followed at all monitoring wells. Figure 3 shows the breakthrough curves of the salt tracer, MS2 and R5. Due to some technical problems with the intake of surface water and during the declogging, injection of water was stopped a few times varying in length from 16 to 57 hours. Time axes of the breakthrough curves were adjusted accordingly so that only the time that pumping was on is given.

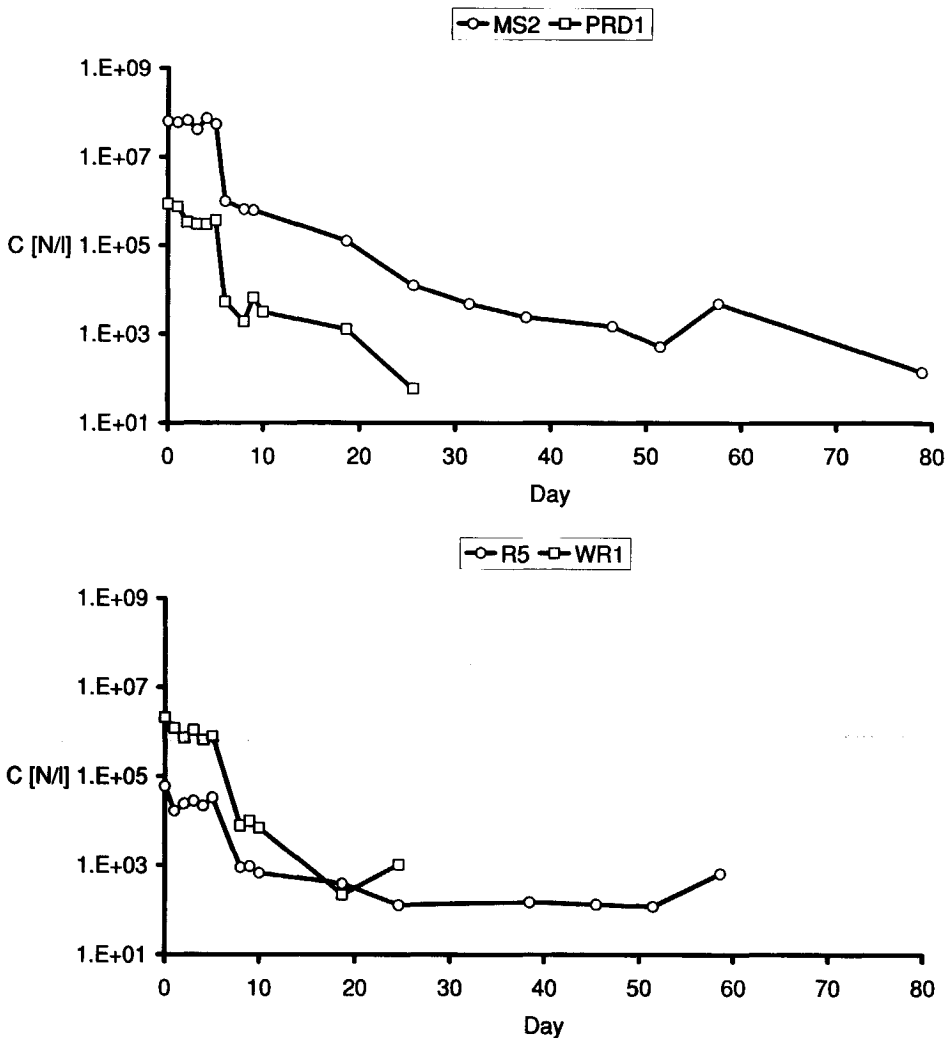


Figure 2 Observed concentrations of the injected microorganisms at injection well IP2.

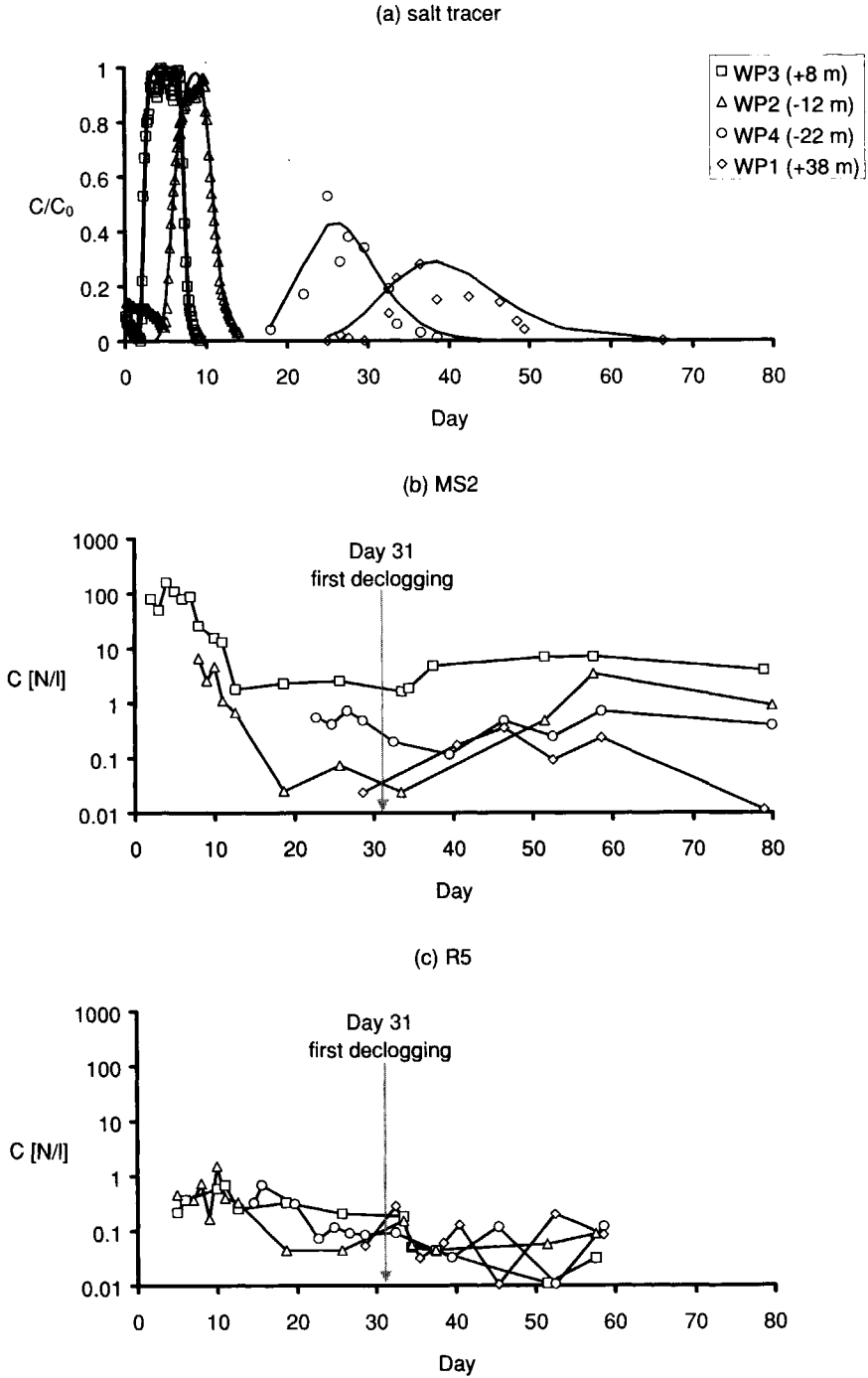


Figure 3 Breakthrough curves of (a) salt tracer (NaCl), (b) MS2) and (c) R5

**Table 3** Values of model parameters.

	Parameter <sup>a</sup>	IP2	WP3	WP1	WP2	WP4
NaCl	x	0.1	+8	+38	-12	-22
	v	-	3.33	1.01	1.98	0.897
	x/v	-	2.4	38	6.1	25
	$\alpha_L$ *	-	0.11	0.66	0.19	0.38
	$\alpha_L/x$	-	0.014	0.017	0.016	0.017
	Total mass (%) <sup>b</sup>		96%	97%	92%	100%
MS2	$\mu_1$	0.10	0.024			
	$k_{att}$	-	6.7	0.65	3.4	0.95
	$\alpha$	-	$1.4 \times 10^{-3}$	$2.0 \times 10^{-4}$	$8.0 \times 10^{-4}$	$2.9 \times 10^{-4}$
PRD1	$\mu_1$	0.054				
R5	$\mu_1$	<sup>c</sup> n.s.				
	$k_{att}$	-	5.1	0.33	1.9	0.55
	$\alpha$	-	$8.0 \times 10^{-3}$	$6.1 \times 10^{-4}$	$3.2 \times 10^{-3}$	$1.0 \times 10^{-3}$
WR1	$\mu_1$	0.083				

<sup>a</sup>Dimensions: x [m], v [m.day<sup>-1</sup>],  $\alpha_L$  [m],  $\mu_1$  and  $k_{att}$  [day<sup>-1</sup>]. Collision efficiency  $\alpha$  is dimensionless. <sup>b</sup>Total mass of salt tracer under breakthrough curve, relative to total injected mass. <sup>c</sup>n.s. = not significantly different from zero.

In Table 3, the estimates of pore water velocity and longitudinal dispersivity are given. The dispersivity values are low which indicates that the sandy layer at the depth of 280 - 310 m is relatively homogeneous. The total mass of salt tracer under the breakthrough curves measured at the monitoring wells was found to be almost constant. This indicates that there is no lateral loss of mass. In other words transverse dispersivity is much smaller than longitudinal dispersivity. This justifies a one-dimensional modeling approach. As expected, MS2 was transported with the same velocity as the sodium chloride. At WP3 (8 m), breakthrough of R5 seemed to be retarded relative to that of sodium chloride, but at WP4 (22 m), it appeared to be faster, while at the other two wells, its breakthrough was more or less concurrent with that of the sodium chloride. It is believed that R5 was transported at the same rate as MS2 and the sodium chloride, but large variations in concentrations in combination with a limited sampling frequency give a misleading picture.

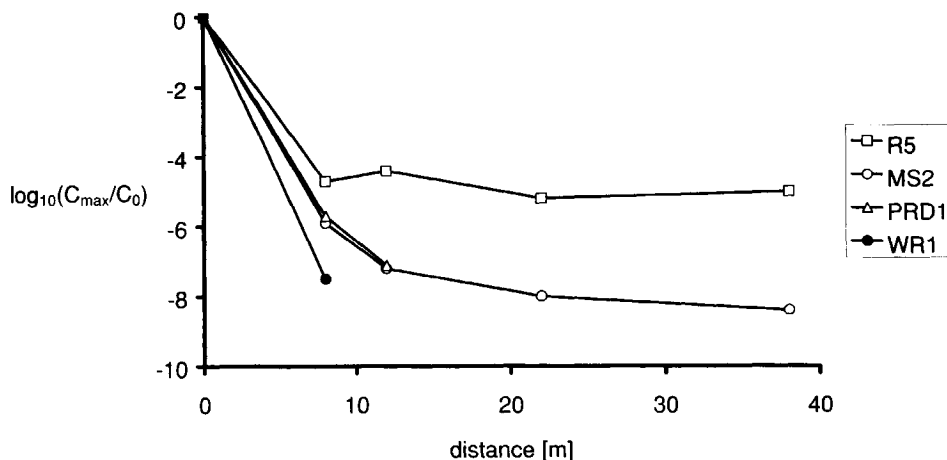


**Figure 4** Removal of microorganisms with distance.

#### 5.4.3 Removal with Distance

The maximum breakthrough concentration at a monitoring well,  $C_{\text{well}}^0$ , was calculated as the mean of breakthrough concentrations over the period of maximum breakthrough; this period was determined on the basis of the sodium chloride experiment. The degree of removal was calculated as the logarithmic reduction in concentration,  $-\log_{10}(C_{\text{well}}^0/C_0)$  (Table 2). For the sake of comparison, we also calculated the degree of reduction as the ratio of the total number passing a monitoring well and the total number of injected microorganisms; there was no difference with the logarithmic reduction in concentration. Figure 4 shows a plot of the logarithmic reductions versus traveled distance. Concentration reductions of MS2 and PRD1 appear to be very similar. MS2- and PRD1-concentrations were attenuated by almost 6  $\log_{10}$  at WP3 (8 m). Reduction of concentrations at WP3 was the smallest for R5 (4.7  $\log_{10}$ ) and the largest for WR1 (7.5  $\log_{10}$ ). It can be seen that MS2-concentrations are gradually reduced at a lower rate as the distance from the injection well increases. R5 also showed a non-linear reduction in concentration with distance. At WP3, reduction was about 4.7  $\log_{10}$ , but from that point on, it was negligible.

#### 5.4.4 Inactivation of Free Microorganisms

Results of inactivation experiments for free microorganisms are shown in Figure 5. Evidently, the inactivation rates are first order under all conditions. Inactivation rate coefficients are given in Table 3. R5 showed no significant inactivation.

The  $\mu_1$ -values for MS2 and WR1 in the water from the injection well were about the same, but about two times less for PRD1. MS2 was found to inactivate at a rate of only 0.024 day<sup>-1</sup> in water from monitoring well WP3 (8 m), four times slower than in water from the injection well and two times slower than PRD1 in water from the injection well.

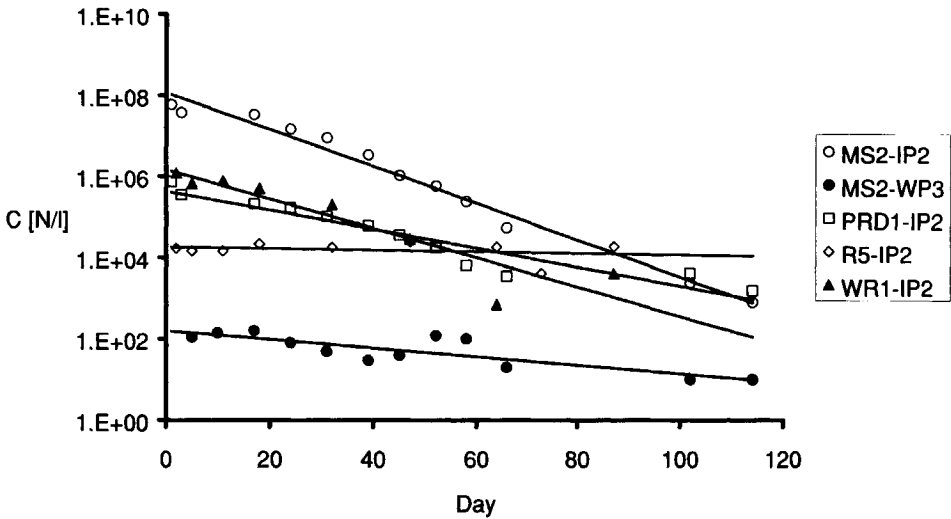


**Figure 5** Inactivation of MS2, PRD1, R5 and WR1 in water from IP2 and WP3 (8 m). Lines are regression lines. See Table 3 for inactivation rate coefficients.

**5.4.5 Estimates of Attachment Rate Coefficients and Collision Efficiencies**

The calculated attachment rate coefficients,  $k_{att}$  and collision efficiencies,  $\alpha$ , are given in Table 3. These values were only calculated for MS2 and R5, because these two microorganisms could be measured at all four monitoring wells. Collision efficiencies for MS2 are low, this indicates relatively unfavorable conditions for attachment. The values of  $\alpha$  are very similar to the ones that were found in our previous study on removal of Bacteriophages by dune recharge (Schijven *et al.*, 1999). In that study, the collision efficiency of the bacteriophages decreased with travel distance from  $1.4 \times 10^{-3}$  at 2.4 m to  $2.4 \times 10^{-4}$  at 30 m. Pieper *et al.* (1997) found slightly higher values for PRD1 in a sewage contaminated aquifer ( $1.4 \times 10^{-3} - 2.6 \times 10^{-3}$ ) at a similar pH (6.0 – 6.7) as in the present field study. Bacterial spores are larger than bacteriophages and have therefore a lower single collector efficiency,  $\eta$  (Yao *et al.*, 1971). Therefore, although R5-concentration was reduced less than that of MS2, its collision efficiency appears to be a few times higher. In a previous study, the collision efficiency for spores of sulfite-reducing clostridia after two meters of passage through fine dune sand was found to be  $9.7 \times 10^{-3}$  (Schijven *et al.*, 1998). This value is only slightly higher than the one found for R5-spores at WP3 (8 m). Also similar collision efficiencies ( $5.4 \times 10^{-3} - 9.7 \times 10^{-3}$ ) were found for small, indigenous bacteria (0.2 – 1.4  $\mu\text{m}$ ) in a field study by Harvey and Garabedian (1991) in the same sewage contaminated aquifer as in the field study of Pieper *et al.* (1997). For an inventory of more collision efficiencies see Schijven and Hassanizadeh (2000).

**Table 4** Results from analysis of water and sediment during declogging.

First declogging							
Time [min]	Sediment <sup>a</sup> [mg.l <sup>-1</sup> ]	Sand % <sup>b</sup>	Debris of plants % <sup>b</sup>	Detritus % <sup>b</sup>	Fe <sub>ox</sub> and Mn <sub>ox</sub> <sup>c</sup> % <sup>b</sup>		
11	5.0 × 10 <sup>-4</sup>	80	5	10	5		
15	7.1 × 10 <sup>-4</sup>	10	5	80	5		
19	2.9 × 10 <sup>-4</sup>	95	0	0	5		
Second declogging							
Time [min]	Turbidity [FTE]	Dissolved Fe [mg.l <sup>-1</sup> ]	TOC [mg.l <sup>-1</sup> ]	Sediment <sup>a</sup> [mg.l <sup>-1</sup> ]	Al <sub>ox</sub> <sup>c</sup> % <sup>b</sup>	Fe <sub>ox</sub> <sup>c</sup> % <sup>b</sup>	Mn <sub>ox</sub> <sup>c</sup> % <sup>b</sup>
4	1.89	12	4.3	1.4 × 10 <sup>-3</sup>	0.14	0.32	0.0024
8	1.87	11	3.3	6.2 × 10 <sup>-3</sup>	0.077	0.13	0.0011
16	0.47	8.7	2.2	8.5 × 10 <sup>-4</sup>	0.070	0.15	0.00090
32	0.25	5.1	1.8	1.3 × 10 <sup>-4</sup>	0.034	0.11	0.00050
64	0.19	3.0	1.6	1.4 × 10 <sup>-4</sup>	0.17	0.41	0.00020
128	0.17	1.8	1.3	9.0 × 10 <sup>-5</sup>	0.071	0.15	0.00080
256	0.16	0.99	1.5	4.0 × 10 <sup>-5</sup>	0.057	0.16	0.00090

<sup>a</sup>Sediment with particles >50 µm; <sup>b</sup>Percentage of dry weight of sediment. <sup>c</sup>Oxidized Al/Fe/Mn

#### 5.4.6 Analysis of Declogging Results

In this section the data obtained after the first and second declogging operations are analyzed. Table 4 shows the analysis of sediments in the water that was pumped up during the first declogging operation. Visual inspection by naked eye and under the microscope showed that in the 11-minute sample, 80% of the sediment consisted of sand, but in the sample after 15 minutes of pumping, the sediment consisted mainly of detritus from copepods. Sediment in the 19-minutes sample consisted mainly of sand again. Comparison of changes in hydraulic head in IP2, in the monitoring well in the gravel pack of IP2 and in WP3 (8 m) indicated that 95% of the collected sediment was located near or at the wall of the borehole and 5% at the openings of the injection screen (Vogelaar, 1999). Apparently, the organic detritus is too large to enter the pores of the aquifer. In all samples, 5% of the sediment consisted of oxidized iron- and manganese-particles. Possibly some of this is the residual iron that originates from the coagulation treatment prior to injection. The first declogging reduced the increase in hydraulic head to a level lower than after the previous declogging prior to this study. However, the hydraulic head was still higher than at the start of the deep well injection in July 1996, indicating that not all of the clogging material was removed.

Figure 6 shows the concentrations of MS2 and R5 measured in the water that was pumped up from the injection well plotted as a function of time. It took about six minutes to pump up the water content of the standing pipe of IP2; after that water from the aquifer was being sampled. In the water that was pumped up from the standing pipe, concentrations of all MS2, PRD1 and R5 were at a similar level as that measured in samples from the gravel pack of IP2 just before declogging. Apparently, the declogging did not cause extra release of microorganisms within a meter distance from the injection well. About 2.5 days after declogging, *i.e.* the travel time of water from IP2 to WP3 (8 m), a rise in concentration of

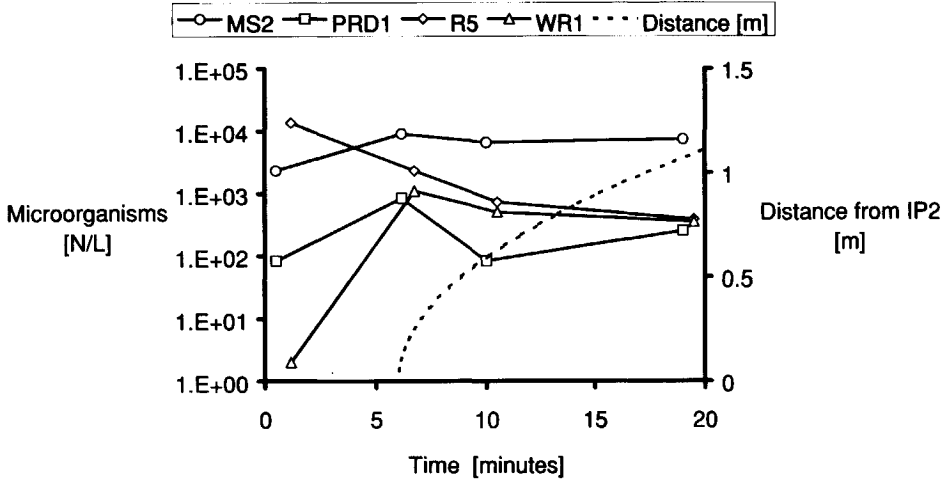


**Figure 6** Analysis of water during first declogging.

MS2 by about a factor of about 3 was measured at WP3 (Figure 3). Also at WP2 (12 m) a rise in concentrations was observed for MS2, this time by about a factor of 100, almost to the same level as at WP3. This rise in concentration was measured more than 6 days after declogging IP2. Probably, the exact time of rise in concentration was missed. Also a rise in concentration of MS2 was observed at WP4 (22 m), 26 days after declogging. No concentration change in relation to the declogging was evident from WP1 (38 m). These observations suggest that at a few meters distance from the injection well, extra release of MS2 had occurred as a consequence of the declogging, and that a pulse of released MS2 was transported along with the water. Colloids may be mobilized by hydrodynamic shear over a wide size range, whereby larger particles will be mobilized before small particles as velocity increases (Ryan and Elimelech, 1996). Hofmann and Schöttler (1998) showed in a study on artificial recharge of groundwater that by shock-wise increases in water velocities the size of suspended colloidal particles may increase by a factor of ten to an average of 1.7  $\mu\text{m}$ . In the case of R5, no rises in concentrations were evident, possibly due to the relatively large variations in the tail concentrations of the R5 breakthrough curves and because concentrations of attached R5 were about  $10^4$  times lower than concentrations of attached MS2.

From Table 4, it can be seen that during the second declogging, turbidity, TOC and the concentration of sediment were initially high. This indicates that most of this material came from within a radius of one meter around the injection well. Also, the concentration of dissolved iron was initially higher, starting at a level of two magnitudes higher than in the pretreated surface water before injection (Table 5). During the four months of ASR, the injection well had turned anoxic. The high concentration of dissolved iron, together with the low oxidized iron content of the sediment, suggest that oxidized iron has dissolved under these anoxic conditions. The oxidized iron content of the sediment from the second declogging was 20 – 50 times lower than from the first declogging.

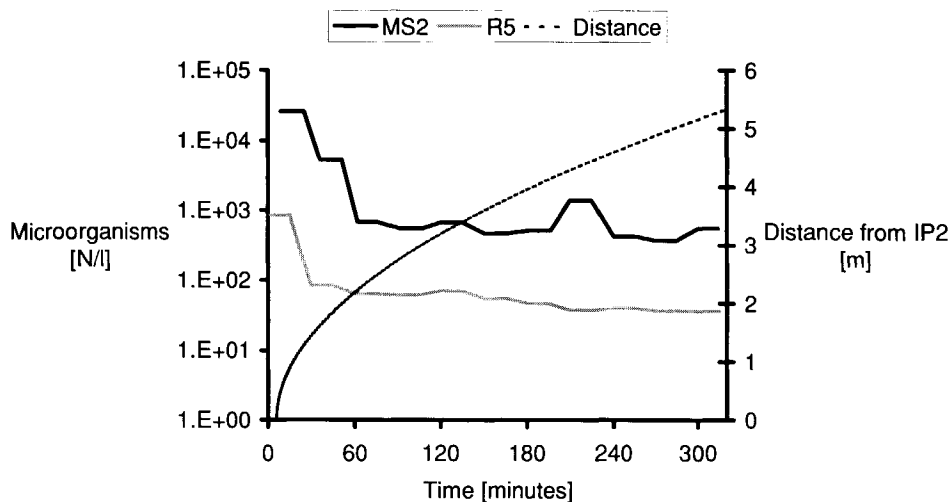


**Figure 7** Analysis of water during second declogging.

Figure 7 shows the measurements of MS2 and R5 in the water that was pumped up from the injection well during the second declogging. Initially, high concentrations of MS2 of up to  $2.6 \times 10^4$  pfp.l<sup>-1</sup> were measured in water coming from a distance of 0 - 1.5 m from IP2. Then, a quick decrease in concentration was seen to a level of  $5 \times 10^2$  pfp.l<sup>-1</sup> in water coming from a distance of 2.5 - 5.5 m. At the beginning of the ASR-experiment, the concentration of MS2 measured at IP2 was 100 pfp.l<sup>-1</sup> but at the end of the ASR-period, concentrations that were 260 times higher were measured. Clearly, MS2 had been released by the declogging procedure. During the first five days of the transport experiment, a total of  $4.3 \times 10^{14}$  MS2 was injected. During the four months of ASR, equilibrium partitioning between free and attached bacteriophages was easily achieved. Because  $k_{att} > k_{det}$ , most of the remaining MS2-phages were attached to the soil. In water from the monitoring screen just outside IP2 a high  $\mu_i$ -value of 0.10 day<sup>-1</sup> for MS2 was found (Table 3). If all MS2-phages were retained within this area, *i.e.* the aquifer was not reached, and if they were inactivated at this high rate, their numbers would have been reduced to  $1.5 \times 10^5$  in the 218 days that had passed since their injection. This is much less than the number of  $1.7 \times 10^9$  that was recovered within 60 minutes in water coming from up to 2 m distance from IP2. It is reasonable to assume that  $\mu_s$  of MS2 is less than or equal to the value measured in water from WP3 (0.024 day<sup>-1</sup>; see Table 3), because the breakthrough tails were flat, but also because the water has turned anaerobic during the four months of ASR. In that case, their numbers would have decreased less than or equal to  $2.3 \times 10^{12}$  in 218 days since injection. This implies that less than or equal to 0.07% of the injected MS2-phages were recovered from a distance of up to 2 m from the injection well. Although it is not clear whether all MS2-phages within this area were detached by the declogging, these calculations suggest that most MS2-phages did penetrate the aquifer farther than two meters from the injection well.

Concentrations of R5 were also initially high (860 per liter) in water pumped up from within 1.5 m of the injection well and then stabilized at about 50 - 60 per liter. During the first five days of the transport experiment,  $7.5 \times 10^{10}$  spores were injected, that were

subsequently reduced by a factor of 3 due to inactivation, but then remained stable (Figure 5). After the second declogging a total of  $4.3 \times 10^7$  was recovered in water from the first meter around the injection well, which is about 0.1%. This indicates that also the majority of R5-spores had entered the aquifer farther than 1.5 meter.

### 5.5 Discussion and Conclusions

Removal of microorganisms from pretreated surface water by deep well injection was studied at a pilot site in The Netherlands. After dosage of the injection water with bacteriophages (MS2 and PRD1), spores of *Clostridium bifermentans* (R5) and *E. coli* (WR1), their breakthrough was followed at different monitoring wells. Within the first 8 meters of soil passage, concentrations of MS2 and PRD1 were reduced by  $6 \log_{10}$ , that of R5-spores by  $5 \log_{10}$  and that of WR1 by  $7.5 \log_{10}$ . Breakthrough of MS2 and R5 could also be followed at larger distances from the injection well. Concentrations of MS2 were reduced only by about  $2 \log_{10}$  in the following 30 m, but the reduction of concentrations of R5 was negligible. Apparently, logarithmic reduction of concentrations decreased non-linearly with distance.

For the purpose of production of safe drinking water, these reductions are more than adequate. Nevertheless, it is important for the design of water treatment systems to understand the non-linear character of concentration reduction with distance. There are several indications that the high initial reduction takes place gradually within the first 8 meters of soil passage, but not in the borehole of the injection well:

1. The maximum concentrations of the microorganisms as measured in the gravel pack at IP2 were not significantly different from the seeding concentration. Only a few percent were retained in the borehole.
2. Concentration reduction of MS2 in the range of 8 – 12 meters from the injection well was still ten times more efficient than at greater distances.
3. During the first declogging no significant release of microorganisms at a distance 1 – 1.5 m from the injection well was observed, but after a period equal to the travel time, a rise in concentrations was observed for MS2 at WP2 (12 m), WP3 (8 m) and WP4 (22 m). This suggests extra release of MS2, probably attached to other colloidal particles, at a distance of more than 1.5 m that was induced by mechanical forces during the declogging. Consequently, these released phages were transported farther downstream.
4. During the second declogging, high numbers of MS2 and R5 were recovered from the injection well, coming from a distance of less than 2 m from the injection well. Still, these numbers represented only a small fraction of the originally injected numbers of microorganisms. This indicates that the majority of injected microorganisms were transported farther than 1.5 m.

During the first two years of its operation, the quality changes of injected water at the pilot site were studied extensively (Stuyfzand, 1999). The clogging of the injection well did not affect chemical quality of the water during soil passage. Table 5 summarizes some of the major redox parameters and the change in their values during soil passage. It shows that dissolved oxygen disappears completely within the first 8 meters of aquifer passage. Within that area, the decrease of the nitrate concentration is also the strongest, accompanied by a strong increase of the sulfate concentration.

**Table 5** Average concentration ( $\mu\text{M}$ ) and concentration change ( $\mu\text{M}$ ) of major redox parameters of injection water during first year of deep well injection (Stuyfzand, 1999) and temperature and pH of injection water during the transport experiment with microorganisms.

	Avg. concentration		Change in concentration			
	IP2	PP1	WP3 (8m)	WP1 (38 m)	WP2 (12 m)	WP4 (22m)
Diss. $\text{O}_2$	310	<16	-300	-330	-300	-320
$\text{NO}_3^-$	310	<8	-87	-340	-190	-270
$\text{SO}_4^{2-}$	650	400	+220	+350	+250	+130
$\text{Fe}_t$	2.1	88	+9.6	+8.8	+1.6	0
$\text{Mn}_t$	0.11	3.8	+0.91	+2.0	+0.91	+4.4
$\text{Ca}^{2+}$	1700	2000				
$\text{Mg}^{2+}$	360	530				
$\text{Cl}^-$	2300	170				
<sup>a</sup> Temp. $^\circ\text{C}$	11.2 (1.8)		12.2 $\pm$ 0.44	12.5 $\pm$ 0.66	12.9 $\pm$ 1.0	12.1 $\pm$ 0.56
<sup>a</sup> pH	7.0 (0.13)		6.6 $\pm$ 0.094	6.7 $\pm$ 0.11	6.8 $\pm$ 0.11	6.6 $\pm$ 0.068

<sup>a</sup> $\pm$  standard error

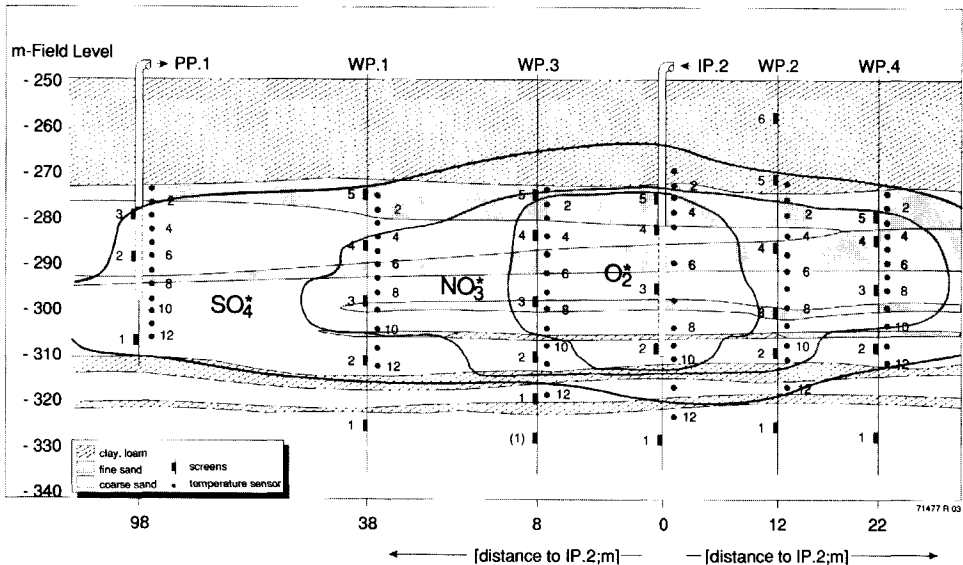


**Figure 8** Redox-zones in the aquifer (Stuyfzand, 1999).  $\text{O}_2$  = dissolved oxygen concentration declining with distance from 10 to 0  $\text{mg}\cdot\text{l}^{-1}$ .  $\text{NO}_3$  = nitrate concentration declining with distance from 20 to 0  $\text{mg}\cdot\text{l}^{-1}$ .  $\text{SO}_4$  = sulfate concentration higher than pretreated surface water due to pyrite oxidation.

Based on geochemical mass balances, Stuyfzand (1999) concluded that dissolved oxygen is completely used up by the oxidation of pyrite (see also Stuyfzand, 1993, 1998). The following redox-zones could be distinguished that are also visualized in Figure 8:

1. The O<sub>2</sub>-zone, up to 10 m, where the water contains oxygen and nitrate, both decreasing with distance.
2. The NO<sub>3</sub>-zone, with no oxygen, but with nitrate, up to 15 m at the level of the number-2 screens.
3. The SO<sub>4</sub>-zone, without oxygen and nitrate, but raised sulfate-concentration as compared to that of the injection water.

As a consequence of pyrite oxidation, ferric oxyhydroxides precipitated in the O<sub>2</sub>-zone. This was also the case in the NO<sub>3</sub>-zone at the level of the number-2 screens, but to a lesser extent, because oxidation of pyrite by nitrate proceeded slower than by oxygen. After 2.3 years of deep well injection, there still is reactive pyrite present in the O<sub>2</sub>-zone. Because oxygen reacts fast with pyrites, the oxygen will not reach the production well before one thousand years (Stuyfzand, 1999). In addition to the oxidation of pyrite, residual iron flocs originating from the coagulation treatment prior to injection may also be filtrated and thus add to the accumulation of ferric oxyhydroxides.

At the ambient pH of 6.8, precipitated ferric, manganese and aluminum oxyhydroxides form positively charged patches on the soil grains and provide favorable attachment sites for negatively-charged viruses (Loveland *et al.*, 1996). Higher attachment of viruses due to the presence of such positively charged patches of ferric oxyhydroxides has been shown in column experiments by Loveland *et al.* (1996) and has been suggested in a column study by Jin *et al.* (1998). It has also been found in two field studies (Pieper *et al.*, 1997; Ryan *et al.*, 1999).

Similar to the approach of Ryan *et al.* (1999), the surface fraction  $f$  of positively charged patches can be calculated from the observed collision efficiencies for MS2 and R5 (Table 3):

$$f = \frac{\alpha_{\text{apparent}} - \alpha_0}{\alpha_{\text{patch}} - \alpha_0} \quad (8)$$

where,  $\alpha_{\text{apparent}}$  is the apparent value of  $\alpha$  as calculated from the value of  $k_{\text{att}}$ . We can assume that the collision efficiency for MS2 and R5 to these patches,  $\alpha_{\text{patch}}$ , approximates the value of 1 owing to electrostatic attraction. The collision efficiency for attachment to the sand without these positively charged patches,  $\alpha_0$ , can be assumed to be similar to the estimate of  $\alpha$  at WP1 (38 m).

This leads to a value of  $f$  for MS2 of 0.12% and for R5 of 0.74% at WP3 (8 m), indicating that surface coverage of the soil grains with positively charged patches is still very low. The values given by Ryan *et al.* (1999) for a 12 000-year-old glacial outwash formation were one order of magnitude higher.

The removal rates of MS2 and PRD1 were almost equal. The very low collision efficiencies found in this study reflect relatively conservative behavior of both MS2 and PRD1 and suggest they are suitable indicators for virus transport. R5 was found to behave even more conservatively. The low estimated values of the collision efficiencies for MS2 and R5 show

that conditions for attachment were generally unfavorable. This is consistent with the concept that in sandy soils with relatively high pH, electrostatic repulsion inhibits attachment (e.g. Bales *et al.*, 1991, 1993; Goyal and Gerba, 1979).

A higher inactivation rate of MS2 was found in water from IP2 compared to that in water from WP3 (8 m). This difference cannot be explained by selection of more stable phages as they are transported through soil. The presence of sub-populations of phages that are inactivated at different rates should be reflected in a non-linear inactivation rate. But this was not the case and inactivation was found to be first order. The water that is injected is oxic (Table 4). It is possible that aerobic bacteria in the vicinity of the injection screen are responsible for the higher inactivation rate as compared to that at the more anaerobic monitoring well at 8 m distance. During a declogging that was carried out before this field experiment, the injection water pumped up during the first 10 minutes from IP2 was analyzed for colony counts at 22 °C and 37 °C and for *Aeromonas* (Vogelaar *et al.*, 1999). Colony counts at 22 °C were in the order of  $10^4$  -  $10^5$  cfp.l<sup>-1</sup> and colony counts at 37 °C were in the order of  $10^3$  cfp.l<sup>-1</sup>. *Aeromonas* concentrations were in the order of 10 - 100 cfp.l<sup>-1</sup>. This confirms the presence of (facultatively) aerobic bacteria in the vicinity of the injection well. Their presence may have enhanced inactivation of bacteriophages. It has been reported that inactivation of viruses may be enhanced by microbial activity (Yates *et al.*, 1987). Jansons *et al.* (1989) found that the inactivation rate of poliovirus 1 in boreholes at a mean dissolved oxygen concentration of 5.4 mg/l was three times higher than at a mean dissolved oxygen concentration of 0.2 mg/l. Also, Jansons *et al.* (1989) found *Pseudomonas maltophilia* in large numbers only in the borehole with a high dissolved oxygen concentration. Inactivation of poliovirus 1 may have been affected directly by a higher dissolved oxygen concentration or, indirectly by microbiological activity due the higher dissolved oxygen concentration. Actively growing bacteria may excrete enzymes that are detrimental to other microorganisms. Also for oocysts of *Cryptosporidium*, microbial activity may result in increased inactivation due to production of chitinases by bacteria (Zuckerman *et al.*, 1997).

This study has increased our understanding of the removal processes for microorganisms at field scale. Attachment of the microorganisms was shown to decrease non-linearly with distance. Within the first 8 meters of soil passage attachment was found to be efficient due to the presence of ferric oxyhydroxides. However, at larger distances, under anoxic conditions, attachment of microorganisms may be very low or negligible. This implies that deep well injection for the removal of microorganisms is adequate due to the existence of a zone where ferric oxyhydroxide deposits actually form. However, reduction of concentrations of microorganisms that incidentally contaminate an anoxic aquifer may be little.

### **Acknowledgements**

This work was carried out on behalf of and funded by Dune Water Company of South Holland and Amsterdam Water Supply, as part of the Research Program of the Dutch Water Companies, and by the Ministry of Housing, Physical Planning and the Environment. The authors wish to thank T. N. Olsthoorn from the Amsterdam Water Supply, H.G. de Jonge and A. de Ruijter from the Dune Water Company of South Holland, and J.H. Peters and M.J.C. van Baar for their contribution in the experimental design. P.J. Stuyfzand is greatly acknowledged for his expert comments regarding the geohydrochemical aspects. The authors greatly acknowledge the hospitality of the Oost Brabant Water Company and the working group on deep infiltration (especially Y. Brekvoort, E. Castenmiller, W.H.A. v.d. Boorn, J.C. Wakker) which have made this field experiment possible and the help and support from J. Thijs and the other workers at the field site. H.A.M. de Bruin, G.B. Engels and R. Voogt are also greatly acknowledged for their work in preparing, dosing, sampling and processing all the microbiological samples. The comprehensive reviewing and useful suggestions by J.N. Ryan are greatly appreciated.

## Chapter 6

# Modeling Virus Adsorption in Batch and Column Experiments

Schijven, J. F., Hassanizadeh, S. M., Dowd, S. E. and Pillai, S. D. 2001d. Modeling virus adsorption in batch and column experiments. *Quant. Microbiol.* In press.

### Abstract

Experiments with batch suspensions, recirculating columns and flow-through columns have been carried out involving a sandy soil and five bacteriophages: MS2, PRD1,  $\phi$ X174, Q $\beta$  and PM2. In batch and recirculating column experiments, attachment and detachment rate coefficients were determined by fitting a two-parameter (attachment and detachment) model. In general, attachment and detachment rate coefficients were not found to be significantly different between the two kinds of experiments. There was one exception, however: MS2 appeared to detach faster in the presence of strong advective flow. In the case of flow-through column experiments, it is shown that a two-site model, with adsorption to equilibrium and kinetic sites, fits the breakthrough curves of all the phages, except PM2, satisfactorily. A one-site kinetic model was found to be appropriate for phage PM2. A small proportion of bacteriophages MS2, PRD1, and Q $\beta$  adsorbed to equilibrium sites, whereas a large proportion of  $\phi$ X174 adsorbed to equilibrium sites. Such a distinction between adsorption to equilibrium and kinetic sites cannot be made in the case of batch or recirculating column experiments. Kinetic attachment rate coefficients were found to be significantly higher for the bacteriophages with presumably stronger negative charge. This may be ascribed to the presence of multivalent cations. Under these conditions, bacteriophage  $\phi$ X174 appears to behave more conservatively than more negatively charged viruses, and may then be a better choice as a relatively conservative tracer for virus transport through the subsurface.

### 6.1 Introduction

Pathogens of major threat to human health are pathogenic viruses. Viruses are a significant cause for waterborne disease outbreaks attributed to the consumption of contaminated groundwater (Craun, 1985). Groundwater is an important source for drinking water that needs to be protected from contamination with viruses. Surface water is also a source for drinking water and is becoming increasingly important. Surface water is contaminated with viruses, mainly due to discharges of wastewater. Viruses can be removed effectively by passage of the surface water through soil, provided travel times and travel distances are adequate.

Processes of major importance that affect virus concentrations during soil passage are adsorption and inactivation (Keswick and Gerba 1980; Yates *et al.*, 1987). Viruses are removed from the liquid phase by the combined effect of adsorption and inactivation, and, in addition, advection and dispersion cause spreading of viruses and thereby result in the attenuation of virus concentrations (Yates and Yates, 1991). In the case of reversible adsorption, one may have equilibrium and/or kinetic adsorption sites. Equilibrium sites are sites where detachment of viruses is relatively fast compared to attachment and advection, allowing an apparent equilibrium to be reached between free and attached viruses within a short time scale. For some other sites, adsorption is kinetically limited relative to flow velocity. Generally speaking, both kinds of adsorption may occur in a given medium. Interactions of viruses with soil are studied at laboratory scale by means of batch and column experiments. In batch experiments, water containing a known number of viruses is mixed with soil and the change in concentration of free virus particles is measured. Initially, free virus concentrations decline with time, but after a short time, they remain almost constant. At that point, equilibrium partitioning of viruses between solid and liquid

phase is attained, because of reversible adsorption. This apparent equilibrium is rapidly reached but not instantaneously and depends on the actual attachment and detachment rates (Gerba, 1984). The kinetic behavior that is operative before apparent equilibrium is reached can be described by virus attachment and detachment from soil. In the case of irreversible attachment, virus concentrations will decline constantly. Over longer periods of time, concentrations can also decline due to inactivation of free and attached viruses (Grant *et al.*, 1993).

A shortcoming of batch experiments is that estimates of adsorption parameters from batch experiments appear to be of limited use in the prediction of virus adsorption in column or field experiments and field situations. For the reasons described momentarily, attachment is overestimated and detachment underestimated. Due to the stirring in a batch experiment, the number of accessible sites for attachment is much higher than in a column or in the field. At the same time, detachment rates in a batch system are presumably lower than under transport conditions influenced by advective flow. Detachment in a soil matrix is limited by diffusion over an energy barrier resulting from virus-soil interactions and by diffusion across a boundary layer near the solid surface (Ryan and Elimelech, 1996). The diffusion coefficient of the virus and the thickness of the boundary layer control the rate of transport across the diffusion boundary layer. Primarily the velocity of the fluid controls diffusion during transport. If this velocity increases, the thickness of the diffusion boundary layer will decrease and detachment of viruses may increase.

In a flow-through column experiment, the effect of adsorption to equilibrium sites is mainly retardation of virus transport and little attenuation of virus concentrations. The effect of adsorption to kinetically limited sites is different however. Due to attachment, virus concentrations are attenuated and due to usually even slower detachment, virus transport is retarded, resulting in long tailing of virus breakthrough.

A third kind of experiment, in which features of batch and column experiments are combined, is the recirculating column experiment. Here, after introducing an initial amount of viruses, the column effluent is continuously fed as influent to the column. Thus, because of viruses circulating through such a column, eventually equilibrium is reached between attached and detached viruses, similarly as in a batch suspension. At the same time, because viruses are transported through a porous medium, attachment and detachment rate coefficients should resemble more those estimated from a flow-through column experiment.

Recently, an extensive set of batch, flow-through column, and recirculating column experiments were carried out by Corapcioglu *et al.* (1997). These experiments were carried out using five bacteriophages: MS2, PRD1,  $\phi$ X174, Q $\beta$  and PM2. These bacteriophages differ in size and isoelectric point. Dowd *et al.* (1998) analyzed the data from the recirculating and flow-through column experiments, but not the data from the batch experiments. Their primary goals were to identify the role of isoelectric points and sizes of the viruses on their adsorption and transport in a sandy soil. The experiments were short enough in duration so that viral inactivation could be neglected. It was found that in the recirculating columns, the percentage viral adsorption correlated negatively with the isoelectric point of the viruses. Similar results were obtained in the flow-through columns for the three smaller viruses (MS2,  $\phi$ X174 and Q $\beta$ ). The adsorption was found to be stronger for PRD1 and PM2, which are larger phages, suggesting a possible correlation between virus size and adsorption. Apparently, viruses that are supposed to be more negatively charged, attached more. Dowd *et al.* (1998) argued that more attachment of

viruses with lower pI could be explained by their attraction to the positively charged diffuse Gouy-layer that surrounds negatively charged soil particles.

The isoelectric point of a virus does not really provide information on its actual electric surface charge. Penrod *et al.* (1995) found strong indications that surface charge of virus particles determines attachment and that this charge is a function of pH. In accordance with DVLO theory, negatively charged viruses attach less at higher pH because of increased electrostatic repulsion (Ryan and Elimelech, 1996; Loveland *et al.*, 1996). At near neutral pH, a virus that has a low pI, is generally expected to have a larger net negative charge, but there are exceptions. At pH-values above 5, the surface charge of MS2 remains constant (Penrod *et al.*, 1995). At pH-values above 6, surface charges of vaccinia virus, reovirus and phage  $\lambda$  are also relatively insensitive to changes in pH (Penrod *et al.*, 1995). At higher pH's, PRD1 (Loveland *et al.*, 1996) and recombinant Norwalk-like virus particles (Redman *et al.*, 1997), however, show a further decrease in their negative charge.

Also contrary to the findings of Dowd *et al.* (1998), most studies have shown that attachment of MS2 is less than or equal to that of most other viruses, including  $\phi$ X174 (Goyal and Gerba, 1979; Herbold-Paschke *et al.*, 1991; Bradford *et al.*, 1993; Farrah and Preston, 1993; Bales *et al.*, 1993; Sobsey *et al.*, 1995; Penrod *et al.*, 1996; Jin *et al.*, 1997; Redman *et al.*, 1997). For an extensive review see Schijven and Hassanizadeh (2000). Dowd *et al.* (1998) fitted observed breakthrough curves from flow-through column experiments with two different models, a one-site kinetic and an equilibrium model; they did not consider the combination. Because both types of sites seem to be present, it is more appropriate to model the experiments with a model combining both equilibrium and kinetic adsorption sites. Concentrations of both PRD1 and PM2 were attenuated more than other phages in the flow-through column experiments, whereas in the recirculating columns percentage of adsorption was found to be the highest for MS2. No explanation was given for these apparently contradictory results.

In the present paper, the results of the batch and circulating column experiments have been used to obtain values for attachment and detachment rate coefficients. These values were compared in order to test the following hypotheses:

1. Attachment rate coefficients in batch experiments are larger than in column experiments, due to the larger number of accessible sites for attachment under batch conditions, and
2. Detachment rate coefficients in batch experiments are smaller than in column experiments, due to the thinner diffusion boundary layer associated with advective flow.

By comparison of batch experiments and recirculating columns, it was investigated whether these experiments are useful for predicting viral transport in flow-through columns. Re-evaluation of the breakthrough curves was carried out by fitting the data to a two-site model in order to assess the contribution of equilibrium and kinetic adsorption sites. Finally, soil and groundwater adsorption characteristics are compared with that of other studies in order to understand why supposedly more negatively charged viruses attached more, contrary to expectations.

## 6.2 Conceptual Model

Consider a situation where viruses can adsorb to two different kinds of sites on solid grains: fast and slow sites (see *e.g.* Bales *et al.*, 1991, 1997, McCaulou *et al.*, 1994). If inactivation of viruses is neglected, the governing equations describing virus transport are as follows (Toride *et al.*, 1995):

$$1 + \frac{\rho_B}{n} k_{eq} \frac{C}{t} = D \frac{\partial^2 C}{\partial x^2} - v \frac{\partial C}{\partial x} - k_{att} C + k_{det} \frac{\rho_B}{n} S^k \quad (1)$$

$$\frac{\rho_B}{n} \frac{\partial S^k}{\partial t} = k_{att} C - k_{det} \frac{\rho_B}{n} S^k \quad (2)$$

where  $C$  is the number of free viruses per unit volume in the aqueous phase, [ $L^{-3}$ ]. The attached virus concentration is given in terms of number of viruses per unit mass of soil, [ $M^{-1}$ ]. The symbol  $S^k$  is used to denote the concentration of viruses attached to slow, *i.e.* kinetic adsorption sites. Further,  $\rho_B$  is the bulk density of the saturated soil, [ $M.L^{-3}$ ];  $n$  is the porosity, [-];  $D$  is the hydrodynamic dispersion coefficient, [ $L^2.T^{-1}$ ];  $v$  is the pore water velocity, [ $L.T^{-1}$ ];  $k_{eq}$  is a distribution coefficient for equilibrium adsorption, [ $M^{-1}.L^3$ ];  $k_{att}$  and  $k_{det}$  are the attachment and detachment rate coefficients for the kinetic sites, respectively, [ $T^{-1}$ ].

For convenience we define a dimensionless distribution coefficient for equilibrium adsorption:

$$k_{eq}^* = \frac{\rho_B}{n} k_{eq} \quad (3)$$

## 6.3 Materials and Methods

### 6.3.1 Soil, Groundwater and Bacteriophages

Sediment and groundwater were originally obtained from a sandy aquifer underlying the Brazos Alluvium. Some major characteristics of the soil and groundwater are summarized in Table 1. A detailed description of this aquifer sediment and groundwater was given in Munster *et al.* (1996). The soil contains virtually no organic matter.

As mentioned earlier, five bacteriophages were used in various experiments: MS2, PRD1, X174, Q and PM2. The origin and characteristics of the bacteriophages, as well as methods for their enumeration were described in Dowd *et al.* (1998).

**Table 1** Soil and groundwater characteristics (Munster *et al.*, 1996)

<i>Brazos alluvium</i>		
Clay		3%
Silt		2%
Sand		95%
Porosity (columns)		0.35
Grain size (lab experiments)	mm	0.2 – 0.5
<i>Groundwater</i>		
Alkalinity (CaCO <sub>3</sub> )	mM	3.0
HCO <sub>3</sub> <sup>-</sup>	mM	11
Ca <sup>2+</sup>	mM	3.7
Cl <sup>-</sup>	mM	1.2
Dissolved solids	mg.l <sup>-1</sup>	694
Hardness (CaCO <sub>3</sub> )	mM	5.4
Fe (dissolved)	mM	0.011
Mg <sup>2+</sup>	mM	1.7
Conductivity	μS.cm <sup>-1</sup>	1088
pH		7.1

### 6.3.2 Batch Experiments

Batch experiments were performed using 50 ml centrifuge tubes (Falcon 2098) containing 5 grams of aquifer material and 9 ml of groundwater to which 1 ml with  $10^6 - 10^{10}$  plaqueforming units (pfu) of bacteriophages were added. Viral lysate was diluted in groundwater to reduce the amount of the suspending media (Tryptone Soy Broth). One ml of the groundwater diluted stock was then added to a time-zero tube which was vortexed, serially diluted, and the virus enumerated to provide an initial phage concentration ( $C_0$ ). The remaining tubes containing groundwater and sediment were inoculated and immediately placed in a shaking incubator at 21°C. One tube at a time was removed at 10 min, 20 min, 40 min, and 90 min and centrifuged at 1000 x g for 2 minutes in order to sediment the soil. The supernatant was then sampled and assayed to determine remaining virus concentrations.

### 6.3.3 Column Experiments

The recirculating and flow-through column experiments have already been described in detail in Dowd *et al.* (1998). Briefly, polyvinyl chloride columns with an inner diameter of 0.05 m were filled with sand up to 0.78 m and saturated with groundwater. The flow-through columns were seeded with two pore volumes of the bacteriophages. Effluent samples were obtained for about 90 minutes. MS2 and PRD1 were introduced together, but the other phages were introduced in separately prepared flow-through columns. One column was made recirculating by connecting the outlet to the inlet of the column. Bacteriophages were injected using a syringe with 20-gauge needle. Here, MS2 and PRD1 were also injected together, but the other phages were each introduced separately, *i.e.* back

to back. Because Q $\beta$  cross-reacts with the host of MS2, Q $\beta$  was injected after MS2 could not be detected anymore. Samples were obtained by injecting 1 ml of phage-free groundwater into the sampling port, waiting for several seconds and then withdrawing a 1-ml aliquot. Samples were obtained at 2.5, 5, 10, 20, 40, 60, 120 and 240 minutes after injection. The pore-water velocity in the recirculating column experiments was 0.17 m.min<sup>-1</sup> and in the flow-through column experiments 0.11 m.min<sup>-1</sup>.

### 6.3.4 Parameter Estimation from Batch and Recirculating Column Experiments

To describe adsorption in experiments with batch suspensions and recirculating columns, the same two-site model given by Equations 1 and 2 may be applied. However, because in both batch and recirculating experiments, the concentration is spatially uniform, dispersion and advection fluxes may be neglected.

Then, the reduced forms of Equations 1 and 2 have the following simple solution:

$$C = C_0 \frac{b + a \exp[-(a + b) t]}{a + b} \quad (4)$$

where

$$a = \frac{k_{att}}{1 + k_{eq}^*} \quad \text{and} \quad b = k_{det}$$

From Equation 4, it can be seen that observed concentrations in time from batch and recirculating column experiments can be fitted with only two parameters, namely  $a$  for attachment and  $b$  for detachment. Due to the absence of advective flux, it is not possible to identify retardation, therefore, we cannot distinguish between equilibrium and kinetic adsorption in batch and recirculating column experiments.

Because free virus concentrations in a batch or recirculating column experiment span several orders of magnitude and because lower concentrations show much larger variation than higher concentrations, Equation 4 and the measured concentrations were logarithmically transformed. A non-linear fitting procedure according to the Levenberg-Marquardt iteration method has been used in Mathematica version 4.0.0.0 to obtain the values for  $a$  and  $b$ .

In order to compare the estimated values for  $a$  and  $b$  between batch and recirculating column experiments, parameters  $a$  and  $b$  in Equation 4 were substituted by:

$$a = a_1 + a_2 y \quad (5)$$

$$b = b_1 + b_2 y \quad (6)$$

where  $y$  is a variable that was introduced to distinguish between the observations of the two types of experiments. In the case of the batch experiment,  $y = 0$  and in the case of the recirculating column experiment,  $y = 1$ . The estimated values of  $a_2$  and  $b_2$  indicate whether the estimated values for  $a$  and  $b$  were significantly different between batch and recirculating column experiments.

In the case that  $a$  showed no significant difference, all batch and recirculating column data were combined, a common value for  $a$  was estimated and separate values for  $b$  were estimated by substitution of the following equation into Equation 4:

$$b = b_1(1 - y) + b_2y \quad (7)$$

Similarly, in the case that  $b$  showed no significant difference, all batch and recirculating column data were combined, a common value for  $b$  was estimated and separate values for  $a$  were estimated by substitution of the following equation into Equation 4:

$$a = a_1(1 - y) + a_2y \quad (8)$$

In the case that neither  $a$  nor  $b$  showed significant differences, all batch and recirculating column data were combined and common values for  $a$  and for  $b$  were estimated.

### 6.3.5 Parameter Estimation from Flow-Through Column Experiments

For fitting the breakthrough curves from the flow-through column experiments, the computer code CXTFIT (Toride *et al.*, 1995) was used. This code is based on analytical solutions of equations 1 and 2. This way, estimated values for  $k_{eq}^*$ ,  $k_{att}$  and  $k_{det}$  were obtained. The fraction of adsorption sites that are always at equilibrium is denoted by  $f$  and was calculated from the adsorption rate coefficients as follows:

$$f = \frac{k_{eq}^*}{k_{eq}^* + \frac{k_{att}}{k_{det}}} \quad (9)$$

## 6.4 Results

### 6.4.1 Batch and Recirculating Column Experiments

Figures 1a through 1e show the fitted adsorption curves for the five phages in the batch and recirculating column experiments and the corresponding parameter values are given in Table 2.

For two of the model viruses ( $\phi$ X174 and Q $\beta$ ), the attachment and detachment rate coefficients did not appear to be significantly different between the batch and recirculating column experiments. In the case of PRD1 and PM2, attachment in the column experiment was found to be significantly different from that seen in the batch experiment, but each phage behaved in the opposite manner that is lower and greater, respectively. Apparently, there was an effect of site accessibility, causing slower attachment of PRD1 in a packed column as compared to a soil suspension. This effect of site accessibility may be related to the larger size of PRD1. There is no obvious explanation for the greater attachment of PM2 in the column experiment. Possibly there was a difference in soil characteristics between the two kinds of experiments. Only with MS2, detachment was significantly greater in the recirculating column experiment, probably caused by the flow of water in the column.

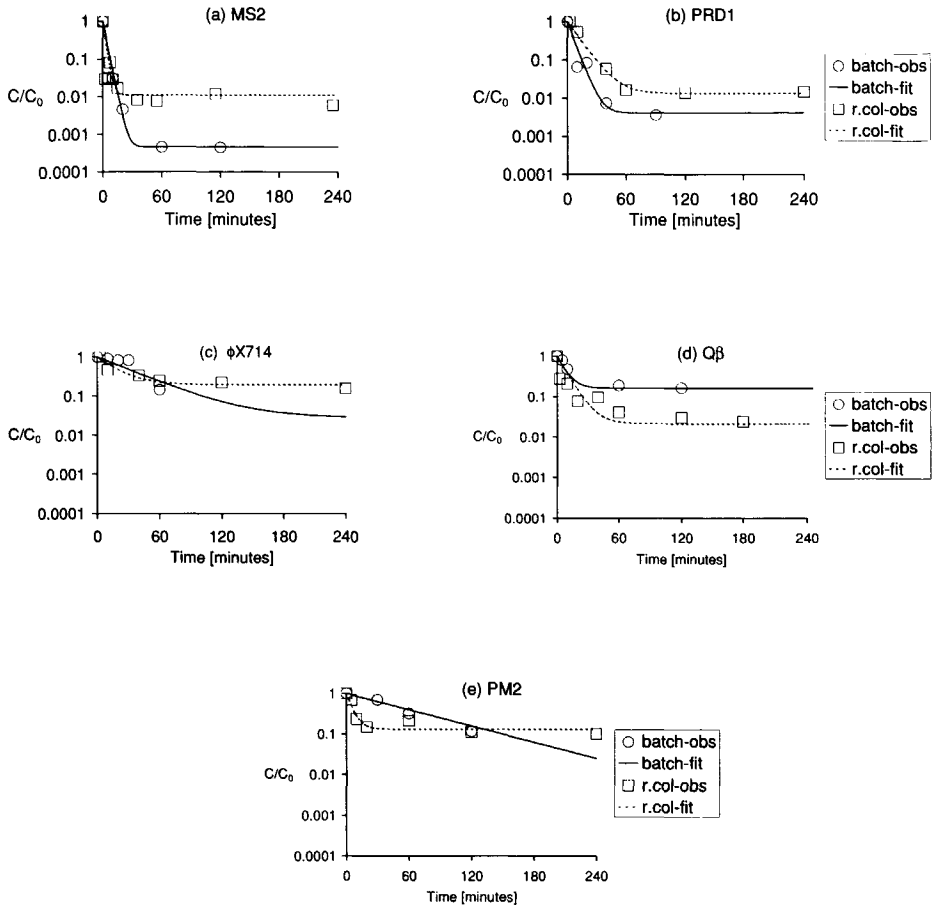


**Figure 1a to 1e** Observations and fitted model in batch and recirculating column-experiments with (a) MS2, (b) PRD1, (c)  $\phi X714$ , (d)  $Q\beta$  and (e) PM2.

**Table 2** *Estimated parameter values of batch and recirculating column experiments*

			Estimate	SE	p (%)
MS2	3-parameter model	<i>a</i>	0.31	0.033	$7.3 \times 10^{-5}$
		<i>b</i> (batch)	0.00015	0.000086	10
		<i>b</i> (r.col)	0.0030	0.0012	2.4
PRD1	3-parameter model	<i>a</i> (batch)	0.16	0.022	0.0081
		<i>a</i> (r.col)	0.076	0.011	0.013
		<i>b</i>	0.00089	0.00029	1.5
$\phi$ X174	2-parameter model	<i>a</i>	0.030	0.0069	0.15
		<i>b</i>	0.0043	0.0021	6.6
Q $\beta$	2-parameter model	<i>a</i>	0.12	0.038	0.84
		<i>b</i>	0.0055	0.0030	8.9
PM2	3-parameter model	<i>a</i> (batch)	0.037	0.015	3.1
		<i>a</i> (r.col)	0.12	0.034	0.83
		<i>b</i>	0.014	0.0060	4.5

Dimensions of *a* and *b* is  $\text{min}^{-1}$ .

**Table 3** *Estimated values of model parameters from flow through column experiments*

	MS2	PRD1	$\phi$ X174	Q $\beta$	PM2
$k_{eq}^*$	0.96	0.75	0.67	0.67	0
$k_{att}$	0.089	0.26	0.017	0.087	0.20
$a = k_{att} / (1 + k_{eq}^*)$	0.045	0.15	0.010	0.053	0.20
$b = k_{det}$	0.0035	0.0042	0.033	0.020	0.00021
<i>f</i>	0.036	0.011	0.56	0.13	0

Dimensions of *a*, *b*,  $k_{att}$  and  $k_{det}$  is  $\text{min}^{-1}$ ;  $k_{eq}^*$  and *f* are dimensionless.

### 6.4.2 Flow-Through Column Experiments

Figure 2a through 2e show the observed breakthrough curves together with best-fit curves obtained from a two-site model (Equations 1 and 2). The corresponding parameter values are given in Table 3. It was assumed that the dispersivity of all columns was the same: 6.4 cm. This value produced the best fitting results for all phages. This is a rather high value and tends to indicate a wide grain size distribution, it may have also been influenced by the very large flow velocity.

Initial breakthrough of all bacteriophages, except PM2, was retarded. Also, all breakthrough curves exhibit long tailing. Therefore, a two-site model was needed to fit the breakthrough curves. In the case of PM2, a one-site kinetic model was found to be more appropriate. The value of  $k_{eq}^*$  ranged between 0.6 and 1 for the retarded phages. In the case of MS2, PRD1, and Q $\beta$ , the values of  $f$  indicated that only a minor part of these phages adsorb to equilibrium sites, whereas  $\phi$ X174 adsorbed for most part to equilibrium sites. In fact, we found that with a one-site equilibrium model, an equally good breakthrough curve could be simulated for  $\phi$ X174. In both cases the tailing was underestimated (not shown). In order to fit the tail part of the breakthrough curve of  $\phi$ X174 the value of  $k_{det}$  was set to 0.033 and the other parameters were evaluated using CXTFIT. In the case of PM2, the measured concentrations along the tail are relatively low and do not have much weight in the fitting procedure. This resulted in overestimation of the tail concentrations and a small estimate for  $k_{det}$ . A visually better fit of the breakthrough tail was obtained by setting the value of  $k_{det}$  to 0.00021 and evaluating the other parameters using CXTFIT.

When comparing the five phages with each other, it can be seen that the value of  $k_{att}$  was lowest for  $\phi$ X174. The values of  $k_{att}$  for MS2 and Q $\beta$  were not significantly different. The value of  $k_{att}$  for PRD1 was not significantly different from that for PM2, but was significantly higher than that of the three other phages. Detachment of PRD1 was found to be one order of magnitude higher than that of PM2.

### 6.4.3 Flow-Through Column Experiments versus Batch and Recirculating Column Experiments

The values of the (a) attachment and (b) detachment rate coefficients from the flow-through column experiments can be compared with those from the batch and recirculating column experiments. Similar values for the attachment rate coefficient were found for the three kinds of experiments in the case of PRD1 and  $\phi$ X174. But in the case of MS2 and Q $\beta$  these values were lower and in the case of PM2 higher in the flow-through column experiments compared to the batch and recirculating column experiments. The values of the detachment coefficients were similar between the experiments only in the case of MS2. They were smaller in the flow-through column experiment in the case of PM2 and greater in the case of the other three phages.

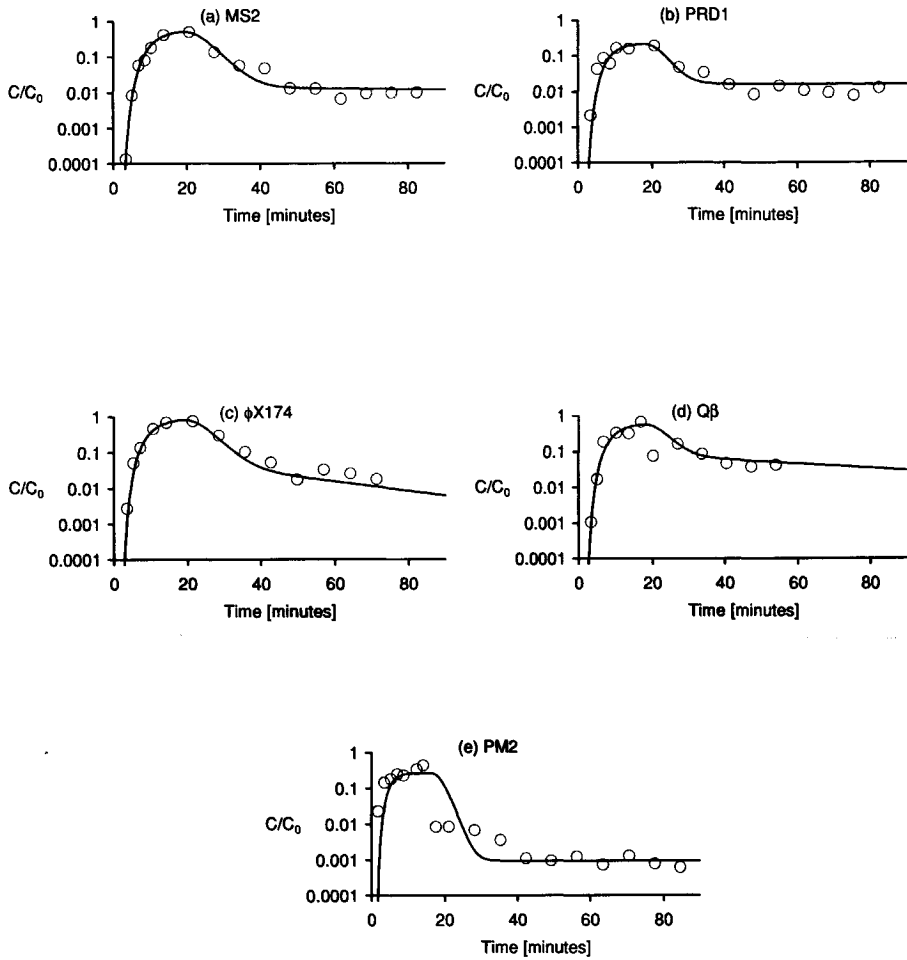


**Figure 2a to 2e** Breakthrough curves of flow-through column experiment with (a) MS2, (b) PRD1, (c)  $\phi$ X174, (d) Q $\beta$  and (e) PM2. The circles represent observations and the lines a 2-site model fit.

## 6.5 Discussion and Conclusions

Mostly, values of attachment and detachment obtained from experiments with batch suspensions were not found to be significantly different from those obtained from the recirculating column experiments. There were a few exceptions however. Bacteriophage MS2 was found to detach faster under the influence of advective flow. PRD1 was found to attach slower in a recirculating column, than in the batch experiment. However, in the flow-through column, the value of attachment for PRD1 was similar to that obtained with the batch experiment suggesting that the difference found between the batch and the recirculating column experiment may not be caused by the presence or absence of advective flow.

To conclude, the first hypothesis that attachment rate coefficients in batch experiments are larger than in column experiments, could not be verified. Also, the second hypothesis, that detachment rate coefficients in batch experiments are smaller than in column experiments is not verified. Only in case of MS2, the detachment rate increased as a consequence of the advective flow of water. This implies that similar attachment and detachment rate coefficients for certain virus-soil combinations from batch and recirculating column experiments may be found, but there may be exceptions, dependent on the type of virus. One would expect similar values of attachment and detachment to be obtained from the two kinds of column experiments. However, here some inconsistencies were found. For example, the attachment rate of MS2 was found to be considerably lower, and the detachment rate of PRD1 was found to be four times higher in the flow-through column than in the recirculating column. The inconsistencies between the two types of column experiments can neither be explained by the characteristics of the bacteriophages, nor by the type of column experiment. It is more plausible to ascribe such inconsistencies to the irreproducibility of column experiments. This may be due to differences in soil characteristics and/or packing of the soil in the different columns. The recirculating column experiments were all carried out using one column, whereas the flow-through column experiments were carried out using four different columns.

In the batch and recirculating column experiments that are presented here, it was found that attachment decreased in the order of MS2, PRD1, Q $\beta$ ,  $\phi$ X174 and PM2. A plausible explanation for the higher attachment of the presumably more negatively charged viruses may be found in the presence of positively charged sites; for example, in the form of ferric oxyhydroxides (Ryan *et al.*, 1999), or in the fact that concentrations of bivalent cations are rather high (Table 1). Bales *et al.* [1991] showed that Ca<sup>2+</sup>-concentrations of 1 – 100  $\mu$ M at pH 7 are sufficient to promote attachment of viruses. Multivalent cations can link viruses and adsorbents of like charge by forming salt bridges between them (Sobsey *et al.*, 1980; Moore *et al.*, 1982, Lipson and Stotzky, 1983) or by charge reversal (Grant *et al.*, 1993). Of course, high concentrations of monovalent cations may also promote attachment by compressing double layers (Lipson and Stotzky, 1983; Grant *et al.*, 1993, Redman *et al.*, 1999), but multivalent cations are believed to be much more effective. The findings from the present study suggest that multivalent cations promote attachment of the more negatively charged viruses even more. Hydrophobic interactions probably do not play a role here, because of the low organic matter content of the soil in this study.

Additional support for the explanation that more negatively charged viruses attach more than less negatively charged viruses, at high concentrations of multivalent cations, may be

found by comparing the present study with the field studies of Pieper *et al.* (1997) and Schijven *et al.* (1999). In these studies, values of  $k_{att}$  for MS2 and PRD1 were found to be 10 to 100 times lower than those from the flow-through column experiments in the present study. Compared to the present study, in the study of Pieper *et al.* (1997), pH was 5.0 – 5.7, electrical conductivity was about two times lower, and concentrations of multivalent cations were less than one-tenth. So, attachment may be lower in the study of Pieper *et al.* (1997), because of lower concentrations of monovalent and multivalent cations. In the study of Schijven *et al.* (1999) compared to the present study, pH was higher (8.3), electrical conductivity was comparable and concentrations of multivalent cations were about half. Attachment may be lower in the study of Schijven *et al.* (1999), because of higher pH and two times lower concentrations of multivalent ions.

This study has shown that similar attachment and detachment rate coefficients for a virus may be found in batch and recirculating column experiments, but there are exceptions, dependent on the type of virus. In batch and recirculating column experiments, no clear distinction can be made between equilibrium and kinetic sites, whereas this is possible in flow-through column experiments. It appeared that  $\phi$ X174 attached for the larger part to equilibrium sites, but MS2, PRD1 and Q $\beta$  for a minor part. PM2 attached only to kinetic sites. The inconsistencies that were found between the two types of column experiments may be due to soil characteristics and/or packing of the soil in the different columns. Therefore, when carrying out column experiments, soil heterogeneities need to be taken into consideration.

Under conditions of high pH in most sandy soils, MS2 can be regarded as a relatively conservative tracer virus, however, in the presence of multivalent cations, bacteriophage  $\phi$ X174 may attach less than MS2. This implies that in the case of soils, at near neutral pH, in the presence of high concentrations of multivalent cations, bacteriophage  $\phi$ X174 may be the better choice for a relatively conservative tracer virus in field and column studies than MS2.

### Acknowledgments

The expert comments of Clyde Munster are highly appreciated. The thorough reviewing and the useful comments of anonymous referees are greatly acknowledged.

## Chapter 7

# Column Experiments for Evaluating Field Data on Virus Removal by Soil Passage through Saturated Dune Sand

Schijven, J. F., de Bruin, H. A. M. and Hassanizadeh, S. M. 2001a. On the nonlinear removal of bacteriophages by passage through saturated dune sand. *Appl. Environ. Microbiol.* Submitted.

Schijven, J. F., de Bruin, H. A. M. and Hassanizadeh, S. M. 2001b. Modeling of bacteriophage transport through saturated dune sand at field and laboratory scale. *Adv. Water Resourc.* Submitted.

Schijven, J. F., de Bruin, H. A. M., Hassanizadeh, S. M. and de Roda Husman, A. M. 2001c. Indicator organisms for removal of pathogenic microorganisms by passage through saturated dune sand. *Appl. Environ. Microbiol.* Submitted.

**Abstract**

Recent studies have shown that removal of microorganisms from groundwater passing through sandy aquifers may be nonlinear. For example, in a field study on dune recharge, bacteriophages MS2 and PRD1 were found to be removed  $3 \log_{10}$  within the first 2.4 m and an additional  $5 \log_{10}$  within the next 27 m. To clarify this non-linear removal, a series of column experiments was carried out. Soil samples were taken along a streamline between the recharge canal and the first monitoring well. Experiments were carried out under conditions similar to the field: the same recharge water, the same temperature ( $5 \pm 3 \text{ }^\circ\text{C}$ ) and the same pore water velocity ( $1.5 \text{ m}\cdot\text{day}^{-1}$ ). Removal of MS2 and PRD1 was compared with that of the less negatively charged bacteriophage  $\phi\text{X174}$ . The high initial removal in the field was found not to be due to heterogeneity of the phage suspensions but mainly due to soil heterogeneity. On one hand, removal of MS2 and PRD1 from two-year-old and freshly prepared suspensions showed a similar linear removal. On the other hand, phage removal rates were found to vary more than a factor ten among columns with the different soil samples; strongly positively correlated with soil organic carbon content, and relatively strongly positively correlated with silt content and the presence of ferric oxyhydroxides. This suggests that the high initial removal in the field may take place within the first few meters of dune passage at a point where the organic carbon content is high, as was indeed observed in the field under the reedy border. The removal rates of MS2 and PRD1 observed in the columns varied across the range of  $0.13 - 2.4 \log_{10} \text{ day}^{-1}$ , which is very close to the range of  $0.11 - 1.8 \log_{10} \text{ day}^{-1}$  that was found in the field study over a distance of 30 meters. This implies that similar removal rates may be found at both laboratory and field scale. However, due to local variations at field scale detailed knowledge on soil heterogeneity may be needed in order to enable a reliable prediction of removal.

The effect of pore water velocity on removal of bacteriophages was investigated. This is of interest for drinking water companies wanting to keep land claim for recharge limited. As expected, a two times higher pore water velocity resulted in an approximately two times lower phage removal with distance.

A one-site kinetic model could not completely fit the breakthrough curves of MS2 and PRD1 in the field study. Considerable discrepancy at the end of the rising and the start of the declining limbs of the breakthrough curves was found. It was assumed that more types of kinetic sites exist due to surface charge heterogeneity of the granular medium. Thus, a two-site kinetic model was developed to analyze the breakthrough curves from the field study as well as from column experiments with bacteriophages MS2, PRD1 and  $\phi\text{X174}$ . Very satisfactory simulations of all breakthrough curves were obtained with the two-site kinetic model. This model can account for the skewness of the rising limb of the breakthrough curve as well as for the smooth transition of the declining limb to the tail of the breakthrough curve. A one-site kinetic model does not follow the curvature of the breakthrough tail, leading to an overestimation of  $\mu_s$ , the inactivation rate coefficient for attached viruses. It is suggested that the two-site kinetic model is generally applicable to fit breakthrough curves of microorganisms. Relatively fast attachment and slow detachment characterize interaction with kinetic site 1, whereas relatively fast attachment and detachment characterize interaction with kinetic site 2. At  $5 \pm 3 \text{ }^\circ\text{C}$ , inactivation of viruses and interaction with kinetic site 2 only provide a minor contribution to removal. The nature

of kinetic site 2 is unknown. Virus removal is mainly determined by the attachment rate to kinetic site 1.

In the field study, very low collision efficiencies were found for MS2 and PRD1, reflecting relatively conservative behavior and suggesting they are suitable indicators for virus transport. But the low collision efficiencies indicate that the soil conditions may be unfavorable for attachment of other (pathogenic) viruses too. From these observations, it was, therefore, not clear whether bacteriophages MS2 and PRD1 are representative for the removal of pathogenic viruses under the given conditions. The role of MS2 and PRD1 was evaluated by comparing their column breakthrough curves with those from bacteriophage  $\phi$ X174 and the human pathogenic viruses Coxsackievirus B4 (CB4) and Poliovirus 1 (PV1), which could not be studied in the field. Virus removal was in the order of  $PV1 > \phi X174 > CB4 \approx PRD1 \approx MS2$ . This can be explained by greater electrostatic repulsion that MS2, PRD1 and CB4 experience compared to the less negatively charged  $\phi$ X174 and PV1. This confirms the findings from many studies that MS2 and PRD1 can be considered as relatively conservative tracers for virus transport in saturated sandy soils at pH 6 – 8 and with a low organic carbon content at low temperatures.

Finally, removal of spores of *Clostridium perfringens* D10 was studied. This pathogen is regarded as an indicator for fecal contamination of drinking water sources. Moreover, Clostridium spores are a potential surrogate for *Cryptosporidium* oocysts, because both are highly persistent in the environment. The spores were found to attach relatively fast, but due to negligible inactivation all spores will eventually break through. Their actual removal with travel time or distance depends on the time period of seeding or contamination.

## 7.1 Introduction

In the Netherlands relies for about 14 % of the total drinking water production on pre-treated surface water that is artificially recharged in dune area. In a field study on the effectiveness of dune recharge for virus removal (Schijven *et al.*, 1999), it was shown that bacteriophages MS2 and PRD1 were removed 3  $\log_{10}$  within the first 2.4 m and only 5  $\log_{10}$  over the next 27 m. When considering MS2 and PRD1 as conservative virus tracers, it may be concluded that dune recharge is an effective way to remove viruses. However, a number of issues remained unclear in this study. These issues are described below.

The first unexplained issue is the high initial removal, *i.e.* the logarithmic reduction in concentration. Several other field and column studies also reported that removal of viruses by soil passage apparently declines with distance (see Schijven and Hassanizadeh, 2000, for a review). This implies that predictions of virus removal at larger distances may be severely overestimated if they are based on removal data from column experiments or from field studies where transport was studied only over short distances. It is therefore important to clarify the cause for the higher initial removal that was observed.

The high initial removal must have been caused by a removal process that existed within the first meters of dune passage, but not thereafter. One explanation may have been heterogeneity in the surface properties of the phage population; phages that are stickier will be removed faster. Another explanation may be spatial heterogeneity of the soil's adsorption characteristics.

One issue related to the modeling of the breakthrough curves remained unexplained. A model accounting for one-site kinetic attachment as well as first order inactivation was employed to simulate the bacteriophage breakthrough curves. Although, a reasonable fitting of the breakthrough curves was obtained, there was considerable discrepancy at the end of the rising and the start of the declining limbs of the breakthrough curves. The reason for this discrepancy has not been determined yet. One may assume that more types of kinetic sites exist due to surface charge heterogeneity of the granular medium. Patch-wise charge heterogeneities are common to all aqueous geologic settings, originating from inherent differences in the surface properties of adjacent crystal faces on mineral grains, and from minerals having bulk- or surface-bound chemical impurities (Ryan and Elimelech, 1996).

Another issue that could not be determined was whether MS2 and PRD1 are good model viruses. In field studies on virus removal by soil passage, bacteriophages are used as surrogates for pathogenic viruses, because concentrations of naturally present pathogenic viruses are usually very low and permission for seeding such viruses in the field is never given. Bacteriophages are harmless, can be seeded in large quantities, and are easy to measure.

Very low collision efficiencies were found for bacteriophages MS2 and PRD1 in the field study by Schijven *et al.* (1999). This reflected their relatively conservative behavior and suggests that they are suitable indicators for virus transport. But the low collision efficiencies indicate that the soil conditions may be unfavorable for attachment of other (pathogenic) viruses too. From these observations, it was, therefore, not clear whether bacteriophages MS2 and PRD1 are representative for the removal of other pathogenic viruses under the given conditions.

In order to investigate the foregoing questions and some other important issues, an extensive series of laboratory experiments was carried out. The major aims of the study were:

1. Investigate the linearity of removal of bacteriophages by passage through dune sand.
2. Evaluate the applicability of a model of adsorption to two different types of kinetic sites.
3. Study the effect of pore water velocity on removal of bacteriophages. This is of interest for drinking water companies wanting to minimize recharge and keeping land claim for recharge projects within limits (Peters, 1996).
4. Evaluate the role of bacteriophages as model viruses by comparing the behavior of three different types of bacteriophages with that of two different types of enteroviruses.
5. Study removal of spores of *Clostridium perfringens*. This pathogen has been used as an indicator of fecal contamination of drinking water sources and supplies for many years (Sartory *et al.*, 1998). Because of its very low inactivation rate, it may be a potential surrogate for oocysts of *Cryptosporidium parvum*.

Laboratory experiments were designed to closely simulate field conditions (Schijven *et al.*, 1999). To that aim, columns were filled with saturated sand from the field. Water from the recharge canal was used. The experiments were all conducted in a cold room at the temperature of the groundwater during the field study ( $5 \pm 3$  °C). The same transport velocity was applied as in the field ( $1.5 \text{ m.day}^{-1}$ ).

## 7.2 Experimental Methods

### 7.2.1 Soil Samples

Samples of dune sand for filling columns were collected along a flow line from the bottom of the recharge canal to the screen of the first monitoring well W1 at 2.4 meters distance. Table 2 lists the locations of the soil samples, denoted A to G. The samples were kept saturated with canal water and transported in stainless steel buckets. Samples of canal water were also collected in 20-liter polyvinylchloride containers. The sand and water samples were refrigerated ( $5 \pm 3$  °C). The soil samples were analyzed for grain size by laser grain size analysis (Konert and Vandenberghe, 1997), for organic carbon content and Al-, Fe- and Mn-oxalate as described in Stuyfzand and van der Jagt (1997). The concentrations of Al-, Fe- and Mn-oxalate largely represent amorphous Al-, Fe- and Mn-oxides and -hydroxides.

### 7.2.2 Microorganisms

Highly concentrated suspensions of MS2 and PRD1 were prepared as described in Schijven *et al.* (1999). In fact, the very same batch suspensions from the field study, which were stored at  $5 \pm 3$  °C for over 2 years, were used in the laboratory experiments. In order to check the role of aging, in one experiment, freshly prepared, highly concentrated suspensions of MS2 and PRD1 were used. A highly concentrated suspension of  $\phi$ X174 was prepared as described in ISO 10705-2 (2000). Part of the highly concentrated bacteriophage suspensions was diluted with 1 g/l peptone-saline to a concentration of  $10^{10} - 10^{11}$  phages per liter. These were used as stock suspensions.

MS2 and PRD1 were selected as model viruses because of their negative charge. MS2 is an icosahedral phage with a diameter of 27 nm and a low isoelectric point (pI) of 3.5. PRD1 is an icosahedral bacteriophage with a diameter of 62 nm with an inner lipid membrane (Bales *et al.*, 1991; Caldentey *et al.*, 1990). Its pI lies between 3 and 4 (Loveland *et al.*, 1997). Bacteriophage  $\phi$ X174 is less hydrophobic than MS2 (Shields and Farrah, 1987), and has a pI of about 6.6 and a size of 23 nm (Fujito and Lytle, 1996; Jin *et al.*, 1997).

The following pathogenic enteroviruses were included in the experiments: A Coxsackievirus B4 (CB4) isolate (RIVM 93-15-7) from recreational surface water and Poliovirus 1 Lsc 2ab (PV1). PV1 is a virus with a diameter of 23 nm and a pI of 6.6 (Bales *et al.*, 1993), but a pI of 7.15 has also been reported (Sobsey *et al.*, 1980). CB4 is in use at our laboratory as a positive control strain for the enumeration of enteroviruses by the plaque method on Buffalo Green Monkey (BGM) cells as described by de Roda Husman *et al.* (2001). Highly concentrated suspensions of CB4 and PV1 were prepared by the cytopathogenic-effect method as described by van Olphen *et al.* (1984).

A highly concentrated suspension of *Clostridium perfringens* strain D10 was prepared as described for *Clostridium bifermentans* strain R5 by Schijven *et al.* (2000).

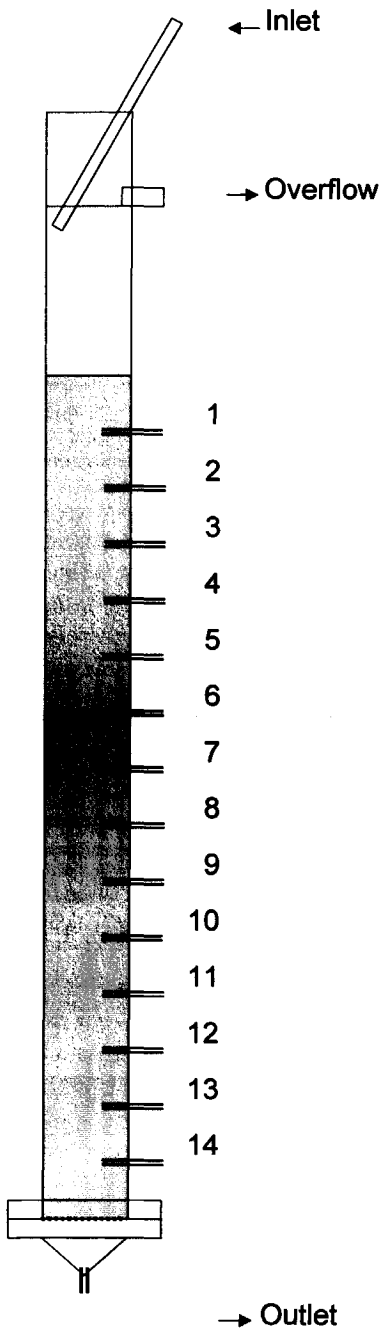


**Figure 1** Schematic representation of a column, filled with sand to a length of 1.5 m. Inner column diameter is 9 cm. Numbers 1 to 14 represent stainless steel samplers, each 10 cm apart.

Prior to each experiment, a seeding suspension was made by adding a selection of these microorganisms in a container with canal water. Initial seeding concentrations were about  $10^7$  to  $10^8$  per liter for each microorganism. MS2 was included in all experiments as a reference.

### 7.2.3. Preparation of Columns

Figure 1 shows a schematic representation of a column; a Perspex pipe was constructed with an inner diameter of 9 cm and a length of 1.9 m. A stainless steel grid for supporting the sand was placed at the bottom of each pipe. An adjustable stainless steel table supported the pipe. Along the pipe, 14 small stainless steel samplers were placed at 10-cm intervals. The pipe was filled with increments of saturated dune sand. During the filling, canal water was flowing upwards. At the same time, the pipe was being tapped in order to distribute the sand evenly and to dislodge air bubbles. The pipe was filled up to a length of 1.5 m. Initially, a thin layer of very fine sand particles settled on top of the column. This layer was removed by suction. One to two days later the flow of water was reversed to downward direction at a rate of  $2.4 \text{ ml}\cdot\text{min}^{-1}$ , corresponding to a pore water velocity of  $2.4 \text{ ml}\cdot\text{min}^{-1}$ . The sand column was kept saturated at all times. The water in the funnel-shaped outlet of the column was gently, but continuously, mixed by means of a magnetic stirrer. This way, the concentration gradient at the lower

boundary of the column was kept to zero. In all experiments, pH of the recharge water was 7.5 – 8.0. At the inlet, canal water was fed and salt and microorganisms were seeded. The overflow kept the level of water in the column constant and led excess of water to the feeding tank. The pump that was connected to the outlet determined the flow rate of water through the column and led the effluent to a disposal tank.

Seven different columns were prepared, each of them filled with different portions of soil samples A to G as described in Table 1. These columns, soil samples and their corresponding lengths (figures inside parentheses, measured from the top of the column) are as follows:

- Column I containing soils A (0 – 0.2 m), B (0.2 – 0.4 m) and C (0.4 – 1.4 m);
- Column II containing soils D (0 – 0.5 m), E (0.5 – 1.0 m) and F (1.0 – 1.4 m);
- Columns III, VI and VII containing soil G, taken near the first monitoring well;
- Columns IV and V containing soil G\*, that was collected at a later date at the same location as soil G.

#### 7.2.4 Salt Breakthrough Experiments

For each column that was constructed, a transport experiment with salt was carried out in order to estimate interstitial flow velocity and medium dispersivity. First, the water on top of the column was removed by pumping to the point where less than one millimeter of water was left on top of the column. Then, it was filled gently with a solution of 750 mg.l<sup>-1</sup> sodium chloride in canal water to the level of the overflow. This way, a sharp front of salt water was introduced to the sand column. The salt solution was fed for a period of 24 hours. At the end of the dosage, the salt solution was replaced by canal water following the same procedure as at the start of the dosage. Samples were taken from sampler number 14, unless otherwise mentioned. Sampling was carried out by continuously pumping from one sampler at a time at a rate of about 0.2 ml.min<sup>-1</sup> for 18 minutes. Samples were collected in glass tubes using a programmable fraction collector. Breakthrough of the salt tracer was established by manually measuring electrical conductivity of the sampled fractions.

#### 7.2.5 Transport Experiments with Microorganisms

Two types of experiments with two different aims were carried out: Experiments to measure overall removal rates and experiments for obtaining breakthrough.

In order to investigate the linearity of removal, soil columns I – V were fed continuously for four days with a suspension of MS2, PRD1 and φX174. In column III, this was continued for 17 days in order to investigate blocking effects. From the second day of seeding, *i.e.* after steady state was established, 1.2-ml samples were taken every day from all sampling points at a flow rate of 0.2 ml.min<sup>-1</sup>. Removal was also measured at a two times higher velocity. To measure inactivation of bacteriophages in the aqueous phase, samples from the column influent and effluent were taken every few days for one to three weeks and analyzed.

In breakthrough experiments, suspensions of microorganisms were seeded for 24 hours and breakthrough was monitored for a period of about a week. In columns III and IV bacteriophages were sampled at 1.4 m. In column VI, MS2 and CB4 were sampled at 0.4 m, and in column VII, MS2, PV1 and D10 were sampled at 0.3 m. Seeding of the microorganisms was carried out following the same procedure as explained for the salt

tracer. Samples were collected automatically every six minutes in glass tubes. The sample tubing consisted of PTFE- and silicone tubing. Prior to each experiment, the tubing was rinsed with a chlorine solution and then with hot tap water. The tubing was tested for interaction with bacteriophages. This was done by pumping seeding suspensions of the bacteriophages through the tubing at a rate of 0.2 ml.min<sup>-1</sup>. Eight replicate influent and effluent samples were analyzed. According to analysis of variance no significant differences between these samples were found. Therefore, we were sure that no attachment of bacteriophages to the sample tubing occurred.

### 7.2.6 Enumeration of Microorganisms

MS2 was assayed as described in ISO 10705-1 (2000) using host strain WG49 (Havelaar *et al.*, 1984). PRD1 was assayed according to ISO 10705-1 using *S. typhimurium* LT2 as the host, omitting nalidixic acid in the top agar layer. Bacteriophage φX174 was assayed according to ISO10705-2 (2000) using WG5 (ACC 700078) as the host.

PV1 and CB4 were enumerated as described by de Roda Husman *et al.* (2000).

To assay the spores of *Clostridium perfringens*, aliquots of 1 ml from sample dilutions were mixed with about 5 ml of molten Sulphite Cycloserine Agar of 45 °C in 9 cm Petri dishes. As soon as this agar had solidified, a layer of about 10 ml of the same agar was poured on top. The plates were incubated for 48 hours at 37 °C in anaerobic jars. The black colonies that had developed were counted.

## 7.3 Modeling Methods

### 7.3.1 Conceptual Model

To investigate whether multiple kinetic sites were present in the Castricum dune sands, a two-site kinetic model was constructed and used for analyzing breakthrough curves obtained in laboratory and field experiments. The aim was to determine whether rate constants for the two kinetic sites are identifiable. The governing equations for an advection-dispersion model, including reversible adsorption to two types of kinetic sites and inactivation of free and attached microorganisms, are as follows:

$$\frac{\partial C}{\partial t} + \frac{\rho_B}{n} \frac{\partial S_1}{\partial t} + \frac{\rho_B}{n} \frac{\partial S_2}{\partial t} = \alpha_L v \frac{\partial^2 C}{\partial x^2} - v \frac{\partial C}{\partial x} - \mu_l C - \mu_{s1} \frac{\rho_B}{n} S_1 - \mu_{s2} \frac{\rho_B}{n} S_2 \quad (1)$$

$$\frac{\rho_B}{n} \frac{\partial S_1}{\partial t} = k_{att1} C - k_{det1} \frac{\rho_B}{n} S_1 - \mu_{s1} \frac{\rho_B}{n} S_1 \quad (2)$$

$$\frac{\rho_B}{n} \frac{\partial S_2}{\partial t} = k_{att2} C - k_{det2} \frac{\rho_B}{n} S_2 - \mu_{s2} \frac{\rho_B}{n} S_2 \quad (3)$$

where  $C$  is the concentration of free phages [pfp.m<sup>-3</sup>];  $S$  is the concentration of attached phages [pfp.kg<sup>-1</sup>];  $t$  is the time [days];  $x$  is the distance [m];  $\alpha_L$  is the dispersivity [m];  $v$  is the average interstitial water velocity [m.day<sup>-1</sup>];  $\rho_B$  is the dry bulk density [kg.m<sup>-3</sup>];  $n$  is the porosity [-];  $k_{att}$  and  $k_{det}$  are the attachment and detachment rate coefficients, respectively

[day<sup>-1</sup>];  $\mu_1$  and  $\mu_s$  are the inactivation rate coefficients of free and attached phages, respectively [day<sup>-1</sup>]. Subscripts 1 and 2 refer to the two different kinetic sites. These equations are subject to boundary conditions  $C = C_0$  at  $x = 0$  and  $\frac{\partial C}{\partial x} = 0$  at  $x = L$ . The initial conditions were zero concentration for all microorganisms.

A numerical model called EQ2KIN was constructed for solving the equations. These equations were discretized numerically using an explicit central finite difference scheme. (see the FORTRAN 77-code in the appendix). Quantities  $v$  and  $\alpha_L$  were found from fitting the salt breakthrough curves using CXTFIT2 (Toride *et al.*, 1995). Estimates of  $\mu_f$  for the bacteriophages were found by measuring their inactivation in column influent and effluent suspensions for a period of one to two weeks. The method for analysis of the inactivation data is described in the following section. Estimates of  $\mu_f$  for the other viruses were found by measuring their inactivation in column influent suspensions. Estimation of parameters  $k_{att1}$ ,  $k_{att2}$ ,  $k_{det1}$ ,  $k_{det2}$  and  $\mu_{s1}$  was carried out by coupling EQ2KIN to the parameter estimation code PEST version 1.07 (Watermark Computing, 1994). The estimation was done by applying log-transformation of the parameters. The value of parameter  $\mu_{s2}$  was assumed to be equal to  $\mu_{s1}$ . Since, the observed concentrations varied relatively more at higher values than at lower values, they were assumed to be log-normally distributed. Therefore, fitting of the breakthrough curves was carried out using log-transformed concentrations. As a measure of goodness of fit, the coefficient of determination  $r^2$  (Toride *et al.*, 1995) was calculated on the basis of  $N$  logarithmically transformed observations  $C_i$  and fitted values  $F_i$ :

$$r^2 = 1 - \frac{\sum_{i=1}^N (\ln C_i - \ln F_i)^2}{\sum_{i=1}^N \left( \ln C_i - \frac{\sum_{i=1}^N \ln C_i}{N} \right)^2} \quad (4)$$

For comparison, a one-site kinetic model was also used for fitting of the breakthrough curves. To that aim the same procedure was followed as for fitting of the two-site kinetic model, but the parameter values for site 2 were set to zero.

Under steady state conditions, the relative contributions of inactivation and adsorption to the removal of viruses by soil passage can be computed analytically. A steady state situation occurs when input of virus continues for long time and may be seen as a worst-case situation. For a steady state situation, Equation 1 and 3 are simplified to:

$$\alpha_L v \frac{\partial^2 C}{\partial x^2} - v \frac{\partial C}{\partial x} = \mu_f C + \mu_{s1} \frac{\rho_B}{n} S_1 + \mu_{s2} \frac{\rho_B}{n} S_2 \quad (5)$$

$$\frac{\rho_B}{n} S_1 = \frac{k_{att1}}{\mu_{s1} + k_{det1}} C \quad (6)$$

$$\frac{\rho_B}{n} S_2 = \frac{k_{att2}}{\mu_{s2} + k_{det2}} C \quad (7)$$

Substitution of Equations 6 and 7 into 5 gives

$$\alpha_L \frac{\partial^2 C}{\partial x^2} - \frac{\partial C}{\partial x} - \frac{\lambda}{v} C = 0 \quad (8)$$

$$\text{where } \lambda = \mu_f + \frac{k_{att1}}{1 + k_{det1}/\mu_{s1}} + \frac{k_{att2}}{1 + k_{det2}/\mu_{s2}} \quad (9)$$

Now, Equation 8 has the following solution:

$$\log_{10} \left( \frac{C}{C_0} \right) = \frac{x}{2.3} \frac{\left( 1 - \sqrt{1 + 4\alpha_L \frac{\lambda}{v}} \right)}{2\alpha_L} \quad (10)$$

where  $C_0$  is the concentration at  $x = 0$ , and  $\log_{10}(C/C_0)$  is a measure of virus removal. It can be shown that for small values of  $\alpha_L$ , the removal rate,  $r$  [ $\text{day}^{-1}$ ], is describe by the following simple equation:

$$r = \frac{-\log_{10} \left( \frac{C}{C_0} \right)}{t} = \frac{\lambda}{2.3} \quad (11)$$

where  $t$  is the travel time defined by  $t = x/v$ .

From Equation 9, the relative contributions of adsorption and inactivation to virus removal can be deduced. The first term in Equation 9 gives the removal rate by inactivation of free virus. The second and last terms give the removal rate of virus due to interaction with kinetic sites. Interaction means the combination of attachment, detachment and inactivation of attached viruses. The parameter values obtained from fitting the breakthrough curves were employed to calculate the removal rates and the contribution of inactivation and interaction with both kinetic sites under steady state conditions.

### 7.3.2 Calculation of Collision Efficiencies

In colloid filtration theory of attachment of colloids, the parameter collision efficiency is introduced as a measure of the intrinsic capacity of the soil (Yao *et al.*, 1971). The collision efficiency is an empirical constant that accounts for electrostatic interactions, in this case, between microorganisms and the porous medium.

Collision efficiencies were calculated using the following equation (Yao *et al.*, 1971):

$$\alpha = \frac{2}{3} \frac{d_g}{(1-n)} \frac{k_{att} v}{\eta} \quad (12)$$

where  $\alpha$  is the collision efficiency and  $\eta$  is the single collector efficiency.

The single collector efficiency  $\eta$  was calculated using the following relationship due to Martin *et al.* (1992):

$$\eta = 1.0 A_s N_{Lo}^{1/8} N_R^{15/8} + 0.00388 A_s N_G^{1.2} N_R^{0.4} + 4 A_s^{1/3} N_{Pe}^{-2/3} \quad (13)$$

Here,  $N_R = d_p / d_c$  accounts for interception,  $N_G = d_p^2 (\rho_p - \rho) g / (18 \mu v n)$  for gravity effects,  $N_{Lo} = 4H / (9 \mu d_p^2 v n)$  for van der Waals interactions, and  $N_{Pe} = d_p v n / D_{BM}$  for diffusion. In these definitions,  $d_p$  and  $d_c$  represent the microorganism particle sizes and soil grain sizes [m], respectively,  $g$  is the gravitational acceleration,  $\rho$  and  $\rho_p$  are the density of water and the microorganism particle, respectively,  $\mu = \rho * 0.000947 / (T + 42.5)^{1.5}$  is the dynamic viscosity [kg/m.s] with  $T$  the water temperature [°C],  $H = 6.2 \times 10^{-21}$  is the Hamaker constant [J] for the bacterium-glass-water interface (Rijnaarts *et al.*, 1995),  $D_{BM} = K_B (T + 273) / (3 \pi d_p \mu)$  is the diffusion coefficient [m<sup>2</sup>/s] with Boltzmann-constant  $K_B = 1.38 \times 10^{-23}$  (J.K<sup>-1</sup>), and  $A_s = 2(1 - \gamma^5) / (2 - 3\gamma + 3\gamma^5 - 2\gamma^6)$  is Happel's porosity-dependent parameter, with  $\gamma = (1 - n)^{1/3}$ . Clostridium spores have an assumed size of 1  $\mu$ m and a buoyant density of 1270 kg.m<sup>-3</sup> (Tisa *et al.*, 1982). Because viruses are small, their transport in the immediate vicinity of the collector surface is dominated by Brownian diffusion. In this case,  $\eta$  is given approximately by the last term in Equation 13. Equation 11 is employed to calculate collision efficiencies  $\alpha_1$  and  $\alpha_2$ , based on  $k_{att1}$  and  $k_{att2}$ , respectively.

### 7.3.3 Analysis of Inactivation Rates and Removal Rates

The inactivation of free bacteriophages is assumed to be first order. As mentioned above, the inactivation rate coefficient of the bacteriophages in water was estimated from the decrease in concentrations with time in samples taken from both column influent and effluent in each experiment. First, inactivation data from different column experiments were compared in order to test whether these data could be pooled. Next, effects of passage through columns on inactivation of free phages were studied by comparing inactivation rates in column influent and effluent.

Removal of the bacteriophages with time or distance is also expected to be first order (see Equation 1). The removal capacities of various soil samples as a function of travel time and distance were determined and compared among soil samples.

Assuming both inactivation and removal are first order, the logarithms of the measured concentrations must decline linearly with either time or distance. Assuming normally distributed errors, a log likelihood function,  $L$ , which includes parameters  $a$  (slope),  $b$

(intercept) and  $s$  (standard error) can be formulated for each set of  $n$  measured concentrations  $C_i$  at time  $t_i$  from an experiment (Hogg and Craig, 1978):

$$L(a, b, s) = 2 \sum_{i=1}^n \left[ \ln(s\sqrt{2\pi}) + \frac{[\ln C_i - (at_i + b)]^2}{2s^2} \right] \quad (14)$$

where  $i$  is the  $i$ -th of  $n$  observations. In the case of inactivation experiments parameter  $a$  equals inactivation rate coefficient  $\mu_i$ , and in the case of the removal experiments it equals removal rate  $r$ .

Values for parameters  $a$ ,  $b$  and  $s$  for the different sets of data or combinations of these sets of data were obtained by maximizing this log likelihood function (equivalent to least squares solution) using numerical optimization in Mathematica 4.0.0 (Wolfram Research, 1999). The question was whether the slopes  $a$  for different sets of data were different or not. This can be done by means of likelihood ratio tests (Cox and Hinkley, 1974). The linear model can be applied to all separate data sets as well as pooled data sets. For pooled data sets, a common value of slope  $a$  was evaluated using the following likelihood function (Hogg and Craig, 1995):

$$L(a, b_1, b_2, \dots, b_m, s) = 2 \sum_{j=1}^m \sum_{i=1}^{n_j} \left[ \ln(s\sqrt{2\pi}) + \frac{[\ln C_{ij} - (at_{ij} + b_j)]^2}{2s^2} \right] \quad (15)$$

for  $m$  experiments with  $n_j$  observations.

The sum of the log likelihoods of the separate data sets is compared to that of the pooled data. The difference is interpreted as a  $\chi^2$ -deviate with number of degrees of freedom equal to the difference in the number of parameters in the pooled data set ( $2+m$ ) and the total number of parameters of all separate data sets ( $3*m$ ) (Teunis et al., 1996). If the log likelihood of the pooled data is found to be significantly higher than that of the sum of the log likelihoods of the separate data sets, then significant differences exist between the data sets. If not, they may be pooled.

In the case of columns I and II, both with three layers of soil ( $0 - x_1$ ,  $x_1 - x_2$ ,  $x_2 - \text{end of column}$ ), a linear model  $f(t) = a_1 t + b$  with slope with slope  $a_1$  was compared with a model defining three slopes  $a_1, a_2, a_3$ , each corresponding to one layer of soil, thus incorporating spatial heterogeneity into the regression model:

$$f(t) = \begin{cases} a_1 t + b & \text{if } 0 \leq t \leq \frac{x_1}{v} \\ a_2(t - t_1) + a_1 t_1 + b & \text{if } \frac{x_1}{v} \leq t \leq \frac{x_2}{v} \\ a_3(t - t_2) + a_2(t_2 - t_1) + a_1 t_1 + b & \text{if } \frac{x_2}{v} \leq t \leq \frac{x_3}{v} \end{cases} \quad (16)$$

## 7.4 Results

### 7.4.1 Soil Analysis

Results of chemical and physical analysis of soil samples are given in Table 1. Grain size distribution was similar for all sand samples, but clay and silt contents were lower in soils B and C. The organic carbon content was higher in samples A, B and D. The values of silt and Fe-oxalate are higher in soil A. Figure 2 shows the variation of the Fe-oxalate concentrations, the organic carbon content and silt content with travel distance at field scale. Parameter values from linear regression analysis are listed in Table 2 and the regression lines are plotted in Figure 2. There appears to be a significant first order decrease with travel distance. In the case of silt content, soils B and C were omitted from regression analysis. Possibly, the silt content may vary irregularly, or silt and clay were partly lost when taking samples B and C from the bottom of the recharge canal.

### 7.4.2 Removal Rates

Figure 3 shows the removal of the bacteriophages with travel distance in columns I, II and III containing soils A to G. Table 3 summarizes the removal rates that were found by fitting the log likelihood-function (Equations 14 and 15). No significant change in removal rate within four days was found for MS2 in none of the columns and for  $\phi$ X174 in column III. But in the other cases, significantly different removal rates between days were found. In columns I and II, both containing three layers of different soil samples, removal rates were found to be significantly different among the different soils for all bacteriophages. It appears that the removal rate is the highest in soil A. This is most apparent for  $\phi$ X174, because removal of this bacteriophage is higher than that of MS2 and PRD1. In soil E, removal of the phages appeared to be very low, even an increase in concentrations with travel time was found. Probably, the samples from soil E in column II contained silt particles with attached phages, causing higher phage counts. These data points were therefore excluded from subsequent analyses.

Table 4 gives the correlation coefficients of soil properties and removal rates. Obviously, sand and silt content are negatively correlated and also the clay content is highly negatively correlated with the sand content. The organic carbon content was found to be highly positively correlated with the silt content. Al-oxalate appeared to be highly positively correlated with the silt and clay content. Mn-oxalate was positively correlated with the sand content. Fe-oxalate was found to be positively correlated with the silt content and highly positively with the organic carbon content.

The removal rates of all three bacteriophages are highly positively correlated with the organic carbon content of the soil. This means that either organic carbon provides attachment sites for the bacteriophages, or that organic carbon and bacteriophages attach to the same type of sites, probably ferric oxyhydroxides of which there are more present in soils A and D. Removal rates of the bacteriophages also show a relatively high and positive correlation with Fe-oxalate and the silt-content, but a low correlation with clay content. Removal rates of the bacteriophages are highly correlated, indicating interaction of the bacteriophages with the same types of kinetic sites.

**Table 1** Chemical and physical analysis of soil samples

Soil sample	A	B	C	D	E	F	G
Distance <sup>a</sup>	0	0	0	0.35	0.7	1.05	1.4
Depth <sup>b</sup>	0-0.05	0.05-0.1	0.1-0.6	0.7-1.0	0.9-1.1	1.2-1.4	1-1.3
L <sup>c</sup>	0.05	0.1	0.35	1.5	1.9	2.3	2.6
T <sup>c</sup>	0.035	0.071	0.25	1.1	1.3	1.7	1.8
Grain size <sup>d</sup>	242	220	214	236	237	239	255
Clay ( $\leq 2 \mu\text{m}$ ) <sup>e</sup>	0.97	0.69	0.67	1.07	1.01	0.92	1.02
Silt ( $> 2$ and $\leq 53 \mu\text{m}$ ) <sup>e</sup>	3.98	1.71	2.08	3.26	2.96	2.38	2.37
Sand ( $> 53 \mu\text{m}$ ) <sup>e</sup>	95.01	97.56	97.24	95.68	96.00	96.70	96.74
f <sub>oc</sub> <sup>e</sup>	0.88	0.50	0.32	0.50	0.16	0.16	0.27
Al-oxalate <sup>f</sup>	0.83	0.55	0.52	0.83	0.86	0.76	0.62
Fe-oxalate <sup>f</sup>	2.8	2.1	2.3	2.4	1.8	1.3	1.1
Mn-oxalate <sup>f</sup>	0.030	0.059	0.031	0.026	0.018	0.019	0.036
Appearance	black	yellow-brown + shells	yellow-brown + shells	black-grey	yellow-brown	yellow-brown-grey	yellow-grey

<sup>a</sup>Distance from bank of recharge canal [m]; <sup>b</sup>Samples A - C relative to bottom of recharge canal [m], samples D - G relative to groundwater level [m]; <sup>c</sup>Travel distance [m] and time [day] approximately along flow line; <sup>d</sup>Geometric mean [ $\mu\text{m}$ ]; <sup>e</sup>%; <sup>f</sup>g/kg dry weight.

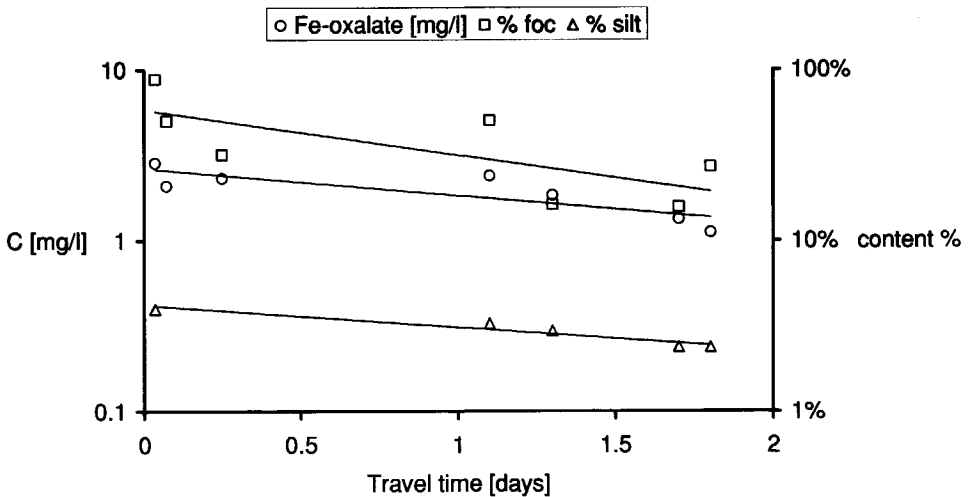


**Figure 2** Change in concentration of Fe-oxalate and contents of f<sub>oc</sub> and silt as a function of travel time.

Column Experiments for Evaluating Field Data on Virus Removal

**Table 2** Regression analysis of soil properties (on log-scale) as a function of travel distance.

	slope	p	intercept	p	Rsqr
ln (Fe-oxalate)	-0.40	0.81%	1.09	0.023%	78%
ln (f <sub>oc</sub> )	-0.65	4.7%	-0.51	12%	58%
ln (silt)	-0.30	0.21%	-3.2	0.00042%	97%

**Table 3** Removal rates  $r$  ( $\log_{10} \text{ day}^{-1}$ ) in soils A to G (columns I to III).

	Column Day	I			II			III
		A	B	C	D	E	F	G
MS2	2	2.7	0.45	0.021	0.75	0.12	0.36	0.54 (0.35-0.73)
	3	2.2	0.65	0.18	0.44	-0.063	0.12	0.59 (0.38-0.80)
	4	1.1	1.9	0.24	0.43	0.17	0.39	
	All	2.0	1.0	0.13	0.54	0.039	0.21	0.57 (0.44-0.70)
PRD1	2	3.0	-0.11	0.10	1.0	-0.27	0.32	0.70 (0.46-0.93)
	3	2.7	1.7	0.39	1.1	-0.34	-0.20	0.61 (0.37-0.85)
	4	1.6	1.9	0.20	0.91	-0.19	1.2	
	All	2.4	1.2	0.23	1.0	-0.26	0.45	0.66 (0.50-0.81)
$\phi$ X174	2	17	1.9	1.4	1.6	0.52	2.6	2.5 (2.3-2.7)
	3	13	4.1	1.2	1.2	-0.037	2.5	2.1 (1.7-2.4)
	4	14	3.3	1.6	1.6	0.22	1.8	
	All	15	3.0	1.4	1.5	0.23	2.3	2.3 (2.0-2.5)

95%-confidence intervals are given between brackets for removal rates in column III with soil G.

**Table 4.** Correlation coefficients of soil properties and removal rates  $r$  ( $\log_{10} \text{ day}^{-1}$ ).

	% sand	% silt	% clay	% f <sub>oc</sub>	Al-oxalate	Mn-oxalate	Fe-oxalate	$r$	
								MS2	PRD1
% silt	-1.00								
% clay	-0.74	0.68							
% f <sub>oc</sub>	-0.67	0.71	0.14						
Al-oxalate	-0.89	0.86	0.80	0.42					
Mn-oxalate	0.52	-0.50	-0.54	0.20	-0.61				
Fe-oxalate	-0.48	0.53	-0.16	0.83	0.25	0.09			
$r$ MS2	-0.61	0.64	0.18	0.92	0.39	0.26	0.57		
$r$ PRD1	-0.72	0.74	0.29	0.95	0.54	0.15	0.62	0.98	
$r$ $\phi$ X174	-0.70	0.74	0.19	0.85	0.48	0.05	0.56	0.92	0.92

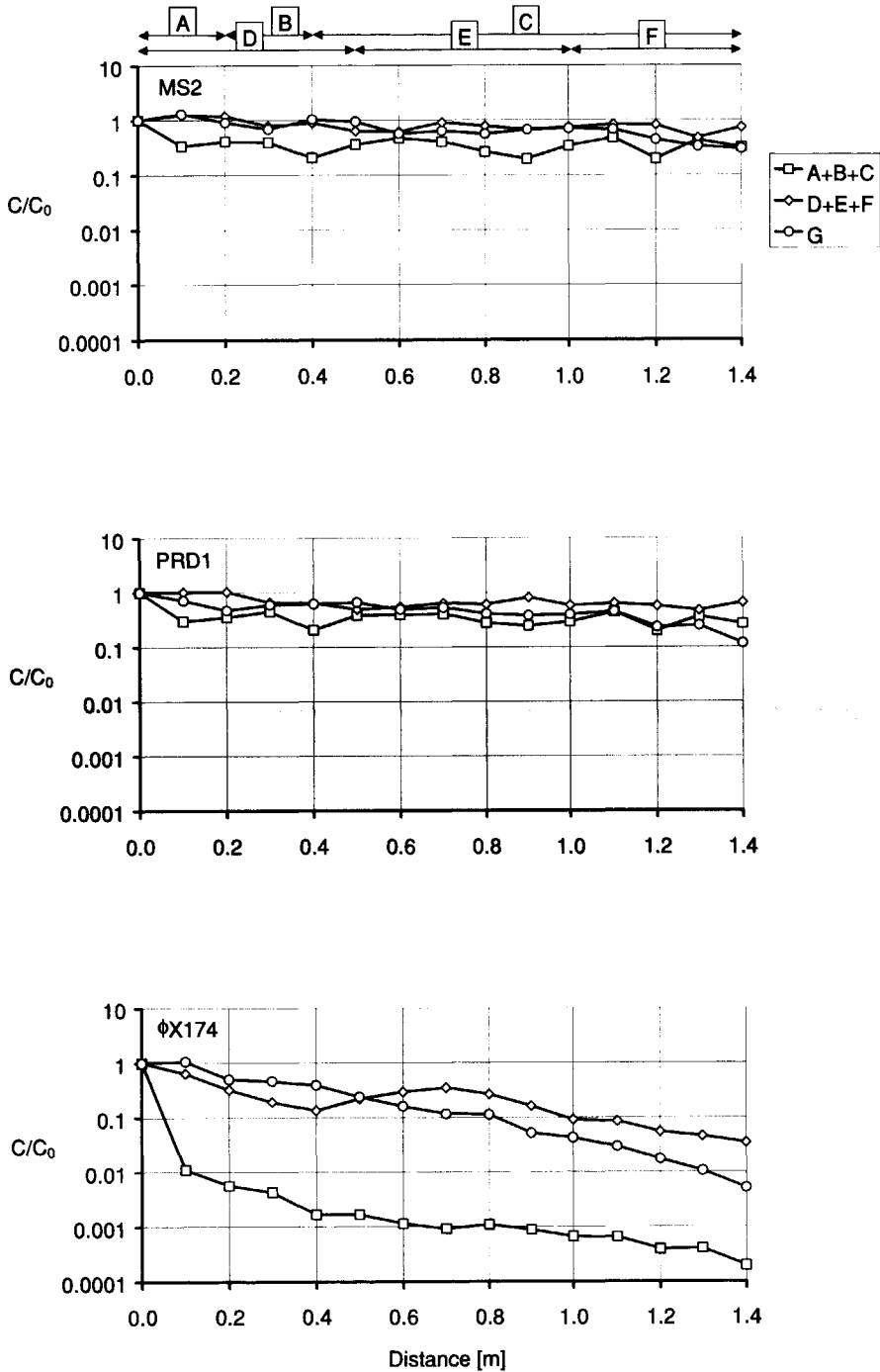


**Figure 3** Removal of bacteriophages with distance after 2 days of seeding in columns I (A+B+C), II (D+E+F) and III (G).

Seeding of bacteriophages in column III containing soil G was continued for a period of 17 days to investigate the possibility of blocking attachment sites with bacteriophages upon prolonged seeding. In the event of blocking, the grain surfaces become progressively occluded, resulting in a decrease in attachment rate. Removal rates are given in Table 5 and plotted with time in Figure 4. Apparently, blocking did not occur. On the contrary, the removal rates of all phages appeared to increase significantly with time. This increase was the same for MS2 and  $\phi$ X74 but three times higher for PRD1. With column IV containing soil G\*, this experiment was repeated, but now seeding was performed for the first three days and again thirty days later. In the intermediate period, the column was not seeded with bacteriophages, only recharge water was fed. In this experiment removal rates did not change significantly. Therefore, the observed increase in removal rates in column III appears to be due to the continuous seeding of bacteriophages.

Table 6 shows the removal rates that were observed in column IV, containing soil G\*, after seeding bacteriophages for two days at a pore water velocity of  $1.7 \text{ m day}^{-1}$ , followed by seeding for one day at a higher velocity of  $3.3 \text{ m day}^{-1}$ . According to colloid filtration theory (Yao *et al.*, 1971), removal rate  $r$  in terms of travel time is proportional to  $v^{1/3}$ , whereas removal rate  $s$  in terms of travel distance is proportional to  $v^{-2.3}$ . In our case,  $v$  was increased by a factor of 1.94, therefore,  $r$  was expected increase by a factor of 1.25 and  $s$  was expected to decrease by a factor of 0.64. It appears that removal rates  $r$  are similar and that removal rate  $s$  are almost halved at the higher velocity. These differences were found to be significant.

Table 6 also shows the removal rates measured in column V containing soil G\*, where freshly prepared suspensions of MS2 and PRD1 were used. Removal of the bacteriophages in this experiment appeared to be linear as well at approximately the same removal rate as in column IV. This means that the initially higher removal of MS2 and PRD1 that was observed in the field was not resulting from sub-populations of phage particles that are removed more efficiently, and that are only present in freshly prepared suspensions.

For columns III, IV and V with only one type of soil (G or G\*), 95% confidence intervals were calculated (Tables 3 and 6) to give an idea of the uncertainty of the observed removal rates. For MS2 and PRD1, the 5%- and 95%-limits differ by a factor of 1.6 – 2.3 in column III (Table 4). For  $\phi$ X174, this ratio is only 1.2 – 1.4. In column IV (Table 7), the 5%- and 95%- limits MS2 and PRD1 differed with factors 2 and 6, respectively, at a pore water velocity of  $1.7 \text{ m.day}^{-1}$ . At a higher pore water velocity ( $3.3 \text{ m.day}^{-1}$ ), these differences were even higher, *i.e.* a factor 33 – 35 for MS2 and PRD1. Whereas for  $\phi$ X174, the ratio of the lower and upper limits of the confidence interval is only 1.5 – 1.7. The confidence interval of the removal rate of  $\phi$ X174 is much smaller because the removal rate is much higher than that of MS2 and PRD1. Removal rates of MS2 were similar in value to those of PRD1 for columns II, IV and V, but that of  $\phi$ X174 was found to be higher in column III.

**Table 5** Removal rates  $r$  ( $\log_{10} \text{ day}^{-1}$ ) of bacteriophages as a function of time in column III (see also Figure 4).

Day	MS2	PRD1	$\phi$ X174
2	0.54	0.70	2.50
3	0.59	0.61	2.06
7	0.65	1.27	2.06
10	0.84	1.88	2.14
14	0.88	1.83	2.34
15	0.66	2.20	2.36
16	0.82	2.04	2.40
17	1.51	2.26	2.57
Intercept ( $-\log_{10}(C/C_0)/t$ at $t=0$ )	0.45	0.48	1.87
Slope ( $-\log_{10}(C/C_0)/t^2$ )	0.035	0.11	0.035
Rsqr	45%	93%	87%
p	6.8%	0.010%	0.24%

First observation of  $\phi$ X174 was considered as an outlier.

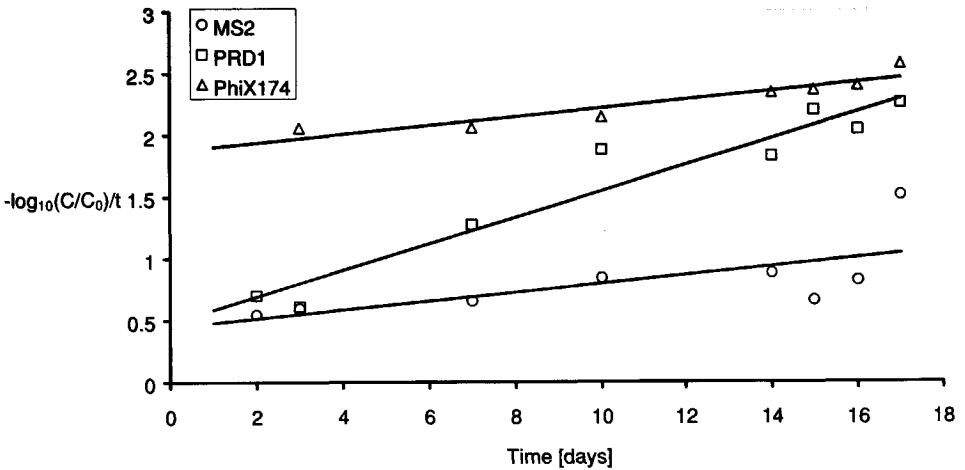


**Figure 4** Removal rates of bacteriophages as a function of time during continuous seeding (see also Table 6).

**Table 6** Removal rate in terms of time ( $t$ ) and distance ( $s$ ) at two velocities in column IV and one velocity in column V with soil G\*.

		IV		V
v [m.day <sup>-1</sup> ]		1.7	3.3	1.6
$r = -\log_{10}(C/C_0)/t$ [day <sup>-1</sup> ]	MS2	0.27 (0.077-0.46)	0.28 (0.24-0.79)	0.56 (0.26-0.87)
	PRD1	0.72 (0.43-1.0)	0.55 (0.030-1.1)	0.53 (0.19-0.70)
	φX174	1.2 (0.90-1.5)	1.3 (0.92-1.6)	1.4 (0.81-1.7)
$s = -\log_{10}(C/C_0)/x$ [m <sup>-1</sup> ]	MS2	0.16 (0.045-0.27)	0.085 (0.072-0.24)	0.36 (0.17-0.56)
	PRD1	0.43 (0.25-0.61)	0.17 (0.0091-0.32)	0.34 (0.12-0.45)
	φX174	0.72 (0.53-0.91)	0.38 (0.28-0.47)	0.92 (0.72-1.1)

95%-confidence intervals are given between brackets.

### 7.4. 3 Inactivation of Free Bacteriophages

Table 7 summarizes the measured values of the inactivation coefficient  $\mu_1$  for the viruses. Likelihood-ratio-tests showed that there were no significant differences between the inactivation rates in column influents and effluents and a single value for the inactivation rate coefficient for each bacteriophage could be estimated. The value of  $\mu_1$  for MS2 is the same as that found for  $\mu_s$  in the field study by Schijven *et al.* (1999). The value of  $\mu_1$  for PRD1 is now found to be lower than in the field study. The value found in the present study is more realistic, because PRD1 is expected to be more stable than MS2 (Yahya *et al.*, 1993). It appears that φX174 is the most stable one.

The estimates of  $\mu_1$  for CB4 and PV1 are based on only a few measurements. CB4 appears to be similarly stable as MS2. A value of 0.012 – 0.04 day<sup>-1</sup> in groundwater at 10 °C of  $\mu_1$  for Coxsackievirus B1 has been reported by Matthess *et al.* (1988), which is lower. Values of 0.01-0.18 day<sup>-1</sup> in groundwater at 10 °C for PV1 have been reported in literature (Matthess *et al.*, 1988; Nasser *et al.*, 1993; Yates *et al.*, 1985). The value of 0.16 day<sup>-1</sup> found in the present study is within this range.

**Table 7** Inactivation rate coefficient  $\mu_1$  [day<sup>-1</sup>].

	N*	$\mu_1$	95% CI
MS2	38	0.082	0.068 – 0.096
PRD1	30	0.044	0.038 – 0.049
φX174	30	0.012	0.0072 – 0.016
CB4	4	0.079	-
PV1	3	0.16	-

\*Number of observations

**Table 8** Experimental conditions of column experiments and of first two monitoring wells in field study.

Column	III	IV	V	VI	VII	W1 <sup>a</sup>	W2 <sup>a</sup>
Column length [m]	1.41	1.42	1.43	0.43	0.27	2.4	3.8
$v$ [m.day <sup>-1</sup> ]	1.6	3.5	1.6	2.0	1.9	1.4	1.6
$\alpha_L$ [m]	0.0075	0.0043	0.0084	0.0015	0.00074	0.0080	0.012

<sup>a</sup>Data from field study (Schijven *et al.*, 1999). Porosity is 0.35.

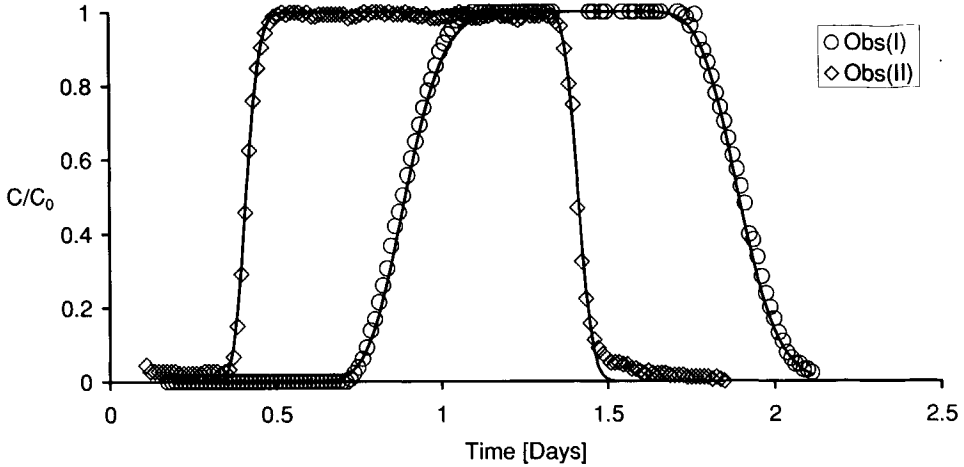
#### 7.4.4 Description of the Breakthrough Curves

Table 8 lists the estimates of  $v$  and  $\alpha_L$  for the column experiments and the first two monitoring wells in the field study. Figure 5 shows the observed and fitted salt breakthrough curves from columns I and II. As can be seen, the limbs of the salt breakthrough curves are perfectly symmetrical, a steady state of  $C/C_0 = 1$  is reached, and excellently fitting breakthrough curves could be obtained.

Figure 6 shows the measured breakthrough curve of MS2 in column I. First, a one-site kinetic model was applied to fit this curve using CXTFIT2 (Toride *et al.*, 1995) with the concentrations on a linear scale. Values for  $k_{att}$ ,  $k_{det}$  and  $\mu_{s1}$  are given in Table 9 under A and correspond with curve A in Figure 6. The value of  $k_{det}$  is higher than that of  $k_{att}$  and the value of  $\mu_{s1}$  is much higher than that of  $\mu_i$ . Curve A fits the measured breakthrough curve very well except for the tail part; this is not considered as satisfactory. The value of  $\mu_s$  determines the slope of the tail and is 50 times higher than the value of  $\mu_i$ , which is considered to be unrealistic. In an analysis of virus inactivation from batch experiments by Schijven and Hassanizadeh (2000), it was found that if values of  $\mu_s$  were higher than that of  $\mu_i$ , this was usually only 2–3 and occasionally 6–8 times higher. Figure 7 shows the corresponding residual values, *i.e.* the differences between observed and fitted concentrations on log scale. Because the tail of curve A deviates from the measured tail, residual values of the tail part become increasingly positive.

In another set of simulations, again a one-site model was used, but this time, we used our model EQ2KIN with log-transformed concentrations and setting the parameter values for site 2 to zero. The corresponding parameter values are given under B in Table 9 and the corresponding curve B is also shown in Figure 6. Note that this curve was forced to fit the maximum breakthrough concentration by giving this concentration extra weight, otherwise the maximum breakthrough concentration would have been underestimated by about 0.5  $\log_{10}$ . The same discrepancies around the rising and declining limbs are found, whereas the tail fits perfectly. These discrepancies are reflected by the residual values in Figure 7 being negative at the rising limb and positive at the declining limb of the breakthrough curve. The value of  $k_{det}$  is now much less than that of  $k_{att}$ .

Finally, the breakthrough curve was fitted by applying the two-site kinetic model. The estimated values are given under C of Table 9. The resulting curve C, in Figure 6, clearly gives a very satisfactory fit to the measurements. This is also reflected by the corresponding residual values in Figure 7, which are randomly scattered around zero, with an average residual of  $-0.0036$  and a variance as small as 0.12. This implies that the assumption of log-normally-distributed concentrations is reasonable. The height of the breakthrough curve is



**Figure 5** Measured salt breakthrough curves *Obs(I)* and *Obs(II)* from column experiments I and II and fitted breakthrough curves (solid lines).

**Table 9** Parameter values (in  $\text{day}^{-1}$ ) estimated from breakthrough of MS2 in column III; *a*, *b*, and *c* in column headings correspond to curves A, B, and C in Fig. 5.

Rate coefficients	A: one-site model (CXTFIT2)	B: one-site model (EQ2KIN)	C: two-site model (EQ2KIN)
$k_{att1}$	4.5	2.2	2.1
$k_{det1}$	5.0	0.074	0.054
$k_{att2}$			8.8
$k_{det2}$			42
$\mu_{s1} = \mu_{s2}$	3.9	0.48	0.43

be mainly determined by the values of  $k_{att1}$ ,  $k_{att2}$ ,  $k_{det2}$  and  $\mu_i$ . The skewness of the climbing and declining limbs is strongly affected by the value of  $k_{det2}$ . After the pulse of viruses has passed, site 2 loses its influence on the shape of the curve because of the high detachment rate of this site. The tail of the breakthrough curve is mainly determined by the values of  $k_{det1}$  and  $\mu_{s1}$ . Because the detachment rate from site 2 is relatively fast, there is little effect of inactivation of viruses that are attached to site 2. Consequently, estimates of  $\mu_{s2}$  may not be meaningful. It was believed to be a reasonable assumption that  $\mu_{s2}$  equals  $\mu_{s1}$ .

All the following curves were fitted with the one-site and two-site kinetic model using log-transformed concentrations and EQ2KIN.

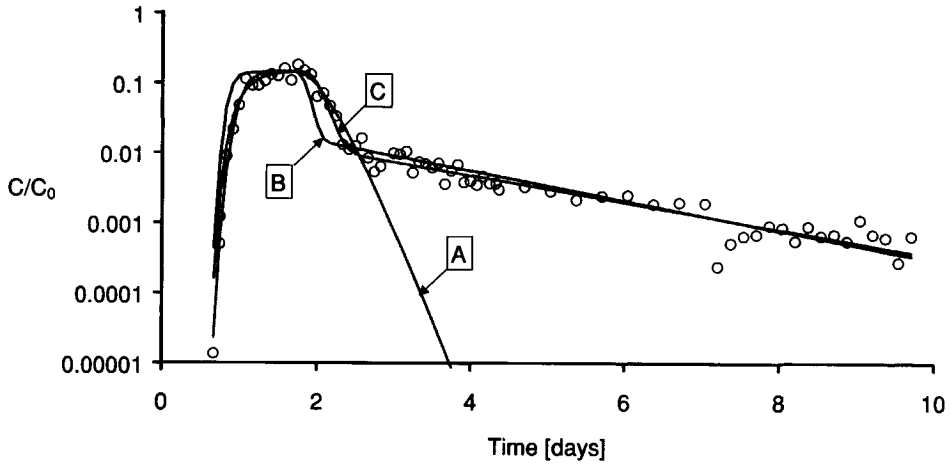


**Figure 6** Measured breakthrough curve (open circles) of MS2 in column III fitted with a one-site kinetic model (curves A and B) and a two-site kinetic model (curve C).

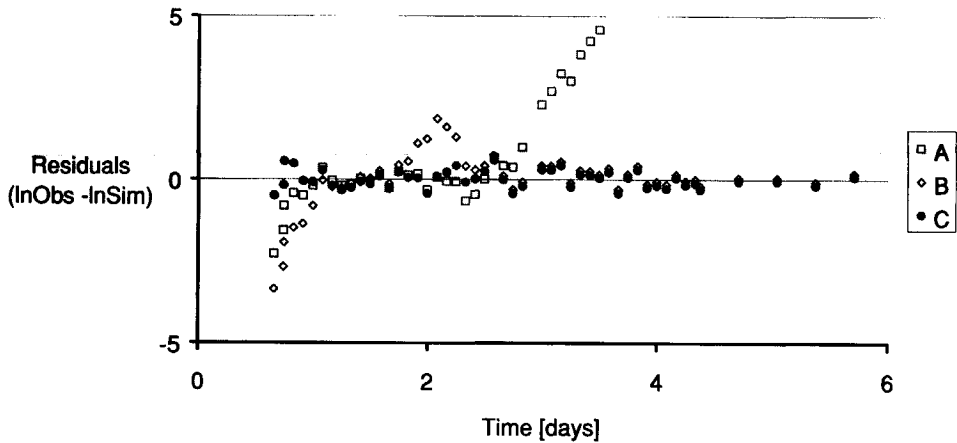


**Figure 7** Residual values (observed minus fitted values) on log-scale corresponding to models A, B and C in Figure 6.

Figures 6, 8 and 9 give the fitted breakthrough curves of the bacteriophages in column III. The corresponding parameter values are given in Table 10. With the one-site model, similar parameter values as for MS2 were obtained for PRD1. However, in the case of PRD1, the tail of the breakthrough curve appears to be curved and becomes flatter at the end. The one-site model does not follow this trend. However, the two-site model does fit the slight bend of the tail. Compared to MS2, the values for  $k_{att2}$  and  $k_{det2}$  are smaller. Also, the estimates of  $\mu_{s1}$  and  $\mu_{s2}$  for PRD1 are now much smaller, and are 50% greater than the  $\mu_1$  value for PRD1. This is in agreement with literature, where for PRD1 the value of  $\mu_s$  was found to be equal or higher than that of  $\mu_1$  (Blanc and Nasser, 1996, Schijven and Hassanizadeh, 2000).

The value of  $\mu_s$  for MS2 is found to be about six times higher than the value of its  $\mu_1$  and is probably overestimated.

The breakthrough curve of  $\phi$ X174 is very much skewed to the right (Figure 9). The one-site model fits this curve badly, but the two-site model fits it very well. The goodness of fit  $r^2$  of the two-site model for  $\phi$ X174 was a bit lower than for MS2 and PRD1. In the case of  $\phi$ X174, the number of counts in the samples from the tail of the breakthrough curve were relatively low, resulting in a large variation in the observed concentrations. Consequently, it was difficult to get a reliable fit of the tail. Bacteriophage  $\phi$ X174 is relatively stable (Table 7), therefore, it was assumed that the inactivation coefficient of attached  $\phi$ X174 has the same value as that of free  $\phi$ X174. The curvature of its breakthrough tail is similar to that of PRD1, which is followed well by the two-site model.

All three bacteriophages attach relatively fast to site 1 and detach only very slowly from this site, whereas both attachment to and detachment from site 2 are fast. Consequently, overall removal is mainly determined by interaction with site 1, and only for a minor part by interaction with site 2. The removal rates that were predicted on the basis of the parameter estimates are a bit higher than the observed removal rates found in the same column (Table 3). The breakthrough experiment in column III preceded the continuous seeding experiment in that column. The predicted removal rate is about 20% higher in the case of PRD1 and  $\phi$ X174, but almost 60% in the case of MS2 than the observed removal rate. In the case of MS2, this difference is in part due to overestimation of  $\mu_{s1}$ .

Although the two-site model appears to fit the breakthrough curves better than the one-site model, leading to more meaningful values of the adsorption and inactivation parameters, it appears that removal rates predicted by either model are very similar in the case of MS2 and PRD1. The reason for this, lies in the fact that  $k_{att1}$  is the most important parameter for determining removal.

Figures 10, 11 and 12 show the fitted breakthrough curves of the bacteriophages in column IV at a two times higher pore water velocity than in column III. Corresponding parameter values are given in Table 10. According to the colloid filtration theory, the value of the attachment rate coefficients are expected to increase with a factor  $2^{1/3}$ , i.e. 1.26 (Yao *et al.*, 1971). In the case of MS2 and PRD1 and the one-site as well as the two-site model, this prediction is fulfilled for  $k_{att1}$ , i.e. falling within the 95%-confidence interval of the estimates of  $k_{att1}$  at twice the pore water velocity. In the case of  $\phi$ X174, the predicted values of  $k_{att1}$  falls just outside this 95%-confidence interval. The values of the other adsorption parameters differ also, but there is no consistent pattern, other than that detachment from site 1 is still relatively slow, and from site 2 relatively fast. In this column, all adsorption parameters of MS2 and PRD1 are now similar in value. As can be seen in Figure 10, the tail of MS2 now appears to flatten at the end, like PRD1. The value of  $\mu_{s1}$  with the two-site model for MS2 is now found to be similar to the value of  $\mu_1$ , whereas estimates with the one-site model are about 6 times higher. Similar values of  $\mu_1$  and  $\mu_s$  for MS2 are consistent with literature (Blanc and Nasser, 1996; Schijven and Hassanizadeh, 2000) and strengthens the suspicion that the value of  $\mu_{s1}$  was overestimated in column III. The removal rates of the bacteriophages predicted from the breakthrough curves in column IV are similar to that observed in column III. Predicted removal with travel distance at twice the pore water velocity in column IV is about half that in column III, confirming the findings from the experiment in column IV where removal rates were measured at the two velocities.

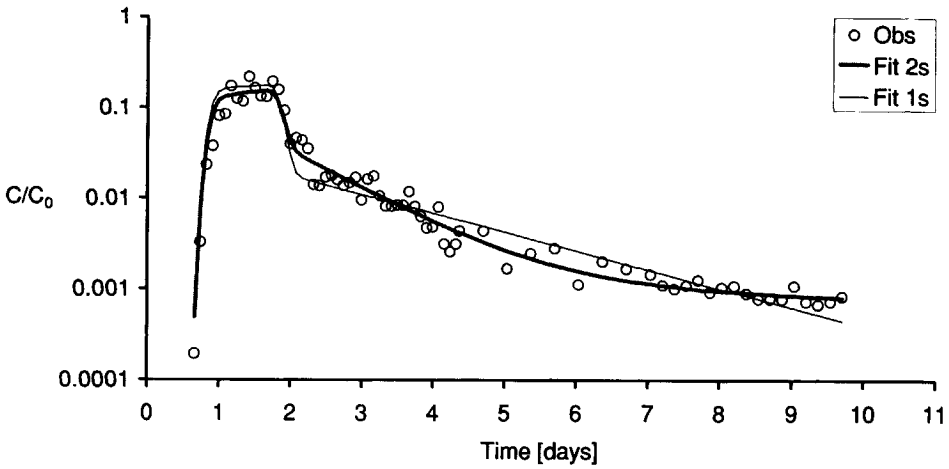


Figure 8 Breakthrough curve of PRD1 in column III. Circles are observations and the lines are the one- and two-site kinetic model fit.

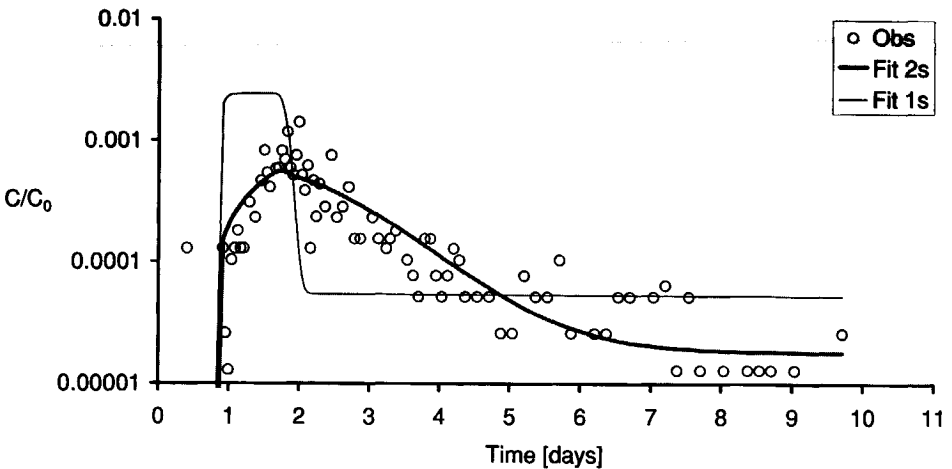


Figure 9 Breakthrough curve of  $\phi$ X174 in column III. Circles are observations and the lines are the one- and two-site kinetic model fit.

**Table 10** Parameter values from fitting breakthrough curves of bacteriophages in columns III and IV.

Column Bacteriophage	One-site model			IV		
	III			IV		
	MS2	PRD1	$\phi$ X174	MS2	PRD1	$\phi$ X174
$k_{ant}$	2.2 (2.1-2.4)	2.0 (1.97-2.12)	7.0 (6.3-7.8)	2.5 (1.8-3.4)	2.5 (2.2-2.8)	10 (9.7-10.5)
$k_{det}$	0.074 (0.050-0.11)	0.085 (0.075-0.096)	0.0039 (0.0031-0.0050)	0.14 (0.098-0.020)	0.089 (0.081-0.098)	0.046 (0.040-0.053)
$\mu_{s1}$	0.48 (0.40-0.58)	0.47 (0.36-0.60)	0.012	0.48 (0.37-0.61)	0.40 (0.33-0.47)	0.53 (0.31-0.89)
$\alpha_1$	0.0010	0.0012	0.0023	0.00061	0.0011	0.0023
$r^2$	80%	95%	-	96%	95%	90%
$\lambda$	2.0	1.8	5.3	2.0	2.1	9.3
% $\mu_1$	4.1%	2.5%	0.2%	4.2%	2.1%	0.1%
% s1	95.9%	97.5%	99.8%	95.8%	97.9%	99.9%
$k_{ant}/\lambda$	1.1	1.2	1.4	1.2	1.2	1.1
$s = -\log_{10}(C/C_0)/x$	0.55	0.48	1.4	0.25	0.26	1.2
$r = -\log_{10}(C/C_0)/t$	0.86	0.76	2.2	0.86	0.91	4.0

Dimension of parameters is day<sup>-1</sup>. The values of  $\mu_{s1}$  and  $\mu_{s2}$  for  $\phi$ X174 were set equal to that of  $\mu_1$ . 95%-confidence intervals are given between brackets. Table 10 is continued on next page.

Table 10 (continued) Parameter values from fitting breakthrough curves of bacteriophages in columns III and IV.

Column	III			IV		
	MS2	PRD1	$\phi$ X174	MS2	PRD1	$\phi$ X174
$k_{ant1}$	2.1 (1.8-2.4)	1.9 (1.83-1.94)	8.0 (7.0-9.2)	2.1 (1.4-2.9)	2.2 (2.0-2.3)	9.5 (9.3-9.8)
$k_{det1}$	0.054 (0.045-0.065)	0.0045 (0.0036-0.0055)	0.0028 (0.0018-0.0045)	0.016 (0.011-0.023)	0.017 (0.016-0.018)	0.0031 (0.0026-0.0037)
$k_{ant2}$	8.8 (6.5-12)	0.47 (0.41-0.53)	2.2 (1.4-3.7)	0.63 (0.58-0.70)	0.48 (0.44-0.53)	0.72 (0.63-0.83)
$k_{det2}$	42 (29-61)	1.1 (0.97-1.3)	1.2 (2.3-4.1)	1.4 (1.3-1.5)	1.6 (1.5-1.8)	0.96 (0.85-1.1)
$\mu_{s1} = \mu_{s2}$	0.43 (0.39-0.47)	0.064 (0.044-0.092)	0.012	0.075 (0.060-0.094)	0.065 (0.058-0.072)	0.012
$\alpha_1$	0.00068	0.0011	0.0024	0.00051	0.00097	0.0022
$\alpha_2$	0.0028	0.00027	0.00086	0.00016	0.00021	0.00016
$r^2$	96%	98%	83%	97%	98%	91%
$\lambda$	2.0	1.8	6.5	1.8	1.8	7.6
% $\mu_1$	4.0%	2.4%	0.2%	4.5%	2.4%	0.2%
% s1	91.5%	96.2%	99.6%	93.6%	96.5%	99.7%
% s2	4.4%	1.4%	0.2%	1.9%	1.0%	0.1%
$k_{ant1}/\lambda$	1.0	1.0	1.2	1.1	1.2	1.2
$s = -\log_{10}(C/C_0)/x$	0.56	0.50	1.8	0.23	0.22	0.95
$r = -\log_{10}(C/C_0)/t$	0.87	0.79	2.8	0.78	0.77	3.3

Dimension of parameters is day<sup>-1</sup>. The values of  $\mu_{s1}$  and  $\mu_{s2}$  for  $\phi$ X174 were set equal to that of  $\mu_1$ . 95%-confidence intervals are given between brackets.

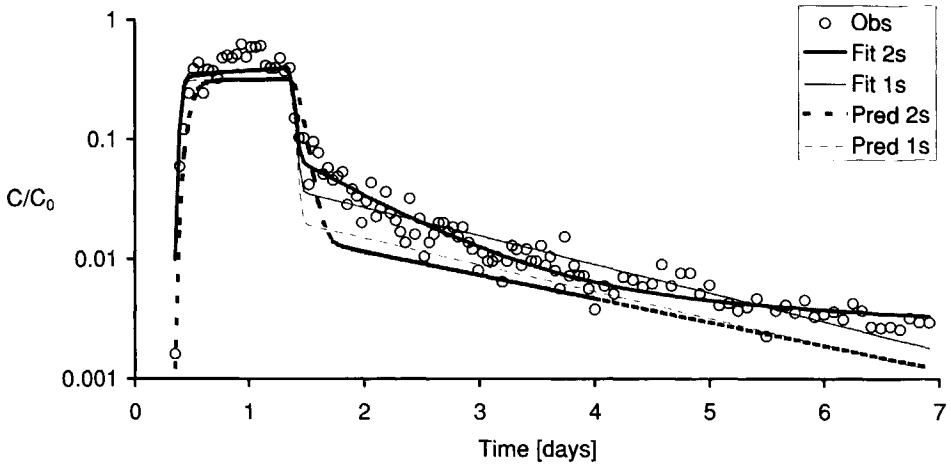


**Figure 10** Breakthrough curve of MS2 in column IV at two times higher pore water velocity. Circles are observations and the lines are the one- and two-site kinetic model fit. The dotted lines are the one- and two-site kinetic model predictions.

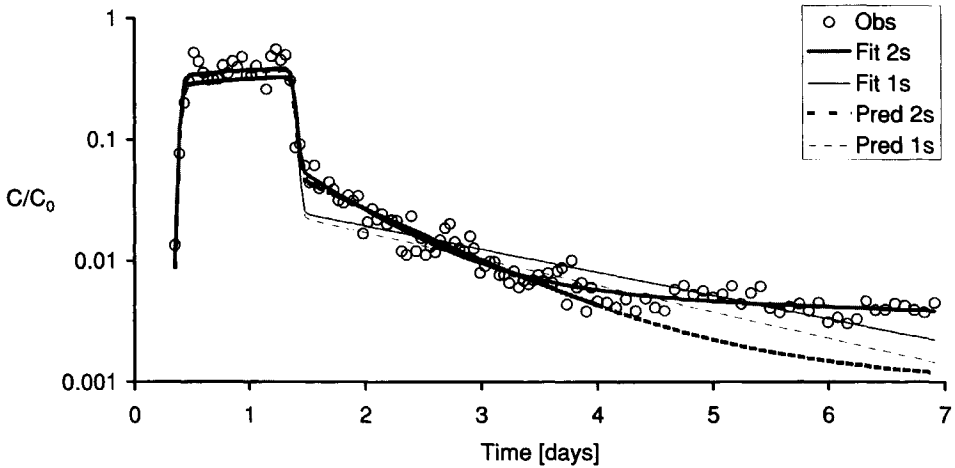


**Figure 11** Breakthrough curve of PRD1 in column IV at two times higher pore water velocity. Circles are observations and the lines are the one- and two-site kinetic model fit. The dotted lines are the one- and two-site kinetic model predictions..

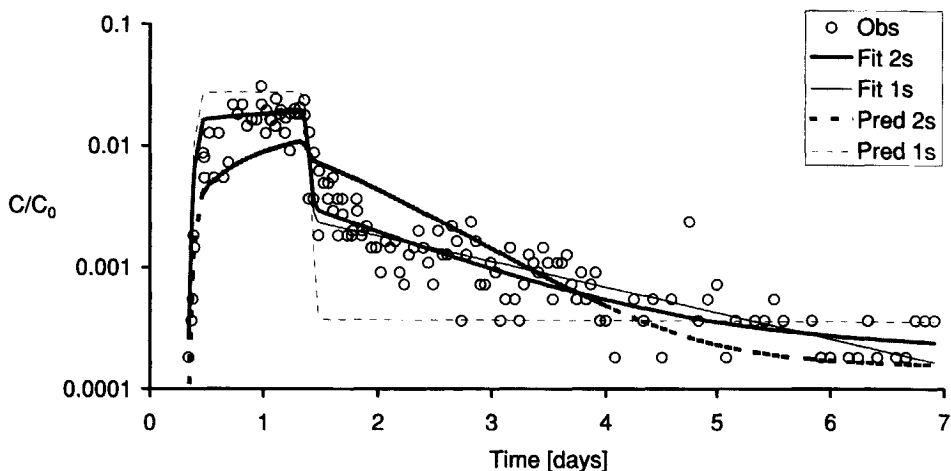


**Figure 12** Breakthrough curve of  $\phi X174$  in column IV at two times higher pore water velocity. Circles are observations and the lines are the one- and two-site kinetic model fit. The dotted lines are the one- and two-site kinetic model predictions..

So far, estimates of parameter determining the breakthrough curves have been obtained by fitting a model to observed breakthrough concentrations. This way, it appeared that a two-site kinetic model gives a better description of the breakthrough curves than a one-site kinetic model. In order to evaluate the two-site model further, parameter values obtained from column III breakthrough curves were used to predict the breakthrough curves from column IV, except for the value of  $k_{att}$ , which was adjusted by a factor of 1.3 as follows from colloid filtration theory. This prediction was carried out applying both the one- and two-site kinetic models. Figures 10, 11 and 12 show these predicted breakthrough curves. In the case of MS2, both the one- and two-site kinetic models slightly under-predict the maximum breakthrough concentration, and also the tail is lower. Both predictions are in fact very similar. This follows from the fact that the tail of the both fitted breakthrough curves of MS2 in column I was straight. The prediction of the PRD1 breakthrough by the two-site model is very good, except for the discrepancy at the extreme part of the tail. The one-site model prediction is very similar to the one-site fitted curve, and shows the same discrepancies at the beginning and the end of the tail of the breakthrough curve. In the case of  $\phi X174$ , the maximum breakthrough concentration is under-predicted by the two-site kinetic model, but it roughly follows the curvature of the tail. The prediction by the one-site kinetic model shows large discrepancies at the climbing limb and at the beginning of the tail of the breakthrough curve.

Overall, predictions by the two-site kinetic model were reasonably good considering the goodness of fits between the predicted and observed concentrations, i.e. 84% (MS2), 89% (PRD1) and 75% ( $\phi X174$ ). However, the same may be said for the predictions by the one-site model for MS2 and PRD1 with goodness of fits of 86% and 93%, respectively. The goodness of fit for the prediction of the  $\phi X174$  breakthrough curve was much lower, 34%.

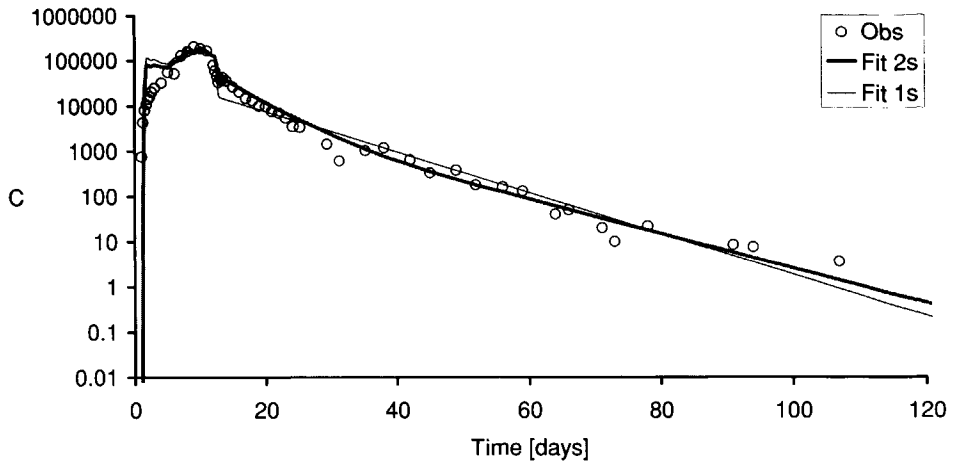


**Figure 13** Breakthrough curve of MS2 at the first monitoring well in field study by Schijven et al. (1999). Circles are observations and the lines are the one- and two-site kinetic model fit.

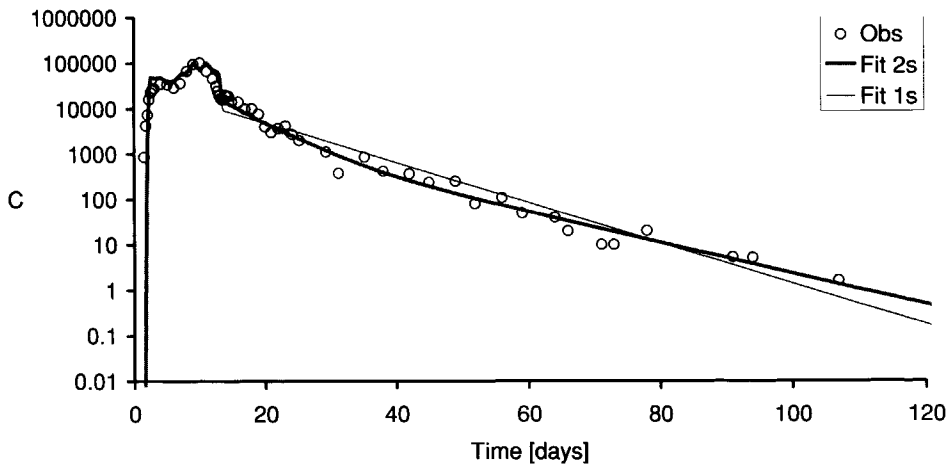


**Figure 14** Breakthrough curve of MS2 at the second monitoring well in field study by Schijven et al. (1999). Circles are observations and the lines are the one- and two-site kinetic model fit.

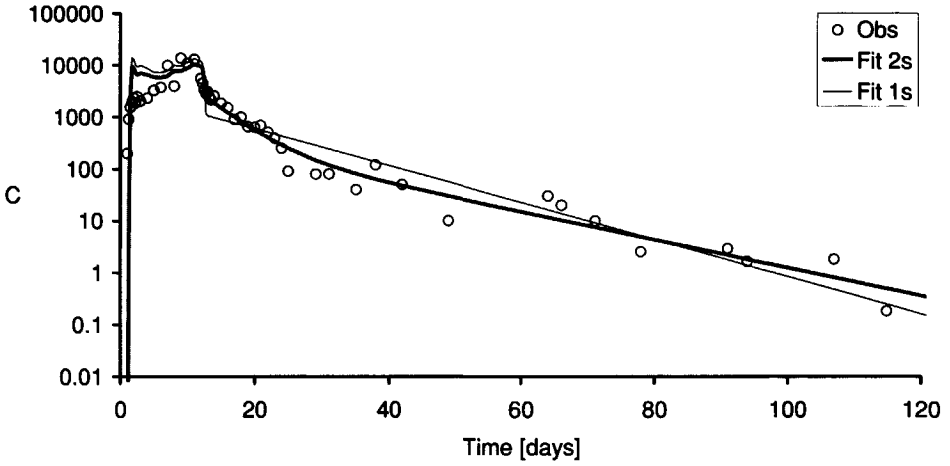


**Figure 15** Breakthrough curve of PRD1 at the first monitoring well in field study by Schijven et al. (1999). Circles are observations and the lines are the one- and two-site kinetic model fit.

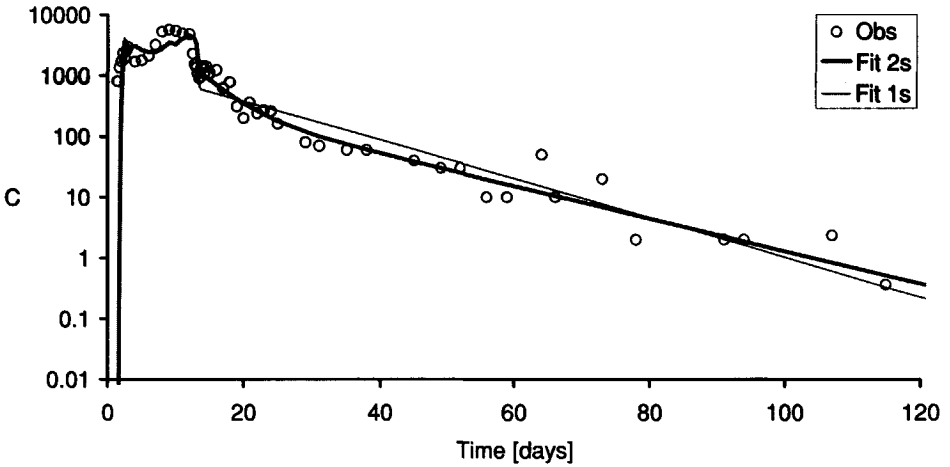


**Figure 16** Breakthrough curve of PRD1 at the second monitoring well in field study by Schijven et al. (1999). Circles are observations and the lines are the one- and two-site kinetic model fit.

**Table 11** Parameter values from fitting breakthrough curves of MS2 and PRD1 from field study at the first two monitoring wells W1 and W2 (Schijven et al., 1999).

One-site model				
column	W1		W2	
	MS2	PRD1	MS2	PRD1
$k_{att1}$	4.1 (3.6-4.8)	4.3 (3.6-5.2)	3.2 (3.1-3.4)	3.4 (3.3-3.5)
$k_{det1}$	0.0024 (0.00068-0.0088)	0.0028 (0.00058-0.014)	0.0035 (0.0018-0.0066)	0.0037 (0.0024-0.0056)
$\mu_{s1}$	0.11 (0.075-0.15)	0.086 (0.055-0.13)	0.11 (0.094-0.13)	0.082 (0.070-0.096)
$\alpha_1$	0.0014	0.0025	0.0011	0.0020
$r^2$	96%	94%	96%	95%
$\lambda$	4.0	4.2	3.2	3.3
% $\mu_1$	0.7%	2.9%	0.9%	3.6%
% s1	99.3%	97.1%	99.1%	96.4%
$k_{att1}/\lambda$	1.0	1.0	1.0	1.0
$s=-\log_{10}(C/C_0)/x$	1.2	1.3	0.86	0.91
$r=-\log_{10}(C/C_0)/t$	1.7	1.8	1.4	1.4
Two-site model				
column	W1		W2	
	MS2	PRD1	MS2	PRD1
$k_{att1}$	4.0 (3.5-4.5)	4.1 (3.5-4.8)	3.1 (2.9-3.2)	3.2 (3.1-3.3)
$k_{det1}$	0.00072 (0.00011-0.0048)	0.00054 (0.000047-0.0071)	0.00048 (0.00019-0.0012)	0.0013 (0.00077-0.0022)
$k_{att2}$	0.64 (0.41-2.6)	0.24 (0.042-130)	0.16 (0.13-0.20)	0.20 (0.15-0.27)
$k_{det2}$	0.17 (0.10-0.28)	0.20 (0.040-1.0)	0.14 (0.067-0.31)	0.26 (0.18-0.36)
$\mu_{s1} = \mu_{s2}$	0.090 (0.060-0.13)	0.066 (0.037-0.12)	0.079 (0.065-0.096)	0.065 (0.054-0.079)
$\alpha_1$	0.0013	0.0025	0.0010	0.0019
$\alpha_2$	0.00014	0.00016	0.000053	0.00011
$r^2$	98%	97%	98%	97%
$\lambda$	4.1	4.3	3.1	3.3
% $\mu_1$	0.7%	2.8%	1.0%	3.6%
% s1	95.9%	95.8%	97.2%	95.2%
% s2	3.4%	1.4%	1.8%	1.2%
$k_{att1}/\lambda$	0.97	0.97	0.98	0.97
$s=-\log_{10}(C/C_0)/x$	1.2	1.3	0.85	0.91
$r=-\log_{10}(C/C_0)/t$	1.7	1.8	1.3	1.4

Dimension of parameters is day<sup>-1</sup>. 95%-confidence intervals are given between brackets.

Figures 13 to 16 give the breakthrough curves of MS2 and PRD1 from the monitoring wells W1 and W2 from the field study by Schijven *et al.* (1999) with corresponding parameter values given in Table 11. The one-site model fit shows the same discrepancies as were noted in the field study (Schijven *et al.*, 1999). Note, that in that study, the height of the tail was adjusted to fit the lower part, whereas in the present fitting, the one-site model fits to an average height. Again, the breakthrough curves could be fitted very well using the two-site model. In these cases, the values of  $k_{att1}$  are higher compared to those in the column experiments, due to the high initial removal that was observed in the field. The values of  $k_{att2}$  are of similar order as in column IV. Remarkably, the values of  $k_{det1}$  and  $k_{det2}$  are lower than those found in the column experiments. The value of  $\mu_{s1}$  for PRD1 is very much the same as that found in the present study. The value of  $\mu_{s1}$  for MS2 from the field study is similar to that found in column IV (and VII). Both the one-site and two-site kinetic models predict the same removal rates.

Figures 17 to 21 show the breakthrough curves from columns VI and VII of CB4, PV1 and spores of *Clostridium perfringens* D10 with MS2 as a reference. CB4 appears attach to a similar extent as MS2. The climbing limb of the breakthrough curve is much more skewed to the right, but the declining limb and the tail of the breakthrough curves of CB4 and MS2 coincide.

The two-site model fit to CB4 breakthrough curve is more skewed to the right than the one-site model fit. A slightly higher removal rate is predicted for CB4 than that for MS2 (Table 12).

The one-site and two-site model simulations of the MS2 breakthrough curve are very similar. In this case the tail of the breakthrough curve appears be very straight, consequently, estimates for  $\mu_s$  are relatively high. The same can be said for CB4.

The breakthrough curve of MS2 in column VI again shows a flattening tail, and again, the estimate of  $\mu_s$  is much higher than that of  $\mu_1$  in the case of the one-site model, but similar to that of  $\mu_1$  in the case of the two-site model. As a consequence, the one-site model appears to predict a higher removal rate than the two-site model. PV1 attaches much faster than MS2, thus a high removal rate is predicted. The values of  $\mu_s$  are similar to that of  $\mu_1$ . The two-site model appears to follow the skewness of the breakthrough curve of PV1 very well, whereas the one-site model does not.

The D10 spores attach very fast. Because inactivation of clostridium spores is negligible, removal can only be due to irreversible adsorption. However, the high detachment rate, evidenced by the relatively high position of the tail of the breakthrough curve, suggests that attachment of the spores is mainly reversible. The detachment rate is high, due to the high number of previously attached spores. The one-site model does not follow the right-skewness of the climbing limb of the breakthrough curve, but the two-site model does.

Column experiments were carried out at low temperature ( $5 \pm 3$  °C), at which inactivation rates are low. As can be seen in Tables 10, 11 and 12, interaction with site 1 accounts for 90 – 98% of removal of MS2, PRD1 and CB4 and almost for 100% for removal of  $\phi$ X174 and PV1. Because  $k_{att1} \gg k_{det1}$ , it follows that  $\lambda = k_{att1}$ , meaning that  $k_{att1}$  is the most important parameter for removal of viruses at low temperatures.

Column Experiments for Evaluating Field Data on Virus Removal

**Table 12** Parameter values from fitting breakthrough curves of microorganisms in columns VI and VII.

One-site model					
Column	VI		VII		
Microorganism	MS2	CB4	MS2	PV1	D10
$k_{att}$	3.0 (2.4-3.6)	3.1 (1.9-4.9)	2.3 (1.4-4.0)	59 (53-65)	32 (18-57)
$k_{det}$	0.067 (0.054-0.084)	0.17 (0.086-0.32)	0.096 (0.019-0.049)	0.016 (0.0046-0.052)	0.086 (0.017-0.44)
$\mu_{s1}$	0.43 (0.37-0.49)	0.53 (0.14-2.1)	1.3 (0.091-1.8)	0.21 (0.061-0.70)	0
$\alpha_1$	0.00086	0.00093	0.00071	0.018	0.087
$r^2$	95%	79%	97%	51%	39%
$\lambda$	2.6	2.4	2.3	55	-
% $\mu_1$	3.2%	3.3%	3.7%	0.3%	-
% $s_1$	92.8%	96.7%	96.3%	99.7%	-
$k_{att}/\lambda$	1.1	1.3	1.0	1.1	-
$s = -\log_{10}(C/C_0)/x$	0.56	0.53	0.53	13	-
$r = -\log_{10}(C/C_0)/t$	1.1	1.0	0.98	23	-
Two-site model					
Column	VI		VII		
Microorganism	MS2	CB4	MS2	PV1	D10
$k_{att1}$	2.0 (1.8-2.3)	2.1 (1.6-2.7)	1.7 (0.36-8.1)	59 (51-68)	15 (6-40)
$k_{det1}$	0.068 (0.054-0.077)	0.054 (0.020-0.15)	0.0037 (0.00079-0.017)	0.0093 (0.00067-0.093)	0.023 (0.0014-0.40)
$k_{att2}$	12 (10-15)	39 (23-65)	0.28 (0.075-1.1)	11 (0.033-2600)	25 (12-49)
$k_{det2}$	77 (65-90)	46 (23-93)	2.7 (1.1-6.4)	17 (0.19-2400)	0.34 (0.067-1.7)
$\mu_{s1} = \mu_{s2}$	0.37 (0.34-0.40)	0.23 (0.097-0.56)	0.089 (0.011-0.73)	0.14 (0.0031-6.2)	0
$\alpha_1$	0.00061	0.00063	0.00052	0.018	0.037
$\alpha_2$	0.0037	0.012	0.000086	0.0034	0.059
$r^2$	98%	85%	98%	55%	74%
$\lambda$	1.9	2.0	1.7	56	-
% $\mu_1$	4.4%	4.0%	4.8%	0.3%	-
% $s_1$	92.4%	86.1%	94.7%	99.6%	-
% $s_2$	3.2%	9.9%	0.5%	0.2%	-
$k_{att1}/\lambda$	1.1	1.1	0.99	1.1	-
$s = -\log_{10}(C/C_0)/x$	0.41	0.44	0.40	13	-
$r = -\log_{10}(C/C_0)/t$	0.81	0.86	0.75	24	-

Dimension of parameters is day<sup>-1</sup>. 95%-confidence intervals are given between brackets.

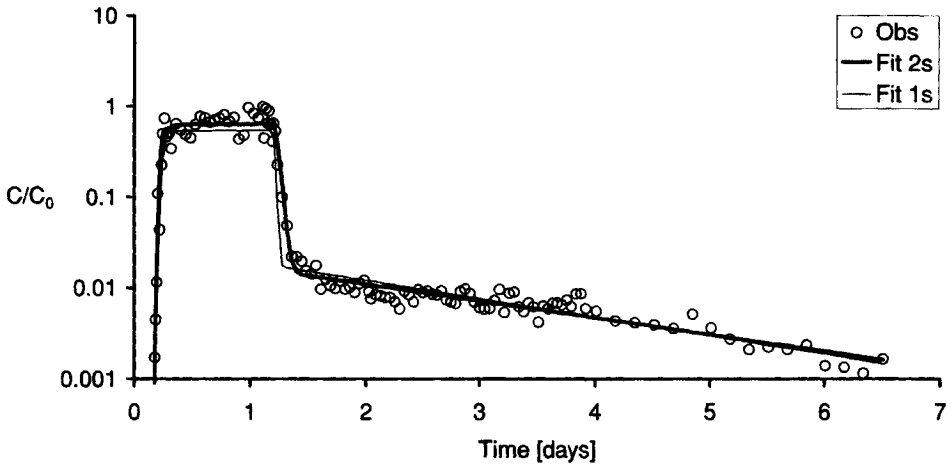


**Figure 17** Breakthrough curve of MS2 in column VI. Circles are observations and the lines are the one- and two-site kinetic model fit.

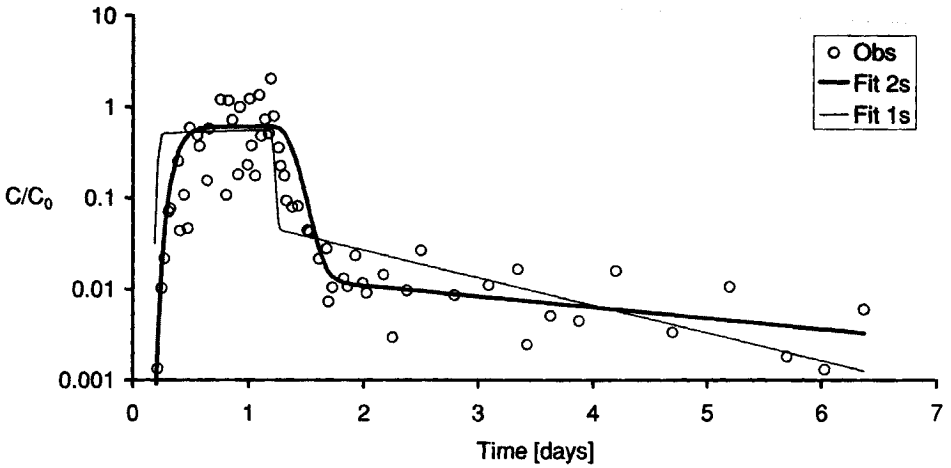


**Figure 18** Breakthrough curve of Coxsackievirus B4 in column VI. Circles are observations and the lines are the one- and two-site kinetic model fit.

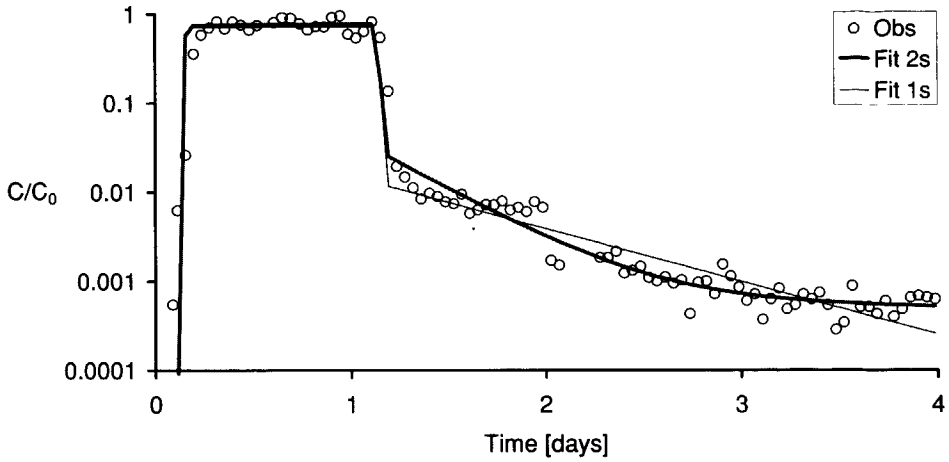


**Figure 19** Breakthrough curve of MS2 in column VII. Circles are observations and the lines are the one- and two-site kinetic model fit.

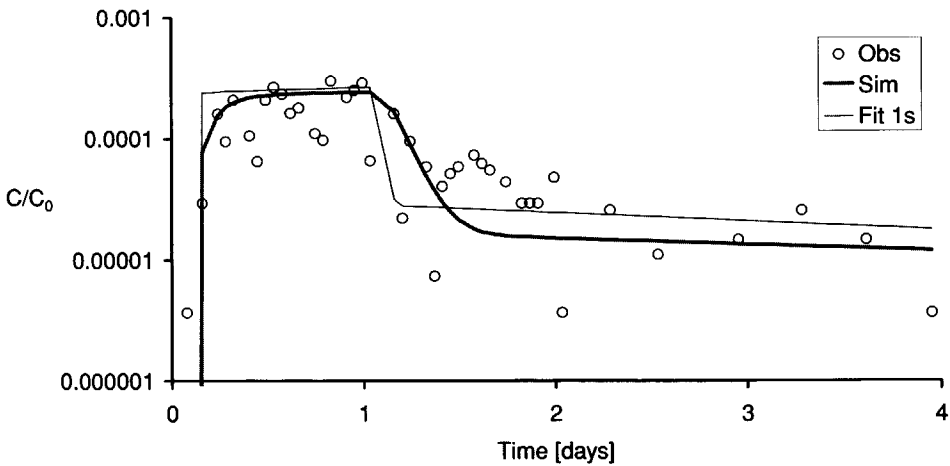


**Figure 20** Breakthrough curve of PV1 in column VII. Circles are observations and the lines are the one- and two-site kinetic model fit.

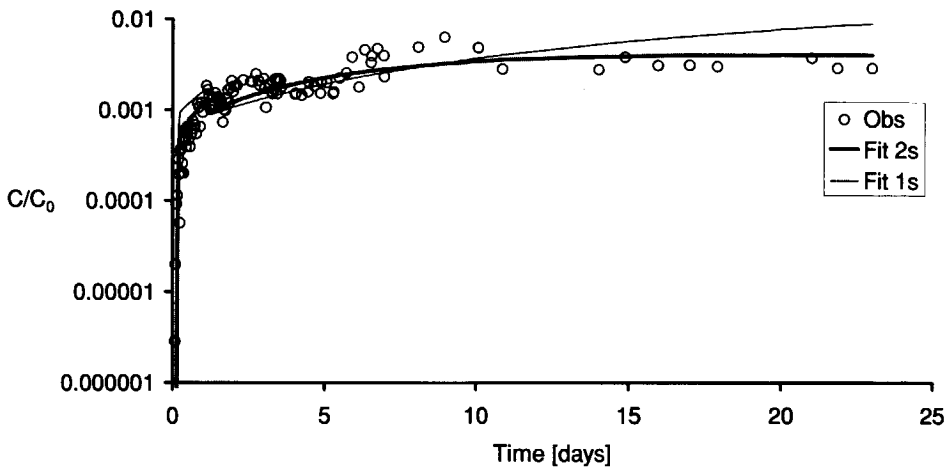


**Figure 21** Breakthrough curve of spores of *Clostridium perfringens* D10 in column VII. Circles are observations and the lines are the one- and two-site kinetic model fit.

In columns III, VI and VII high values of  $k_{att2}$  and  $k_{det2}$  for MS2 were found. In the other cases, including the field observations, lower values of  $k_{att2}$  and  $k_{det2}$  were found that were similar compared to those observed for PRD1 and  $\phi$ X174. The high values of  $k_{att2}$  and  $k_{det2}$  that were found for MS2 may have been overestimated, due to the overestimation of  $\mu_{s1}$ . Values of collision efficiencies  $\alpha_1$  and  $\alpha_2$  are also given in Tables 10, 11 and 12. In the column experiments, the value of  $\alpha_1$  for MS2 lies between 0.00051 and 0.00068, that for PRD1 between 0.00097 and 0.0011 and that of  $\phi$ X174 between 0.0022 and 0.0024. The values of  $\alpha_1$  for MS2 and PRD1 that were obtained from the field data are about two times higher, due to the initial high removal. The value of  $\alpha_1$  for CB4 is 0.00063, which is very similar to that of MS2. An  $\alpha_1$  of 0.018 is found for PV1. Bales *et al.* (1993) reported values of 0.0040 – 0.0072 in columns with silica beads at pH 7, meaning that more sites for attachment are available for PV1 in the dune sand compared to silica beads. DeBorde *et al.* (1999) reported a minimum collision efficiency for poliovirus 1 (CHAT strain) of 0.019 in a sand and gravel aquifer at pH 7.2.

The values of  $\alpha_2$  vary stronger than those of  $\alpha_1$ . In the column experiments,  $\alpha_2$  for MS2 varies between 0.00014 and 0.0028,  $\alpha_2$  for PRD1 varies between 0.00011 and 0.00027, and  $\alpha_2$  for  $\phi$ X174 varies between 0.00016 and 0.00086.

The collision efficiency  $\alpha_1$  for the clostridium spores is much higher: 0.037.

## 7.5 Discussion and Conclusions

### 7.5.1 Linearity of Removal of Bacteriophages by Passage through Dune Sand.

Two possible causes have been considered for the nonlinear removal of bacteriophages in our earlier field study: heterogeneity in the phage population and heterogeneity in soil properties.

Removal of the bacteriophages within each soil sample increased linearly with travel time. We may therefore conclude that the nonlinear removal that was observed in the field study was not due to heterogeneity of the bacteriophages. In the field study, freshly prepared suspensions of MS2 and PRD1 were used. In the present study, these suspensions were used again after two years of storage. To study the possibility of sub-populations of bacteriophages that are inactivated and/or attached faster and, therefore, have disappeared in the two-year old suspensions, removal of MS2 and PRD1 from the freshly prepared and two-year old suspensions was compared. Removal appeared to elapse in a linear fashion at similar rates for both fresh and two-year-old stock suspensions of MS2 and PRD1..

Although removal rates were found to be higher in soil A and B, this does not fully explain the high removal that was observed during the field study (Schijven *et al.*, 1999), since soils A and B account for only the first 5 – 10 cm of soil passage in the field. The removal within soil A suggests a nonlinear behavior, because the removal rate appears to be higher in the first than in next 10 cm. The removal rates of the bacteriophages were found to vary more than a factor 10 among various soils. Most probably, this variation was mainly due to the variation in organic carbon content, to which the removal rates were highly positively correlated. Possibly, the soil that lies between the bottom of the recharge canal and the first monitoring well contains more organic carbon than the sampled soils suggest. This is supported by the findings from a soil sample that was taken in the field study by Schijven *et al.* (1999). This sample was taken from approximately the same location as soil sample D and was found to have a five-fold higher organic carbon content (about 2.7 %). The sample location was right under the reedy border. This could imply that the initial high removal occurred somewhere between the point of infiltration and the first monitoring well, instead of within the first centimeters of infiltration and was due to adsorption to bonded organic matter that was locally present at higher concentrations.

For comparison between removal rates from the column experiments and the field study by Schijven *et al.* (1999), details of removal and removal rates from the field study are given in Table 13. Concentrations of MS2 and PRD1 decreased about  $3 \log_{10}$  within the first 2.4 m at a rate of  $1.8 \log_{10} \text{ day}^{-1}$  (Figure 22). Thereafter, another  $3.5 - 3.8 \log_{10}$  was removed over a distance of 15 m at a rate of  $0.36 - 0.40 \log_{10} \text{ day}^{-1}$ . Finally, over the next 13 m, an additional  $1.6 - 1.9 \log_{10}$  was removed at a rate of  $0.11 - 0.14 \log_{10} \text{ day}^{-1}$ . The removal rates that were found for MS2 and PRD1 between the first and second monitoring well in the field study (Table 13) are similar to the ones found in column III, IV and V with soil G and G\*, taken near the first observation well. The removal rates of MS2 and PRD1 in soil A were a bit higher than the initial removal rates found in the field.

Overall, one can say that the removal rates of MS2 and PRD1 observed in the column experiments with soils taken between the recharge canal and the first monitoring well vary

**Table 13** Removal and removal rates of MS2 and PRD1 at field scale (Schijven et al., 1999).

Well	Travel distance [m]	Travel time [day]	Removal ( $-\log_{10}(C/C_0)$ )		Removal rate from well to well ( $-\log_{10}(C/C_0)/t$ ; $\text{day}^{-1}$ )	
			MS2	PRD1	MS2	PRD1
	0	0	0	0		
W1	2.4	1.7	3.0	2.9	1.8	1.8
W2	3.8	2.4	3.3	3.3	0.40	0.53
W3	6.4	4.0	4.9	4.0	1.0	0.40
W4	10	6.5	5.6	4.4	0.30	0.18
W5	17	11	6.5	6.7	0.18	0.49
W6	30	25	8.4	8.3	0.14	0.11

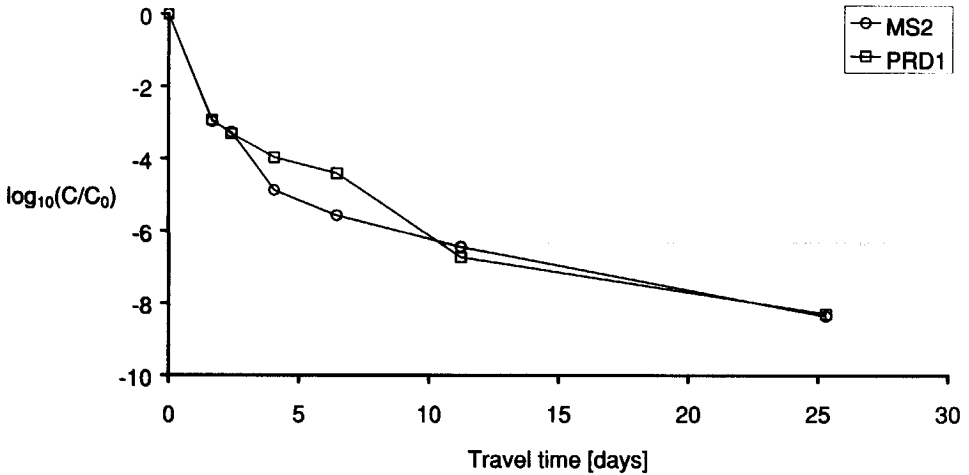


**Figure 22** Removal of MS2 and PRD1 at field scale as a function of travel time (Schijven et al., 1999).

over a very similar range ( $0.13 - 2.4 \log_{10} \text{day}^{-1}$ ) as the removal rates observed in the field study over a distance of 30 meters ( $0.11 - 1.8 \log_{10} \text{day}^{-1}$ ). However, considerable variation in removal rates was also found within each experiment over the days of observation in the columns with soils A – F. This variation is probably due to uncertainties in the measurements. According to the 95%-confidence intervals that were calculated for the removal rates of the bacteriophages in column II, IV and V with 1.5 m of soils G and G\*, predictions of removal may vary by a factor two to three.

Nevertheless, the main source for uncertainty in predicting removal at field scale is heterogeneity of the soil properties. Therefore, detailed knowledge on soil heterogeneity is needed in order to be able to predict removal at field scale.

The effect of a two times higher pore water velocity appeared to be an approximately two times lower removal with distance but there is little effect on removal rate with time. This implies that colloid filtration theory (Yao *et al.*, 1971) may be valid for this range of pore water velocities, and that collision efficiencies are constant within this range of pore water velocities. As we have seen, removal rates are mainly determined by attachment. Assuming that this also applies to the high initial removal at field scale, colloid filtration theory predicts that at a two times higher pore water velocity removal of MS2 and PRD1 after 30 m of dune passage will have decreased from 8 log<sub>10</sub> to 5 log<sub>10</sub>. At the present pore water velocity, one can predict that a removal of 12 log<sub>10</sub> will be achieved at the production well at 60-m travel distance. At twice the pore water velocity, a removal of 8 log<sub>10</sub> may be achieved at the production well.

During 17 days of continuous seeding of bacteriophages in column III with soil G, removal rates appeared to increase linearly with time. This increase was on average 0.035 day<sup>-1</sup> for both MS2 and φX174, and 0.11 day<sup>-1</sup> for PRD1. The cause for this increase is not clear. It cannot be explained by an increase of inactivation of free bacteriophages. For example in the case of MS2 or PRD1, a 100-fold increase of  $\mu_1$  would be needed to account for the observed increase. Similarly strong increases of  $\mu_{s1}$  and  $\mu_{s2}$  would be needed, and these are very unlikely. In the field study by Schijven *et al.* (1999), only a small increase in inactivation of MS2 and PRD1 was observed in water from the first monitoring well compared to that in recharge water. However, an increase by a factor of approximately 2.5 for MS2, 5 for PRD1 and 1.4 for φX174 of  $k_{att}$  would account for the observed increases in removal rate.

### 7.5.2 Applicability of a Two-Site Kinetic Advection Dispersion Model.

All breakthrough curves from the column as well as from the field experiments could be fitted very satisfactorily using a two-site kinetic model. The tails of the breakthrough curves appeared to flatten at the end, which could not be fitted with the one-site model. In some experiments with MS2, this flattening of the tail of the breakthrough curve was not clearly observed, leading to about 6 times higher estimates of  $\mu_s$ . Apparently, it is important to measure breakthrough tails long enough to get a good estimate of  $\mu_s$ . Tails that are measured too short may lead to an overestimation of  $\mu_{s1}$ . In addition, it may lead to overestimation of the values of  $k_{att2}$  and  $k_{det2}$ . Overestimation of  $\mu_s$  always occurs, when applying a one-site kinetic model. However, overestimation of  $\mu_{s1}$  has little effect on removal when  $k_{det1} \ll 1$  and  $\mu_{s1} > k_{det1}$ .

Breakthrough curves that appear to be very skewed to the right, like that of φX174, are fitted badly using a one-site kinetic model but good using a two-site kinetic model. Similarly shaped breakthrough curves, *i.e.* with the rising limb skewed to the right and with a smooth transition of the declining limb to the tail, have been observed in other studies with bacteriophages and bacteria (*e.g.* Bales *et al.*, 1991; 1993; DeBorde *et al.*, 1998, 1999; Dowd *et al.*, 1998; Hornberger *et al.*, 1992; Kinoshita *et al.*, 1993; McCaulou *et al.*, 1994), suggesting that the two-site kinetic model is generally applicable.

Predicted removal rates from the parameter estimates obtained by fitting a breakthrough curve are in reasonable agreement with the observed removal rates. Moreover, a removal rate of 0.8 log<sub>10</sub> day<sup>-1</sup> of MS2 was predicted from all breakthrough curves of MS2. In these

experiments it was found that estimates of  $k_{att1}$ -values from breakthrough curves are highly reproducible. Interaction with kinetic site 2, under the assumption that  $\mu_{s2}$  equals  $\mu_{s1}$ , has a minor contribution to removal. Generally,  $k_{att1} \gg k_{det1}$ ,  $k_{att2} \leq k_{det2}$  and  $k_{att2} < k_{att1}$ . At low temperatures, and therefore low inactivation rates,  $k_{att1}$  mainly determines virus removal. The uncertainty in the estimate of  $k_{att1}$  is usually smaller than that in the measured removal rates. This implies that predicted removal rates from breakthrough curves are more accurate.

### 7.5.3 Bacteriophages as Model Viruses for Pathogenic Viruses.

The values of  $k_{att1}$  for MS2 and PRD1 were found to be lower than that of  $\phi$ X174. A similar difference in adsorption was also found between MS2 and  $\phi$ X174 in Ottawa sand at pH 7.5 by Jin *et al.* (1997, 2000) and between MS2 and PV1 by Bales *et al.* (1993). At pH 7.5 – 8.0, the dune sand is predominantly negatively charged and conditions are unfavorable for attachment to negatively charged viruses. Therefore, one may argue that the virus-grain interaction is the rate-limiting step for attachment and not the transport (*e.g.* by diffusion) to attachment sites (Ryan and Elimelech, 1996). Farrah *et al.* (1991) showed that differences in attachment rates of MS2 and PV1 to diatomaceous earth with zeta-potentials ranging from -12 mV to -71 mV, due to different coatings with metallic salts, increased with a more negative zeta-potential. Similarly, Bales *et al.* (1993) showed that at pH 7, attachment of PV1 to silica beads was 2 – 3 times higher than that of MS2, but about the same at pH 5 – 5.5. Thus, the different extent of interaction with site 1 can be explained by greater electrostatic repulsion that MS2 and PRD1 experience compared to the less negatively charged  $\phi$ X174 and PV1.

The removal rates between the bacteriophages are highly positively correlated, which indicates that the bacteriophages interact with the same types of kinetic sites. The removal rates of all three bacteriophages are very highly positively correlated with the organic carbon content of the soil, and to a lesser extent with Fe-oxalate and the silt-content. Because removal rates are mainly determined by attachment to site 1, one may reason that sites of type 1 are composed of organic carbon, and/or ferric oxyhydroxides to which organic matter is attached. The dune recharge system has been in operation for about fifty years (Peters, 1992). Thus, the organic matter has probably already fully occupied the available binding sites of ferric oxyhydroxides, which form favorable (positively charged) sites (Ryan and Elimelech, 1996).

The bonded organic matter originates from plants, roots, humus and organic matter in the infiltrating water. Such organic matter is capable of binding both charged and uncharged particles. MS2, PRD1 are the most hydrophobic viruses, but  $\phi$ X174 exhibits little if any hydrophobic character (Shields and Farrah, 1987; Lytle and Routson, 1995). But in the case of elution from nitrocellulose membranes by a nonionic surfactant,  $\phi$ X174 and MS2 exhibited a similar hydrophobic binding potential (Lytle and Routson, 1995). MS2 was also found to be more hydrophobic than  $\phi$ X174 in the studies by Thompson *et al.* (1998) and Jin *et al.* (2000). Hydrophobic interactions with solid surfaces have also been suggested to play a role for PV1 (Farrah *et al.*, 1981; Shields and Farrah, 1983; Wait and Sobsey, 1983). Thus, depending on the nature of the bonded organic carbon, the interaction of MS2, PRD1 and PV1 with the bonded organic matter may be hydrophobic.

Because removal of MS2 and PRD1 has been measured at both laboratory and field scale and was also compared with that of other microorganisms at laboratory scale, it is possible

to predict removal of these microorganisms relative to MS2 and PRD1 at field scale. The attachment rate of CB4 was found to be similar to that of MS2. This means that CB4 is probably a strongly negatively charged virus. Clearly, CB4 will be removed by  $8 \log_{10}$  after 30 m of dune passage like MS2, and PV1 much more. These viruses cover the range of slightly to strongly negatively charged viruses. In batch experiments with different soils at pH 7 – 8, CB4 (V216) and CB4 (V240) were found to adsorb similarly low as, or, in some cases, lower than MS2 (Goyal and Gerba, 1979; Gerba *et al.*, 1981). In these experiments, adsorption of PV1 was much higher. It may be concluded that MS2 and PRD1 represent the low adsorptive behavior of negatively charged viruses and may therefore be considered as (relatively) worst case viruses under these conditions. According to the breakthrough curves adsorption of MS2 and PRD1 was very similar, but observed removal rates in columns I to IV were usually higher for PRD1 compared to those for MS2. Many studies support the conclusion that MS2 can be considered as a relatively conservative tracer for virus transport in saturated sandy soils at pH 6 – 8 and with a low organic carbon content, because under those conditions it showed little or no adsorption (Bales *et al.*, 1989; Powelson *et al.*, 1990; Herbold-Paschke *et al.*, 1991; Kinoshita *et al.*, 1993; Jin *et al.*, 1997; Schijven *et al.*, 1999). In most soils, attachment of MS2 is also relatively low compared to most other viruses (Goyal and Gerba, 1979; Herbold-Paschke *et al.*, 1991; Bradford *et al.*, 1993; Farrah and Preston, 1993; Bales *et al.*, 1993; Sobsey *et al.*, 1995; Penrod *et al.*, 1996; Redman *et al.*, 1997; Jin *et al.*, 1997; DeBorde *et al.*, 1999). Furthermore, removal of naturally occurring F-specific RNA bacteriophages at a nearby dune recharge site has been shown to be similar to that of MS2 (Schijven *et al.*, 1998).

With some exceptions, similar values of  $k_{att2}$  and  $k_{det2}$  were found for the bacteriophages. The differences that exist in hydrophobicity and surface charge between the bacteriophages suggest that their interaction with sites of type 2 is neither electrostatic nor hydrophobic. The second site effect on the breakthrough curves may be of physical nature, *e.g.* distribution between mobile and immobile regions of water.

#### 7.5.4 Removal of Spores of *Clostridium perfringens*.

This pathogenic microorganism is interesting because of its optimal size (1  $\mu\text{m}$ ) for transport (Yao *et al.*, 1971) and its very low inactivation rate. Because of the latter property it may be a potential surrogate for oocysts of *Cryptosporidium parvum*. Although D10 spores attach relatively fast, due to negligible inactivation all spores will eventually break through. Actual removal with travel time or distance depends on the time period of seeding or contamination. By simulating breakthrough of the D10 spores in the case of continuous seeding, an almost constant rise in concentration up to the value of the initial seeding concentration will occur at a given travel distance. This simulation is shown in Figure 23 at a travel distance of 1 meter.  $C/C_0$  increases at a rate of  $3.2 \times 10^{-5} \text{ day}^{-1}$ . This implies that after approximately 86 years  $C/C_0$  equal to one will have been reached.

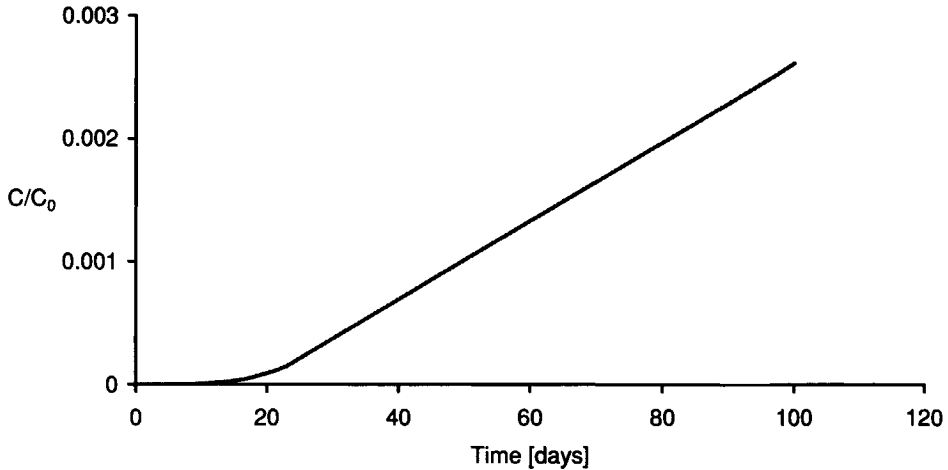


**Figure 23** Predicted increase in concentration of of spores of *Clostridium perfringens* D10 at one meter travel distance as a function of time during continuous seeding.

#### Acknowledgements

*Clostridium perfringens* strain D10 was kindly provided by W.A.M. Hijnen (Kiwa, Nieuwegein, The Netherlands). W. Hoogenboezem and J. Bergsma (PWN Water Supply Company North-Holland, The Netherlands) are greatly acknowledged for their support in obtaining sand samples, soil and water analyses. L.C. Rietveld and M. v.d. Meulen (Technical University Delft) are thanked for the design and construction of the Perspex column supports. G.B. Engels, F.M. Schets, W.J. Lodder and A.M. Holwerda are thanked for support in microbiological analyses and for providing CB4 and PV1. P.F.M. Teunis is specially thanked for his support in statistical analysis and for his expert comments. A.M. de Roda Husman is greatly acknowledged for her expert comments.

## Chapter 8

# Kinetic Modeling of Virus Removal in Heterogeneous Porous Media

Schijven, J. F. and Simunek J. 2001. Kinetic modeling of virus removal in heterogeneous porous media. *J. Contam. Hydrol.* Submitted.

## Abstract

Bacteriophage removal by soil passage in two field studies was re-analyzed with the goal to investigate differences between one- and two-dimensional modeling approaches, differences between one- and two-site kinetic sorption models, and the role of heterogeneities in the soil properties. The first study involved removal of bacteriophages MS2 and PRD1 by dune recharge, while the second study represented removal of MS2 by deep well injection. In both studies, removal was higher during the first meters of soil passage than thereafter. The software packages HYDRUS-1D and HYDRUS-2D, which simulate water flow and solute transport in one- and two-dimensional variably saturated porous media, respectively, were used. The two codes were modified by incorporating reversible adsorption to two types of kinetic sites.

Tracer concentrations were used first to calibrate flow and transport parameters of both models before analyzing transport of bacteriophages. The one-dimensional one-site model did not fully describe the tails of the measured breakthrough curves of MS2 and PRD1 from the dune recharge study. While the one-dimensional one-site model predicted a sudden decrease in virus concentrations immediately after the peaks, measured data displayed much smoother decline and tailing. The one-dimensional two-site model simulated the overall behavior of the breakthrough curves very well. The two-dimensional one-site model predicted a more gradual decrease in virus concentrations after the peaks than the one-dimensional one-site model, but not as good as the one-dimensional two-site model. The dimensionality of the problem hence can partly explain the smooth decrease in concentration after peak breakthrough. The two-dimensional two-site model provided the best results. Values for  $k_{att2}$  and  $k_{det2}$  could not be determined at the last two of four monitoring wells, thus suggesting that either a second type of kinetic sites is present in the first few meters of dune passage and not beyond the second monitoring well, or that effects of soil heterogeneity and dimensionality of the problem overshadowed this process. Variations between single collector efficiencies were relatively small, whereas collision efficiencies varied greatly. This implies that the nonlinear removal of MS2 and PRD1 is mainly caused by variations in interactions between grain and virus surfaces rather than by physical heterogeneity of the porous medium.

Similarly, a two-site model performed better than the one-site model in describing MS2 concentrations for the deep well injection study. However, the concentration data were too sparse in this study to have much confidence in the fitted parameters.

## 8.1 Introduction

Much interest exists, worldwide, in removing viruses by soil passage, either for protection of groundwater, or as treatment of surface water that is subsequently used for drinking water. Both groundwater as well as surface water may be contaminated with pathogenic viruses from various fecal sources (e.g., Yates, 1985; Havelaar *et al.*, 1993). A considerable amount of research has been carried out on the processes that determine virus removal by soil passage, both at the laboratory and field scale (see Schijven and Hassanizadeh, 2000, for a review). Virus removal during subsurface transport is due to a complex interplay of processes, of which inactivation and adsorption are of major importance (Yates *et al.*,

1987). In sandy aquifers, adsorption is reversible and kinetically limited, while likely several types of kinetic sites exist (Hassanizadeh and Schijven, 2000, Schijven *et al.*, 2001b). In addition, processes of advection, dispersion and dilution cause spreading of viruses and thus affect virus concentrations.

Transport and removal of viruses even in field studies is often still modeled as a one dimensional problem, assuming constant and steady-state water flow and considering only longitudinal dispersion (e.g., Bales *et al.*, 1997; DeBorde *et al.*, 1999; Pieper *et al.*, 1997; Ryan *et al.*, 1999; Schijven *et al.*, 1999, 2000). In reality, field situations are generally much more complex because of temporal and spatial variations in water flow velocities, diverging or converging flow lines, the effects of transverse dispersion and dilution. For these reasons a two-dimensional, or even a three-dimensional, transport model may be needed.

Another complication in understanding field-scale virus transport is that removal rates of viruses are often higher initially than further along the transport pathway (Bales *et al.*, 1995; DeBorde *et al.*, 1998; Pieper *et al.*, 1997; Ryan *et al.*, 1999; Schijven *et al.*, 1999, 2000). This may be due to heterogeneity within the soil environment at various scales (Schijven and Hassanizadeh, 2000), such as spatial variations of preferential attachment sites formed by ferric oxyhydroxides (Schijven *et al.*, 2000, 2001a) or, possibly, in the soil organic matter content (Schijven *et al.*, 2001a).

In the present study, data on virus removal from two field studies (Schijven *et al.*, 1999, 2000) were re-analyzed with the goal to investigate (1) differences between one- and two-dimensional modeling approaches, (2) differences between one- and two-site kinetic sorption models, and (3) the role of heterogeneities in subsurface hydraulic properties on virus removal. The first study involved removal of bacteriophages MS2 and PRD1 by dune recharge at Castricum, The Netherlands (Schijven *et al.*, 1999), while the second study represented removal of MS2 by deep well injection at Someren, The Netherlands (Schijven *et al.*, 1999). Details about both studies will be given below. Bacteriophages MS2 and PRD1, used in both field studies, represent the low adsorptive behavior of negatively charged viruses and therefore may represent a relatively worst case scenario in terms of rapid virus transport (Schijven and Hassanizadeh, 2000). This was confirmed by results from column experiments with dune sand from the Castricum field site (Schijven *et al.*, 2001c), which showed that a negatively charged pathogenic virus, Coxsackievirus B4, was removed almost as little as MS2, while a less negatively charged virus, Poliovirus 1, was removed much more effectively.

For our analyses we used the software packages HYDRUS-1D (Šimůnek *et al.*, 1998) and HYDRUS-2D (Šimůnek *et al.*, 1999), which simulate water flow and solute transport in one- and two-dimensional variably saturated porous media, respectively. The two codes were adapted by incorporating reversible adsorption to two types of kinetic sites. Data from the two field studies were previously analyzed using one-dimensional analytical models, assuming constant flow velocities, a homogeneous soil environment, and constant reaction and transport parameters between the source of bacteriophages and several collecting wells. In this study we will consider the two-dimensionality of both field problems, two-site kinetic sorption, and the heterogeneity of subsurface.

## 8.2 Brief Description of Field Experiments

### 8.2.1 Removal of MS2 and PRD1 by Dune Recharge

Removal of bacteriophages MS2 and PRD1 during dune recharge has been studied at Castricum, The Netherlands. Details of this field experiment and an extensive evaluation of the results are found in Schijven *et al.* (1999). The site consists of fine aeolian dune sands that form a phreatic aquifer around 10 m thick, with a hydraulic conductivity of about 12 m day<sup>-1</sup> (at a water temperature of 5 °C) and an effective porosity of approximately 0.35. Surface water infiltrates the sand through a number of parallel canals that are about 120 m apart. Water is produced through rows of wells that are placed along midlines of the canals. Within one of the canals, a 150-m<sup>2</sup> compartment was constructed using PVC sheeting along wooden poles. The distance from this compartment to extraction well PCQ414 was 63 m, with a water travel time of approximately 40 days. Almost perpendicular to the bank of the canal, six monitoring wells, W1 to W6, were installed up to a distance of 30 m (Figure 1). Well screens W1 to W4 were 0.25 m long and well screens W5 and W6 0.50 m long. The well screens were positioned at different depths to locate them along a calculated flow line. Table 1 lists the exact locations of these screens.

Prior to the dosage of the water with bacteriophages, sodium chloride was added to the compartment as a conservative salt tracer to estimate the interstitial flow velocity and the medium dispersivity. The chloride concentration of the water in the compartment was increased in one step from 150 mg.l<sup>-1</sup> to 750 mg.l<sup>-1</sup> and kept at this level for exactly 7 days. This represented an increase of electric conductivity (EC) from 890  $\mu\text{S.cm}^{-1}$  to about 2700  $\mu\text{S.cm}^{-1}$ . For a period of 35 days, the EC was measured at 10 minutes intervals in the six monitoring wells by means of fixed EC-sensors connected to a data logger. Dosage of the water with phages started by emptying bottles with a phage concentration of  $2.5 \times 10^{13}$  plaqueforming particles (pfp) of MS2 and  $2.5 \times 10^{12}$  pfp of PRD1 at the center of the compartment. This was done in order to raise the concentration in the compartment immediately to about  $10^8$  and  $10^7$  pfp.l<sup>-1</sup>, respectively. Although we tried to keep the concentrations constant by pumping phages from 1000-l containers into the compartment for a period of exactly eleven days, they varied by a factor of about two due to variations in power supply to the dosage pump. Water samples from the compartment and monitoring wells were taken regularly for a period of four months. The field study was performed during winter, when water temperatures were low and inactivation hence was minimal. The inactivation rate of phages in the water phase was measured both in the field and by means of laboratory experiments.

Concentrations of MS2 and PRD1 were reduced about 3 log<sub>10</sub> within the first 2.4 m and another 5 log<sub>10</sub> in a linear fashion within the following 27 m. The higher initial removal rate was investigated in more detail in column experiments (Schijven *et al.*, 2001a). Bacteriophage removal rates were found to be highly and positively correlated with soil organic carbon content and to a lesser extent with the presence of ferric oxyhydroxides. Hence, we believe that the high initial removal within the first meters of dune passage is due to attachment to preferable sites formed by ferric oxyhydroxides and/or organic carbon, that may be locally high under the reedy border of the recharge canal.

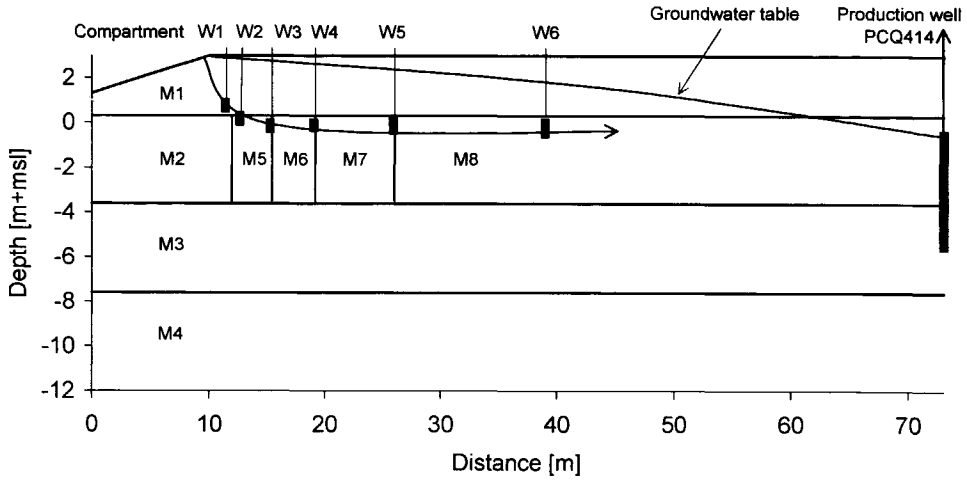


**Figure 1.** Schematic cross section of the dune recharge field site with a source compartment and monitoring wells W1 to W6. The curved arrow indicates the flow path. Depth is given in meters above sea level (msl). M1 to M8 denote the different materials.

**Table 1** Location of monitoring screens at the field site for the dune recharge experiment (Vogelaar et al., 1997).

Monitoring screen	Horizontal distance to bank of canal [m]	Top of screen [m + msl]	Bottom of screen [m + msl]	Mean hydraulic head [m + msl]
W1	1.40	0.89	0.64	2.37
W2	2.65	0.3	0.05	2.26
W3	5.30	-0.03	-0.28	2.07
W4	9.05	0.03	-0.22	1.83
W5	15.95	0.17	-0.33	1.44
W6	29.00	0.01	-0.49	0.77

msl is the mean sea level

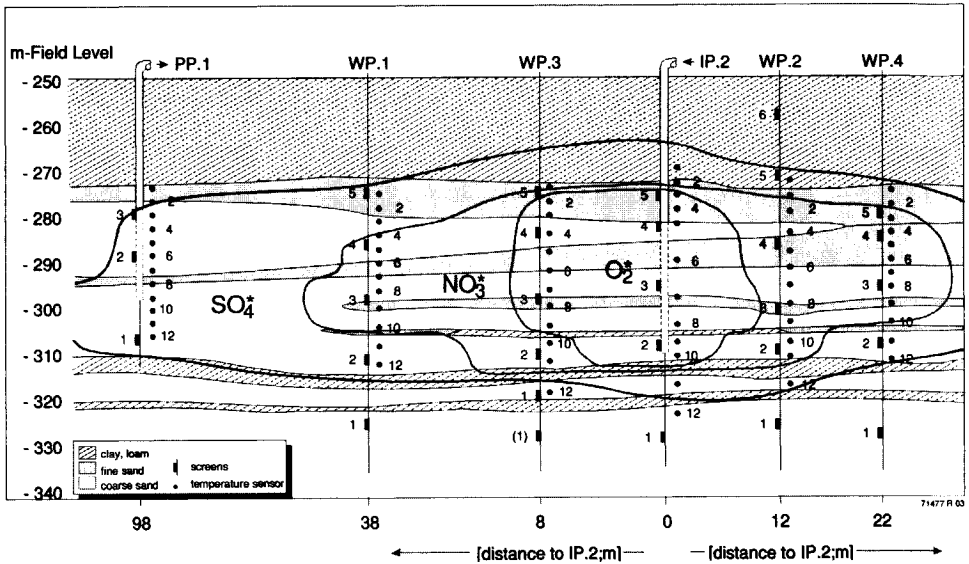


**Figure 2** Schematic cross section of a field site with injection well IP2, monitoring wells WP1 to WP4 and production well PP1. Samples were taken from the number-2 screens. Also shown are the redox-zones in the aquifer (Stuyfzand, 1999).  $^*O_2$  = dissolved oxygen concentration declining with distance from 10 to 0  $mg.l^{-1}$ .  $NO_3$  = nitrate concentration declining with distance from 20 to 0  $mg.l^{-1}$ .  $SO_4$  = sulfate concentration higher than pretreated surface water due to pyrite oxidation (Schijven *et al.*, 2000).

### 8.2.2 Removal of MS2 by Deep Well Injection

Removal of MS2 by deep well injection was studied at a field site near Someren, The Netherlands. Details of this study are given in Schijven *et al.* (2000). Pre-treated surface water was injected at a depth of 280 – 310 m below the surface (Figure 2). A 50-m thick layer of clay overlies the highly permeable aquifer. The aquifer itself lies on top of another 2–3 m thick clay layer. The aquifer consists of several sandy layers (fluvial sediments) that differ in permeability. Water was abstracted at a distance of 98 m from the injection point, from a depth interval of 278 to 298 m below the surface. Monitoring wells were located at distances of 8 m (WP3), 12 m (WP2), 22 m (WP4) and 38 m (WP1) from the injection well along the line of flow symmetry connecting IP2 and PP1. Samples were taken from 2-m long polyvinylchloride (PVC) screens at a depth of 310 m below the surface. The screens were all situated within the same layer of sand with the highest permeability ( $25 m.day^{-1}$ ).

Sodium chloride was injected as a conservative tracer to estimate the interstitial flow velocity of the injected water and the dispersivity of the porous medium. For a period of exactly five days, 265 kg NaCl in 880 liter was injected each day into the main injection pipeline through which pretreated surface water was injected at a rate of  $960 m^3.day^{-1}$ . This resulted in a salt concentration of  $0.275 kg.m^{-3}$  in the injection water, with the electrical conductivity (EC) of the injection water increasing in one step from  $450 \mu S.cm^{-1}$  to about  $1000 \mu S.cm^{-1}$ . During the first two weeks of the tracer study, the EC was measured

automatically at the number-2 screens of IP2, WP3 (8 m) and WP2 (12 m) at 4-hour intervals. EC-measurements in samples from the number-2 screens of WP1 (38 m) and WP4 (22 m) were carried out manually at daily and weekly intervals. A phage concentration of  $7.0 \times 10^7$  pfp.l<sup>-1</sup> of MS2 was applied to the injection well for a period of 5 days. The inactivation rate of MS2 in the water phase was measured in a sample from the injection water, and from the water collected after 8 m of soil passage.

Within the first 8 meters of soil passage, concentrations of MS2 were reduced by 6 log<sub>10</sub>, but only by about 2 log<sub>10</sub> in the following 30 m. This non-linear removal was ascribed to preferable attachment of MS2 to patches of ferric oxyhydroxides that are present within the first 8 meters from the injection point, but not thereafter (Schijven *et al.*, 2000).

### 8.3 Theory

#### 8.3.1 Conceptual Model

##### 8.3.1.1 Water Flow

Because of the unsaturated nature of part of the transport domain of the dune recharge experiment at Castricum, subsurface flow was simulated with the variably-saturated (Richards') equation as follows:

$$\frac{\partial \theta}{\partial t} = \frac{\partial}{\partial x_i} \left[ K(h) \left( K_{ij}^A \frac{\partial h}{\partial x_j} + K_{iz}^A \right) \right] \quad (1)$$

where  $x_i$  represents the spatial coordinate [m], with  $x_2=z$  taken here to be positive upward for the vertical cross section (i.e., for dune recharge experiment) and  $x_2=y$  for flow in a horizontal plane (i.e., the deep well injection experiment),  $t$  is time [day],  $\theta$  is the water content [ $\text{m}^3 \text{m}^{-3}$ ],  $h$  is the pressure head [m],  $K$  is the hydraulic conductivity [ $\text{m day}^{-1}$ ], and  $K_{ij}^A$  are components of a dimensionless anisotropy tensor. Knowledge of the functional relationships relating the water contents and the hydraulic conductivities to the pressure heads, in addition to the initial and boundary conditions, is needed to numerically solve Equation 1. An advantage of the Richards equation is that it can be used to describe simultaneously flow in both the saturated and unsaturated zones. Equation 1 hence can be applied to variably saturated water flow in the dune recharge experiment, and to fully saturated flow in the deep well injection experiment.

##### 8.3.1.2 Solute and Virus Transport

Transport of the conservative (NaCl) tracer is described using the convection-dispersion equation. In two-dimensional form, this equation is as follows:

$$\frac{\partial \theta c}{\partial t} = \frac{\partial}{\partial x_i} \theta D_{ij} \frac{\partial c}{\partial x_j} - q_i \frac{\partial c}{\partial x_i} \quad (2)$$

where  $c$  is the tracer solution concentration [ $\text{g m}^{-3}$ ],  $q_i$  is the  $i$ -th component of the volumetric flux density [ $\text{m day}^{-1}$ ], and  $D_{ij}$  is the dispersion coefficient tensor [ $\text{m}^2\text{day}^{-1}$ ] defined as (Bear, 1972):

$$\theta D_{ij} = \lambda_L |q| \delta_{ij} + (\lambda_L - \lambda_T) \frac{q_i q_j}{|q|} + \theta D_d \tau \delta_{ij} \quad (3)$$

where  $D_d$  is the molecular diffusion coefficient in free water [ $\text{m}^2\text{day}^{-1}$ ],  $\tau$  is a tortuosity factor [-],  $|q|$  is the absolute value of the Darcian fluid flux density [ $\text{m day}^{-1}$ ],  $\delta_{ij}$  is the Kronecker delta function, and  $\lambda_L$  and  $\lambda_T$  are the longitudinal and transverse dispersivities [m], respectively.

Schijven *et al.* (1999) used a one-dimensional (1D) one-site kinetic sorption model to describe the transport of viruses at both field sites. They assumed that both attachment and detachment of viruses to the solid phase could be described using a first-order kinetic rate process. The governing equations describing 1D virus transport are then as follows:

$$\theta \frac{\partial C}{\partial t} + \rho_B \frac{\partial S}{\partial t} = \lambda_L \theta v \frac{\partial^2 C}{\partial x^2} - \theta v \frac{\partial C}{\partial x} - \mu_i \theta C - \mu_s \rho_B S \quad (4)$$

$$\rho_B \frac{\partial S}{\partial t} = k_{att} \theta C - k_{det} \rho_B S - \mu_s \rho_B S \quad (5)$$

where  $C$  is the concentration of free phages [ $\text{pfp m}^{-3}$ ],  $S$  is the concentration of attached phages [ $\text{pfp kg}^{-1}$ ],  $\theta$  is the water content [ $\text{m}^3\text{m}^{-3}$ ], assumed here to be equal to porosity  $n$  [-] for the fully saturated conditions,  $v$  ( $=q/\theta$ ) is the average interstitial water velocity [ $\text{m day}^{-1}$ ],  $\rho_B$  is the dry bulk density [ $\text{kg m}^{-3}$ ],  $k_{att}$  and  $k_{det}$  are attachment and detachment rate coefficients, respectively [ $\text{day}^{-1}$ ]; and  $\mu_i$  and  $\mu_s$  are inactivation rate coefficients of the free and attached phages, respectively [ $\text{day}^{-1}$ ]. It was shown that this one-site sorption model could not accurately duplicate the tailing of virus breakthrough curves measured at various monitoring wells (Schijven *et al.*, 1999), nor the breakthrough curves measured on the laboratory samples (Schijven *et al.*, 2001b).

Hassanizadeh and Schijven (2000) later showed that the breakthrough curves of bacteriophages MS2 and PRD1 in the column experiments could be better described by means of a convection-dispersion model that incorporates adsorption to two types of kinetic sites. Their model assumes that the sorption sites on the solid phase can be divided into two fractions with different properties and various attachment and detachment rate coefficients.

The governing equations of the two-site sorption model are as follows (Hassanizadeh and Schijven, 2000; Schijven *et al.*, 2001b):

$$\theta \frac{\partial C}{\partial t} + \rho_B \frac{\partial S_1}{\partial t} + \rho_B \frac{\partial S_2}{\partial t} = \lambda_1 \theta v \frac{\partial^2 C}{\partial x^2} - \theta v \frac{\partial C}{\partial x} - \mu_1 \theta C - \mu_{s1} \rho_B S_1 - \mu_{s2} \rho_B S_2 \quad (6)$$

$$\rho_B \frac{\partial S_1}{\partial t} = k_{att1} \theta C - k_{det1} \rho_B S_1 - \mu_{s1} \rho_B S_1 \quad (7)$$

$$\rho_B \frac{\partial S_2}{\partial t} = k_{att2} \theta C - k_{det2} \rho_B S_2 - \mu_{s2} \rho_B S_2 \quad (8)$$

where all variables are the same as for equations (4) and (5), with the subscripts 1 and 2 referring to the two different kinetic sites.

### 8.3.2 Numerical Model

The governing water flow (1) and solute transport (2-8) equations were solved numerically subject to appropriate initial and boundary conditions using the HYDRUS-1D (Šimčnek *et al.*, 1998) and HYDRUS-2D (Šimčnek *et al.*, 1999) models for the one- and two-dimensional problems, respectively. Galerkin-type linear finite element methods were used for the spatial discretization, and a finite difference method for temporal discretization. A fully implicit mass conservative modified Picard iteration scheme (Celia *et al.*, 1990) was used to solve the Richards' equation.

HYDRUS-1D and HYDRUS-2D simulate water flow and solute transport in variably saturated porous media. The two codes considered the concept of two-site sorption (Selim *et al.*, 1977; van Genuchten and Wagenet, 1989) to permit consideration of nonequilibrium adsorption-desorption reactions. The two-site sorption concept assumes that the sorption sites can be divided into two fractions, with sorption on one fraction of the sites (the type-1 sites) being instantaneous, and with sorption on the remaining (type-2) sites being time-dependent. The HYDRUS codes hence permitted only one type of sorption sites to be kinetic. To make the codes applicable to our study, HYDRUS-1D and HYDRUS-2D were both modified by implementing reversible kinetic adsorption to two sets of kinetic sites as modeled with Eqs. (6) to (8).

### 8.3.3 Inverse Modeling

Solute transport and reaction parameters, as well as saturated hydraulic conductivities and porosities were obtained by calibrating the HYDRUS-1D and HYDRUS-2D model solutions against the measured data. This was done by iteratively changing model parameters and thus improving model fits to the measured data until a desired degree of precision is obtained. The objective function, SSQ, which was minimized during the parameter estimation procedure, contains weighted residuals between the measured data and the model predictions:

$$SSQ(\mathbf{b}, \mathbf{q}) = \sum_{j=1}^m \left( v_j \sum_{i=1}^{n_j} w_{ij} [q_j^*(\mathbf{x}, t_i) - q_j(\mathbf{x}, t_i, \mathbf{b})]^2 \right) \quad (9)$$

where the right-hand side represents weighted deviations between the measured and calculated space-time variables (e.g., concentrations and/or pressure heads at different times in the flow domain). In this term,  $m$  is the number of different sets of measurements,  $n_j$  is the number of measurements in a particular measurement set,  $q_j^*(\mathbf{x}, t_i)$  represents specific measurements at time  $t_i$  for the  $j^{\text{th}}$  measurement set at location  $\mathbf{x}$ ,  $q_j(\mathbf{x}, t_i, \mathbf{b})$  are the corresponding model predictions for the vector of optimized parameters  $\mathbf{b}$  (e.g.,  $K_s$ ,  $n$ ,  $\lambda_L$ ,  $k_{att}$  and  $k_{det}$ ), and  $v_j$  and  $w_{ij}$  are weights associated with a particular measurement set or point, respectively. Minimization of SSQ was accomplished using the Levenberg-Marquardt nonlinear minimization algorithm (Marquardt, 1963).

## 8.4 Analysis of the Dune Recharge Experiment

### 8.4.1 Water Flow and Tracer Transport

Two types of analyses were carried out with data collected during the dune recharge experiment. First, HYDRUS-1D was used to optimize the hydraulic (*i.e.*, the saturated hydraulic conductivity and porosity) and solute transport (*i.e.*, longitudinal dispersivity and attachment and detachment constants) parameters along a one-dimensional flow path, similarly as in previous studies (Schijven *et al.*, 1999, 2000). In the initial analyses we assumed that the different parameters were constant between the source of tracer or phages and particular wells. However, because model parameters calibrated against data measured at one well often could not reproduce concentrations at the other wells, in later analysis we allowed various variables to vary between individual wells. For comparison purposes we list in Table 2 results obtained previously by (Schijven *et al.*, 1999) using the one-dimensional one-site sorption model as modeled with the CXTFIT2 code (Toride *et al.*, 1995). The optimized dispersivities and average pore-water velocities were fitted to the EC and virus data assuming stream tubes from the source to a particular well and with the aquifer having homogeneous properties and constant porosity  $n$  of 0.35.

Table 3 presents stream-tube dispersivities and average pore-water velocities as fitted with the HYDRUS-1D code to the measured EC data. As expected, the optimization results are almost identical to those in Table 2, thus verifying the numerical solution in the HYDRUS-1D code. Optimized pore-water velocities were smaller for the first well (W1), almost constant for the next four wells, and then significantly lower for the last well (W6). The optimized longitudinal dispersivities were very small (on the order of 1 cm) with the exception of the last well, for which we obtained a dispersivity of 8 cm. Although excellent agreement was obtained between measured and fitted concentrations for a particular well (not shown), the optimized parameters could not always be used successfully to predict concentrations at other locations.

**Table 2** Estimated values of model parameters determined using the CXTFIT2 analytical model (one-dimensional, one-site kinetic sorption) from individual breakthrough curves of NaCl, MS2 and PRD1 for the dune recharge experiment (Schijven *et al.*, 1999).

Solute	Variable	Units	Wells					
			W1	W2	W3	W4	W5	W6
	$X$	m	2.4	3.8	6.4	10.2	17.1	30.1
NaCl	$\nu$	m.day <sup>-1</sup>	1.41	1.56	1.59	1.57	1.52	1.19
	$\lambda_{\nu}^*$	m	0.008	0.012	0.017	0.017	0.0096	0.08
MS2	$\mu_l$	day <sup>-1</sup>	0.03	0.03	0.03	0.03	0.03	0.03
	$\mu_s$	day <sup>-1</sup>	0.085	0.092	0.092	0.092	0.092	0.092
	$k_{att}$	day <sup>-1</sup>	4.1	3.2	2.8	2.0	1.3	0.8
	$k_{det}$	day <sup>-1</sup>	0.00087	0.0016	0.0026	0.0018	0.00052	0.0030
PRD1	$\mu_l$	day <sup>-1</sup>	0.12	0.12	0.12	0.12	0.12	0.12
	$\mu_s$	day <sup>-1</sup>	0.071	0.067	0.067	0.067	0.067	0.067
	$k_{att}$	day <sup>-1</sup>	4.0	3.1	2.2	1.5	1.3	0.7
	$k_{det}$	day <sup>-1</sup>	0.00077	0.0011	0.0018	0.0025	0.0021	0.0034

$X$  is the distance along a streamline

To improve the prediction of concentrations at all wells simultaneously, in the second step of our one-dimensional analyses we assumed that several variables could change between different wells. We defined an objective function using EC breakthrough curves from all 6 wells, assumed a constant water flux in the subsurface equal to the arithmetic average of the fluxes in Table 3, used longitudinal dispersivities between individual wells equal to those optimized for particular breakthrough curves, and optimized the porosities between the source and the first well, and between all subsequent two consecutive wells. Although the pore-water velocities could vary along a stream tube depending upon the porosity, the volumetric flux  $q$  must be constant unless sources or sinks are present. This optimization assumes that instead of using different stream tubes with particular pore velocities and dispersivities for each well, the solute arriving at the first well is moved further to the second well (with different porosities and dispersivities between the first two wells), and then to the third well, etc. Results of the optimization are given in Table 4 and in Figure 3. Notice an excellent correspondence between the measured and fitted EC data. We obtained a large value of porosity between wells W5 and W6 (equal to 0.6), which causes a relatively small value of the optimized flux for the breakthrough curve of well W6, including its late arrival time.

For the two-dimensional analyses the transport domain was first divided into four major material layers: the surface layer M1 (from 3.0 to 0.4 m relative to the mean sea level), two intermediate layers M2 (0.4 to -3.5 m) and M3 (-3.5 to -7.5 m), and the less permeable layer M4 (-7.5 to -12 m) at the bottom of the transport profile (Figure 1). These four layers were determined from bore profiles (Vogelaar *et al.*, 1997). As boundary conditions we used a constant head in the source pool, corresponding to the height of the ponded water,

**Table 3** One-dimensional optimizations using EC data from the dune recharge experiment and assuming stream tubes from a source to a particular well having constant properties ( $n=0.35$ ). Each breakthrough curve was optimized independently using HYDRUS-1D.

Well	$q$ [m.day <sup>-1</sup> ]	$\lambda_i$ [m]	$v$ [m.day <sup>-1</sup> ]	SSQ
W1	0.49±0.001	0.0069±0.0005	1.4	0.0020
W2	0.54±0.001	0.010±0.0007	1.54	0.0043
W3	0.55±0.0015	0.016±0.0016	1.57	0.013
W4	0.56±0.0008	0.016±0.001	1.6	0.0069
W5	0.53±0.0008	0.0074±0.0004	1.51	0.030
W6	0.41±0.0008	0.083±0.0054	1.17	0.033

**Table 4** One-dimensional optimization using EC data from the dune recharge experiment and assuming the presence of one stream tube from the source through all wells. All EC data were analyzed simultaneously using HYDRUS-1D; porosities and dispersivities varied between wells. For dispersivities see Table 3.

Well	W1	W2	W3	W4	W5	W6	SSQ
Porosity	0.384	0.282	0.338	0.352	0.371	0.596	0.00115
	±0.0020	±0.0044	±0.0026	±0.0022	±0.0011	±0.0013	

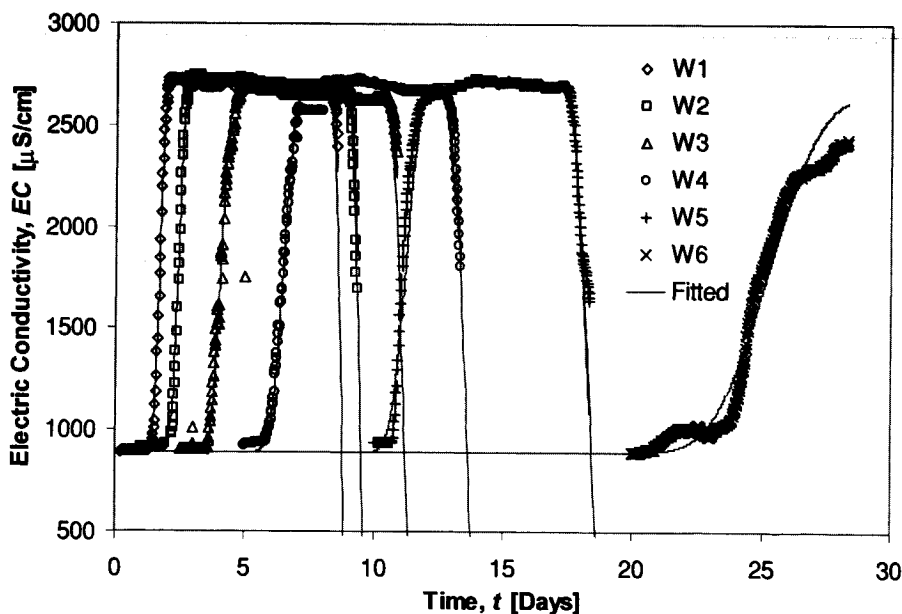


**Figure 3** Measured and optimized EC data assuming a stream tube from the source through all wells of the dune recharge experiment. All EC data were analyzed simultaneously using HYDRUS-1D; porosities and dispersivities varied between wells.

**Table 5** Two-dimensional simulations of EC data from the dune recharge experiment. All EC data were analyzed simultaneously using HYDRUS-2D.

Material	M1	M2	M5	M6	M7	M8	M3	M4
$K_s$	9.55	11.2	11.2	11.2	11.2	11.2	26.0	2.0
[m.day <sup>-1</sup> ]	±1.84	±1.71	±1.71	±1.71	±1.71	±1.71	±4.40	
Porosity	0.388	0.308	0.419	0.403	0.326	0.502	0.350	0.350
	±0.0078	±0.060	±0.021	±0.0187	±0.0100	±0.0081		

and a constant flux along the active part of the pumping well, corresponding to the pumping rate. Next we calibrated HYDRUS-2D by optimizing the saturated hydraulic conductivities for these boundary conditions against the mean hydraulic heads recorded for all 6 wells. Defining the objective function using only the mean hydraulic heads in the observation wells produced conductivities that predicted unrealistic arrival times for the tracer fronts at these monitoring wells. Thus, in the next step, we defined the objective function using also values of the mean flux along the streamline as obtained from the one-dimensional analysis of the tracer fronts. This calibration led to the saturated hydraulic conductivities for particular soil layers as given in Table 5 for materials M1 through M4.

In order to obtain better description of the EC breakthrough curves at particular monitoring wells, material layer M2 was further subdivided into another 5 submaterials (M2, M5, M6, M7, and M8), corresponding to areas between individual wells. We did this additional subdivision only for material layer M2 since this was the only layer for which we had information on NaCl and phages concentrations. Material M2 was situated between the left side of the transport domain and well W2, material M5 was between wells W2 and W3, M6 between W3 and W4, M7 between W4 and W5, and material M8 to the right of well W5 (Figure 1). We then calibrated the porosities of each of these materials using all measured breakthrough curves simultaneously. The results of the two-dimensional analyses of water flow and the EC data are given in Table 5. The optimizations produced similar agreement between measured and optimized NaCl breakthrough curves as those given in Figure 3 for the one-dimensional numerical analysis.

Calibrated values of the saturated hydraulic conductivity, porosity and longitudinal dispersivity were assumed to correctly describe the solute transport system and were used in our subsequent analyses of virus transport.

#### 8.4.2 Analysis of Virus Transport

In the case of the dune recharge study, the measured inactivation coefficients of free bacteriophages, as well as the inactivation coefficients of attached bacteriophages, determined from the slope of the tails of the breakthrough curves, were reported by Schijven *et al.* (1999). The inactivation rate coefficients of virus attached to site 2 were assumed to be the same as those for site 1. All inactivation coefficients were assumed to be known and were not further included in the inverse analysis. The observations were assumed to be log-normally distributed and hence logarithmically transformed prior to the fitting procedure.

Application of the one-dimensional one-site kinetic sorption stream-tube transport model produced a reasonable fit of the breakthrough curves except for considerable discrepancy at the end of the rising and the start of the declining limbs of the breakthrough curves (Schijven *et al.*, 1999). Table 2 lists the corresponding parameter values.

The measured MS2 and PRD1 breakthrough data were subsequently analyzed with the one- and two-dimensional HYDRUS-1D and HYDRUS-2D models using both the one-site and two-site kinetic sorption models. Attachment and detachment coefficients were again optimized sequentially starting with the breakthrough curve measured at well W1, then moving forward to well W2, and so on. In several optimization runs model parameters were determined simultaneously from two corresponding breakthrough curves. Optimized parameter values determined from the MS2 and PRD1 breakthrough curves, using both one- and two-dimensional analyses and one- and two-site kinetic sorption models, are given in Tables 6 and 7, respectively. Measured and optimized MS2 and PRD1 breakthrough curves for the different models and viruses are presented in Figures 4 through 11.

The description of all breakthrough curves using models of various dimensionality and complexity is reasonably good. However, as can be seen from Figures 4 and 8, the one-dimensional one-site model does not completely describe the tails of the measured breakthrough curves. While the one-dimensional one-site model predicts a sudden decrease of virus concentrations immediately after their peak, measured data display a relatively smooth transition of the declining limb to the more straight later part of the tail. The one-dimensional two-site model did fit the overall shape of the breakthrough curves very well (Figures 5 and 9).

Figures 6 and 10 show fits obtained using the two-dimensional model and assuming one-site sorption. The two-dimensional one-site model predicted a more gradual decrease of the virus concentrations after the peaks than the one-dimensional one-site model, but not as good as the one-dimensional two-site model. While the two-dimensional one-site model seems to follow the course of the MS2 tail reasonably well, this is less so for PRD1. Apparently, dimensionality of the problem can partly explain the smoother appearance of the concentration after peak breakthrough. Still, the two-dimensional two-site model fitted (visually as well as based on SSQ values) the breakthrough curve better.

With the two-site model, both one- and two-dimensional, estimates of  $k_{att2}$  and  $k_{det2}$  for MS2 and PRD1 at W2 were highly uncertain. The value of  $k_{att1}$  at W2 for both MS2 and PRD1 was relatively low, thus suggesting that little adsorption occurred in the vicinity of W2. This may explain the large uncertainty found in the estimates of  $k_{det2}$  at W2. Notice also that the models fitted the maximum breakthrough concentration at W2 very well, but generally underestimated the maximum breakthrough at W1. This is because of the skewness of the climbing limb of the breakthrough curve at W1. At W3 and W4, values for  $k_{att2}$  and  $k_{det2}$  could not be determined with a two-dimensional model. When the attachment coefficients for the second type of sorption sites were small (often estimated with large confidence intervals) or could not be determined altogether, then obviously also the detachment coefficients could not be determined. This suggests that a second type of kinetic sites is either present only in the first few meters of dune passage (due to the presence of organic carbon), but not beyond W2, or that the effects of soil heterogeneity and dimensionality of

**Table 6** Parameter values for MS2 breakthrough curves for the dune recharge experiment. One stream tube from source through all wells was considered in one-dimensional optimizations. Optimizations were carried out sequentially from well to well.

	$k_{att1}$	$k_{der1}$	$k_{att2}$	$k_{der2}$	SSQ	$\eta^c$	$\alpha^d$
<b>1D One-site</b>							
W1	4.48 $\pm 0.170$	0.00195 $\pm 0.00050$			0.0391	0.53	$1.4 \times 10^{-3}$
W2	0.548 $\pm 0.241$	$3.6 \times 10^{-8}$ $\pm 0.0061$			0.0386	0.66	$8.1 \times 10^{-5}$
W3	2.50 $\pm 0.105$	0.0121 $\pm 0.00270$			0.0140	0.58	$5.6 \times 10^{-4}$
W4	0.822 $\pm 0.0887$	0.0252 $\pm 0.0120$			0.0135	0.60	$2.1 \times 10^{-4}$
<b>1D Two-site</b>							
W1	4.28 $\pm 0.0969$	0.000862 $\pm 0.00020$	0.838 $\pm 0.231$	0.0413 $\pm 0.135$	0.0188	0.53	$1.3 \times 10^{-3}$
W2	0.585 $\pm 0.173$	$1 \times 10^{-6a}$ $\pm 0.00006$	0.963 $\pm 1.55$	2.10 $\pm 6.58$	0.0269	0.66	$8.6 \times 10^{-5}$
W3	2.17 $\pm 0.0708$	0.003110 $\pm 0.00096$	0.0001 <sup>a</sup> $\pm 0.406$	NA	0.0058	0.58	$4.8 \times 10^{-4}$
W4	0.827 $\pm 0.0666$	0.0150 $\pm 0.0069$	0.0001 <sup>a</sup> $\pm 1.56$	NA	0.0112	0.60	$2.1 \times 10^{-4}$
<b>2D One-site</b>							
W1	5.87 $\pm 0.161$	0.00132 $\pm 0.00028$				0.52	$1.8 \times 10^{-3}$
W2	0.415 $\pm 0.143$	0.181 $\pm 0.0885$			0.0295 <sup>b</sup>	0.37	$1.4 \times 10^{-4}$
W3	1.74 $\pm 0.0756$	0.00209 $\pm 0.00186$				0.42	$6.1 \times 10^{-4}$
W4	0.0001 $\pm 1.59$	NA			0.0324 <sup>b</sup>	0.49	$3.3 \times 10^{-8}$
<b>2D Two-site</b>							
W1	4.51 $\pm 0.278$	0.00132 $\pm 0.00042$	1.45 $\pm 0.363$	0.215 $\pm 0.0759$		0.52	$1.4 \times 10^{-3}$
W2	0.447 $\pm 0.321$	0.00202 $\pm 0.00538$	0.0001 $\pm 0.486$	NA	0.0175 <sup>b</sup>	0.37	$1.5 \times 10^{-4}$
W3	1.57 $\pm 3.50$	0.00804 $\pm 0.0209$	0.291 $\pm 6.84$	52.1 $\pm 1086.9$		0.42	$5.5 \times 10^{-4}$
W4	0.0001 $\pm 1.05$	NA	0.0001 $\pm 0.550$	NA	0.0183 <sup>b</sup>	0.49	$3.3 \times 10^{-8}$

<sup>a</sup>Parameter fixed or constraint reached; <sup>b</sup>In the 2D case, breakthrough curves from wells W1 and W2 (and W3 and W4) were optimized simultaneously; <sup>c</sup>Single collector efficiency; <sup>d</sup>collision efficiency associated with  $k_{att1}$

**Table 7** Parameter values for PRD1 breakthrough curves for the dune recharge experiment. One stream tube from source through all wells was considered in one-dimensional optimizations. Optimizations were carried out sequentially from well to well.

	$k_{att1}$	$k_{det1}$	$k_{att2}$	$k_{det2}$	SSQ	$\eta^c$	$\alpha^d$
<b>1D One-site</b>							
W1	4.56	0.00217			0.051	0.30	$2.5 \times 10^{-3}$
	$\pm 0.153$	$\pm 0.000052$					
W2	0.280	$1 \times 10^{-6}$			0.062	0.37	$7.41 \times 10^{-5}$
	$\pm 0.308$	$\pm 0.0129$					
W3	1.57	0.0353			0.027	0.33	$6.2 \times 10^{-4}$
	$\pm 0.136$	$\pm 0.000892$					
W4	120.	167.			0.062	0.33	$5.4 \times 10^{-2}$
	$\pm 617.$	$\pm 898.$					
<b>1D Two-site</b>							
W1	4.45	0.00116	0.876	0.524	0.026	0.30	$2.4 \times 10^{-3}$
	$\pm 0.0927$	$\pm 0.00022$	$\pm 0.243$	$\pm 0.170$			
W2	0.517	0.00583	1.42	1.86	0.0435	0.37	$1.4 \times 10^{-4}$
	$\pm 0.247$	$\pm 0.00638$	$\pm 1.33$	$\pm 3.36$			
W3	0.975	0.00756	0.442	1.230	0.00153	0.33	$3.9 \times 10^{-4}$
	$\pm 0.0741$	$\pm 0.00302$	$\pm 0.460$	$\pm 1.76$			
W4	36.8	56.8	0.101	0.00942	0.0624	0.33	$1.7 \times 10^{-2}$
	$\pm 682.$	$\pm 1071.$	$\pm 0.101$	$\pm 0.0481$			
<b>2D One-site</b>							
W1	5.59	0.00175			0.0622	0.29	$3.1 \times 10^{-3}$
	$\pm 0.298$	$\pm 0.00056$					
W2	0.471	0.0302			0.0622 <sup>b</sup>	0.21	$2.7 \times 10^{-4}$
	$\pm 0.222$	$\pm 0.0166$					
W3	0.215	0.536				0.24	$1.3 \times 10^{-4}$
	$\pm 0.304$	$\pm 1.47$					
W4	0.001 <sup>a</sup>	$8.1 \times 10^8$			0.0910 <sup>b</sup>	0.27	$6.0 \times 10^{-8}$
<b>2D Two-site</b>							
W1	4.90	0.00175	0.961	0.282	0.0139	0.29	$2.7 \times 10^{-3}$
	$\pm 0.393$	$\pm 0.00078$	$\pm 0.475$	$\pm 0.2403$			
W2	0.437	0.00840	0.001 <sup>a</sup>	NA	0.0517 <sup>b</sup>	0.21	$2.5 \times 10^{-4}$
	$\pm 1.804$	$\pm 0.0437$	$\pm 3.55$				
W3	0.181	0.162	0.001 <sup>a</sup>	NA		0.24	$1.1 \times 10^{-4}$
	$\pm 0.296$	$\pm 0.631$	$\pm 0.687$				
W4	0.818	88.2	0.001 <sup>a</sup>	NA	0.103 <sup>b</sup>	0.27	$4.9 \times 10^{-4}$
	$\pm 410.5$	too large	$\pm 2.05$				

<sup>a</sup>Parameter fixed or constraint reached; <sup>b</sup>In the 2D case, breakthrough curves from wells W1 and W2 (and W3 and W4) were optimized simultaneously; <sup>c</sup>Single collector efficiency; <sup>d</sup>collision efficiency associated with  $k_{att1}$

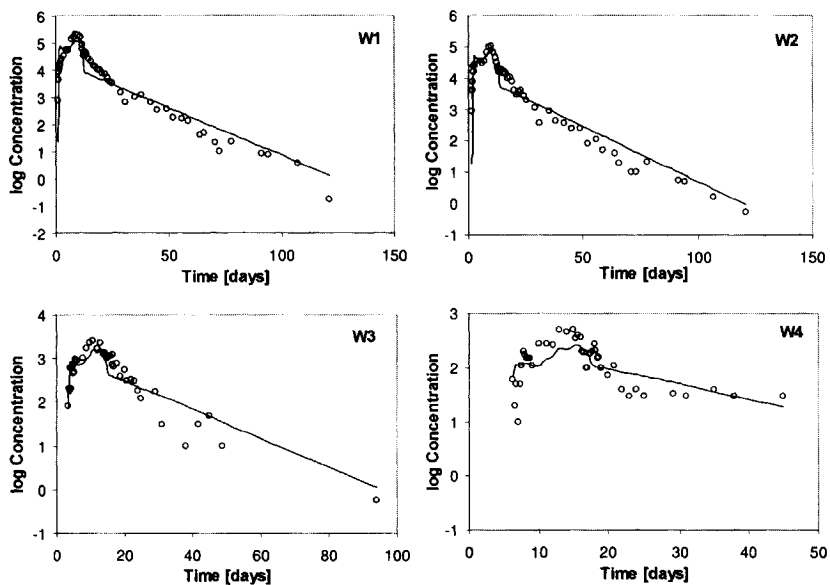


**Figure 4** MS2, 1D, one-site Measured and optimized MS2 breakthrough curves for the dune recharge experiment. One-dimensional one-site model was used in sequential optimizations. Dots are observations; the line is the model fit.

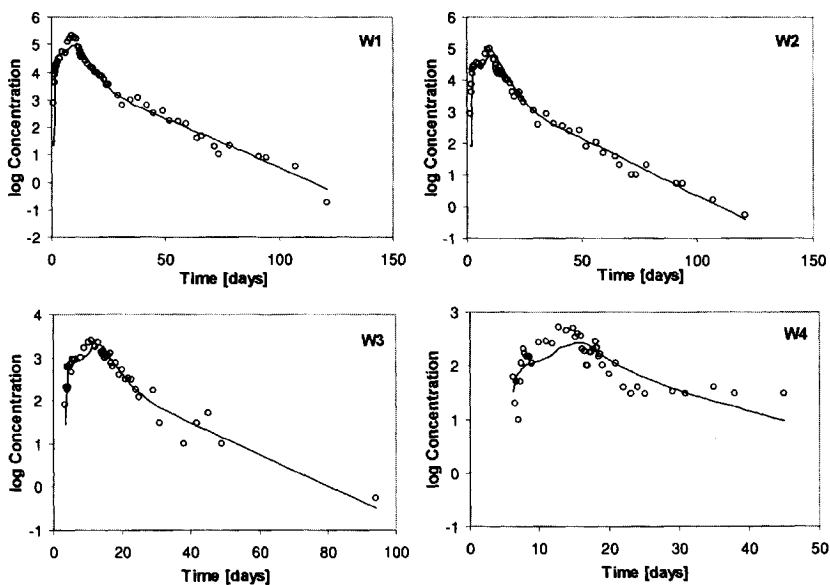


**Figure 5** MS2, 1D, two-site Measured and optimized MS2 breakthrough curves for the dune recharge experiment. One-dimensional two-site model was used in sequential optimizations. Dots are observations; the line is the model fit.

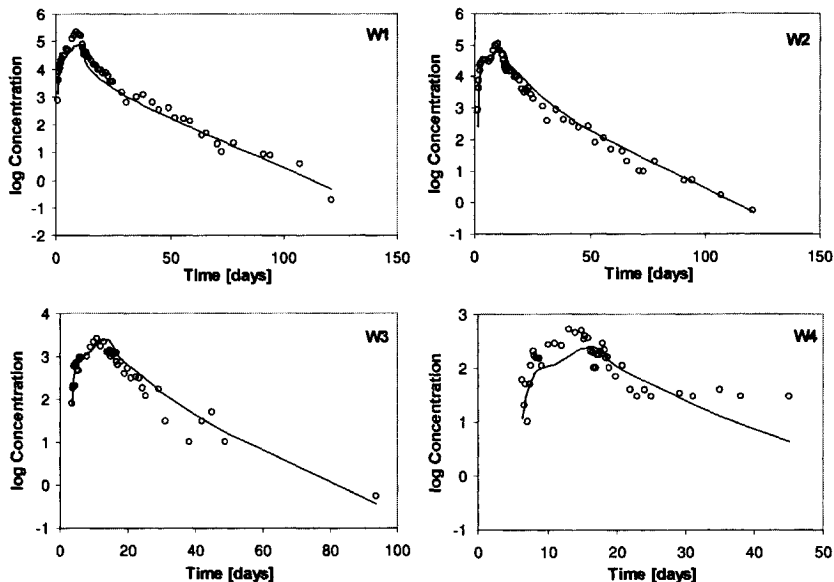


**Figure 6** MS2, 2D, one-site Measured and optimized MS2 breakthrough curves for the dune recharge experiment. Two-dimensional one-site model was used in sequential optimizations. Dots are observations; the line is the model fit.

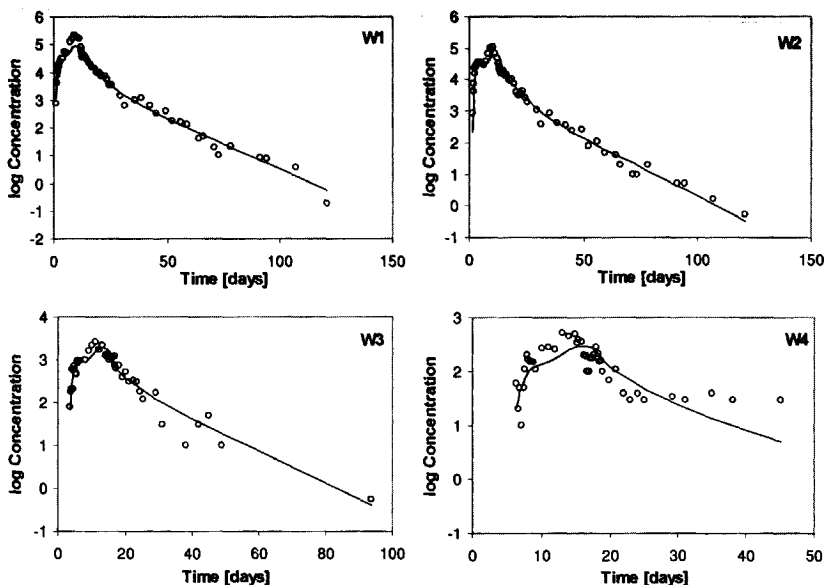


**Figure 7** MS2, 2D, two-site Measured and optimized MS2 breakthrough curves for the dune recharge experiment. Two-dimensional two-site model was used in sequential optimizations. Dots are observations; the line is the model fit.

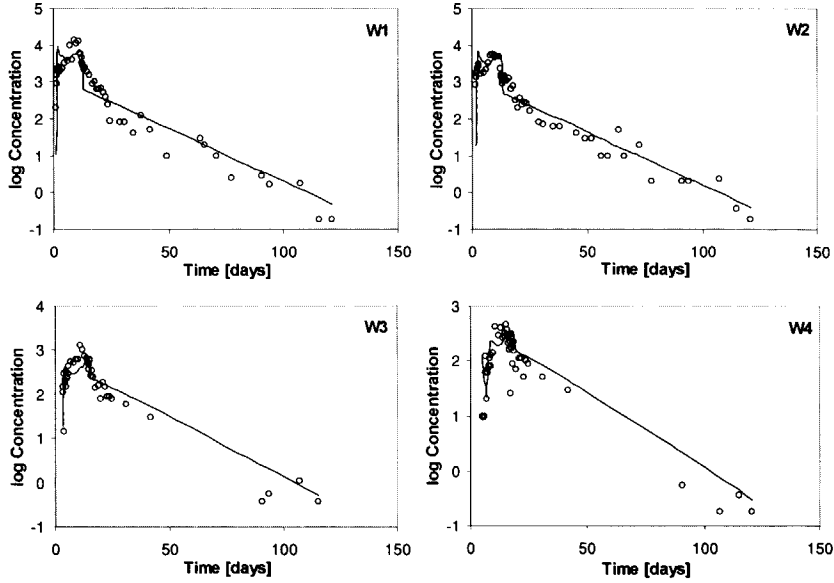


**Figure 8** PRD1, 1D, one-site Measured and optimized PRD1 breakthrough curves for the dune recharge experiment. One-dimensional one-site model was used in sequential optimizations. Dots are observations; the line is the model fit.

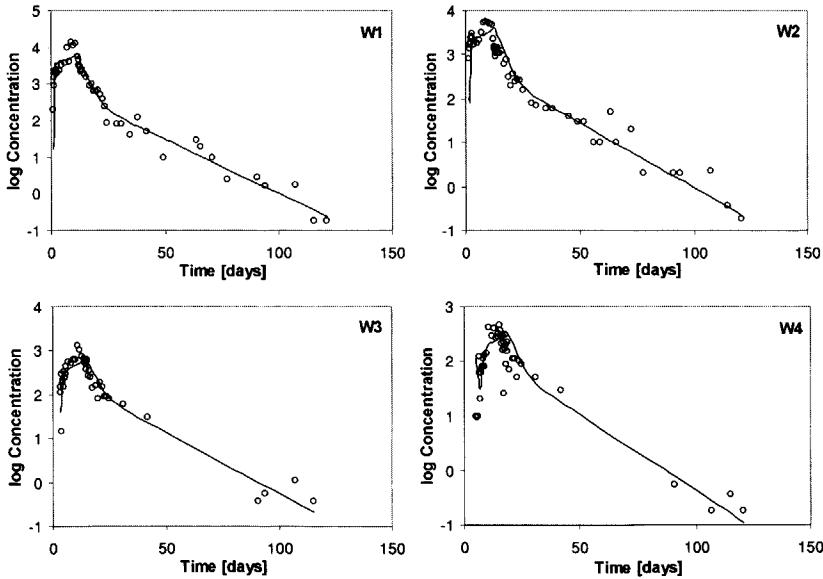


**Figure 9** PRD1, 1D, two-site Measured and optimized PRD1 breakthrough curves for the dune recharge experiment. One-dimensional two-site model was used in sequential optimizations. Dots are observations; the line is the model fit.

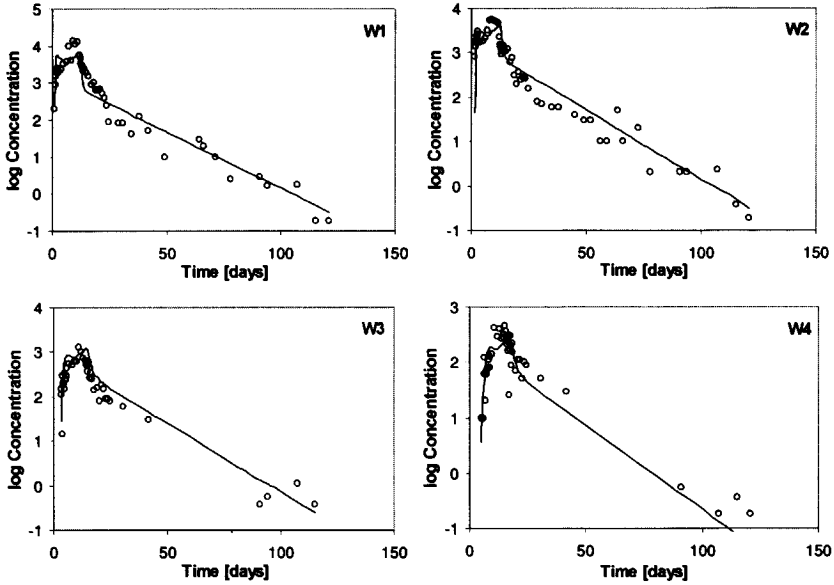


**Figure 10** PRD1, 2D, one-site *Measured and optimized PRD1 breakthrough curves for the dune recharge experiment. Two-dimensional one-site model was used in sequential optimizations. Dots are observations; the line is the model fit.*

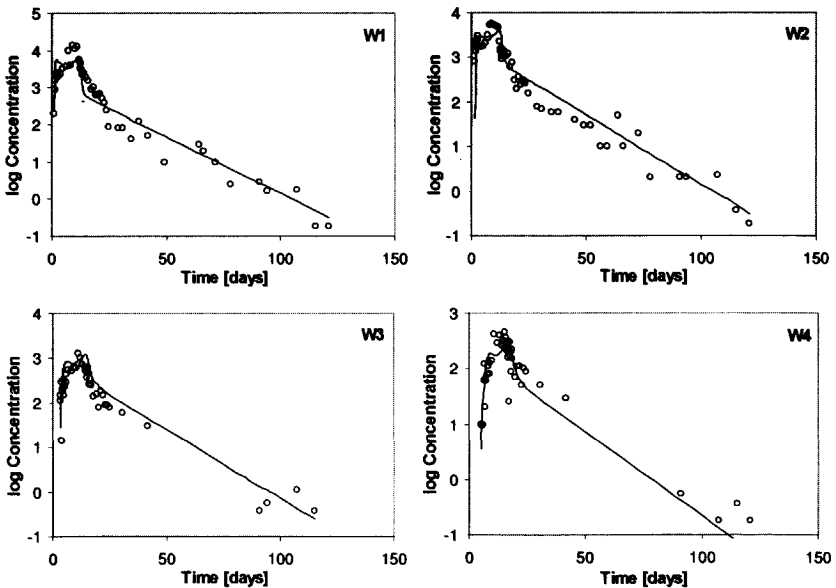


**Figure 11** PRD1, 2D, two-site *Measured and optimized PRD1 breakthrough curves for the dune recharge experiment. Two-dimensional two-site model was used in sequential optimizations. Dots are observations; the line is the model fit.*

the problem overshadowed this process. The latter explanation seems more plausible since the two-site kinetic sorption process was determined independently on laboratory soil columns (Hassanizadeh and Schijven, 2000; Schijven *et al.*, 2001b). Most of the interaction with the type-1 sites took place before W2, and thus had the greatest effects on the shapes of the breakthrough curves at the subsequent wells. Beyond W2 little attachment took place and the minor changes in the shape of the breakthrough curves are then mainly due to effects of dispersion.

Estimates of  $k_{att1}$  between the four different models were quite similar. For both MS2 and PRD1, the highest values were found at W1, reflecting the high initial removal rate that occurred within the first few meters of dune recharge. The other estimates of  $k_{att1}$  were lower, varying between 0.0 and 2.5. These variations reflect differences in adsorption properties of the soil and determine variations in removal rates. No attachment could be determined between wells W3 and W4 using a two-dimensional model for both bacteriophages. When modeling breakthrough from the source to a particular well the variations in rates were less explicit (see Table 2). This is because the higher initial attachment rate was redistributed along the entire stream tube, which leads to gradually decreasing attachment coefficients for wells further along the streamline.

Tables 6 and 7 also list corresponding single collector and collision efficiencies associated with  $k_{att1}$  (for equations, see Schijven *et al.*, 2001b). The single collector efficiency is the rate at which particles, in our case viruses, strike a soil grain divided by the rate at which particles move towards the grain and represents the physical factors determining particle collision. The collision efficiency is the efficiency with which collided particles remain attached to the soil grains due to electrostatic interaction. Variations between single collector efficiencies were relatively small, whereas collision efficiencies varied greatly. This implies that the nonlinear removal of MS2 and PRD1 is mainly caused by variations in the interactions between grain and virus surfaces, rather than by physical heterogeneities of the porous medium. This is in agreement with findings from the column experiments (Schijven *et al.*, 2001a) where removal was found to be strongly and positively correlated with such surface characteristics as soil organic carbon content and ferric oxyhydroxide content.

### 8.5 Deep Well Injection Experiment

#### 8.5.1 Analyses of Water Flow and Tracer Transport

Because of the dimensionality of this problem, only two-dimensional modeling was considered. We simulated the deep well injection experiment on a horizontal quadrilateral transport domain of 200 m times 100 m that was perpendicular to the monitoring, pumping and injecting wells. The transport domain was discretized into two finite element meshes (3508 and 13136 finite elements) with a very fine spatial discretization around the injecting and pumping wells and in the area between the two wells. Coarser discretizations were used towards the external boundaries. Wells IP2 and PP1 were simulated as circles with a diameter of 80 cm and were discretized using 15 or 25 nodes for the coarser and finer finite element mesh, respectively. A finer finite element mesh was used for simulation of NaCl transport because the small dispersivities and the absence of sorption and inactivation led to

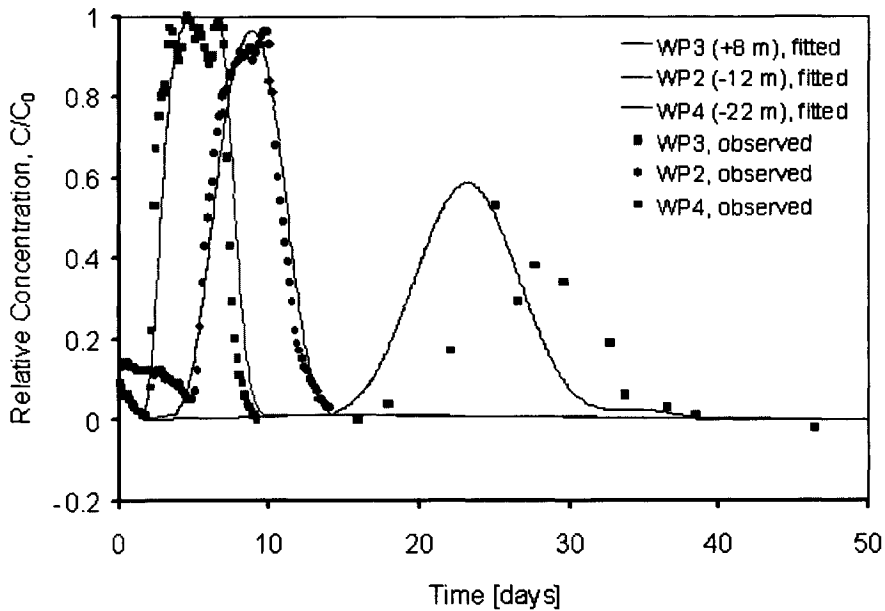


**Figure 12** Measured and optimized NaCl breakthrough curves at three wells for the deep well injection experiment. The distance in the legend corresponds with the location of the monitoring well with respect to the injection and pumping well, with positive number corresponding with monitoring well located between the two major wells.

relatively large Peclet numbers over the transport domain, a situation that usually leads to significant numerical oscillations. Coarser meshes could be used for the virus transport calculations since the sorption and inactivation produced considerably smoother (dispersed) curves.

Injection and pumping rates ( $13 \text{ m day}^{-1}$ ) were used as boundary conditions for water flow, and relative concentrations of injected water for solute transport. NaCl concentrations measured at wells WP2, WP3, and WP4 were used to calibrate the longitudinal dispersivity of the aquifer. Results of the calibration for the optimized value of the longitudinal dispersivity of  $0.163 \text{ cm}$  are shown in Figure 12. Note that without any calibration of the water flow field, the fit of the first two breakthrough curves was excellent, while only third breakthrough curve arrived slightly later than calculated. Also notice that the tracer not only moved in the direction of the pumping well (monitoring well WP3), but also in the opposite direction (monitoring wells WP2 and WP4). Good calibration of the tracer breakthrough curves at wells WP2 and WP3 should be adequate for our subsequent virus transport analysis. The breakthrough curves for MS2 at WP1 and WP4 were not analyzed because of the limited number of measurements at these wells.

**Table 8** Parameter values for MS2 breakthrough curves for the deep well injection experiment.

Model	$\mu_l$	$\mu_s$	$k_{att1}$	$k_{det1}$	$k_{att2}$	$k_{det2}$	SSQ
One-site (2 wells)	0.024*	0.163 $\pm 0.0812$	6.276 $\pm 0.597$	0.0165 $\pm 0.0206$			0.672
Two-site (2 wells)	0.024*	0.0551 $\pm 0.438$	4.91 $\pm 5.30$	0.00170 $\pm 0.0143$	1.68 $\pm 6.12$	0.479 $\pm 2.01$	0.599
One-site (1st well)	0.024*	0.112 $\pm 0.0487$	5.85 $\pm 0.187$	0.00278 $\pm 0.00210$			0.0789
One-site (2nd well)	0.024*	0.121 $\pm 0.065$	2.49 $\pm 0.060$	0.000366 $\pm 0.00050$			0.0690

\*Parameter fixed.

### 8.5.2 Analysis of Virus Transport

Calibrated value of the longitudinal dispersivity and the independently determined saturated hydraulic conductivity and porosity were used as starting points of the virus transport analyses. Again, both one-site and two-site kinetic sorption models were used in the analyses of the MS2 breakthrough curves at wells WP2 and WP3. Optimization results for both models are given in Table 8 and in Figures 13 and 14. In one set of optimization runs we assumed that the transport parameters are constant throughout the subsurface (Figure 13). In the second set of optimization runs we allowed the immobilization, attachment, and detachment coefficients to be different in the direction of each well (Figure 14). The second set of optimizations we ran only for the one-site kinetic sorption model.

Similarly as for the dune recharge study, the two-site model performs better than the one-site model in predicting the measured MS2 concentrations, both in terms of the peak concentration and subsequent declining concentrations (Figure 13). Also, similarly as for the dune recharge study, the sum of the attachment coefficients  $k_{att1}$  and  $k_{att2}$  for the two-site model is approximately equal to the attachment coefficient  $k_{att1}$  for the one-site model. Attachment to the type-2 sites is again significantly slower than attachment to the type-1 sites, with detachment from the type-2 sites faster than that from the type-1 sites. This leads to much larger residence time for MS2 on the type-1 sites and more MS2 becoming attached to these sites compared to sites-2. Thus, again, attachment to type-1 sites mainly determines virus removal. Because of the sparseness of MS2 data, the confidence of optimized parameters is relatively small, especially for the two-site model. The estimates of  $\mu_s$  from the one-site model are very high and likely an overestimation, whereas that from the two-site model approximates that of  $\mu_l$ . Possibly the value of  $\mu_s$  is very similar to that of  $\mu_l$ , because the tails of the breakthrough curves may be even flatter. This is indicated by the three to four observations that make up the later part of the tails.

Excellent agreement between measured and optimized MS2 concentrations was obtained when we allowed the immobilization, attachment, and detachment coefficients for the one-site kinetic sorption model to vary in the direction of each well (Figure 14). Obviously, this can be explained by the fact that WP3 (8 m) lies within the oxygen zone, whereas WP2 (12 m) lies outside this zone (Figure 2). Within the oxygen zone, favorable sites of ferric

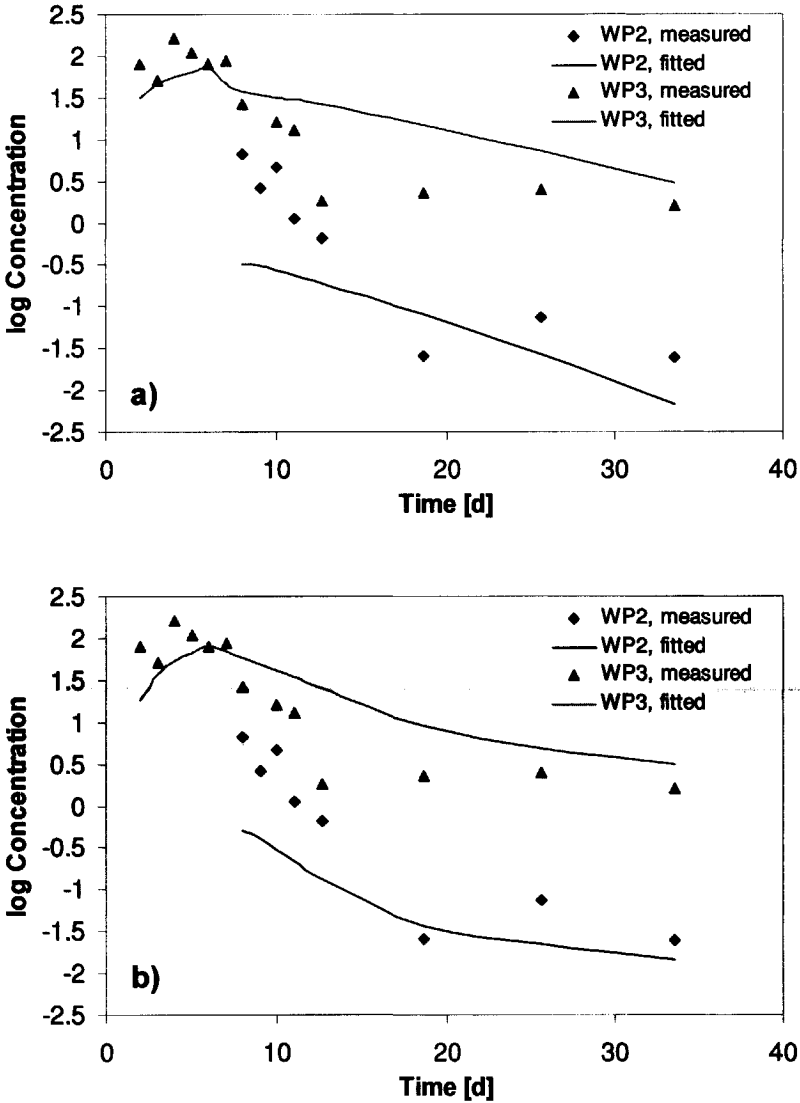


**Figure 13** Measured and optimized MS2 breakthrough curves at two observation wells for the deep well injection experiment assuming homogeneous subsurface. Two-dimensional one-site (a) and two-site (b) kinetic sorption models were used in the optimization.

oxyhydroxides are present, but not beyond that zone (Schijven *et al.*, 2000). The MS2 concentration data were, however, too sparse to fit parameters for the two-site kinetic sorption model with varying parameters in the two directions. Possibly, some improvement may be expected when assuming  $\mu_s$  is equal  $\mu_i$ .

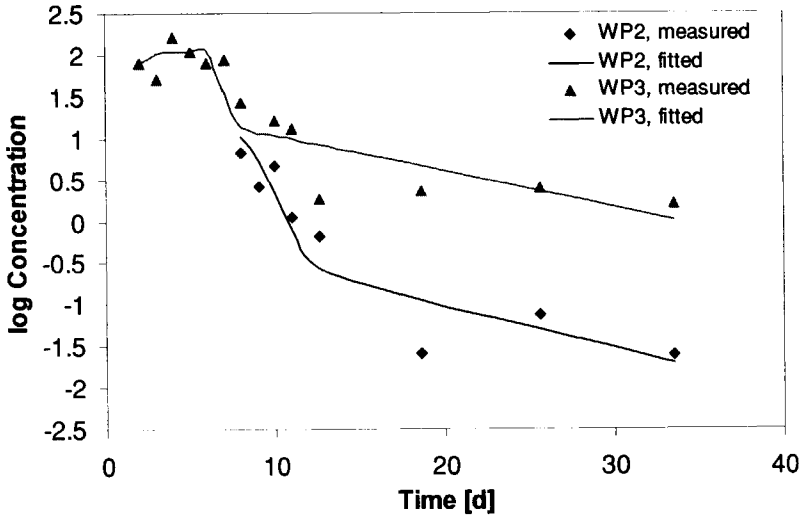


**Figure 14** Measured and optimized MS2 breakthrough curves at two observation wells for the deep well injection experiment assuming heterogeneous subsurface. Two-dimensional one-site kinetic sorption model was used in the optimization.

## 8.6 Concluding Remarks

We implemented a reversible two-site kinetic sorption model into the HYDRUS-1D and HYDRUS-2D numerical codes and used the resulting models to analyze the transport of MS2 and PRD phages in two field studies. Differences between the one- and two-dimensional modeling approaches, differences between the one- and two-site kinetic models, and the role of heterogeneities in the soil properties were investigated.

For the dune recharge experiment, the one-dimensional one-site model did not completely describe the tails of the measured breakthrough curves. While the one-dimensional one-site model predicted a sudden decrease in the virus concentrations immediately after their peaks, measured data displayed a relatively smooth transition of the declining limb to the later straight part of the tail. The one-dimensional two-site model fitted the course of the breakthrough curves very well. The two-dimensional one-site model predicted a more gradual decrease in the virus concentrations after their peaks than the one-dimensional one-site model, but not as good as the one-dimensional two-site model. Because the two-dimensional one-site sorption model could describe the measured breakthrough curves already reasonably well, the breakthrough curves did not provide enough information for successful estimation of two-site sorption parameters. Transverse dispersion seemed to partially explain features of the breakthrough curve that were thought to be the effects of a second type of kinetic sites when the one-dimensional model was used. Apparently, dimensionality of the problem can partly predict the smooth decrease in concentration after peak breakthrough. Still, the two-dimensional two-site model did provide better predictions of the breakthrough curves, partly due to the higher order of freedom (more fitted parameters) of the inverse solution. Values for  $k_{att2}$  and  $k_{des2}$  could not be determined at the larger distances from the source (third and fourth monitoring wells) using the two-

dimensional model, thus suggesting that either a second type of kinetic sites is present within the first few meters of dune passage, but not beyond the second monitoring well, or that effects of soil heterogeneity and dimensionality of the problem overshadowed this process. Variations between single collector efficiencies were relatively small, whereas collision efficiencies varied greatly. This implies that the nonlinear removal of MS2 and PRD1 is mainly caused by variations in interactions between grain and virus surfaces rather than by physical heterogeneity of the porous medium.

Similarly, a two-site model performed better than the one-site model in describing MS2 concentration for the deep well injection study. However, the concentration data were too sparse in this study to have much confidence in the fitted parameters.

### **Acknowledgements**

S. M. Hassanizadeh and M. Th. van Genuchten are greatly acknowledged for their expert comments.

## Chapter 9

# Virus Removal by Soil Passage at Field Scale and Groundwater Protection

Schijven, J. F. and Hassanizadeh, S.M. 2001. A procedure for predicting virus removal by soil passage. Groundwater. In preparation.

Schijven, J. F. and Hassanizadeh, S.M. 2001. Groundwater vulnerability to virus contamination in sandy aquifers: A worst case approach. Appl. Environ. Microbiol. In preparation.

**Abstract**

In the present study, theoretical and practical knowledge about virus removal in terms of process parameters and boundary conditions at field scale was summarized. The aims were to evaluate prediction of virus removal by soil passage as a treatment in drinking water production and prediction of a zone that allows 9 log<sub>10</sub>-protection of groundwater wells from virus contamination.

Removal rates of bacteriophages from field studies were summarized in order to identify some typical cases that can be used to predict virus removal by soil passage at sites under similar conditions. Virus removal can be interpreted as a function of collision efficiencies  $\alpha_\beta$  and  $\alpha_\lambda$ , inactivation rate coefficient  $\mu_1$ , rate parameter  $\gamma$ , pore water velocity  $v$ , porosity  $n$ , the grain size  $d_c$  and the water temperature. Initial high removal is determined by  $\alpha_\beta$ , which decreases exponentially at a rate  $\gamma$  to a constant base removal rate that is determined by  $\alpha_\lambda$  and  $\mu_1$ . Collision efficiencies  $\alpha_\beta$  and  $\alpha_\lambda$  depend on the fraction and nature of heterogeneously distributed patches of favorable sites for attachment.

In order to predict virus removal in a particular field situation, detailed knowledge about the soil properties is required, which may be obtained from geochemical analyses of soil samples and be supported by studying attachment of MS2 in column experiments.

Bacteriophage MS2 may be considered as a conservative tracer virus. Similarly, from analysis of different soil samples along a flow line, one may estimate  $\gamma$ . *E.g.*  $\gamma$  may be related to a decrease in dissolved oxygen with travel time. At higher pH, electrostatic repulsion between the surfaces of viruses and soil grains is higher, which is reflected by lower values of the collision efficiency. The collision efficiency of MS2 is assumed to decrease by a factor 0.9 for every increase in pH by one tenth.

As a first step in a vulnerability analysis of Dutch groundwater well systems to virus contamination, a hypothetical case was simulated to calculate the travel distance and time that are required for 9-log<sub>10</sub> protection against virus contamination. To that aim, a selection was made of phreatic aquifers in The Netherlands that were anoxic and the pH of the water was 7 or higher. These conditions may be as unfavorable for attachment as in the anoxic part of the aquifer from a deep well injection study, where the removal rate for bacteriophage MS2 was found to be 0.081 day<sup>-1</sup>, *i.e.* 0.024 day<sup>-1</sup> due to inactivation and 0.057 day<sup>-1</sup> due to attachment to the soil grains. This corresponds to a collision efficiency of  $1.5 \times 10^{-5}$ .

The same conditions may apply to many confined aquifers. Protection zones that assure virus removal of 9 log<sub>10</sub> were determined for this selection of phreatic aquifers, applying worst case values for the inactivation rate coefficient and collision efficiency for MS2. Virus was assumed to be originating from a sewage pipe lying at the groundwater table leaking continuously at rate of 1 m<sup>3</sup>.day<sup>-1</sup>. Virus concentration was found to be reduced by 3.1 to 4.0 log<sub>10</sub> at the abstraction well due to mixing. To account for an additional 5.0 to 5.9 log<sub>10</sub> removal of virus by attachment and inactivation, travel times of 209 to 442 days are needed, depending on abstraction rates, aquifer thickness and grain size of the sand. This is about three to seven times longer than the current guideline of 60 days. Only horizontal transport was considered, *i.e.* protective effects of confining layers and vertical transport through (un)saturated zones were not considered, but, on the other hand, leakage rates may be higher and concentrations of human pathogenic viruses in raw wastewater may possibly be higher too.

### 9.1 Removal Rates from Field Studies

In the present study, theoretical and practical knowledge about virus removal in terms of process parameters and boundary conditions at field scale was summarized. The aims were to evaluate prediction of virus removal by soil passage as a treatment in drinking water production and prediction of a zone that allows 9 log<sub>10</sub>-protection of groundwater wells from virus contamination.

Only relatively few well-defined field studies on virus removal by soil passage exist. In this section, removal data from these field studies as well as relevant conditions are summarized. The aim is to identify some typical cases that can be used to predict virus removal at other sites under similar conditions. As pointed out by Schijven and Hassanizadeh (2000), removal of virus often appears to be higher near the source than further away from the source. A high initial removal may be explained by special attachment sites that are present in the first meters of soil passage but rapidly decrease with travel distance or travel time in an exponential fashion, like sites formed by ferric oxyhydroxides in a deep well injection study (Schijven *et al.*, 2000), or by ferric oxyhydroxides and organic carbon in a dune recharge study (Schijven *et al.*, 2001a). Thus, under steady state conditions and assuming negligible dispersion, virus removal can be described by:

$$v \frac{dC}{dx} + [\beta \exp(-\gamma) + \lambda]C = 0 \quad (1)$$

where  $\beta$  is the maximum attachment rate coefficient to favorable attachment sites [T<sup>-1</sup>],  $\gamma$  is the rate coefficient with which the attachment rate decreases due to an exponential decrease in the number of attachment sites with travel time [T<sup>-1</sup>]. Parameter  $\lambda$  is the base removal rate coefficient due to attachment to a constant base level of attachment sites, and due to inactivation of viruses [T<sup>-1</sup>]. At low temperatures, inactivation is usually much slower than attachment.

After substituting  $dx = vdt$ , equation (1) has the following solution:

$$C = \exp\left[\frac{\beta}{\gamma} \exp(-\gamma) - \lambda\right] C^* \quad (2)$$

where,  $C^*$  is an integration constant.

Subject to boundary conditions  $C^* = C_0 \exp\left(-\frac{\beta}{\gamma}\right)$  at  $t = 0$ , where  $C_0$  is the initial virus concentration. Therefore, virus removal is described by:

$$\log_{10}(C/C_0) = \frac{1}{2.3} \left\{ \frac{\beta}{\gamma} [\exp(-\gamma) - 1] - \lambda \right\} \quad (3)$$

where,  $\log_{10}(C/C_0)$  defines removal.

At  $t = 0$ , the initially high removal rate  $\frac{d[\log_{10}(C/C_0)]}{dt}$  is determined by  $-\frac{1}{2.3}(\beta + \lambda)$ .

Equation (3) has been used to fit field data from Bales *et al.* (1995, 1997), Pieper *et al.* (1997), DeBorde *et al.* (1998, 1999), Ryan *et al.* (1999) and Schijven *et al.* (1998, 1999, 2000). The results are shown in Figures 1a – 1c. In most of these studies, removal of bacteriophages MS2 or PRD1 was measured. These bacteriophages represent low adsorbing negatively charged viruses (Schijven and Hassanizadeh, 2000; Chapter 7).

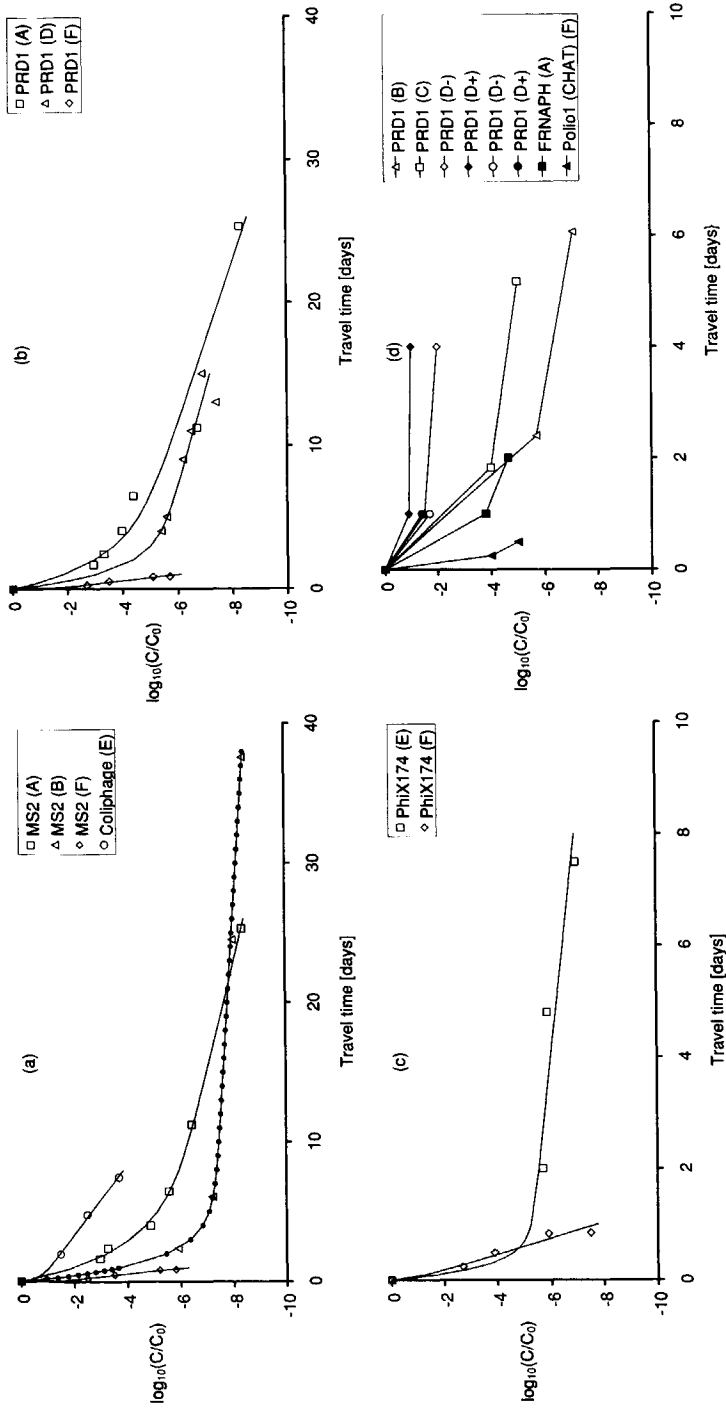
Values of parameters  $\beta$ ,  $\gamma$  and  $\lambda$  were found by fitting equation 1 to the field data and are listed in Table 1. Corresponding values of single collector efficiencies ( $\eta_\beta$  and  $\eta_\lambda$ ) and collision efficiencies ( $\alpha_\beta$  and  $\alpha_\lambda$ ) of the viruses were calculated applying equations (18) and (19) from Chapter 2. A default value of  $0.024 \text{ day}^{-1}$  for the inactivation rate coefficient  $\mu_i$  was applied in these calculations. This is the low value that was found for MS2 in the deep well injection study by Schijven *et al.* (2000). Table 2 gives hydrologic and chemical properties of the aquifers from the field studies. The aquifers are denoted A to F and are ordered according to grain size.

In some cases, only two to three measurements of removal with time were available (Bales *et al.*, 1997; Pieper *et al.*, 1997; DeBorde *et al.*, 1999; Ryan *et al.*, 1999; Schijven *et al.*, 1998, 2000). These removal data are shown in Figure 1d. For these data, equation (1) was not applied, but, for the sake of comparison, removal rates were calculated from the linear increase in time.

**Aquifer A** contains very fine dune sand. The initial removal rate was found to be strongly and positively correlated with soil organic carbon content and to a lesser extent with the content of ferric oxyhydroxides (Schijven *et al.*, 2001a). Due to the high pH, conditions for attachment are unfavorable, as evidenced by the low collision efficiencies.

**Aquifer B** contains fine sand. Initially, collision efficiency  $\alpha_\beta$ , and thus the initial removal rate, is higher than in aquifer A due to the presence of favorable attachment sites in the form of ferric oxyhydroxides together with a lower pH. However, collision efficiency  $\alpha_\lambda$  and the base removal rate coefficient  $\lambda$  in aquifer B are lower than that in aquifer A. This difference can be explained neither by the difference in pH nor by the difference in temperature. Higher pH is less favorable for attachment and at lower temperature the inactivation rate is lower. Therefore, there must be fewer sites for attachment in the anoxic part of aquifer B than in aquifer A. Eventually, 8- $\log_{10}$  removal was achieved in both aquifers.

The sand in aquifer C is coarser, but otherwise similar to A or B, but hydraulic conductivity is lower in C. Similar removal rates and collision efficiencies for PRD1 were found in aquifers B and C. The collision efficiencies for PRD1 in aquifer C were not calculated because data on grain size and temperature were not reported. However, collision efficiencies of 0.0028 – 0.003 at pH 7.4 and of 0.00085 – 0.0016 at pH 8.4 were reported by the investigators (Bales *et al.*, 1997). In aquifer C, pH is higher than in B. Probably, more favorable sites are available in aquifer C than initially in B.



Figures 1a – 1d. Removal of bacteriophages and poliovirus 1 in relation with travel time in sandy aquifers. See corresponding parameter values in Table 1 and aquifer properties in Table 2.

Table 1 Removal rate parameter values from field studies.

Figure	Virus	Aquifer	$\beta^a$	$\gamma$	$\lambda^a$	$\eta_B$	$\eta_A$	$\alpha_6$	$\alpha_5$	Reference
6a	MS2	A	5.0	0.43	0.30	0.61	0.57	$1.2 \times 10^{-3}$	$7.2 \times 10^{-5}$	Schijven <i>et al.</i> , 1999
	MS2	B	12	0.71	0.081	0.36	0.88	$2.6 \times 10^{-3}$	$1.5 \times 10^{-5}$	Schijven <i>et al.</i> , 2000
	MS2	F	6.4	2.5	12	0.10	0.10	$2.2 \times 10^{-2}$	$4.2 \times 10^{-3}$	DeBorde <i>et al.</i> , 1999
6b	Coliphages	E	15	9.8	0.92	0.25	0.25	$6.1 \times 10^{-2}$	$3.7 \times 10^{-3}$	DeBorde <i>et al.</i> , 1998
	PRD1	A	8.5	0.53	0.41	0.34	0.32	$3.8 \times 10^{-3}$	$6.9 \times 10^{-5}$	Schijven <i>et al.</i> , 1999
	PRD1	D-	9.9	0.88	0.35	0.20	0.26	$1.8 \times 10^{-2}$	$6.7 \times 10^{-4}$	Bales <i>et al.</i> , 1995
6c	PRD1	F	103	32	11	0.056	0.056	$6.7 \times 10^{-2}$	$6.9 \times 10^{-3}$	DeBorde <i>et al.</i> , 1999
	$\phi$ X174	E	129	11	0.56	0.25	0.25	$5.2 \times 10^{-1}$	$2.2 \times 10^{-3}$	DeBorde <i>et al.</i> , 1998
	$\phi$ X174	F	0.62	0	18	0.10	0.10	$2.4 \times 10^{-4}$	$6.6 \times 10^{-3}$	DeBorde <i>et al.</i> , 1999
6d			$\lambda_1^a$	$\lambda_2^a$	$\eta_1$	$\eta_2$	$\alpha_1$	$\alpha_2$		
	PRD1	B	5.5	0.87	0.20	0.45	$2.1 \times 10^{-3}$	$2.1 \times 10^{-4}$		Schijven <i>et al.</i> 2000
	PRD1	C	5.1	0.69						Bales <i>et al.</i> , 1997
	PRD1	D-	3.5	0.39	0.26	0.26	$7.3 \times 10^{-3}$	$7.8 \times 10^{-4}$		Pieper <i>et al.</i> , 1997
	PRD1	D+	2.1	0.076	0.26	0.26	$4.4 \times 10^{-3}$	$1.0 \times 10^{-6}$		Pieper <i>et al.</i> , 1997
	PRD1	D-	3.9		0.26		$8.1 \times 10^{-3}$			Ryan <i>et al.</i> , 1999
	PRD1	D+	3.2		0.26		$6.7 \times 10^{-3}$			Ryan <i>et al.</i> , 1999
FRNAPH's <sup>b</sup>	A	8.7	1.9						Schijven <i>et al.</i> 1998	
	Polio 1	F	37	9.2	0.10	0.10	$1.3 \times 10^{-2}$	$3.3 \times 10^{-3}$		Deborde <i>et al.</i> , 1999

<sup>a</sup>Parameter values  $\beta$ ,  $\gamma$  and  $\lambda$  were estimated by applying equation (1);  $\lambda_1$  and  $\lambda_2$  were calculated from the increase in removal in time between to adjacent points in time; dimension of  $\gamma$ ,  $\lambda$ ,  $\lambda_1$  and  $\lambda_2$  is day<sup>-1</sup>; parameter  $\beta$  is dimensionless. <sup>b</sup>F-specific RNA-bacteriophages

**Table 2.** *Hydrologic and chemical properties of the studied sandy aquifers (A - F)<sup>a</sup>*

	A	B	C	D <sup>+</sup> <sup>b</sup>	D <sup>-</sup> <sup>b</sup>	E	F
Grain size (mm)	0.20-0.24	0.27	fine to medium	0.5	0.5	2.4	1.25-12
Porosity	0.35	0.32	0.3	0.39	0.39	0.2	0.15
Clay %	0.5-0.8	0.9	0-15	<1	<1		
Silt %	1-4	1.1					
Sand %	95-98	98		>99	>99		
Gravel %	0	0					
Hydraulic conductivity (m.d <sup>-1</sup> )	12	25	6	110	110	240-300	900-13800
Pore water velocity (m.d <sup>-1</sup> )	1.2-2	1	1.9	0.2-1	0.2-1	1-2.9	27
foc %	0.1-0.4	0.17	0.03	1	<0.01		
Surface Fe (III) (g.kg <sup>-1</sup> )	0.7-1.7			0.20	0.26		
PH	7.3-8.3	6.6-6.8	7.4-7.5	5.8-6.7	5-5.8	6-6.4	7.2
EC	900	450		250-450	30-100	300-800	288
Temp	2-5	12		15	16	9-12	10.3
Dissolved oxygen (mg.l <sup>-1</sup> )	1.1-9.7	10 → <0.5		0-0.5	4.5-11		3.5
Nitrate (mM)		0.31 → <0.008		0.3	<0.01		
Sulfate (mM)		0.65 → 0.40		0.36	0.085		
Bicarbonate (mM)	2.4-2.8	5.6-6.2		0.64	0.028		
DOC (mg.l <sup>-1</sup> )	1.5-2.4	0.55		2-4.4	0.3-1		
Ca <sup>2+</sup> (mM)	2.2-2.3	1.7-2		0.21	0.028		
Mg <sup>2+</sup> (mM)	0.52-0.63	0.36-0.53		0.13	0.037		

<sup>a</sup>See Table 1 for references. <sup>b</sup>D<sup>+</sup> and D<sup>-</sup>: the same aquifer, but D<sup>+</sup> is a sewage contaminated zone, whereas D<sup>-</sup> is an uncontaminated zone.

The sand of aquifer D is also coarser than in A or B, and the hydraulic conductivity is much higher. Aquifer D consists of a sewage contaminated (D+) and uncontaminated zone (D-). In D+, organic matter occupies favorable attachment sites. Nevertheless, similar collision efficiencies for PRD1 were reported in aquifer D+ as in A and C. But, removal rates in D+ are lower than in A or C due to a combination of a lower transport velocity and coarser sand, leading to lower values of the single collector efficiency (fewer collisions). Organic matter limits attachment in D+ by occupying attachment sites, whereas a higher pH is the limiting factor in A and C. In aquifer D-, removal rates and collision efficiencies are higher than in aquifer D+, because in D-, attachment sites are not blocked by organic matter. The sand in aquifer E is coarse, the hydraulic conductivity and pore water velocity are higher. The initial removal rate of coliphages is similar to that of MS2 in B, but the base removal rate is ten times higher in E compared to that in B. The initial removal of  $\phi X174$  in aquifer E is very high, but its base removal rate is only about twice that of MS2 in aquifer A. Bacteriophage  $\phi X174$  is expected to attach much more than MS2 because its surface charge is less negative than that of MS2. The relatively low base removal rates in aquifer E are probably due to the coarseness of the soil, which lead to low single collector efficiencies.

In aquifer F, we have the coarsest sand and, by far, the highest hydraulic conductivity and pore water velocity. In aquifer F we find the highest removal rates. This is also reflected by the relatively high collision efficiencies, suggesting the presence of favorable attachment sites.

From the data shown in Figures 1a and 1b, it is possible to identify a worst case situation, *i.e.* where interaction with the soil grains is very low, due to the absence or blocking of preferable sites for attachment. In aquifers B and D+, very low base removal rates of  $0.08 \text{ day}^{-1}$  were found for MS2 and PRD1, respectively. In aquifer B, the low removal rate of MS2 took place in the anoxic part of the aquifer with few sites for attachment. In aquifer D+, attachment of PRD1 was limited due to the presence of organic matter occupying attachment sites. This latter condition may represent a situation of virus contamination from a wastewater source.

To conclude, pH and the presence of favorable sites for attachment seem to be the major factors determining attachment of virus to the soil grains. This is in line with observations by Elimelech *et al.* (2000), where pH together with the presence of heterogeneously distributed patches of iron oxide coatings were found to be the key factors in determining attachment of colloids to soil. In this study, differences in ionic strength were found to be of little importance. Ionic strengths in aquifers A to F are generally low, *i.e.* in the order of  $10^{-2} \text{ M}$ , therefore, possible effects of different ionic strengths may be neglected.

One may now raise the question, whether it is possible to predict virus removal in a particular field situation.

Here, virus removal is presented as a function of collision efficiencies  $\alpha_{\beta}$  and  $\alpha_{\lambda}$ , inactivation rate coefficient  $\mu_i$ , rate parameter  $\gamma$ , pore water velocity  $v$ , porosity  $n$ , the grain size  $d_c$  and the water temperature. Collision efficiencies are linearly dependent on the fraction of heterogeneously distributed patches of favorable sites for attachment (Elimelech *et al.*, 2000). In the case of 100% coating with favorable sites,  $\alpha$  is equal to one. Thus, collision efficiencies  $\alpha_{\beta}$  and  $\alpha_{\lambda}$  are both determined by the fraction and nature of favorable attachment sites that are present. This requires detailed knowledge about the soil properties that may be obtained from geochemical analyses of soil samples and be supported by

studying attachment of MS2 in column experiments. Similarly, from analysis of different soil samples along a flow line, one may estimate  $\gamma$ . *E.g.*  $\gamma$  may be related to a decrease in dissolved oxygen with travel time.

At higher pH, electrostatic repulsion between the surfaces of viruses and soil grains is higher, which is reflected by lower values of the collision efficiency. The decrease in collision efficiency of MS2 due to an increase in pH can be derived from the data from the column studies by Bales *et al.* (1991, 1993), Kinoshita *et al.* (1993) and Penrod *et al.* (1996): In the pH range of 3.5 to 7,  $\alpha$  decreases by a factor 0.9 for every increase in pH by 0.1. *E.g.* pH in aquifer A is 2 units higher than in aquifer B. This suggests that the collision efficiency of PRD1 would be about ten times lower in aquifer A, assuming the same dependency of the collision efficiency of PRD1 on pH as MS2. Indeed, collision efficiencies of PRD1 are about ten times lower in aquifer A than in aquifer D-. But ferric oxyhydroxides in aquifer A may be a factor of five higher than in aquifer B, which suggests that collision efficiencies in A should be five times higher due to the presence of more favorable sites. Possibly, the surface iron, as it is presented here, is not directly comparable between the two aquifers, because different methods of analysis were applied. In Table 2, only the soil in these two aquifers was analyzed for the presence of ferric oxyhydroxides, so information on the presence of favorable sites in aquifers from field studies is very limited. In the deep well injection study by Schijven *et al.* (2000), where initial high removal could be explained by the presence of sites of ferric oxyhydroxides due to pyrite oxidation, no quantitative information was available about the amount of favorable sites. But, if for a given site, the fraction of favorable sites as a function of travel time is known, and pH, grain size, porosity and temperature are known, one should be able to derive values for  $\beta$ ,  $\gamma$  and  $\lambda$ . Then, by applying equation (3) one can calculate (non-linear) removal of MS2 as a function of travel time. Of course, in the case of similar situations as the well characterized dune recharge site (Schijven *et al.*, 1999) and deep well injection site (Schijven *et al.*, 2000), one may also reasonably assume that removal rates are the same as at these sites.

## 9.2 Protection of Groundwater Well Systems

As a first step in a vulnerability analysis of Dutch groundwater well systems to virus contamination, the following hypothetical case was simulated to calculate the travel distance and time that are required for sufficient protection against virus contamination: Water is abstracted continuously from a phreatic aquifer. At a distance  $R$  from the abstraction well and right at the groundwater table, a sewage pipe is continuously leaking and thus contaminating the groundwater with viruses. We assume that a steady state condition has been reached. In this case, only horizontal transport in the direction of the abstraction well is considered. A leaking sewage pipe below the groundwater table would not leak sewage water, but drain the groundwater. Protective effects of confining layers and of vertical transport through (un)saturated layers are not considered. This is in line with the current guidelines (CBW, 1980). According to these guidelines, no activities other than water abstraction are allowed within the protection area that is delineated by a groundwater travel time of 60 days. The protective effects of confining or semi-permeable layers are not considered, because local differences in the thickness of confining layers due to irregularities and effects of erosion are regarded as a considerable source of uncertainty for protection.

Under steady state conditions, virus transport is described by:

$$\frac{dC}{dr} - \alpha_L \frac{d^2C}{dr^2} + \frac{\lambda}{v} C = 0 \quad (4)$$

where,  $C$  is the concentration of virus [ $L^{-3}$ ],  $r$  is the distance from the well [ $L$ ] and  $\alpha_L$  is the dispersivity [ $L$ ]. Detachment is neglected, because it is usually much slower than attachment. Attachment to a second type of site is not considered, because it only has a minor contribution to removal (Schijven *et al.*, 2001b). This means that removal rate coefficient  $\lambda = k_{att} + \mu_1$  [ $T^{-1}$ ], where  $k_{att}$  is the attachment rate coefficient [ $T^{-1}$ ] and  $\mu_1$  is the inactivation rate coefficient of free viruses [ $T^{-1}$ ].

Pore water velocity  $v$  [ $LT^{-1}$ ] increases in the direction of the abstraction well according to:

$$v = -\frac{Q}{2\pi nr} \quad (5)$$

where  $Q$  is the abstraction rate [ $L^3T^{-1}$ ],  $n$  is the porosity and  $h$  is the aquifer thickness [ $L$ ].

According to colloid filtration (Yao *et al.*, 1971), the attachment rate coefficient  $k_{att}$  can be calculated as follows:

$$k_{att} = \frac{3(1-n)}{2} \frac{\alpha A_s^{1/3}}{d_c} \left( \frac{D_{BM}}{d_c n v} \right)^{2/3} v \quad (6)$$

where,  $d_c$  is the average diameter of the single collector (soil grain), [ $L$ ] and  $\alpha$  is the collision efficiency.  $A_s = 2(1-\gamma^5)/(2-3\gamma+3\gamma^5-2\gamma^6)$  is Happel's porosity dependent parameter, with  $\gamma = (1-n)^{1/3}$ .  $D_{BM} = K_B(T+273)/(3\pi d_p \mu)$  is the diffusion coefficient, [ $L^2T^{-1}$ ];  $K_B = 1.38 \times 10^{-23}$  is the Boltzmann constant [ $J.K^{-1}$ ];  $T$  is the water temperature [ $^{\circ}C$ ];  $d_p$  is the virus particle size [ $L$ ];  $\mu$  is the dynamic viscosity [ $ML^{-1}T^{-1}$ ];

Substitution of equations (5) and (6) into (4) gives:

$$\frac{dC}{dr} - \alpha_L \frac{d^2C}{dr^2} - (k_1 r^{2/3} + k_2 r) C = 0 \quad (7)$$

where,  $k_1 = \frac{3(1-n)}{2} \frac{\alpha A_s^{1/3}}{d_c} \left( \frac{D_{BM} 2\pi h}{d_c Q} \right)^{2/3}$  and  $k_2 = \frac{2\pi n h}{Q} \mu_1$ .

As an extra simplification, dispersion will be neglected. This is justified by the low dispersion that was found in the sandy aquifers A and B (Chapters 4 and 5). Thus, equation (7) has the following analytical solution:

$$\ln(C) = \frac{3}{5}k_1r^{5/3} + \frac{1}{2}k_2r^2 + C^* \quad (8)$$

Where,  $C^*$  is an integration constant.

Subject to boundary conditions  $C_R = C_0 \frac{q}{Q_R}$  at  $r = R$ , where  $C_0$  is the initial virus

concentration in the sewage pipe [ $L^{-3}$ ],  $C_R$  is the virus concentration in the aquifer at  $R$  [ $L^{-3}$ ],  $q$  is the leakage rate of sewage water [ $L^3T^{-1}$ ], and  $Q_R$  is the flow rate in the aquifer at  $R$  [ $L^3T^{-1}$ ]. It is assumed that virus attachment is not affected by the size of the hole through which viruses are leaking. Therefore, the virus concentration at  $R$  is described by:

$$\ln(C_R) = \frac{3}{5}k_1R^{5/3} + \frac{1}{2}k_2R^2 + C^* \quad (9)$$

Subject to boundary conditions  $C_A = C_W \frac{Q_R}{Q_A}$  at  $r = W$ , where  $C_A$  is the virus concentration in

the abstracted water [ $L^{-3}$ ],  $C_W$  is the virus concentration at  $W$  [ $L^{-3}$ ],  $W$  is the radius of the well [ $L$ ], and  $Q_A$  is the abstraction rate [ $L^3T^{-1}$ ]. The virus concentration at  $W$  is described by:

$$\ln(C_W) = \frac{3}{5}k_1W^{5/3} + \frac{1}{2}k_2W^2 + C^* \quad (10)$$

By substitution of boundary conditions, subtracting equation (9) from (10), and neglecting  $W$ , because  $W \ll R$  one obtains the equation for calculating virus removal:

$$\log_{10}\left(\frac{C_A}{C_0}\right) = -\frac{1}{2.3}\left(\frac{3}{5}k_1R^{5/3} + \frac{1}{2}k_2R^2\right) + \log_{10}\left(\frac{q}{Q_A}\right) \quad (11)$$

Where, removal is described by attachment to the soil grains (first right term), by inactivation (second right term), and dilution (third right term).

A selection was made of 16 Dutch groundwater well systems located in phreatic sandy aquifers where the screens of the production wells are at a depth of less than 25 m (REGWAT, 1989). From these aquifers, a subset of ten aquifers was selected, in which pH of the abstracted water is 7 or higher and levels of dissolved oxygen and nitrate are less than 0.5 mg.l<sup>-1</sup>. In addition, it was assumed that no pyrite is present. Under these conditions, one may assume that preferential sites for attachment of viruses are absent. The absence of confining layers together with the shallowness of the aquifers and unfavorable conditions for attachment make it a reasonable assumption qualifying these groundwater well systems as relatively vulnerable.

The water quality data as well as the aquifer properties of the ten selected aquifers – denoted Aq1 to Aq10 – are listed in Table 3 (Pastoors, 1992; REWAB, 2000). The water quality data are averages, minimum and maximum values over the period 1991 – 1999 (REWAB, 2000). Sulfate content of the abstracted water from all these aquifers is higher

than 0.009 mM. Thus, together with the low oxygen and nitrate levels, these aquifers can be designated as anoxic (Stuyfzand and Lüers, 1996). As it appears, the conditions in aquifers Aq1 to Aq10 may be equally unfavorable for attachment as in the anoxic part of aquifer B, which was qualified in the previous section as a worst case situation for virus removal. Note that many deeper aquifers with confining layers are also anoxic, and pH of the water is approximately 7 (REWAB, 2000).

For the anoxic part of aquifer B, the removal rate coefficient  $\lambda$  for bacteriophage MS2 was found to be  $0.081 \text{ day}^{-1}$ . In the corresponding field study (Schijven *et al.*, 2000), a value of  $0.024 \text{ day}^{-1}$  for  $\mu_1$  of MS2 was measured at the monitoring well at 8 m, near the outer limits of the oxic zone. Thus, a value of  $k_{att}$  equal to  $0.057 \text{ day}^{-1}$ , and a value of the collision efficiency equal to  $1.5 \times 10^{-5}$  can be estimated. In this situation, the contributions of attachment and inactivation to removal of MS2 are similar. MS2 may be considered here as a worst case virus tracer, *i.e.* it attaches less to soil than most viruses. A value of  $\mu_1$  equal to  $0.024 \text{ day}^{-1}$  for MS2 in groundwater at  $12^\circ\text{C}$  is low and similar to that of several human pathogenic viruses in groundwater at  $10^\circ\text{C}$  (see Schijven and Hassanizadeh, 2000 for an overview). Moreover, the flat tails of the breakthrough curves of MS2 in the field study by Schijven *et al.* (2000) suggest that inactivation of MS2 may even be lower further downstream into the anoxic part of the aquifer. If so, the contribution of attachment was higher. Sewage water has a high content of dissolved organic matter, which may compete with viruses for the same attachment sites, and thus limit attachment of virus. This effect is not considered

In domestic wastewater at two large sewage treatment plants in The Netherlands, geometric mean concentrations of 34 and 190 enteroviruses per liter were found (Hoogenboezem *et al.*, 2000) and at another sewage treatment plant 250 enteroviruses per liter (Lodder *et al.*, 2001). Based on an infection risk of 1 per  $10^4$  persons per year and assuming rotavirus infectivity, the maximum allowable concentration level of viruses at the abstraction well would be  $1.8 \times 10^{-7}$  viruses per liter (Regli *et al.*, 1991). This implies that virus concentrations in domestic wastewater from a leaking pipe should be reduced by  $9 \log_{10}$  at the point of groundwater abstraction. In the studies by Lodder *et al.* (1999, 2001), concentrations of NLV viruses in raw wastewater at a sewage treatment plant in The Netherlands were in the order of  $10^4$  to  $10^6$  RNA-containing particles per liter as determined by PCR. NLV are the most common viral pathogens with epidemic gastroenteritis in adults (Kapikian *et al.*, 1996). The concentrations of infectious Norwalk-like Caliciviruses are probably much lower. However, it is possible that concentrations of infectious human pathogenic viruses in domestic wastewater are significantly higher than 200 viruses per liter, implying that virus removal by more than  $9 \log_{10}$  is needed for NLV.

Currently, no information on leakage rates is available (R. Hermans, RIONED, pers. comm.). In this hypothetical case, a leakage rate  $q$  of  $1 \text{ m}^3 \cdot \text{day}^{-1}$  was assumed. Such a low leakage rate may remain unnoticed for quite some time.

**Table 3** Hydrologic and chemical properties of selected Dutch phreatic aquifers (Aq1 –Aq10). (Pastoors, 1992; REWAB, 2000)

	Aq1	Aq2	Aq3	Aq4	Aq5	Aq6	Aq7	Aq8	Aq9	Aq10
Grain size [mm]	0.50 <sup>a</sup>	0.50 <sup>a</sup>	0.25 <sup>b</sup>	0.25 <sup>b</sup>	0.50 <sup>a</sup>	0.50 <sup>a,c</sup>	0.50 <sup>a,c</sup>	0.25 <sup>b,c</sup>	0.25 <sup>b</sup>	0.25 <sup>b,d</sup>
Hydraulic conductivity [m.d <sup>-1</sup> ]	10-40	30	-	-	35	30	30	15	Low	Low
pH	7.0	7.2	7.3	7.4	7.3	7.1	7.1	7.2	8.0	7.2
EC [ $\mu$ S.cm <sup>-1</sup> ]	478	212	572	485	657	624	808	740	549	615
Temperature [°C]	13.6	10.6	10.9	10.7	10.1	10.5	10.7	10.5	10.0	9.8
Dissolved oxygen [mg.l <sup>-1</sup> ]	<0.50	<0.50	<0.50	<0.50	<0.35	<0.44	<0.50	0.20	0.35	0.46
Nitrate [mM]	<0.061	0.21	0.49	0.44	0.076	<0.0037	<0.0047	<0.0068	<0.0037	<0.011
Sulfate [mM]	0.33	0.27	0.60	0.51	0.79	0.45	0.99	0.53	0.36	1.0
Bicarbonate [mM]	4.8	1.1	5.0	4.4	5.3	5.5	6.5	5.2	2.6	3.8
DOC [mg.l <sup>-1</sup> ]	-	-	-	-	3.8	5.3	6.1	1.9	-	3.6
Ca2+ [mM]	2.3	0.71	3.3	2.9	3.0	2.7	3.5	2.8	1.5	2.3
Mg2+ [mM]	0.42	0.20	0.25	0.12	0.37	0.43	0.48	0.56	0.33	0.46
$\alpha \times 10^{-06}$	12	9.8	8.9	8.0	8.9	11	11	9.8	4.2	9.8
Q [m <sup>3</sup> .day <sup>-1</sup> ]	8219	3096	-	-	1781	1370	8219	9589	-	4658
h [m]	Variable	30	10-20	10-20	25	23	20	25	20	20
log <sub>10</sub> (Q/q)	3.9	3.5	-	-	3.3	3.1	3.9	4.0	-	3.7
9 – log <sub>10</sub> (Q/q)	5.1	5.5	-	-	5.7	5.9	5.1	5.0	-	5.3
t <sub>T</sub> [days]	-	408	-	-	442	434	342	209	-	235
s <sub>S</sub> [m]	-	196	-	-	169	153	357	270	-	223

Porosity is 0.35 (default value). <sup>a</sup>Moderately coarse sand, low silt content. <sup>b</sup>Relatively fine sand, silt containing. <sup>c</sup>Many thin clay-layers.

<sup>d</sup>Clayey on top of the aquifer. <sup>e</sup>Collision efficiency is  $1.5 \times 10^{-5}$  at pH 6.8, and is lowered by a factor 0.9 for each 0.1 pH higher. Inactivation rate coefficient is 0.039 day<sup>-1</sup>. <sup>f</sup>T is travel time and <sup>g</sup>S is setback distance of 9 log<sub>10</sub>-protection zone.

From equation (9), and applying the values of the collision efficiency and inactivation rate coefficient for MS2 as found in aquifer B, required travel times and setback distances that assure  $9 \log_{10}$  removal were calculated for six of the selected phreatic aquifers. For the other four aquifers, data on the aquifer thickness or the abstraction rate were not known. The results are also listed in Table 3. Figures 2a and 2b show removal as a function of travel time and distance, respectively. Depending on the abstraction rate, the dilution factor varies between 3.1 and  $4.0 \log_{10}$ , therefore an additional 5.0 to  $5.9 \log_{10}$  removal of virus is needed. To achieve this, travel times of 209 to 442 days are needed, depending on abstraction rates, aquifer thickness and grain size of the sand. As can be seen in Figure 2a, removal rates are higher in Aq8 and Aq10 than in the other aquifers due to the finer sand. At a higher transport velocity, removal with distance is less, but this is partly compensated by a higher dilution factor (Figure 2b). Based on these simulations, one may conclude that the current guideline of a 60-days travel time is inadequate, and that travel times of about three to seven times the current guideline are needed for sufficient protection against virus contamination.

Currently, all provinces in The Netherlands employ the 60-days travel time, except for Gelderland and Zeeland, where a travel time of one year is employed, and Flevoland, where a travel distance of 200 m is employed (Eck and Huisman, 1990).

Major factors that determine the size of the protection zone are virus attachment to the solid medium, virus inactivation, leakage rate, and the maximum allowable virus concentration in drinking water. Worst case assumptions concerning virus attachment and inactivation were based on observed behavior of bacteriophage MS2 and may be considered reasonable. Of course, in particular cases, attachment may be greater, *e.g.* where preferential sites in the form of ferric oxyhydroxides are available. Possibly, attachment is also affected by the calcium-ion content of the water, which appears to vary a factor of four. Local effects of organic matter on virus attachment were not considered either. This implies that investigation of aquifer and soil properties in more detail may be worthwhile. Moreover, spatial variation of water quality data of the abstracted water may also be taken into consideration.

The worst case depicted here may be even worse, because of higher leakage rates and the possibility of higher concentrations of pathogenic viruses in raw wastewater. But these worsening factors may already have been compensated by protective effects of confining layers and vertical transport through (un)saturated zones.

Future studies on vulnerability of groundwater wells to virus contamination should include investigating the frequency, probability and extent of leakage rates. The physical and chemical characteristics of the porous medium should be studied in more detail in order to evaluate the extent of virus attachment. Finally, effects of confining layers and vertical transport through (un)saturated zones may also be taken into consideration.

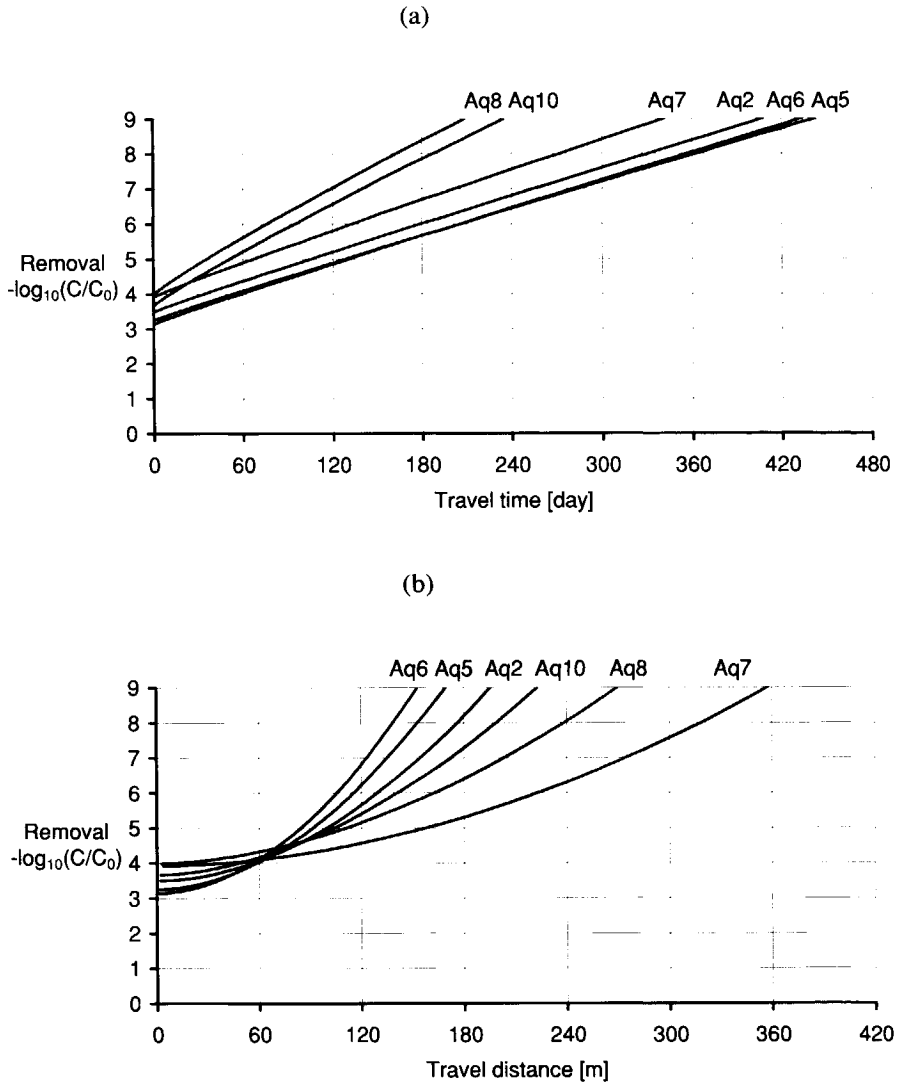


**Figure 2** Virus removal in six phreatic aquifers as a function of travel time (a) and travel distance (b).

Compared to the removal capabilities of sandy aquifers, removal of viruses in karst, fractured bedrock and gravel aquifers may be lower. Such aquifers are identified as sensitive to fecal contamination by the US EPA's proposed Ground Water Rule (EPA, 2000). These aquifers have in common that more permeable pathways exist that allow very high flow rates of viruses (Rossi *et al.*, 1994; Paul *et al.*, 1995, 1997). In such pathways, the single collector efficiency will be very low, and consequently, there will be little attachment. Due to the high transport rate, inactivation will also be minimal. In gravel, removal of slug-injected bacteriophages T7 and H40/1 was only 2  $\log_{10}$  over a travel distance of 50 meters (Rossi, 1994; Rossi *et al.*, 1994). But this is about the same removal rate as for MS2 in a sandy anoxic aquifer. In fact, T7 and H40/1 were probably removed more effectively than MS2, considering the coarseness of gravel. Even, considerable removal may be found in fractured rock, *e.g.* about 6- $\log_{10}$  removal of MS2 over a distance of 20 m in limestone (Paul *et al.*, 1997) or 1- $\log_{10}$  removal of MS2 and PRD1 over a distance of 0.5 m in a clay-rich till (Hinsby *et al.*, 1996). Nevertheless, it is obvious that preferred pathways, like fractures and breaches, will contribute greatly to the uncertainty in the removal capabilities of a certain aquifer.

In The Netherlands, this condition is not very relevant, except for karst aquifers in the south of Limburg and in Twente with water flow velocities of 10 – 100  $\text{m}\cdot\text{day}^{-1}$  (CBW, 1980). Due to the high uncertainties that are introduced by the presence of preferred pathways, tracer studies at field scale may be needed.

### Acknowledgements

G. van Drecht, C.R. Meinardi, J.H.C. Mülschlegel and M.J.H. Pastoors are greatly acknowledged for fruitful discussions and expert comments. P. Cleij, C.R. Meinardi, J.H.C. Mülschlegel and M.J.H. Pastoors are also highly acknowledged for providing hydrologic and water quality data.

# **Summary, Conclusions and Recommendations**

## Virus Removal From Groundwater by Soil Passage Modeling, Field and Laboratory Experiments

Jack Schijven

### Summary, conclusions and recommendations

#### Scope and objectives

In The Netherlands, about two-thirds of all drinking water is delivered from groundwater and one-third from surface water. About 39% of the surface water, which is used for drinking water production, is treated by soil passage, like in riverbank filtration and in dune recharge with pretreated surface water.

Groundwater may become contaminated with viral, bacterial and protozoan pathogens from fecally contaminated water, e.g. from artificially recharged surface water, septic tanks or leaking sewage pipes. Surface water is contaminated with pathogenic microorganisms, mainly due to discharges of wastewater and by manure run-off from agricultural land.

For many decades, no data on waterborne disease have been associated with fecal contamination of (artificial) groundwater in The Netherlands. However, pathogens like enteric viruses and the pathogenic protozoa *Cryptosporidium* and *Giardia* are ubiquitously present in the Dutch surface waters. Therefore, adequate treatment of surface water, which is used as the source for drinking water production, must be guaranteed under all circumstances.

Groundwater, not from artificial recharge, can be protected from contamination with pathogenic microorganisms by applying adequate setback distances between sources of contamination and production wells using the soil as a barrier. Surface water can be treated effectively to remove pathogens by means of passage through the subsurface, provided travel times and travel distances are adequate. According to current guidelines a travel time of at least 60 days is required at wellhead protection areas. For riverbank filtration the travel time varies between 0.5 and 30 years and for artificial recharge of pretreated surface water between 35 and 135 days. The travel time of 60 days is assumed to be adequate to inactivate pathogenic bacteria to the degree that no health risk exists. However, for decades, viruses and, more recently, protozoa have been recognized as pathogens of major health concern. Due to their persistence in the environment and their infectivity, enteric viruses and the pathogenic protozoa *Cryptosporidium* and *Giardia* may be considered as the most critical waterborne pathogens for drinking water production. Because of this environmental persistence, a travel time of 60 days may be too short for sufficient inactivation of viruses and pathogenic protozoa. On the other hand, attachment to the soil grains during soil passage may contribute significantly to their removal.

This raises the question to what extent the hygienic quality of drinking water is guaranteed.

In 2001, a different policy for production of safe drinking water in The Netherlands has been incorporated into legislation. This approach is based on a maximum acceptable infection risk of one per 10 000 persons per year associated with drinking water consumption and dose-response relationships for pathogens and has resulted in using

maximum allowable concentrations in drinking water. In the case of viruses, the maximum allowable concentration is  $1.8 \times 10^{-7}$  viruses per liter, which is based on the dose response relationship of rotavirus and poliovirus 3, as a worst-case. This implies that virus concentrations in surface water need to be reduced 5 to 8  $\log_{10}$  in order to produce drinking water in which maximum allowable concentrations are not exceeded. This raises the question what travel times and travel distances are needed to achieve such reductions by soil passage.

Compliance with these maximum allowable concentrations can only be assessed by analysis of very large volumes of drinking water, *i.e.* in the order of  $10^5 - 10^7$  liters. This is considered to be impracticable and another approach for determining compliance must be followed. Concentrations of pathogenic microorganisms in treated water can be calculated from the concentrations in source water and the effectiveness of the water treatment. The effectiveness of the water treatment can be determined by means of a computational model. In the case of soil passage as a water treatment, a model is needed that describes the fate and transport of the pathogenic microorganisms during soil passage.

Clearly, there is a need to study the behavior of these pathogens in order to provide information for the evaluation of new and existing drinking water production systems from (artificial) groundwater and to be able to evaluate the protection guideline of 60 days. The research presented in this thesis was mainly aimed at understanding, quantifying and modeling the processes that govern the removal of viruses by soil passage. More specifically, the research objectives were as follows:

1. To assess removal of model and pathogenic microorganisms by soil passage.
2. To study to what extent and in what manner the processes adsorption and inactivation contribute to this removal.
3. To develop a model that adequately describes removal of pathogenic microorganisms by soil passage.
4. To evaluate the role of model microorganisms as surrogates to pathogenic microorganisms.
5. To calculate a protection zone of a groundwater well system for adequate removal of viruses in a worst case scenario.

The research comprised theoretical work, extensive fieldwork, laboratory experiments and modeling. Although the focus is mainly on virus removal, some bacteria that serve as fecal indicators have been studied as well. Bacteriophages were used as surrogates for pathogenic viruses.

### Efficiency of soil passage as a water treatment to remove viruses

Two field studies, at a dune recharge site and a deep well injection pilot site, were conducted in order to measure removal of bacteriophages MS2 and PRD1. In both studies, pretreated recharge water was seeded with these phages. By dune passage concentrations of both phages were reduced by  $8 \log_{10}$  within 30 m of travel distance, corresponding to 25 days of travel time. At the deep well injection site, MS2 was removed by  $8 \log_{10}$  within 38 m of travel distance, corresponding to 40 days of travel time. Assuming MS2 is poorly removed compared to other (pathogenic) viruses, it may be concluded that soil passage as in dune recharge and deep well injection is a very efficient way for removing viruses. The required removal is achieved in less than 60 days.

The major removal process was found to be attachment of the bacteriophages to the soil grains. Detachment was very slow. The temperature at the field studies was  $12^\circ\text{C}$  or lower, hence inactivation rates were low. Near the point of infiltration or injection, virus removal was found to be much higher than further away in the direction of the production well. By dune recharge, concentrations of both phages were reduced about  $3 \log_{10}$  over the first 2.4 m and another  $5 \log_{10}$  over the following 27 m. By deep well injection, concentrations of MS2 and PRD1 were reduced by  $6 \log_{10}$  over the first 8 m of soil passage. But in the following 30 m, concentrations of MS2 were reduced by only about  $2 \log_{10}$ .

From column experiments it appeared that the high initial removal was due to heterogeneity of attachment properties of the soil. Phage removal rates were found to vary more than a factor ten between columns with the different soil samples and were strongly positively correlated with soil organic carbon content, and relatively strongly positively with silt content and the presence of ferric oxyhydroxides. This suggests that the high initial removal may take place within the first meters of dune passage at a point where the organic carbon content is high, as was indeed observed in the field under the reedy border. Both the bacteriophages and organic matter probably attach to favorable sites of ferric oxyhydroxides that are more abundant in the first meters of soil passage, but the phages may, possibly, also attach to sites provided by bonded organic matter.

The high initial removal that was observed in the deep well injection study could be ascribed to favorable attachment to patches of ferric oxyhydroxides that were present within 8 meters distance from the injection point due to pyrite oxidation, but not thereafter. Ferric oxyhydroxides provide positively charged patches on to which fast attachment of the negatively charged microorganisms may take place. This implies that deep well injection for the removal of viruses is adequate due to the existence of a zone where ferric oxyhydroxide deposits actually form. However, removal of viruses that incidentally contaminate an anoxic aquifer may be little. Under that condition no patches of ferric oxyhydroxides have formed from pyrite oxidation.

The effect of pore water velocity on removal of bacteriophages was investigated in column experiments. This is of interest for drinking water companies wanting to keep land claim for artificial recharge limited. As expected, a two times higher pore water velocity resulted in an approximately two times lower phage removal with distance. It can be predicted for the dune recharge site that at the current pore water velocity virus removal of  $12 \log_{10}$  will be achieved at the production well at a distance of 60 m. At twice the pore water velocity still  $8 \log_{10}$  virus removal will be achieved.

## Model viruses

In a literature review some frequently used bacteriophages were evaluated as model viruses. MS2 and PRD1 meet the requirements for worst-case model viruses, at water temperatures less than about 10° C, at pH 6 – 8 and if the soil does not contain too many hydrophobic sites and not too many multivalent cations. Under those conditions, these bacteriophages attach little to the soil grains compared to other (pathogenic) viruses due to their strong negative charge and their inactivation rate is low. This was also shown in column experiments with dune sand by comparison with pathogenic viruses.

Bacteriophage  $\phi$ X174 may be a relatively conservative model virus, because of its low hydrophobicity and stability. F-specific RNA bacteriophages that are present in surface water or treated wastewater that is used for recharging groundwater, consist of stable and poorly adsorbing viruses. F-specific RNA bacteriophages may, therefore, be very useful naturally occurring worst-case viruses.

In laboratory experiments that were re-analyzed, kinetic attachment rate coefficients were found to be significantly higher for bacteriophages with presumably stronger negative charge. This is contrary to the expectation that a more negatively charged virus attaches less to the soil grains due to stronger electrostatic repulsion. Presumably, the more negatively charged viruses attached more due to the presence of multivalent cations that enable cation bridging or charge reversal. Another possibility may be an abundance of favorable sites, but data on the characteristics of the soil were lacking in that respect. Anyway, attachment rate coefficients were very high, meaning that conditions for attachment were highly favorable. Under such conditions, bacteriophage  $\phi$ X174 appears to behave more conservatively than more negatively charged viruses, like MS2 and PRD1, and may then be a better choice as relatively conservative tracer for virus transport through the subsurface.

## Removal of bacteria by soil passage

In addition to studying virus removal by soil passage, removal of fecal indicator bacteria was investigated as well. Fecal indicator bacteria, especially clostridium spores, may penetrate sandy aquifers as well as viruses. Nevertheless, viruses may still be considered as more critical for the effectiveness of soil passage due to their infectivity. Removal of spores of *Clostridium perfringens* (D10) was also studied in a column experiment. This pathogen is regarded as an indicator for fecal contamination of drinking water sources. Moreover, *Clostridium* spores are potential surrogates for *Cryptosporidium* oocysts, because both are highly persistent in the environment. The spores were found to attach relatively fast, but because of their very long survival all spores break through eventually. Their actual removal with travel time or distance depends on the time period of seeding or contamination.

### Modeling of virus removal

Literature on models that describe subsurface transport of viruses and the factors that determine the extent of adsorption and inactivation was reviewed extensively. These models include terms for advection and dispersion, as well as for adsorption and inactivation. Both equilibrium and kinetic adsorption were considered. It was concluded that under saturated conditions and at temperatures below 15 °C, where inactivation is low, kinetically limited attachment and detachment mainly govern removal of viruses during subsurface transport and determine the shape of breakthrough curves. At pH 7 – 8, adsorption will mainly be reversible. Usually, attachment rates are faster than detachment rates. Little or no retardation due to equilibrium adsorption is found. At pH 7 and higher, conditions are generally unfavorable for attachment, but viruses may preferentially attach to a minor surface fraction of soil grains that is positively charged. All this is in line with the findings from the field studies on virus removal by dune recharge and deep well injection. Dissolved organic matter decreases virus attachment by competition for the same binding sites and thus reduces attachment. Bonded organic matter may provide hydrophobic binding sites for viruses and thus enhance attachment. Dissolved organic matter may disrupt hydrophobic bonds. The enhancing and attenuating effects of organic matter are difficult to quantify and may be responsible for considerable uncertainty when predicting virus removal.

Values of inactivation rate coefficients for attached viruses were calculated using literature data from batch studies. Enhanced or reduced inactivation is found to be virus-specific and almost independent of adsorption. Temperature is the most important factor that influences virus inactivation. Probably, the inactivation rates of free and attached viruses change similarly with temperature.

In the dune recharge study, parameter values for adsorption and inactivation were obtained from fitting an analytical, one-site kinetic model (CXTFIT2) to the breakthrough curves of bacteriophages MS2 and PRD1. Although, a reasonable fitting of the breakthrough curves was obtained, there was considerable discrepancy at the end of the rising and the start of the declining limbs of the breakthrough curves. One may assume that more types of kinetic sites exist due to surface charge heterogeneity of the granular medium. Thus, a numerical code for a two-site kinetic model (EQ2KIN) was written to analyze the breakthrough curves from the dune recharge study as well from the column experiments with dune sand. Very satisfactory fits of all breakthrough curves were obtained with the two-site model. This model can account for the skewness of the rising limb of the breakthrough curve and for the smooth transition of the declining limb to the tail of the breakthrough curve. A one-site kinetic model cannot follow the curvedness of the breakthrough tail, leading to an overestimation of the inactivation rate coefficient for attached viruses. It is suggested that a two-site kinetic model is generally applicable to fit breakthrough curves of microorganisms. Relatively fast attachment and slow detachment characterize interaction with kinetic site 1, whereas relatively fast attachment, but equal or faster detachment, characterizes interaction with kinetic site 2. It was shown that interaction of viruses with sites of type 2 only had a minor contribution to virus removal. Moreover, at low temperatures, where virus inactivation is low, attachment to kinetic site 1 mainly determines virus removal.

In the column experiments, it was shown that a two times higher pore water velocity resulted in an approximately two times lower removal with distance, but a nearly constant removal rate. This implies that colloid filtration theory may be valid for this range of pore water velocities, and that collision efficiencies are constant within this range of pore water velocities.

Literature data from batch and column experiments using five different bacteriophages were re-analyzed. In batch and recirculating column experiments, attachment and detachment rate coefficients were not found to be significantly different between the two kinds of experiments. There was one exception, however: MS2 appeared to detach faster in the presence of strong advective flow.

In flow-through column experiments, it was found that a two-site model, with adsorption to equilibrium and kinetic sites, fitted the breakthrough curves of all the bacteriophages, except PM2, satisfactorily. A one-site kinetic model was found to be appropriate for this latter phage. However, it was also noticed that a large dispersion coefficient was needed to fit the curves. Estimates of dispersion from a salt tracing experiment were not conducted. Most, likely, these breakthrough curves can be described better with a two-site kinetic model and applying a more realistic value for dispersion. Similar attachment and detachment rate coefficients for certain virus-soil combinations from batch and recirculating column experiments may be found, but there may be exceptions, dependent on the type of virus.

So far, removal of viruses was modeled as a one-dimensional problem, assuming a constant and steady state water flow and considering only longitudinal dispersion. In reality, the situation is much more complex because of the temporal and spatial variations in water flow velocities, and because of effects of transverse dispersion and dilution. Bacteriophage removal by soil passage in the two field studies was re-analyzed with the goal to investigate differences between one- and two-dimensional modeling approaches, differences between one- and two-site kinetic sorption models, and the role of heterogeneities in the soil properties. The first study involved removal of bacteriophages MS2 and PRD1 by dune recharge, while the second study represented removal of MS2 by deep well injection. In both studies, removal was higher during the first meters of soil passage than thereafter. The software packages HYDRUS-1D and HYDRUS-2D were modified by incorporating reversible adsorption to two types of kinetic sites.

The one-dimensional two-site model simulated the overall behavior of the breakthrough curves of MS2 and PRD1 from the dune recharge study very well. The two-dimensional one-site model predicted a more gradual decrease in virus concentrations after the peaks than the one-dimensional one-site model, but not as good as the one-dimensional two-site model. The dimensionality of the problem hence can partly explain the smooth decrease in concentration after peak breakthrough. The two-dimensional two-site model provided the best results. The non-linear removal of MS2 and PRD1 is mainly caused by variations in interactions between grain and virus surfaces rather than by physical heterogeneity of the porous medium.

Similarly, a two-site model performed better than the one-site model in describing MS2 concentrations for the deep well injection study. However, the concentration data were too sparse in this study to have much confidence in the fitted parameters.

### Virus removal at field scale

Theoretical and practical knowledge about virus removal in terms of process parameters and boundary conditions at field scale was summarized. Removal rates of bacteriophages from field studies were analyzed in order to identify some typical cases that can be used to predict virus removal by soil passage at sites under similar conditions. Virus removal can be interpreted as a function of collision efficiencies  $\alpha_\beta$  and  $\alpha_\lambda$ , inactivation rate coefficient  $\mu_1$ , rate parameter  $\gamma$ , pore water velocity  $v$ , porosity  $n$ , the grain size  $d_c$  and the water temperature. Initial high removal is determined by  $\alpha_\beta$ , which decreases exponentially at a rate  $\gamma$  to a constant base removal rate that is determined by  $\alpha_\lambda$  and  $\mu_1$ . Collision efficiencies  $\alpha_\beta$  and  $\alpha_\lambda$  depend on the fraction and nature of heterogeneously distributed patches of favorable sites for attachment.

In order to predict virus removal in a particular field situation, detailed knowledge about the soil properties is required, which may be obtained from geochemical analyses of soil samples and be supported by studying attachment of MS2 in column experiments. This conclusion is supported by the findings from column experiments that were designed to mimic the field conditions during dune recharge. The removal rates of MS2 and PRD1 varied across a very similar range as in the field study. The values of inactivation rate coefficients for free and attached viruses were found to be the same at field and laboratory scale.

Similarly, from analysis of different soil samples along a flow line, one may estimate  $\gamma$ . *E.g.*  $\gamma$  may be related to a decrease in dissolved oxygen with travel time. At higher pH, electrostatic repulsion between the surfaces of viruses and soil grains is higher, which is reflected by lower values of the collision efficiency. The collision efficiency of MS2 is assumed to decrease by a factor 0.9 for every increase in pH by one tenth.

### Calculation of protection zone for groundwater well systems: A worst-case approach

As a first step in a vulnerability analysis of Dutch groundwater well systems (not artificially infiltrated) to virus contamination, a hypothetical case was simulated to calculate the travel distance and time that are required for 9- $\log_{10}$  protection against virus contamination. To that aim, a selection was made of phreatic aquifers in The Netherlands that were anoxic and the pH of the water was 7 or higher. These conditions may be as unfavorable for attachment as in the anoxic part of the aquifer from a deep well injection study. This corresponds to a collision efficiency of about  $1.5 \times 10^{-5}$ .

The same conditions may apply to many confined aquifers. Protection zones that assure virus removal of 9  $\log_{10}$  were determined for this selection of phreatic aquifers, applying worst case values for the inactivation rate coefficient and collision efficiency for MS2. Virus was assumed to be originating from a sewage pipe lying at the groundwater table leaking continuously at rate of  $1 \text{ m}^3 \cdot \text{day}^{-1}$ . Virus concentration was found to be reduced 3 to 4  $\log_{10}$  at the abstraction well due to mixing. To account for an additional 5 to 6  $\log_{10}$  removal of virus by attachment and inactivation, travel times of about three to seven times longer than the current guideline of 60 days are needed. Only horizontal transport was considered, *i.e.* protective effects of confining layers and vertical transport through (un)saturated zones were not considered, but, on the other hand, leakage rates may be higher and concentrations of human pathogenic viruses in raw wastewater may possibly be higher too.

## Major results and conclusions

Soil passage as a treatment for drinking water production, as applied in dune recharge and deep well injection, is a very efficient way to remove viruses. Bacteriophage MS2 was removed by  $8 \log_{10}$  within 25 to 40 days. Bacteriophages MS2 and PRD1 can be considered as worst-case model viruses in saturated sandy soils at pH 6 – 8 with a low organic carbon content and at low temperature. MS2 and PRD1 are strongly negatively charged and attach therefore at least as poorly to soil grains as other (pathogenic) viruses. In addition, they are relatively stable at temperatures below 12 °C. F-specific RNA bacteriophages are useful naturally occurring worst-case viruses.

At a temperature below 12 °C, where inactivation is low, attachment of bacteriophages to the soil grains is the most important removal process. Attached phages detach slowly.

In the field studies, much more virus removal took place near the point of injection than further downstream. This high initial removal is due to attachment to favorable sites that are present in higher numbers within the first meters of soil passage. Possibly, the high initial removal at the dune recharge site occurred at a location where the soil organic carbon content is high. Both bacteriophages as organic matter probably attach to the same favorable sites formed by ferric oxyhydroxides, which are present in higher numbers. Presumably, the phages attach also to sites consisting of bonded organic matter.

The high initial removal that was observed in the deep well injection study could be ascribed to favorable attachment to ferric oxyhydroxides that were present within 8 m of the injection well, but not thereafter. A model that describes attachment to two types of sites can account for the skewness of the rising limb of the breakthrough curve and for the smooth transition of the declining limb to the tail of the breakthrough curve. A one-site kinetic model cannot follow the curvedness of the breakthrough tail, leading to an overestimation of the inactivation rate coefficient for attached viruses. Relatively fast attachment and slow detachment characterize interaction with kinetic site 1, whereas relatively fast attachment, but equal or faster detachment, characterizes interaction with kinetic site 2. It was shown that interaction of viruses with sites of type 2 only had a minor contribution to virus removal.

Fecal indicator bacteria and especially clostridium spores may penetrate sandy aquifers as well as viruses. Nevertheless, viruses may still be considered as more critical due to their infectivity. Because clostridium spores are very stable, their actual removal depends on the time period of contamination.

Virus removal can be interpreted as a function of collision efficiencies  $\alpha_\beta$  and  $\alpha_\lambda$ , inactivation rate coefficient  $\mu_1$ , rate parameter  $\gamma$ , pore water velocity  $v$ , porosity  $n$ , the grain size  $d_c$  and the water temperature. Initial high removal is determined by  $\alpha_\beta$ , which decreases exponentially at a rate  $\gamma$  to a constant base removal rate that is determined by  $\alpha_\lambda$  and  $\mu_1$ . Collision efficiencies  $\alpha_\beta$  and  $\alpha_\lambda$  depend on the fraction and nature of heterogeneously distributed patches of favorable sites for attachment.

According to a hypothetical worst case approach protection zones of groundwater well systems (not artificially infiltrated) with three to seven times longer than the current guideline of 60 days are needed to assure virus removal of  $9 \log_{10}$ .

### Recommendations

From various field studies it became apparent that high initial virus removal often takes place due to the presence of more favorable attachment sites within the first few meters of soil passage. In order to predict virus removal in a particular field situation, detailed knowledge about the soil properties is required, which may be obtained from geochemical analyses of soil samples and be supported by studying attachment of MS2 in column experiments. It is highly recommended to investigate the quantitative relationship between virus attachment, pH and the fraction of favorable attachment sites on the surface of the sand grains.

It is recommended to conduct such a prediction and validate it by measuring virus removal, using MS2 as a model virus.

In the hypothetical case to calculate a protection zone for phreatic aquifers, only horizontal transport was considered and, *i.e.* protective effects of confining layers and vertical transport through (un)saturated zones were not included. It is recommended to investigate these protective effects and to include them in the vulnerability analysis of a given groundwater system. The major uncertain factor is leakage of wastewater. Further investigation of the probability and extent of such leaks is necessary. There are indications that concentrations of human pathogenic viruses in raw wastewater may be higher. Further investigation of concentrations of important human pathogenic viruses in raw wastewater is also necessary.

Finally, the before mentioned approach to predict virus removal and subsequent validation may also be applied to groundwater well systems.

# **Samenvatting, Conclusies en Aanbevelingen**

## Virusverwijdering uit Grondwater door Bodempassage Modellering, Veld- en Laboratoriumexperimenten

Jack Schijven

### Samenvatting, conclusies en aanbevelingen

#### Achtergrond en doelstellingen

Ongeveer tweederde van al het drinkwater in Nederland is afkomstig van grondwater en eenderde van oppervlaktewater. Ongeveer 39% van het oppervlaktewater dat gebruikt wordt voor drinkwaterproductie wordt behandeld door middel van bodempassage, zoals bij oeverfiltratie en duinfiltratie van voorgezuiverd oppervlaktewater.

Grondwater zou besmet kunnen raken met pathogene virussen, bacteriën en protozoa van fecaal verontreinigd water, zoals van kunstmatig geïnfilterd oppervlaktewater, septische tanks en lekkende rioolpijpen. Oppervlaktewater is besmet met pathogene micro-organismen, voornamelijk ten gevolge van lozingen van (on)gezuiverd afvalwater en door uit- en afspoeling van dierlijke mest van landbouwgronden. Gedurende vele tientallen jaren zijn in Nederland geen gegevens bekend over infectieziekten die geassocieerd konden worden met fecale verontreiniging van (kunstmatig) grondwater. Echter, pathogenen zoals enterovirussen en de pathogene protozoa *Cryptosporidium* en *Giardia* zijn alom aanwezig in de Nederlandse oppervlaktewateren. Adequate zuivering van oppervlaktewater, dat wordt ingenomen voor drinkwaterproductie, moet derhalve onder alle omstandigheden gegarandeerd kunnen worden.

Grondwater kan beschermd worden tegen besmetting met pathogene micro-organismen door handhaving van een voldoende grote afstand tussen de plaats van besmetting en de winputten. Hierbij dient de bodem als barrière. Pathogenen kunnen effectief uit oppervlaktewater worden verwijderd door middel van bodempassage met inachtneming van voldoende grote afstanden en/of voldoende lange verblijftijden. Volgens de huidige richtlijnen is een verblijftijd van tenminste 60 dagen nodig om grondwaterwinningen te beschermen. Bij oeverfiltratie varieert de verblijftijd tussen 0,5 en 30 jaar en bij kunstmatige infiltratie van voorgezuiverd oppervlaktewater tussen 35 en 135 dagen. De verblijftijd van 60 dagen werd voldoende geacht om pathogene bacteriën zodanig af te laten sterven dat geen risico voor de volksgezondheid meer bestaat. Echter, het is reeds tientallen jaren bekend dat virussen en, recenter, protozoa het meest bedreigend zijn voor de volksgezondheid. Als gevolg van hun persistentie in het milieu en hun infectiviteit worden virussen en de pathogene protozoa *Cryptosporidium* en *Giardia* is de verwijdering van deze pathogenen bij drinkwaterproductie meest cruciaal. Door hun persistentie in waterige milieus kan een verblijftijd van 60 dagen te kort zijn voor voldoende afsterving. Echter, hechting van deze pathogenen aan zandkorrels tijdens bodempassage kan significant bijdragen aan hun verwijdering. Dit alles leidt tot de vraag in hoeverre de hygiënische kwaliteit van drinkwater gegarandeerd is.

In het nieuwe Waterleidingbesluit (2001) is opgenomen dat de kans op infectie door pathogenen ten gevolge van drinkwaterconsumptie niet hoger dan één per 10 000 personen

per jaar mag zijn. Met behulp van deze risico-eis, drinkwaterconsumptie en dosisrespons relaties van pathogenen kunnen maximum toelaatbare concentraties aan pathogenen in drinkwater worden berekend. In het geval van virussen is deze concentratie gebaseerd op de dosisrespons relatie van rotavirus en poliovirus 3 als "worst-case" en bedraagt  $1,8 \times 10^{-7}$  virussen per liter. Gegeven de virusconcentraties in Nederlands oppervlaktewater moeten deze concentraties 5 tot 8  $\log_{10}$  gereduceerd moeten worden om drinkwater te leveren waarin de maximum toelaatbare concentratie niet wordt overschreden. Dit leidt tot de vraag welke verblijftijden en afstanden nodig zijn om een dergelijke concentratieafname door bodempassage te bewerkstelligen.

Of de maximaal toelaatbare concentratie niet wordt overschreden kan alleen maar worden bepaald aan de hand van onderzoek aan zeer grote monsters drinkwater van  $10^5 - 10^7$  liter. Dit is onpraktisch, derhalve wordt een andere benadering gevolgd om vast te stellen of aan de concentratienorm wordt voldaan. De concentraties pathogene micro-organismen in gezuiverd water kunnen worden berekend uit de concentraties in het ruwe water en de effectiviteit van de waterzuivering. De effectiviteit van de waterzuivering kan worden vastgesteld aan de hand van een rekenmodel. In het geval van bodempassage, is een model nodig om het transport en gedrag van pathogene micro-organismen tijdens bodempassage te beschrijven.

Er is dus informatie nodig over het gedrag van pathogene micro-organismen tijdens bodempassage te bestuderen ter evaluatie van de effectiviteit van bodempassage als zuiveringstap in nieuwe en bestaande situaties en van de beschermingsrichtlijn van 60 dagen verblijftijd voor grondwaterwinningen. Het onderzoek in dit proefschrift was hoofdzakelijk gericht op het begrijpen, kwantificeren en modelleren van de processen die de verwijdering van virussen tijdens bodempassage bepalen. De specifieke doelstellingen van onderzoek waren als volgt:

1. De verwijdering bepalen van model- en pathogene micro-organismen door bodempassage.
2. Bepalen in welke mate en op welke manier processen als hechting en afsterving bijdragen tot de verwijdering.
3. Ontwikkelen van een rekenmodel dat de verwijdering van pathogene micro-organismen door bodempassage adequaat beschrijft.
4. Evalueren van de rol van model micro-organismen als surrogaat voor pathogene micro-organismen.
5. Berekenen van een beschermingsgebied van een grondwaterwinning dat groot genoeg is voor afdoende virusverwijdering in een worst case scenario.

Het onderzoek omvatte theoretisch werk, uitgebreid veldwerk, laboratoriumexperimenten en modellering. Hoewel de aandacht hoofdzakelijk gericht was op virusverwijdering, is tevens de verwijdering van enkele fecale indicatorbacteriën onderzocht. Bacteriofagen werden onderzocht als surrogaat voor pathogene virussen.

### **Effectiviteit van bodempassage als zuiveringstap voor virusverwijdering**

Twee veldstudies, op een locatie voor duininfiltratie en op een proeflocatie voor diepinfiltratie, werden uitgevoerd om verwijdering van bacteriofagen MS2 en PRD1 te meten. In beide studies werd deze fagen aan het voorgezuiverde infiltratiewater gedoseerd.

Door duinpassage werden de concentraties van beide fagen met  $8 \log_{10}$  gereduceerd binnen 30 m (25 dagen verblijftijd). Door diepinfiltratie werd MS2  $8 \log_{10}$  verwijderd over een afstand van 38 meter (40 dagen verblijftijd). Omdat MS2 relatief slecht verwijderd wordt ten opzichte van de meeste (pathogene) virussen is, kan worden geconcludeerd dat bodempassage, zoals bij duin- en diepinfiltratie, een zeer efficiënte manier is om virussen te verwijderen. De vereiste reductie wordt dus in minder dan 60 dagen bereikt.

Het belangrijkste verwijderingsproces bleek hechting van de bacteriofagen aan de zandkorrels te zijn. De gehechte fagen kwamen langzaam weer los. De temperatuur tijdens de veldstudies was  $12\text{ }^{\circ}\text{C}$  of lager, waardoor hun afsterving zeer langzaam verliep. Vlakbij het infiltratiepunt vond veel meer virusverwijdering plaats dan verderop in de richting van de winput. Tijdens duinpassage werden de faagconcentraties ongeveer  $3 \log_{10}$  gereduceerd over de eerste 2.4 m en vervolgens nog eens  $5 \log_{10}$  over de volgende 27 m. Tijdens diepinfiltratie werden de concentraties MS2 en PRD1  $6 \log_{10}$  gereduceerd over de eerste 8 m bodempassage. Maar de concentraties MS2 werden in de daaropvolgende 30 m slechts ongeveer  $2 \log_{10}$  gereduceerd.

Uit kolomproeven bleek dat de hoge initiële verwijdering het gevolg was van heterogeniteit in de hechtingseigenschappen van de bodem. De verwijdering was namelijk sterk positief gecorreleerd met het gehalte aan organisch koolstof en relatief sterk positief met het lutumgehalte en de aanwezigheid van amorfe ijzerhydroxiden. Waarschijnlijk vond de hoge initiële verwijdering plaats binnen de eerste meters duinpassage op een plek waar het organisch koolstofgehalte hoog is. Zowel de bacteriofagen als organisch materiaal hechten waarschijnlijk aan de gunstige hechtingsplaatsen gevormd door amorfe ijzerhydroxiden die in hogere mate aanwezig zijn in de eerste meters bodempassage, maar de fagen hechten vermoedelijk ook aan plaatsen op de zandkorrels bestaande uit gebonden organisch materiaal.

De hoge initiële verwijdering die in het onderzoek naar diepinfiltratie werd waargenomen kon worden toegeschreven aan gunstige hechting op plekken met amorfe ijzerhydroxiden die aanwezig waren binnen 8 meter van het injectieput ten gevolge van pyrietoxidatie, maar niet daarbuiten. Amorfe ijzerhydroxiden vormen positief geladen plaatsen op negatief geladen zandkorrels, waaraan snelle hechting van negatief geladen micro-organismen kan plaatsvinden. Dit betekent dat tijdens diepinfiltratie virussen zeer effectief worden verwijderd in een zone waar amorfe ijzerhydroxiden neerslaan. Echter, de verwijdering van virussen die incidenteel een anoxisch (zuurstofloos) watervoerend pakket besmetten kan zeer laag zijn, omdat daar geen gunstige hechtingsplaatsen gevormd zijn door pyrietoxidatie.

Het effect van de poriewatersnelheid op de verwijdering van bacteriofagen werd onderzocht met behulp van kolomproeven. Dit is van belang voor drinkwaterleidingbedrijven die de ruimte benodigd voor kunstmatige infiltratie willen beperken. Volgens verwachting resulteerde een twee keer hogere poriewatersnelheid in een ongeveer twee keer lagere faagverwijdering in relatie tot de afstand. Het kan worden voorspeld dat door duinfiltratie bij de huidige poriewatersnelheid een virusverwijdering van  $12 \log_{10}$  wordt bereikt bij de winput op een afstand van 60 m en dat bij een twee keer hogere poriewatersnelheid nog steeds  $8 \log_{10}$  virusverwijdering wordt bereikt.

## Modelvirussen

In een literatuuroverzicht werden enkele vaak gebruikte bacteriofagen geëvalueerd als modelvirussen. MS2 en PRD1 voldoen aan de eisen die gesteld worden aan "worst-case" modelvirussen, bij watertemperaturen lager dan ongeveer 10° C, bij pH 6 – 8 en als de grond niet teveel hydrofobe plekken en niet teveel meerwaardige kationen bevat. Onder dergelijke omstandigheden hechten deze bacteriofagen minder aan de zandkorrels dan andere (pathogene) virussen ten gevolge van hun sterk negatieve lading, terwijl hun afsterving heel laag is. Dit werd nog eens getoond in kolomproeven met duinzand door vergelijking met pathogene virussen.

Bacteriofaag  $\phi$ X174 kan als relatief conservatief modelvirus worden beschouwd vanwege zijn lage hydrofobiciteit en hoge stabiliteit. F-specifieke RNA-bacteriofagen in oppervlaktewater of gezuiverd afvalwater dat wordt gebruikt voor kunstmatige aanvulling van grondwater bestaan uit stabiele en slecht hechtende virussen. Daarom kunnen F-specifieke RNA-bacteriofagen als nuttige natuurlijk voorkomende "worst-case" virussen worden gezien.

Laboratoriumexperimenten uit de literatuur werden opnieuw geanalyseerd. Hierbij werden kinetische hechtingscoëfficiënten gevonden die significant hoger waren voor bacteriofagen met vermoedelijk sterker negatieve lading. Dit is in tegenstelling tot de verwachting dat een sterker negatief geladen virus minder aan zandkorrels hecht ten gevolge van een sterkere elektrostatische afstoting. Vermoedelijk hechten sterker negatief geladen virussen meer door de aanwezigheid van meerwaardige kationen. Meerwaardige kationen kunnen kationbruggen vormen of ladingsomkering bewerkstelligen. Een andere mogelijkheid is een overvloed aan gunstige (positief geladen) hechtingsplaatsen, echter gegevens daarover ontbreken. Hechtingscoëfficiënten waren erg hoog, hetgeen betekent dat de condities voor hechting zeer gunstig zijn. Onder zulke omstandigheden blijkt bacteriofaag  $\phi$ X174 zich conservatiever te gedragen dan sterker negatief geladen virussen, zoals MS2 en PRD1.

## Verwijdering van bacteriën door bodempassage

Naast virusverwijdering door bodempassage werd verwijdering van fecale indicatorbacteriën onderzocht. Fecale indicatorbacteriën en vooral clostridiumsporen kunnen even goed als virussen in zandige bodems doordringen. Desalniettemin kunnen virussen nog steeds worden beschouwd als meest cruciaal voor de effectiviteit van bodempassage op grond van hun infectiviteit. Verwijdering van sporen van *Clostridium perfringens* (D10) werd ook onderzocht in een kolomexperiment. Deze pathoogeen wordt beschouwd als een indicator voor fecale verontreiniging van drinkwaterbronnen. Clostridiumsporen zijn bovendien potentieel surrogaat voor oöcysten van *Cryptosporidium* omdat beide zeer persistent zijn in het milieu. De sporen hechten relatief snel, maar ten gevolge van hun zeer lange overleving zullen ze uiteindelijk toch doorbreken in het water na bodempassage. De eigenlijke verwijdering als functie van verblijftijd of afstand hangt af van de tijdsduur van besmetting.

## Modellering van virusverwijdering

Literatuur over modellen voor virustransport door de bodem en de factoren die de mate van hechting en afsterving bepalen werd uitgebreid beschreven. Deze modellen omvatten termen voor zowel advection en dispersie als voor hechting en afsterving. Zowel evenwichts- als kinetische hechting werd beschouwd. Er werd geconcludeerd dat onder verzadigde condities en bij temperaturen lager dan 15 °C, wanneer afsterving laag is, virusverwijdering voornamelijk wordt bepaald door kinetische gelimiteerde hechting en onthechting en dat dit proces voornamelijk de vorm van doorbraakcurven bepaald. Hechting bij pH 7 – 8 is voornamelijk reversibel. Hechting verloopt gewoonlijk sneller dan onthechting. Het virustransport wordt niet tot nauwelijks vertraagd door evenwichtsadsorptie. De condities voor hechting zijn in het algemeen ongunstig bij een pH van 7 en hoger, maar virussen kunnen preferentieel hechten aan een kleine fractie op de oppervlakken van zandkorrels die positief geladen zijn. Dit alles is in overeenstemming met de bevindingen van de veldstudies naar virusverwijdering door duin- en diepinfiltratie.

Opgelost organisch materiaal verlaagt hechting van virussen door competitie om dezelfde hechtingsplaatsen. Gebonden organisch materiaal kan daarentegen ook hydrofobe hechtingsplaatsen voor virussen leveren en daarmee virushechting bevorderen. Opgelost organisch materiaal kan hydrofobe verbindingen verbreken. De versterkende en verzwakkende effecten van organisch materiaal zijn moeilijk te kwantificeren en kunnen de oorzaak zijn van grote onzekerheid in de voorspelling van virusverwijdering.

Waarden van afstervingscoëfficiënten voor gehechte virussen werden berekend aan de hand van de literatuurgegevens van schudproeven. Versterkte en verzwakte afsterving bleek virusspecifiek te zijn en bijna onafhankelijk van hechting. Temperatuur is de belangrijkste factor, die virusafsterving bepaalt. De afstervingscoëfficiënten van vrije en gehechte virussen veranderen in dezelfde mate onder invloed van de temperatuur.

In de duininfiltratiestudie werden parameterwaarden voor hechting en afsterving verkregen door de doorbraakcurven van bacteriofagen MS2 en PRD1 te simuleren met een analytisch model (CXTFIT2) dat hechting aan één type kinetische hechtingsplaatsen veronderstelt. Hoewel een redelijke simulatie van de doorbraakcurven verkregen werd, was er een behoorlijke discrepantie aan het einde van de stijgende en het begin van de dalende flanken van de doorbraakcurven. Men kan aannemen dat er meerdere typen kinetische hechtingsplaatsen bestaan ten gevolge van heterogeniteit in oppervlaktelading van het granulaire medium. Daarom werd een numerieke code geschreven voor een model dat hechting aan twee type plaatsen beschrijft (EQ2KIN) om de doorbraakcurven van de duininfiltratiestudie en van kolomexperimenten met duinzand te analyseren. Heel bevredigende simulaties van alle doorbraakcurven werden verkregen met dit model. Dit model kan de scheefheid van de stijgende flank van de doorbraakcurve volgen alsmede de geleidelijke overgang van de dalende flank naar de staart van de doorbraakcurve. Een model dat maar één type hechtingsplaatsen beschouwt kan de buiging van de staart van de doorbraakcurve niet volgen, hetgeen leidt tot een overschatting van de afstervingscoëfficiënt voor gehechte virussen. Er werd gesuggereerd dat het model voor twee typen hechtingsplaatsen algemeen toepasbaar is op doorbraakcurven van micro-organismen. Relatief snelle hechting en langzaam loslaten kenmerkt de interactie met de hechtingsplaats van type 1, terwijl relatief snelle hechting maar evenzo snel of sneller loslaten de interactie met de hechtingsplaats van type 2 kenmerkt. Getoond werd dat

interactie van virussen met hechtingsplaatsen van type 2 slechts een ondergeschikte bijdrage levert aan de virusverwijdering. Bij lage temperaturen, verloopt afsterving langzaam en bepaalt hechting aan plaatsen van type 1 hoofdzakelijk de virusverwijdering.

Uit kolomexperimenten bleek dat een twee keer hogere poriewatersnelheid een ongeveer twee keer lagere verwijdering in relatie tot de afstand tot gevolg heeft, maar dat de verwijderingsnelheid bijna constant blijft. Dit betekent dat binnen dit bereik van poriewatersnelheden de colloïdfiltratietheorie valide is en dat botsingsefficiënties constant zijn.

Literatuurgegevens van batch- en kolomproeven met vijf verschillende bacteriofagen werden opnieuw geanalyseerd. In batch- en recirculerende kolomproeven werden hechtigen- en onthechtigcoëfficiënten gevonden, die niet significant verschilden tussen de twee typen proeven. Echter, er was een uitzondering: MS2 bleek sneller los te laten bij een sterkere waterstromsnelheid.

In doorstroomkolomproeven werd gevonden dat met een model, dat hechting aan evenwichts- en kinetische plaatsen veronderstelt, de doorbraakcurven van alle bacteriofagen, behalve PM2, goed kon worden beschreven. Een model voor slechts één type kinetische hechtingsplaatsen was voldoende om de doorbraakcurve van deze faag te beschrijven. Echter, ook werd opgemerkt dat het nodig was om een grote dispersiecoëfficiënt toe te passen om de doorbraakcurven te simuleren. Tijdens de proeven waren geen schattingen gedaan van dispersie met behulp van een zouttracer. Deze doorbraakcurven kunnen zeer waarschijnlijk beter worden beschreven met het model voor twee typen kinetische hechtingsplaatsen in combinatie met een realistischer waarde voor dispersie.

Tot dusver werd virusverwijdering gemodelleerd als een ééndimensionaal probleem, met de aanname van een constante waterstroom met alleen longitudinale dispersie. In werkelijkheid is de situatie veel complexer vanwege tijdelijke en ruimtelijke variaties in waterstromsnelheden en vanwege effecten van transversale dispersie en verdunning. Verwijdering van bacteriofagen door bodempassage in de twee eerder genoemde veldstudies werd opnieuw geanalyseerd met het doel de verschillen tussen een één- en tweedimensionale benadering en met de verschillen tussen beschouwing van één en twee typen hechtingsplaatsen, alsmede de rol van heterogeniteit in de bodemeigenschappen te onderzoeken. De softwarepakketten HYDRUS-1D en HYDRUS-2D werden hiertoe gebruikt en aangepast.

Het ééndimensionale model voor twee typen hechtingsplaatsen simuleerde de doorbraakcurven van MS2 en PRD1 tijdens duininfiltratie zeer goed. Het tweedimensionale model voor één type hechtingsplaats voorspelde een meer graduele afname in virusconcentraties na de piekdoorbraak dan het ééndimensionale model voor één type hechtingsplaats, maar niet zo goed als het ééndimensionale model voor twee typen hechtingsplaatsen. De dimensionaliteit van het probleem kan aldus de geleidelijke buiging van de staart van de doorbraakcurve gedeeltelijk verklaren. Het tweedimensionale model voor twee type hechtingsplaatsen leverde de beste resultaten. De niet-lineaire verwijdering van MS2 en PRD1 kan voornamelijk toegeschreven worden aan verschillen in de interacties tussen de oppervlakken van zandkorrels en virussen en niet zozeer aan fysische heterogeniteit van het poreuze medium.

Evenzo bleek het model voor twee typen hechtingsplaatsen beter MS2 concentraties in de diepinfiltratiestudie te beschrijven dan het model voor één type hechtingsplaatsen. Het aantal meetgegevens was echter te beperkt om veel vertrouwen te kunnen hebben in de geschatte waarden van de parameters.

### Virusverwijdering op veldschaal

Theoretische en praktische kennis over virusverwijdering in termen van procesparameters en randvoorwaarden op veldschaal werd samengevat. Verwijderingsnelheden van bacteriofagen uit verschillende veldstudies werden geanalyseerd om enkele typische gevallen te identificeren, die toegepast kunnen worden om virusverwijdering door bodempassage te voorspellen op plaatsen waar soortgelijke condities gelden. Virusverwijdering kan worden opgevat als een functie van botsingsefficiënties  $\alpha_\beta$  en  $\alpha_\lambda$ , afstervingscoëfficiënt  $\mu_i$ , parameter  $\gamma$ , poriewatersnelheid  $v$ , porositeit  $n$ , zandkorrelgrootte  $d_c$  en de watertemperatuur. Initieel hoge verwijdering wordt bepaald door  $\alpha_\beta$ , welke exponentieel afneemt met een snelheid  $\gamma$  tot een constante basisverwijderingsnelheid, welke vervolgens wordt bepaald door  $\alpha_\lambda$  en  $\mu_i$ . Botsingsefficiënties  $\alpha_\beta$  en  $\alpha_\lambda$  hangen af van de fractie en de aard van heterogeen verdeelde plekken van gunstige hechtingsplaatsen.

Teneinde virusverwijdering in een gegeven veldsituatie te voorspellen is gedetailleerde kennis van de bodemeigenschappen nodig. Deze kan worden verkregen uit geochemische analyse van monsters grond en kan worden ondersteund door hechting van MS2 in kolomproeven te onderzoeken. Deze conclusie vindt ondersteuning in de bevindingen van kolomproeven die bedoeld waren om de veldomstandigheden tijdens duininfiltratie na te bootsen. De verwijderingsnelheden van MS2 en PRD1 varieerden over een zeer gelijk bereik als in de veldstudie. De waarden van de afstervingscoëfficiënten voor vrije en gehechte virussen bleken hetzelfde te zijn op veld- en laboratoriumschaal.

Evenzo kan uit de analyse van verschillende monsters grond langs één stroombaan een schatting worden gemaakt van  $\gamma$ . Parameter  $\gamma$  kan bijvoorbeeld gerelateerd zijn aan een afname van het gehalte aan opgeloste zuurstof als functie van de verblijftijd. Bij hogere pH is de elektrostatische afstoting tussen de oppervlakken van virussen en zandkorrels groter. Dit wordt weergegeven in de vorm van lagere waarden van de botsingsefficiëntie. De botsingsefficiëntie van MS2 wordt verondersteld met een factor 0,9 af te nemen voor elke toename van de pH met 0,1.

### Berekening grondwaterbeschermingsgebied: een “worst-case” benadering

Als een eerste stap naar een analyse van de kwetsbaarheid voor virusbesmetting van Nederlandse waterwinningen van grondwater (niet afkomstig van kunstmatige infiltratie) werd een hypothetische situatie gesimuleerd om de afstand en verblijftijd te berekenen die nodig zijn om 9-log<sub>10</sub>-bescherming te bieden tegen virusbesmetting vanuit een lekkend riool. Er werd een selectie gemaakt van freatische winningen in Nederland, die anoxisch (zuurstofloos) zijn, en waarvan de pH van het water 7 of hoger is. Deze condities mogen als ongunstig voor hechting worden gezien, zoals was waargenomen in het anoxische gedeelte van het watervoerende pakket in de diepinfiltratiestudie. Dezelfde condities kunnen van toepassing zijn op veel watervoerende pakketten onder afdekkende lagen. Beschermingszones die een virusverwijdering van 9 log<sub>10</sub> garanderen werden berekend voor de selectie van freatische winningen onder toepassing van de “worst-case” waarden voor de

afstervingscoëfficiënt en botsingsefficiëntie van MS2. Aangenomen werd dat virussen ononderbroken uit een rioolpijp lekten ter hoogte van de grondwaterspiegel met een volumestroom  $1 \text{ m}^3 \cdot \text{dag}^{-1}$ . De virusconcentraties namen af met 3 tot 4  $\log_{10}$  bij de winput ten gevolge van menging. Om vervolgens 5 tot 6  $\log_{10}$  virusverwijdering door hechting en afsterving te garanderen zijn volgens de berekeningen verblijftijden van ongeveer drie tot zeven keer de huidige richtlijn van 60 dagen nodig. Alleen horizontaal transport werd beschouwd, dat wil zeggen dat met beschermende effecten van afdekkende lagen en verticaal transport door (on)verzadigde zones geen rekening werd gehouden. Aan de andere kant kunnen lekkages groter zijn en zijn mogelijk de concentraties aan menspathogene virussen in ongezuiverd rioolwater hoger.

### Belangrijkste resultaten en conclusies

Bodempassage als zuiveringstap voor de drinkwaterbereiding, zoals toegepast bij duin- en diepinfiltratie, is een zeer efficiënte manier om virussen te verwijderen. Bacteriofaag MS2 werd 8  $\log_{10}$  verwijderd binnen 25 tot 40 dagen. Bacteriofagen MS2 en PRD1 gelden als "worst-case" modelvirussen in verzadigde zandige bodems bij pH 6 – 8 met een laag gehalte aan organisch koolstof en bij lage temperatuur. MS2 en PRD1 zijn sterk negatief geladen en hechten daardoor minstens zo slecht aan zandkorrels als andere (pathogene) virussen. Bovendien zijn ze relatief stabiel bij temperaturen lager dan 12 °C. F-specifieke RNA-bacteriofagen kunnen als nuttige natuurlijk voorkomende "worst-case" virussen worden gezien.

Bij een temperatuur van 12 °C of lager, wanneer afsterving laag is, is hechting van de bacteriofagen het belangrijkste verwijderingsproces aan de zandkorrels. De gehechte fagen komen slechts langzaam weer los.

In de veldstudies vond vlakbij het infiltratiepunt veel meer virusverwijdering plaats dan verderop in de richting van de winput. Deze hoge initiële verwijdering is het gevolg van hechting aan gunstige hechtingsplaatsen, die in hogere mate aanwezig zijn binnen de eerste meters van de bodempassage. Vermoedelijk vond de hoge initiële verwijdering plaats binnen de eerste meters duinpassage op een plek waar het organisch koolstofgehalte hoog is. Zowel de bacteriofagen als organisch materiaal hechten waarschijnlijk aan dezelfde gunstige hechtingsplaatsen gevormd door amorfe ijzerhydroxiden die daar in hogere mate aanwezig zijn, maar de fagen hechten vermoedelijk ook aan plaatsen op de zandkorrels bestaande uit gebonden organisch materiaal.

De hoge initiële verwijdering die in het onderzoek naar diepinfiltratie werd waargenomen kon worden toegeschreven aan gunstige hechting aan plekken met amorfe ijzerhydroxiden die aanwezig waren binnen 8 meter van het injectieput, maar niet daarbuiten.

Het model dat hechting aan twee type plaatsen beschrijft bleek de scheefheid van de stijgende flank van de doorbraakcurve te kunnen volgen alsmede de geleidelijke overgang van de dalende flank naar de staart van de doorbraakcurve. Een model dat maar één type hechtingsplaatsen beschouwt kan de buiging van de staart van de doorbraakcurve niet volgen, hetgeen leidt tot een overschatting van de afstervingscoëfficiënt voor gehechte virussen. Relatief snelle hechting en langzaam loslaten kenmerkt de interactie met de hechtingsplaats van type 1, terwijl relatief snelle hechting maar evenzo snel of sneller loslaten de interactie met de hechtingsplaats van type 2 kenmerkt. Interactie van virussen met hechtingsplaatsen van type 2 levert slechts een ondergeschikte bijdrage aan de virusverwijdering.

Fecale indicatorbacteriën en vooral clostridiumsporen kunnen even ver als virussen in zandige bodems doordringen. Desalniettemin kunnen virussen nog steeds worden beschouwd als meest kritisch op grond van hun infectiviteit. Doordat clostridiumsporen zeer stabiel zijn, hangt hun verwijdering af van de tijdsduur van besmetting.

Virusverwijdering kan worden opgevat als een functie van botsingsefficiënties  $\alpha_\beta$  en  $\alpha_\lambda$ , afstervingscoëfficiënt  $\mu_i$ , parameter  $\gamma$ , poriewatersnelheid  $v$ , porositeit  $n$ , zandkorrelgrootte  $d_c$  en de watertemperatuur. Initieel hoge verwijdering wordt bepaald door  $\alpha_\beta$ , welke exponentieel afneemt met een snelheid  $\gamma$  tot een constante basisverwijderingsnelheid, welke vervolgens wordt bepaald door  $\alpha_\lambda$  en  $\mu_i$ . Botsingsefficiënties  $\alpha_\beta$  en  $\alpha_\lambda$  hangen af van de fractie en de aard van heterogeen verdeelde plekken van gunstige hechtingsplaatsen.

Volgens een hypothetische “worst-case” benadering zijn beschermingszones voor grondwaterwinningen (niet kunstmatig geïnfilteerd) met verblijftijden van drie tot zeven keer de huidige richtlijn van 60 dagen nodig om een virusverwijdering van  $9 \log_{10}$  garanderen.

### Aanbevelingen

Uit verschillende veldstudies is gebleken dat virusverwijdering veelal in sterkere mate plaatsvindt gedurende de eerste meters van de bodempassage ten gevolge van het daar in hogere mate aanwezig zijn van gunstige hechtingsplaatsen. Teneinde virusverwijdering in een gegeven veldsituatie te voorspellen is derhalve gedetailleerde kennis van de bodemeigenschappen nodig. Deze kan worden verkregen uit geochemische analyse van monsters grond en kan worden ondersteund door hechting van MS2 in kolomproeven te onderzoeken.

Het is daarbij zeer aanbevelenswaard om de kwantitatieve relatie op te helderen tussen hechting van virussen, pH en de fractie aan gunstige hechtingsplaatsen op de oppervlakken van de zandkorrels.

Het is aan te bevelen om voor een bepaalde locatie een voorspelling uit te voeren en vervolgens deze voorspelling te valideren door meting van de virusverwijdering aan de hand van MS2 als modelvirus.

In de hypothetische kwetsbaarheidanalyse van freatische grondwaterwinningen werd alleen horizontaal transport beschouwd, dat wil zeggen dat beschermende effecten van afdekkende lagen en verticaal transport door (on)verzadigde zones niet beschouwd werden. Het verdient aanbeveling om deze beschermende effecten nader te onderzoeken en mee te laten wegen in de kwetsbaarheidanalyse voor een gegeven grondwaterwinning. Grote onbekende is het lekdebiet van rioolwater. Nader onderzoek naar de kans op en de mate van rioollekken is nodig. Er bestaan aanwijzingen dat de concentraties aan menspathogene virussen in ongezuiverd rioolwater hoger kunnen zijn, derhalve is nader onderzoek naar de concentraties van belangrijke menspathogene virussen in rioolwater noodzakelijk.

Tenslotte kan de hierboven genoemde aanpak om virusverwijdering door bodempassage te voorspellen ook worden toegepast en gevalideerd voor grondwaterwinning

# References

## References

---

- Abu-Ashour, J., Joy, D. M., Lee, H., Whiteley, H. R. and Zelin S. 1994. Transport of microorganisms through soil. *Water, Air Soil and Pollution* 75, 141-158.
- Albinger, O., Biesemeyer, B. K., Arnold, R. G. and Logan B. E. 1994. Effect of bacterial heterogeneity on adhesion to uniform collectors by monoclonal populations. *FEMS Microbiol. Letters* 124, 321-326.
- Armon, R. and Cabelli, V. J. 1988. Phage f2 desorption from clay in estuarine water using non ionic detergents, beef extract and chaotropic agents. *Can. J. Microbiol.* 34, 1022-1024.
- Babich, H. and Stotzky, G. 1980. Reductions in inactivation rates of bacteriophages by clay minerals in lake water. *Water Res.* 14, 185-187.
- Bales, R. C., Gerba, C. P., Grondin, G. H. and Jensen S. L. 1989. Bacteriophage transport in sandy soil and fractured tuff. *Appl. Environ. Microbiol.* 55, 2061-2067.
- Bales, R. C., Hinkle, S. R., Kroeger, T. W. and Stocking, K. 1991. Bacteriophage adsorption during transport through porous media: Chemical perturbations and reversibility. *Environ. Sci. Technol.*, 25: 2088-2095.
- Bales, R. C., Li, S., Maguire, K. M., Yahya, M. T. and Gerba, C. P. 1993. MS-2 and poliovirus transport in porous media: hydrophobic effects and chemical perturbations. *Water Resour. Res.*, 29: 957-963.
- Bales, R. C., Li, S., Maguire, K. M., Yahya, M.T., Gerba, C. P. and Harvey, R. W. 1995. Virus and bacteria transport in a sandy aquifer, Cape Cod, MA, *Ground Water* 33, 653-661.
- Bales, R. C., Li, S., Yeh, T. C. J., Lenczewski, M. E. and Gerba, C. P. 1997. Bacteriophage and microsphere transport in saturated porous media: Forced-gradient experiment at Borden, Ontario, *Water Resour. Res.*, 33: 639-648.
- Bear, J. 1972. *Dynamics of Fluid in Porous Media*. Elsevier, New York.
- Belnap, D. M. and Stevens, A.C. 2000. Déjà vu all over again: the similar structures of bacteriophage PRD1 and adenovirus. *Trends in microbiology.* 8: 91-93.
- Bitton, G. 1980. *Introduction to environmental virology*, *John Wiley & Sons*, New York, pp. 1-28.
- Bitton, G. and Mitchell, R. 1974. Effects of colloids on the survival of bacteriophages in seawater. *Water Res.* 10, 323-327.
- Bitton, G., Farrah, S. R., Ruskin, R. H., Butner, J. and Chou, Y. J. 1983. Survival of pathogenic and indicator organisms in groundwater. *Ground Water* 21, 405-410.
- Blanc, R. and Nasser, A. 1996. Effect of effluent quality and temperature on the persistence of viruses in soil. *Water Sci. Tech.* 33, 237-242.
- Bouwer, E. J., and Rittman, B. E. 1992. Comment on "Use of colloid filtration theory in modeling movement of bacteria through a contaminated aquifer". *Environ. Sci. Tech.* 26, 400-401.
- Bradford, S. M., Bradford, A. W. and Gerba, C. P. 1993. Virus transport through saturated soils. *Wiener Mitteilungen, Wien* 12, 143-147.
- Brush, C. F., Ghiorse, W. C., Anguish, L. J., Parlange J. Y. and Grimes, H. G. 1999. Transport of *Cryptosporidium parvum* oocysts through saturated columns. *J. Environ. Qual.* 28, 809-815.
- Burge, W. D. and Enkiri, N. K. 1978. Virus adsorption to five soils. *J. Environ. Qual.* 7, 73-76.

- Caldentey, J., Bamford, J. K. H. and Bamford, D. H. 1990. Structure and assembly of bacteriophage PRD1, an *Escherichia coli* virus with a membrane. *J. Struct. Biol.* 104, 44-51.
- Camper, A. K., Hayes, J. T., Sturman, P. J., Jones, W. L. and Cunningham A. B. 1993. Effects of motility and adsorption rate coefficients on transport of bacteria through saturated porous media. *Appl. Environ. Microbiol.*, 59: 3455-3462.
- CBW. Commissie Bescherming Waterwingebieden. 1980. Richtlijnen en aanbevelingen voor de bescherming van waterwingebieden. VEWIN-RID (In Dutch).
- Celia, M. A., Bouloutas, E. T. and Zarba, R. L. 1990. A general mass-conservative numerical solution for the unsaturated flow equation. *Water Resour. Res.* 26, 1483-1496.
- Chrysiopoulos, C. V. and Sim, Y. 1996. One-dimensional virus transport in homogeneous porous media with time-dependent distribution coefficient. *J. Hydrol.* 185, 199-219.
- Chung, H. and Sobsey, M. D. 1992. Survival of F-specific coliphages, *Bacteroides fragilis* phages, hepatitis A virus (HAV) and poliovirus 1 in seawater and sediment. *Water Sci. Tech.* 27, 425-428.
- Corapcioglu, M. Y., Munster, C. and Pillai, S. D. 1997. Field experiments and modeling of virus transport in groundwater. US EPA, Texas A&M University.
- Cox, D. C. and Hinkley, D. V. 1974. *Theoretical statistics*, Chapman and Hall, London, p 313 cf.
- Craun, G. F. and Calderon, R. 1996. Microbial risks in groundwater systems. Epidemiology of waterborne outbreaks. pp. 9- 20 In: *Under the microscope. Examining microbes in groundwater.* Am. Water Works Assoc. Res. Found., Denver, Colorado.
- Craun., G. F. 1985. Summary of waterborne illness transmitted through contaminated groundwater. *J. Environ. Health*, 48, 122-127.
- D'Antonio, R. G., Winn, R. E. and Taylor, J. P. 1985. A waterborne outbreak of cryptosporidiosis in normal hosts. *Ann. Intern. Med.* 312, 647-648.
- Dangendorf, F., Hernst, S. and Kistemann, Th. 2000. A GIS approach for analyzing the distribution of gastrointestinal diseases with respect to water supply structures in Rhein-Berg (Germany). Proceedings of 10<sup>th</sup> health related water microbiology symposium, IWA, Paris, HRM28.
- De Roda Husman, A. M., Holwerda, A. M. and Lodder, W. J. 2001. Comparison of the BGM monolayer and suspended plaque assay for the detection of entero- and reoviruses in water. In preparation.
- DeBorde, D. C., Woessner, W. W., Kiley, Q. T. and Ball, P. N. 1999. Rapid transport of viruses in a floodplain aquifer. *Water Res.* 33, 2229-2238.
- DeBorde, D. C., Woessner, W. W., Lauerman, B. and Ball P. N. 1998. Virus occurrence in a school septic system and unconfined aquifer. *Ground Water* 36, 825-834.
- Di Fazio, R and Vurro, M. 1994. Experimental test using rhodamine WT as tracer. *Adv. Water Resourc.* 17, 375-378.
- Dizer, H., Nasser, A. and Lopez, J. M. 1984. Penetration of different human pathogenic viruses into sand columns percolated with distilled water, groundwater or wastewater. *Appl. Environ. Microbiol.* 47, 409-415.
- Dowd, S. E., Pillai, S. D., Wang, S. and Corapcioglu, M. Y. 1998. Delineating the specific influence of virus isoelectric point and size on virus adsorption and transport through sandy soils. *Appl. Environ. Microbiol.* 64, 405-410.

## References

---

- Eck, Ph. G. and Huisman, D. F. M. J. Grondwaterbeschermingsbeleid. Een vergelijking van het beleid der provincies. 1990. Landbouwwuniversiteit Wageningen (in Dutch).
- Elimelech, M., Nagai, M., Ko, C. H. and Ryan, J. N. 2000. Relative insignificance of mineral grain zeta potential to colloid transport in geochemically heterogeneous porous media. *Environ. Sci. Technol.* 34:2143-2148.
- EPA, US Environmental Protection Agency. 2000. National Primary Drinking Water Regulations: Ground Water Rule. Proposed Rule. *Federal Register*, 10: 30194-30274.
- Farrah, S. R. 1982. Chemical factors influencing adsorption of bacteriophage MS2 to membrane filters. *Appl. Environ. Microbiol.* 43, 659-663.
- Farrah, S. R. and Preston, D. R. 1993. Adsorption of viruses to sand modified by in situ precipitation of metallic salts. *Wiener Mitteilungen, Wien* 12, 25-29.
- Farrah, S. R., Preston, D. R., Toranzos, G. A., Girard, M., Erdos, G. A. and Vasuhdivan, V. 1991. Use of modified diatomaceous earth for removal and recovery of viruses in water. *Appl. Environ. Microbiol.* 57, 2502-2506.
- Farrah, S. R., Shah, D. O. and Ingram, L. O. 1981. Effects of chaotropic and antichaotropic agents on elution of poliovirus on membrane filters. *Proc. Natl. Acad. Sci. USA* 78, 1229-1232.
- Formentin, K., Rossi, P. and Aragno, M. 1997. Determination of bacteriophage migration and survival potential in karstic groundwaters using batch agitated experiments and mineral colloidal particles. *Tracer Hydrology* 97, 39-46.
- Frost, F. J., Craun, G. F. and Calderon, R. L. 1996. Waterborne disease surveillance. *J. Am. Water Works Assoc.* 88, 66-75.
- Fujito, B. T. and Lytle, C. D. 1996. Elution of viruses by ionic and nonionic surfactants. *Appl. Environ. Microbiol.* 62, 3470-3473.
- Funderburg, S. W., Moore, B. E., Sagik, B. E. and Sorber C. A. 1981. Viral transport through soil columns under conditions of saturated flow. *Water Res.* 15, 703-711.
- Furtado, C., Adak, G. K., Stuart, J. M., Wall, P. G., Evans, H. S. and Casemore, D. P. 1998. Outbreaks of waterborne infectious intestinal disease in England and Wales, 1992-5. *Epidemiol. Infect.* 121, 109-119.
- Gantzer, C., Quignon, F. and Schwartzbrod, L. 1994. Poliovirus-1 adsorption onto and desorption from montmorillonite in seawater, survival of the adsorbed virus. *Environ. Technol.* 15, 271-278.
- Gerba, C. P. 1984. Applied and theoretical aspects of virus adsorption to surfaces. *Adv. Appl. Microbiol.* 30, 133-168.
- Gerba, C. P. 1996. What are the current microbiological and public health issues in drinking water? In: *Under the microscope. Examining microbes in groundwater.* Am. Water Works Assoc. Res. Found., Denver, Colorado. 39-47.
- Gerba, C. P., Goyal, S. M., Cech, I. and Bogdan, G. F. 1981. Quantitative Assessment of the adsorptive behaviour of viruses to soils. *Environ. Sci. Technol.* 15, 940-944.
- Gerba, C. P., Keswick, B. H., Dupont, H. L., and Fields, H. A. 1984. Isolation of rotavirus from drinking water. *Monogr. Virol.* 15, 119-125.
- Gerba, C. P. and Lance, J. C. 1978. Poliovirus removal from primary and secondary sewage effluent by soil filtration. *Appl. Environ. Microbiol.* 36, 247-51.
- Gerba, C. P. and Schaiberger, G. E. 1975. Effect of particulates on virus survival in seawater. *J. Water Pollut. Control Fed.* 47, 93-103.
- Gerba, C. P., Stagg, C. H. and Abadie, M. G. 1978. Characterisation of sewage solid-associated viruses and behaviour in natural waters. *Water Res.* 12, 805-812.

- Gerba, C. P., Yates, M. V. and Yates, S. R. 1991. Quantitation of factors controlling viral and bacterial transport in the subsurface. In: Modeling the environmental fate of microorganisms, edited by C. J. Hurst, pp. 77-88, Am. Soc. for Microbiol., Washington DC.
- Goyal, S. M. and Gerba, C. P. 1979. Comparative adsorption of human enteroviruses, simian rotavirus, and selected bacteriophages to soils. *Appl. Environ. Microbiol.* 38, 241-247.
- Grant, S. B. 1994. Virus coagulation in aqueous environments. *Environ. Sci. Technol.* 28, 928-933.
- Grant, S. B. 1995. Inactivation kinetics of viral aggregates. *J. Environ. Engin.* 121, 311-319.
- Grant, S. B., List, E. J. and Lidstrom, M. E. 1993. Kinetic analysis of virus adsorption and inactivation in batch experiments. *Water Resour. Res.* 29, 2067-2085.
- GWR, U. S. EPA. 2000. National Primary Drinking Water Regulations: Ground Water Rule. Proposed Rule. *Federal Register*, 10 (65), 30194-30274.
- Hancock, C. M., Rose, J. B. and Callahan, M. 1998. Crypto and Giardia in US groundwater. *J. AWWA.* 90, 58-61.
- Harter, T., Wagner, S. and Atwill E. R. 1999. Colloid transport and filtration of *Cryptosporidium parvum* in sandy soils and aquifer sediments. *Environ. Sci. Tech.*
- Harvey R. W. 1997. Microorganisms as tracers in groundwater injection and recovery experiments: a review. *FEMS Microbiol. Rev.* 20, 461-472.
- Harvey, R. W. and Garabedian, S. P. 1991. Use of colloid filtration theory in modeling movement of bacteria through a contaminated sandy aquifer. *Environ. Sci. Technol.* 25: 178-185.
- Hassanizadeh, S. M. and Schijven, J. F. 2000. Use of bacteriophages as tracers for the study of removal of viruses. In: *Tracers and Modeling in Hydrogeology*, ed. A. Dassargues. Proceedings of TRAM2000 held in Liege, Belgium, 23-26 May 2000, pp. 167-174.
- Havelaar, A. H. 1986. F-specific bacteriophages as model viruses in water treatment processes. Ph. D. Thesis, University of Utrecht, The Netherlands 240 pp.
- Havelaar, A. H. 1993. Bacteriophages as models of enteric viruses in the environment. *ASM News* 59, 614-619.
- Havelaar, A. H., Hogeboom, W. M. and Pot, R. 1984. F-specific RNA-bacteriophages in sewage: methodology and occurrence. *Water Sci. Technol.* 17, 645-655.
- Havelaar, A. H., van Olphen, M. and Drost, Y. C. 1993. F-specific RNA bacteriophages are adequate model organisms for enteric viruses in fresh water. *Appl. Environ. Microbiol.* 59, 2956-2962.
- Havelaar, A. H., van Olphen, M. and Schijven, J. F. 1995. Removal and inactivation of viruses by drinking water treatment processes under full scale conditions. *Water. Sci. Technol.* 31: 55-62.
- Hejkal, T. W., Wellings, F. M., Lewis, A. L. and LaRock, P. A. 1981. Distribution of viruses associated with particles in wastewater. *Appl. Environ. Microbiol.* 41, 628-634.
- Hendry, M. J., Lawrence, J. R. and Maloszewski, P. 1997. The role of sorption in the transport of *Klebsiella oxytoca* through saturated silica sand. *Ground Water*, 35: 575-584.
- Herbold-Paschke, K., Straub, U., Hahn, T., Teutsch, G. and Botzenhart, K. 1991. Behaviour of pathogenic bacteria, phages and viruses in groundwater during transport and adsorption. *Water Sci. Tech.* 24, 301-304.

## References

---

- Hijnen, W. A. M., Veenendaal, D., van der Speld, W. M. H., Visser, A., Hoogenboezem, W. and van der Kooij, D. 2000. Enumeration of faecal indicator bacteria in large water volumes using on site membrane filtration to assess water treatment efficiency. *Water Res.* 34: 1659-1665.
- Hinsby, K., McKay, L. D., Jorgensen, P., Lenczewski, M. and Gerba C. P. 1996. Fracture aperture measurements and migration of solutes, viruses and immiscible creosote in a column of clay-rich till. *Ground Water* 34, 1065-1075.
- Hofmann, T. and Schöttler, U. 1998. Microparticle facilitated transport of contaminants during artificial groundwater recharge. Proceedings of the Third International Symposium on Artificial Recharge of Groundwater, A.A. Balkema, Rotterdam, The Netherlands, pp. 205-210.
- Hogg, C. V. and Craig, A. T. 1995. Introduction to mathematical statistics. Englewood Cliffs, N. J., Prentice Hall.
- Hoogenboezem, W., Ketelaars H. A. M., Medema G. J., Rijs, G. B. J. and Schijven, J. F. 2000. *Cryptosporidium* en *Giardia*: voorkomen in rioolwater, mest en oppervlaktewater met zwem- en drinkwaterfunctie. RIWA/RIVM/RIZA-rapport. ISBN 9036953324.
- Hornberger G. M., Mills, A. L. and Herman, J. S. 1992. Bacterial transport in porous media: Evaluation of a model using laboratory observations. *Water Resour. Res.* 28, 915-938.
- Houba, V. J. G., Van der Lee, J. J., Novoamsky, I. and Wallinga I. 1989. Soil and plant analysis; a series of syllabi. Part 5: Soil analysis procedures, 5<sup>th</sup> edition. Wageningen University, The Netherlands.
- Hurst, C. J., Gerba, C. P. and Cech, I. 1980. Effects of environmental variables and soils characteristics on virus survival in soil. *Appl. Environ. Microbiol.* 40, 1067-1079.
- Hurst, C. J., Wild, D. K. and Clark, R. M. 1992. Comparing the accuracy of equation formats for modelling microbial population decay rates. In: "Modelling the metabolic and physiologic activities of micro-organisms", pp. 149-175 (C.J. Hurst, ed., John Wiley & Sons. Inc., New York).
- ISO (International Organization for Standardization). 1995. Water quality - Detection and enumeration of F-specific RNA-bacteriophages - Part 1: Method by incubation with a host strain., *ISO 10705-1*, Geneva.
- ISO (International Organization for Standardization). 2000. Water quality - Detection and enumeration of bacteriophages - Part 1: Enumeration of F-specific RNA-bacteriophages, *ISO 10705-1*, Geneva.
- ISO (International Organization for Standardization). 2000. Water quality - Detection and enumeration of bacteriophages - Part 2: Enumeration of somatic coliphages, *ISO 10705-2*, Geneva.
- Jansons, J., Edmonds, L. W., Speight, B. and Bucens, M. R. 1989a. Movement of viruses after artificial recharge. *Water Res.* 23, 293-299.
- Jansons, J., Edmonds, L. W., Speight, B. and Bucens, M. R. 1989b. Survival of viruses in groundwater. *Water Res.* 23, 301-306.
- Jin, Y., Chu, Y. and Li, Y. 2000. Virus removal and transport in saturated and unsaturated sand columns. *J. Contam. Hydrol.* 43, 111-128.
- Jin, Y., M. V. Yates, Thompson, S.S. and Jury, W. A. 1997. Sorption of viruses during flow through saturated sand columns. *Environ. Sci. Technol.* 31, 548-55.
- Kapikian, A. Z., Estes, M. K. and Chanock, R. M. 1996. Norwalk group of viruses, pp. 783-810. In Field, B. N., Knipe, D. M., Howley, P. M., Chanock, R. M., Melnick, J. L.,

- Monath, T. P., Roizman, B. and Straus, S. E. (eds.) *Fields Virology*, 3<sup>rd</sup> ed. vol. 1. Lippincott-Raven, Philadelphia, Pa.
- Keswick, B. H. and Gerba, C. P. Viruses in groundwater. 1980. *Environ. Sci. Technol.* 14, 1290-1297.
- Keswick, B. H., Gerba, C. P., Secor, S. L. and Cech, I. 1982. Survival of enteric viruses and indicator bacteria in groundwater. *J. Environ. Sci. Health.* A12, 903-912.
- Kinoshita, T., Bales, R. C., Maguire, K. M. and Gerba, C. P. 1993. Effect of pH on bacteriophage transport through sandy soils. *J. Cont. Hydrol.* 14, 55-70.
- Knorr, N. 1937. Die Schutzzonenfrage in der Trinkwasser-hygiene. *Das Gas- und Wasserfach* 80 : 330-355.
- Konert, M. and Vandenberghe, J. 1997. Comparison of laser grain size analysis with pipette and sieve analysis: an solution for the underestimation of the clay fraction. *Sedimentology.* 44, 523-535.
- Lahti, K. and Hiisvirta, L. 1995. Causes of waterborne outbreaks in community water systems in Finland: 1980-1992. *Water Sci. Tech.* 31, 33-36.
- Lance, J. C., Gerba, C. P. and Wang, D. S. 1982. Comparative movement of different enteroviruses in soil columns. *J. Environ. Qual.* 11, 347-351.
- Landry, E. F., Vaughn, J. M., Vicalet, T. J., and Mann, R. 1983. Accumulation of sediment-associated viruses in shellfish. *Appl. Environ. Microbiol.* 46, 673-682.
- Levine, A. D., Tchobanoglous, G. and Asano, T. 1985. Characterisation of the size distribution of contaminants in wastewater: treatment and reuse implications. *J. Water Pollut. Control. Fed.* 57, 805-816.
- Li, S. 1993. Modeling biocolloid transport in saturated porous media. Ph.D. thesis, University of Arizona, Tucson.
- Liew, P. F. and Gerba, C. P. 1980. Thermostabilization of enteroviruses by estuarine environment. *Appl. Environ. Microbiol.* 40, 305-308.
- Lipson, S. M. and Stotzky, G. 1983. Adsorption of reovirus to clay minerals: effects of cation-exchange capacity, cation saturation and surface area. *Appl. Environ. Microbiol.* 46, 673-682.
- Lodder, W. J., Nijst, O. E. M., Holwerda, A., Leenen, E. J. T. M. and de Roda Husman, A. M. 2001. Presence of human caliciviruses in Dutch surface waters. In preparation.
- Lodder, W. J., Vinjé, J., van der Heide, R., de Roda Husman, A. M., Leenen, E. J. T. M. and Koopmans, M. P. G. 1999. Molecular detection of Norwalk-like caliciviruses in sewage. *Appl. Environ. Microbiol.* 65, 5624-5627.
- Loveland, J. P., Ryan, J. N., Amy, G. L. and Harvey, R. W. 1996. The reversibility of virus attachment to mineral surfaces. *Colloids and Surfaces. A: Physicochemical and Engineering Aspects.* 107, 205-221.
- Lytle, C. D. and Routson, L. B. 1995. Minimised virus binding for test barrier materials. *Appl. Environ. Microbiol.* 61, 643-649.
- Macler, B. A. 1996. Developing the Ground Water Disinfection Rule. *J. Am. Water Works. Assoc.* 88, 47-55.
- Marquardt, D. W. 1963. An algorithm for least-squares estimation of nonlinear parameters, *J. Soc. Ind. Appl. Math.* 11:431-441.
- Martin, R. E., Bouwer, E. J. and Hanna, L. M. 1992. Application of clean bed filtration theory to bacterial deposition in porous media. *Environ. Sci. Technol.* 26, 1053-1058.
- Matthess, G., Pekdeger, A., and Schroeter, J. 1988. Persistence and transport of bacteria and viruses in groundwater - a conceptual evaluation. *J. Contam Hydrol.* 2, 171-188.

## References

---

- McCaulou, D. R., Bales R. C. and McCarthy, J. F. 1994. Use of short-pulse experiments to study bacteria transport through porous media. *J. Contam. Hydrol.*, 15: 1-14.
- McCaulou, D. R., Bales, R. C. and Arnold, R. G. 1995. Effect of temperature-controlled transport of bacteria and microspheres through saturated sediment. *Water Resour. Res.*, 31: 271-280.
- McKay, L. D., Gillham, R. W. and Cherry, J. A. 1993. Field experiments in a fractured clay till. 2. Solute and colloid transport. *Water Resour. Res.* 29, 3879-3890.
- Medema, G. J. and Havelaar, A. H. 1994. Microorganisms in water: A health risk. National Institute of Public Health and the Environment, Bilthoven. Report 289202002 (in Dutch).
- Medema, G. J., Ketelaars, H. A. M. and Hoogenboezem, W. 1996. *Cryptosporidium* and *Giardia* in the Rhine and the Meuse. RIVM/RIWA-report. Report 289202 015 (in Dutch).
- Medema, G. J., Schijven, J. F., de Nijs, A. C. M. and Elzenga, J. G. 1997. Modeling of the discharge of *Cryptosporidium* and *Giardia* by domestic sewage and their dispersion in surface water. In: Proceedings Int. Symp. On Waterborne Cryptosporidium. Newport Beach CA, USA.
- Metcalf, T. G., Rao, V. C and Melnick, J. L. 1984. Solid associated viruses in a polluted estuary. *Monog. Virol.* 15, 97-110.
- Miettinen, I. T., Zacheus, O., von Bonsdorff, C. H. and Vartiainen, T. 2000. Waterborne epidemics in Finland 1998 -99. Proceedings of 10<sup>th</sup> health related water microbiology symposium, IWA, Paris, HRM2.
- Moore, G. T, Cross, W. M., McGuire, C. D., Mollohan, C. S., Gleason, N. N., Healy, G. R. and Newton, L. H. 1969. Epidemic giardiasis at a ski resort. *New England J. Med.* 281, 402.
- Moore, R. S., Taylor and D. H., Sturman, L. S. 1982. Adsorption of reovirus by minerals and soils. *Appl. Environ. Microbiol.* 44, 852-859.
- Moore, R. S., Taylor, D. H. and Sturman, L. S. 1981. Poliovirus adsorption by 34 minerals and soils. *Appl. Environ. Microbiol.* 42, 963-975.
- Mülschlegel, J. H. C. and Kragt, F. J. 1998. Waterwinning en waterverbruik bij doelgroepen. National Institute of Public Health and the Environment, Bilthoven. Report 703717003 (in Dutch).
- Munster, C. L., Mathewson, C. C. and Wroblewski, C. L. 1996. *Environmental Engineering and Geosciences* 2, 517-530.
- Nasser, A., Tchorch, Y., and Fattal, B. 1993. Comparative survival of *E. coli*, F<sup>+</sup>bacteriophages, HAV and poliovirus 1 in wastewater and groundwater. *Water Sci. Tech.* 27, 401-407.
- Ouyang, Y., Shinde, D., Mansell, R. S. and Harris, W. 1996. Colloid-enhanced transport of chemicals in subsurface environments: A review. *Crit. Rev. Environ. Sci. Tech.* 26, 189-204.
- Park, N. S., Blandford, T. N. and Huyacorn, P. S. 1994. VIRALT- A model for simulating viral transport in groundwater. Documentation and user's guide. Version 3.0, HydroGeologic, Herndon, VA.
- Park, N. S., Blandford, T. N., Wu, Y. S. and Huyacorn, P. S. 1995. CANVAS- A composite analytical-numerical model for viral and solute transport simulation. Documentation and user's guide. Version 2.1, HydroGeologic, Herndon, VA.

- Pastours, M.J.H. 1992 National Groundwater Model; Conceptual model description, National Institute of Public Health and the Environment, Bilthoven. Report 714305004 (in Dutch).
- Paul, J. H., Rose, J. B. and Jiang, S. C. 1997. Evidence for groundwater and surface marine water contamination by waste disposal wells in the Florida Keys. *Water Res.* 31, 1448-1454.
- Paul, J. H., Rose, J. B., Brown, J., Shinn, E. A., Miller, S. and Farrah S. R. 1995. Viral tracer studies indicate contamination of marine waters by sewage disposal practices in Key Largo, Florida. *Appl. Environ. Microbiol.* 61, 2230-2234.
- Payment, P., Morin, E. and Trudel, M. 1988. Coliphages and enteric viruses in the particulate phase of river water. *Can. J. Microbiol.* 34, 907-910.
- Pedly, S. and Howard, G. The public health implications of microbiological contamination of groundwater. *Quart. J. Engin. Geol.* 1997. 30, 179-188.
- Penrod, S. L., Olson, T. M. and Grant, S. B. 1995. Whole particle microelectrophoresis for small viruses. *J. Coll. Interface Sci.* 173, 521-523.
- Penrod, S. L., Olson, T. M. and Grant, S. B. 1996. Deposition kinetics of two viruses in packed beds of quartz granular media. *Langmuir*, 12, 5576-5587.
- Peters, J. H. 1996. Are there any blueprints for artificial recharge? Proceedings of an International Symposium on Artificial Recharge of groundwater, Helsinki, Nordic Hydrological Program NHP Report no, 38.
- Peters, J. H., Slings, Q. L. and Stakelbeek, A. 1992. Open infiltratie Nieuwe Stijl, H<sub>2</sub>O, 25, 532-537 (in Dutch).
- Pieper, A. P., Ryan, J. N., Harvey, R. W., Amy, G. L., Illangasekare, T. H. and Metge, D. W. 1997. Transport and recovery of bacteriophage PRD1 in a sand and gravel aquifer: Effect of sewage-derived organic matter. *Environ. Sci. Technol.* 31, 1163-1170.
- Poletika, N. N., Jury, W. A. and Yates, M. V. 1995. Transport of bromide, simazine, and MS-2 coliphage in a lysimeter containing undisturbed, unsaturated soil. *Water Resour. Res.* 31, 801-810.
- Powelson, D. K. and Gerba, C. P. 1994. Virus removal from sewage effluents during saturated and unsaturated flow through soil columns. *Water Res.* 28, 2175-2181.
- Powelson, D. K., Gerba, C. P. and Yahya, M. T. 1993. Virus transport and removal in wastewater during aquifer recharge. *Water Res.* 27, 583-590.
- Powelson, D. K., Simpson, J. R. and Gerba, C. P. 1990. Virus transport and survival in saturated and unsaturated flow through soil columns. *J. Environ. Qual.* 19, 396-401.
- Powelson, D. K., Simpson, J. R. and Gerba, C. P. 1991. Effects of organic matter on virus transport in unsaturated flow. *Appl. Environ. Microbiol.* 57, 2192-2196.
- Pyne, R. D. G. 1995. Groundwater recharge and wells: a guide to aquifer storage and recovery. CRC Press, Inc. (Lewis Publ.), Boca Raton (FL, USA).
- Rao, V. C., Siedel, K. M., Goyal, S. M., Metcalf, T. G. and Melnick, J. L. 1984. Isolation of enteroviruses from water, suspended solids and sediments from Galveston Bay: Survival of poliovirus and rotavirus adsorbed to sediment. *Appl. Environ. Microbiol.* 48, 404-409.
- Redman, J. A., Grant, S. B., Olson, T. M., Adkins, J. M., Jackson, J. L., Castillo, M. S. and Yanko, W. A. 1999. Physicochemical mechanisms responsible for the filtration and mobilization of a filamentous bacteriophage in quartz sand. *Water Res.* 33, 43-52.

## References

---

- Redman, J. A., Grant, S. B., Olson, T. M., Hardy, M. E. and Estes, M. K. 1997. Filtration of recombinant Norwalk virus particles and bacteriophage MS2 in quartz sand: Importance of electrostatic interactions. *Environ. Sci. Technol.* 31, 3378-3383.
- Regli, S., Rose, J. B., Haas, C. N. and Gerba, C. P. 1991. Modeling the risk from *Giardia* and viruses in drinking water. *J. Am. Water Works Assoc.* 213, 76-84.
- REGWAT. 1989. Registratie en verwerking van waterkwantiteitsgegevens van waterleidingbedrijven en industrie. ISDIV database, Rijksinstituut voor Volksgezondheid en het Milieu, Laboratorium voor Bodem- en Grondwateronderzoek.
- Rehman, L. L. C., Welty, C. and Harvey, R. W. 1999. Stochastic analysis of virus transport in aquifers. *Water Resour. Res.* 35, 1987-2006.
- REWAB. 2000. Registratie en verwerking van waterkwaliteitsgegevens van waterleidingbedrijven 1991-1998. ISDIV database, Rijksinstituut voor Volksgezondheid en het Milieu, Laboratorium voor Water- en Drinkwateronderzoek.
- Rijnaarts, H. H. M., Norde, W., Bouwer, E. J., Lyklema, J. L. and Zehnder, A. J. B. 1995. Reversibility and mechanism of bacterial adhesion. *Colloids Surf. B.*, 4: 5-22.
- Rose, J. B. 1998. Occurrence and significance of *Cryptosporidium* in water. *J. Amer. Water Works Assoc.* 80, 53-58.
- Rossi, P. 1994. Advances in biological tracer techniques for hydrology and hydrogeology using bacteriophages. Ph.D. Thesis, University of Neuchatel, Switzerland, 200 pp.
- Rossi, P., De Carvalho-Dill, A., Muller, I. and Aragno, M. 1994. Comparative tracing experiments in a porous aquifer using bacteriophages and fluorescent dye on a test field located at Wilerwald (Switzerland) and simultaneously surveyed on a local scale by radio-magneto-tellury (12-240 kHz). *Environ. Geol.* 23, 192-200.
- Ryan, J. N. and Elimelech, M. 1996. Colloid mobilization and transport in groundwater. *Colloids and Surfaces. A: Physicochemical and Engineering Aspects* 107, 1-56.
- Ryan, J. N., Elimelech, M., Ard, R. A., Harvey, R. W. and Johnson, P. R. 1999. Bacteriophage PRD1 and silica colloid transport and recovery in an iron oxide-coated sand aquifer. *Environ. Sci. Technol.* 33, 63-73.
- Sakoda, A., Sakai, Y., Hayakawa, K. and Suzuki, M. 1997. Adsorption of viruses in water environment onto solid surfaces. *Water Sci. Tech.* 35, 107-114.
- Sartory, D. P., Field, M., Curbishley, S. M. and Pritchard, A. M. 1998. Evaluation of two media for the membrane filtration enumeration of *Clostridium perfringens* from water. *Lett. Appl. Microbiol.* 27, 323-327.
- Schijven, J. F. and Hassanizadeh, S. M. 2000. Removal of viruses by soil passage: overview of modeling, processes and parameters. *Crit. Rev. Environ. Sci. Technol.*, 30: 49-127.
- Schijven, J. F. and Hassanizadeh, S.M. 2001. A procedure for predicting virus removal by soil passage. *Groundwater*. In preparation.
- Schijven, J. F. and Hassanizadeh, S.M. 2001. Groundwater vulnerability to virus contamination in sandy aquifers: A worst case approach. *Appl. Environ. Microbiol.* In preparation.
- Schijven, J. F. and Rietveld, L. C. 1996. How do field observations compare with models of microbial removal? pp 105-114. In: *Under the microscope. Examining microbes in groundwater*. Am. Water Works Assoc. Res. Found., Denver, Colorado.
- Schijven, J. F. and Simunek J. 2001. Kinetic modeling of virus removal in heterogeneous porous media. *J. Contam. Hydrol.* Submitted.

- Schijven, J. F., Annema, J. A., de Nijs, A. C. M., Theunissen, J. J. H. and Medema, G. 1995. Enteroviruses in surface waters in The Netherlands – Emission and distribution calculated with PROMISE and WATNAT – a pilot study. National Institute of Public Health and the Environment, Bilthoven. Report 289202006 (in Dutch).
- Schijven, J. F., de Bruin, H. A. M., Engels, G. B. and Leenen, E. J. T. M. 1999. Emission of *Cryptosporidium* and *Giardia* by domestic farm animals. National Institute of Public Health and the Environment, Bilthoven. Report 289202 023 (in Dutch).
- Schijven, J. F., de Bruin, H. A. M. and Hassanizadeh, S. M. 2001a. On the nonlinear removal of bacteriophages by passage through saturated dune sand. Appl. Environ. Microbiol. Submitted.
- Schijven, J. F., de Bruin, H. A. M. and Hassanizadeh, S. M. 2001b. Modeling of bacteriophage transport through saturated dune sand at field and laboratory scale. Adv. Water Resour. Submitted.
- Schijven, J. F., de Bruin, H. A. M., Hassanizadeh, S. M. and de Roda Husman, A. M. 2001c. Indicator organisms for removal of pathogenic microorganisms by passage through saturated dune sand. Appl. Environ. Microbiol. Submitted.
- Schijven, J. F., Hassanizadeh, S. M., Dowd, S. E., Pillai, S. D. 2001d. Modeling virus adsorption in batch and column experiments, Quant Microbiol. In press.
- Schijven, J. F., Hoogenboezem, W., Hassanizadeh, S. M. and Peters, J. H. 1999. Modelling removal of bacteriophages MS2 and PRD1 by dune infiltration at Castricum, the Netherlands. Water Resour. Res. 35: 1101-1111.
- Schijven, J. F., Hoogenboezem, W., Nobel, P. J., Medema, G., Stakelbeek, A. 1998. Reduction of FRNA-bacteriophages and faecal indicator bacteria by dune infiltration and estimation of sticking efficiencies, Water Sci. Technol. 38, 127-131.
- Schijven, J. F., Medema, G. J., de Nijs, A. C. M. and Elzenga, J. G. 1996. Emission and dispersion of *Cryptosporidium*, *Giardia* and enteroviruses via domestic wastewater. National Institute of Public Health and the Environment, Bilthoven, The Netherlands. Report number 289202014 (in Dutch).
- Schijven, J. F., Medema, G., Vogelaar, A. J. and Hassanizadeh, S. M. 2000. Removal of microorganisms by deep well injection. J. Contam. Hydrol. 44, 301-327.
- Schijven, J. F., Medema, G. J., de Nijs, A. C. M. and Elzenga, J. G. 1996. Emission and distribution of *Cryptosporidium*, *Giardia* and enteroviruses via domestic wastewater. National Institute of Public Health and the Environment, Bilthoven. Report 289202 014 (in Dutch).
- Selim, H. M., Schulin, R. and Flüher, H. 1987. Transport and ion exchange of calcium and magnesium in an aggregated soil. Soil Sci. Soc. Am. J. 51(4): 876-884.
- Shields, P. A. and Farrah, S. R. 1983. Influence of salts on electrostatic interactions between poliovirus and membrane filters. Appl. Environ. Microbiol. 45, 526-531.
- Shields, P. A. and Farrah, S. R. 1987. Determination of the electrostatic and hydrophobic character of enteroviruses and bacteriophages, abstr, Q-82. Program Abstr. 87<sup>th</sup> Annu. Meet. Amer. Soc. Microbiol. American Society for Microbiology, Washington, D.C.
- Sim, Y. and Chrysikopoulos, C. V. 1995. Analytical models for one-dimensional virus transport in saturated porous media. Water Resour. Res. 31, 1429-1437.
- Sim, Y. and Chrysikopoulos, C. V. 1996. One-dimensional virus transport in porous media with time-dependent inactivation rate coefficients. Water Resour. Res. 32, 2607-2611.
- Sim, Y. and Chrysikopoulos, C. V. 1998. Three-dimensional analytical models for virus transport in saturated porous media. Transport in Porous Media 30, 87-112.

## References

---

- Šimůnek, J., Šejna, M., and van Genuchten, M. Th. 1999. The HYDRUS-2D software package for simulating two-dimensional movement of water, heat, and multiple solutes in variably saturated media. Version 2.0, *IGWMC - TPS - 53*, International Ground Water Modeling Center, Colorado School of Mines, Golden, Colorado, 251 pp.
- Šimůnek, J., Šejna, M., and van Genuchten, M. Th. 1998. The HYDRUS-1D software package for simulating the one-dimensional movement of water, heat, and multiple solutes in variably-saturated media. Version 2.0, *IGWMC - TPS - 70*, International Ground Water Modeling Center, Colorado School of Mines, Golden, Colorado, 202 pp.
- Simizu, Y., Sogabe, H. and Terashima, Y. 1998. The effects of colloidal humic substances on the movement of non-ionic hydrophobic organic contaminants in groundwater. *Water Sci. Tech.* 38, 159-167.
- Singh, S. N., Bassous, M., Gerba, C. P. and Kelley, L. M. 1986. Use of dyes and proteins as indicators of virus adsorption to soils. *Water Res.* 20, 267-272.
- Sinton, L. W., Finlay, R. K., Pang, L. and Scott, D. M. 1997. Transport of bacteria and bacteriophages in irrigated effluent into and through an alluvial gravel aquifer. *Water Air and Soil Pollution* 98, 17-42.
- Smith, E. M., Gerba, C. P. and Melnick, J. L. 1978. Role of sediment in the persistence of enteroviruses in the estuarine environment. *Appl. Environ. Microbiol.* 35, 685-689.
- Sobsey, M. D., Dean, C. H., Knuckles, M. E. and Wagner, R. A. 1980. Interaction and survival of enteric viruses in soil materials. *Appl. Environ. Microbiol.* 40, 92-101.
- Sobsey, M. D., Hall, R. M. and Hazard, R. L. 1995. Comparative reductions of hepatitis A virus, enteroviruses and coliphage MS2 in miniature soil columns. *Water Sci. Tech.* 31, 203-209.
- Sobsey, M. D., Shields, P. A., Hauchmann, F. H., Hazard, R. L. and Caton, L. W. 1986. Survival and transport of hepatitis A virus in soils, groundwater, and wastewater. *Water Sci. Tech.* 18, 97-106.
- Stuart, A. and Ord, J. K. 1987. Kendall's advanced theory of statistics 1: Distribution theory. *Charles Griffin and Co.*, London, 5<sup>th</sup> edition.
- Stuyfzand, P. J. 1993. Hydrochemistry and hydrology of the coastal dune area of the Western Netherlands, Ph.D. Dissertation, the Vrije Universiteit, Amsterdam, ISBN 90-74741-01-0, 366 pp.
- Stuyfzand, P. J. 1998. Quality changes upon injection into anoxic aquifers in The Netherlands: Evaluation of 11 experiments. Proceedings of the Third International Symposium on Artificial Recharge of Groundwater. A.A. Balkema, Rotterdam, The Netherlands, pp. 283-291.
- Stuyfzand, P. J. 1999. Deep well injection in Zuid-Oost Nederland (DIZON) Final report on quality changes during soil passage. Kiwa, Nieuwegein, The Netherlands, Report KOA 99.054 (in Dutch).
- Stuyfzand, P. J. and Lüers F. 1996. Gedrag van milieugevaarlijke stoffen bij oeverfiltratie en kunstmatige infiltratie. Effecten van bodempassage gemeten langs stroombanen. Kiwa, Nieuwegein. Mededeling 125 (In Dutch).
- Stuyfzand, P. J. and van der Jagt, H. 1997. Toelichting op de anorganisch-chemische analysemethoden voor grond in het LAM van Kiwa. Kiwa, Nieuwegein, The Netherlands, Report OA 96.116 (in Dutch).
- Swanton, S. W. 1995. Modelling colloid transport in groundwater; the prediction of colloid stability and retention behaviour. *Adv. in Colloid and Interface Science* 54, 129-208.

- Taylor, D. H., Bellamy, A. R. and Wilson, A. T. 1980. Interactions of bacteriophages R17 and reovirus type III with the clay mineral allophane. *Water Res.* 14, 339-346.
- Taylor, D. H., Moore, R. S. and Sturman, L. S. 1981. Influence of pH and electrolyte composition on adsorption of poliovirus by soils and minerals. *Appl. Environ. Microbiol.* 42, 976-984.
- Teunis, P. F. M., van der Heijden, O. G., van der Giessen J. W. B. and Havelaar, A. H. 1996. The dose-response relation in human volunteers for gastro-intestinal pathogens., RIVM Report 284550002, 97 pp.
- Theunissen, J. J. H., Nobel, P. J., van de Heide, R., de Bruin, H. A. M., van Veendendaal, D., Lodder, W. J., Schijven, J. F., Medema, G. J., and van de Kooij, D. 1998. Enterovirus concentrations at intake points for drinking water production. National Institute of Public Health and the Environment, Bilthoven. Report 289202 013 (in Dutch).
- Thompson, S. S., Flury, M., Yates, M. V. and Jury, W. A. 1998. Role of the air-water-solid interface in bacteriophage sorption experiments. *Appl. Environ. Microbiol.* 64, 304-309.
- Tim, U. S. and Mostaghimi, S. 1991. Model for predicting virus movement through soils. *Ground Water* 29, 251-259.
- Tisa, L. S., Koshikawa, T. and Gerhardt, P. 1982. Wet and dry bacterial spore densities determined by buoyant sedimentation. *Appl. Environ. Microbiol.* 43: 1307-1310.
- Toride, N., Leij, F.J. and van Genuchten, M. T. 1995. The CXTFIT code for estimating transport parameters from laboratory or field tracer experiments. Version 2.0. US Salinity Laboratory, Agricultural Research Service, US Department of Agriculture, Riverside, California, Report No. 137.
- Van Genuchten, M. Th., and Wagenet, R. J. 1989. Two-site/two-region models for pesticide transport and degradation: Theoretical development and analytical solutions. *Soil Sci. Soc. Am. J.* 53: 1303-1310.
- Van Olphen, M., Kapsenberg, J. G., van de Baan, E., and Kroon, W. A. 1984. Removal of enteric viruses from surface water at eight waterworks in The Netherlands. *Appl. Environ. Microbiol.*, 47, 927-932.
- VEWIN 1998. Waterleidingstatistiek 1997. Vereniging van Exploitanten van Waterleidingbedrijven in Nederland. (in Dutch). ISSN 0922-8101.
- Vilker, V. L., Meronek, G. C. and Bulter, P. C. 1983. Interaction of poliovirus with montmorillonite clay in phosphate-buffered saline. *Eviron. Sci. Technol.* 17, 631-634.
- Vilker, V.L. and Burge, W.D. 1980. Adsorption mass transfer model for virus transport in soils. *Water Res.* 14, 783-790.
- Vogelaar A. J. 1999. Deep well injection in the southeast of The Netherlands (DIZON): Clogging and declogging of injection well IP2. Kiwa, Nieuwegein, The Netherlands, Report KOA 99.035 (in Dutch).
- Vogelaar, A. J., van Baar, M. J. C., Peters, J. H. and Bergsma J. 1997. Report of NaCl-tracer experiments in December 1996 at Castricum. Kiwa, Nieuwegein, The Netherlands, report SWI 97.115 (in Dutch).
- VROM 1995. Infectierisico van virussen en parasitaire protozoa via drinkwater. Notitie ter voorbereiding van beleidsstandpunt. Concept 17 maart 1995. Directie DWL, VROM, Den Haag.
- Wait, D. A. and Sobsey, M. D. 1983. Method for recovery of enteric viruses from estuarine sediments with chaotropic agents. *Appl. Environ. Microbiol.* 46, 379-385.

## References

---

- Wang, D. S., Gerba, C. P. and Lance, J. C. 1981. Effect of soil permeability on virus removal through soil. *Appl. Environ. Microbiol.* 42, 83-88.
- Woody, M. A. and Cliver, D. O. 1995. Effects of temperature and host cell growth phase on replication of F-specific RNA coliphage Q beta. *Appl. Environ. Microbiol.* 61: 1520-1526.
- Yahya, M. T., Galsomies, L., Gerba, C. P. and Bales, R. C. 1993. Survival of bacteriophages MS2 and PRD1 in groundwater. *Water Sci. Tech.* 27, 409-412.
- Yao, K. M., Habibian, M. T. and O'Melia, C. R. 1971. Water and waste water filtration: concepts and applications. *Environ. Sci. Technol.* 5, 1105-1112.
- Yates, M. V., Yates, S. R., Wagner J. and Gerba C. P. 1987. Modelling virus survival and transport in the subsurface. *J. Contam. Hydrol.* 1, 329-345.
- Yates, M. V. 1985. Septic tank density and groundwater contamination. *Ground Water* 23: 586-591.
- Yates, M. V. 1995. Field evaluation of the GWDR's natural disinfection criteria. *J. Am. Water Works Assoc.* 87, 76-85.
- Yates, M. V. and Ouyang, Y. 1992. VIRTUS, a model of virus transport in unsaturated soils. *Appl. Environ. Microbiol.* 58, 1609-1616.
- Yates, M. V. and Yates, S. R. 1987. A comparison of geostatistical methods for estimating virus inactivation rates in groundwater. *Water Res.* 21, 1119-1125.
- Yates, M. V. and Yates, S. R. 1988. Virus survival and transport in groundwater. *Water Sci. Tech.* 20, 301-307.
- Yates, M. V. and Yates, S. R. 1991. Modeling microbial transport in the subsurface: a mathematical discussion. In: *Modeling the environmental fate of microorganisms*, edited by C. J. Hurst, pp. 48-76, Am. Soc. for Microbiol., Washington DC.
- Yates, M. V., Gerba, C. P. and Kelley, L. M. 1985. Virus persistence in groundwater. *Appl. Environ. Microbiol.* 49, 778-781.
- Yates, M. V., Yates, S. R., Wagner, J. and Gerba, C. P. 1987. *Journal of Contaminant Hydrology* 1, 329-345.
- Yates, M. V., Yates, S. R., Warrick, A. W. and Gerba, C. P. 1986. Use of geostatistics to predict virus decay rates for determination of septic tank setback distances. *Appl. Environ. Microbiol.* 52, 479-483.
- Zuckerman, H., Gold D., Shelef, G., Yuditsky, A. and Armon, R., 1997. Microbial degradation of *Cryptosporidium parvum* by *Serratia marcescens* with high chitinolytic activity. *Proc. Int. Symp. on waterborn Cryptosporidium*, Newport Beach, CA.

---

**This dissertation was based on the following publications**

**Publications in refereed journals**

1. **Schijven, J. F.**, Hoogenboezem, W., Nobel, P. J., Medema, G. J. and Stakelbeek, A. 1998. Reduction of FRNA-bacteriophages and faecal indicator bacteria by dune infiltration and estimation of sticking efficiencies. *Water Sci. Technol.* 38, 127-131.
2. **Schijven, J. F.**, Hoogenboezem, W., Hassanizadeh, S. M., Peters, J. H. 1999. Modelling removal of bacteriophages MS2 and PRD1 by dune recharge at Castricum, Netherlands. *Water Resour. Res.* 35, 1101-1111.
3. **Schijven, J. F.**, Hassanizadeh, S. M. 2000. Removal of viruses by soil passage: overview of modeling, processes and parameters. *Crit. Rev. Environ. Sci. Tech.* 31, 49-125.
4. **Schijven, J. F.**, Hassanizadeh, S. M., Dowd, S. E. and Pillai, S. D. 2001. Modeling virus adsorption in batch and column experiments. *Quant. Microbiol.* In press.
5. **Schijven, J. F.**, Medema, G. J., Vogelaar, A. J. and Hassanizadeh, S. M. 2000. Removal of microorganisms by deep well injection. *J. Contam. Hydrol.* 44, 301-327.
6. **Schijven, J. F.** and Simunek, J. 2001. Kinetic modeling of virus removal in heterogeneous porous media. *J. Contam. Hydrol.* Submitted.
7. **Schijven, J. F.**, de Bruin, H. A. M. and Hassanizadeh, S. M. 2001. On the nonlinear removal of bacteriophages by passage through saturated dune sand. *Appl. Environ. Microbiol.* Submitted.
8. **Schijven, J. F.**, de Bruin H. A. M and Hassanizadeh, S.M. 2001. Modeling of bacteriophage transport through saturated dune sand at field and laboratory scale. *Adv. Water Resour.* Submitted.
9. **Schijven J. F.**, de Bruin, H. A. M., Hassanizadeh, S. M. and de Roda Husman, A. M. 2001. Indicator organisms for removal of pathogenic microorganisms by passage through saturated dune sand. *Appl. Environ. Microbiol.* Submitted.

**Publications in preparation**

10. **Schijven, J. F.** and Hassanizadeh, S.M. 2001. A procedure for predicting virus removal by soil passage. *Groundwater.* In preparation.
11. **Schijven, J. F.** and Hassanizadeh, S.M. 2001. Groundwater vulnerability to virus contamination in sandy aquifers: A worst case approach. *Appl. Environ. Microbiol.* In preparation.

**Chapters of Books or Conference Proceedings and publications in non-refereed journals**

12. **Schijven, J. F.** and Rietveld, L. C. 1996. How do field observations compare with models of microbial removal? In: *The 1996 Proceedings of the Groundwater Foundation's 12<sup>th</sup> Annual Fall Symposium*, Boston, Massachusetts. 105-114
13. **Schijven, J.F.** and Hassanizadeh, S.M. 1998. An overview of modelling removal of viruses by soil passage. To appear in *Proceedings of Future Groundwater Resources at Risk*, Changchun, P.R. China.

## References

---

14. Hoogenboezem, W., **Schijven, J. F.**, Nobel, P. J. and Bergsma, J. De verwijdering van bacteriofagen tijdens duinpassage, *H2O*, 1999; 22: 29-31 (in Dutch).
15. Peters, J.H., **Schijven, J. F.**, Hoogenboezem, W., van Baar, M. J. C., Bergsma, J., Nobel, P. J., Stakelbeek, A. and Vogelaar, A. J. 1997. Fate of pathogens and consequences for the design of artificial recharge systems. In: 2.Deutsch-Niederländischer workshop Künstliche Grundwasseranreicherung, Schwerte (D)
16. Peters, J. H., **Schijven, J. F.**, Hoogenboezem, W., van Baar, M.J.C., Bergsma, J., Nobel, P. J., Stakelbeek, A. and Vogelaar, A. J. 1998. Fate of pathogens and consequences for the design of artificial recharge systems. In: Artificial recharge of groundwater (Peters, J.H. Ed.), A.A. Balkema, Rotterdam.
17. Hassanizadeh, S. M. and **Schijven, J.F.** 2000. Use of bacteriophages as tracers for the study of removal of viruses. In: Tracers and Modeling in Hydrogeology, ed. A. Dassargues (Proceedings of TRAM'2000 held in Liege, Belgium, 23-26 May 2000), pp. 167-174.
18. **Schijven, J. F.** and Hassanizadeh, S.M. 2000. Modeling of virus transport and removal in the subsurface. In:Encyclopedia of Environmental Microbiology, John Wiley and Sons. Eds. G.I Bitton, C. P. Gerba. Submitted.
19. **Schijven, J. F.**, Berger, P. and Miettinen, I. T. 2000. Removal of pathogens, surrogates, indicators and toxins using bank filtration. In: Bank filtration for water supply. Kluwer Academic, C. Ray (Ed.) Submission March 2001.

---

## Curriculum vitae

Jack Schijven (Jacobus Franciscus) werd op 3 februari 1957 geboren te Heerle (Noord-Brabant). Hij behaalde zijn HAVO-diploma in 1974 te Bergen op Zoom. In de periode 1975-1979 volgde hij het Hoger Natuurwetenschappelijk Onderwijs aan het Dr. Struycken-instituut Etten Leur. Vanaf 1980 was hij werkzaam als researchanalist op de afdeling Experimentele Cytologie van het Nederlands Kankerinstituut, Het Antoni van Leeuwenhoekhuis te Amsterdam. Hij verrichtte experimenteel onderzoek aan oncogenen met behulp van cytologische en moleculair-biologische technieken.

Intussen was zijn interesse voor automatisering gewekt en behaalde hij in de periode 1984 tot 1986 verschillende AMBI-certificaten op het gebied van informatica, alsmede het diploma wetenschappelijk programmeur PASCAL/FORTRAN. In 1989-1991 bekwaamde hij zich in UNIX-systeembeheer en in 1991 behaalde hij het AMBI-certificaat datacommunicatie en netwerken.

Vanaf 1986 is hij als onderzoeks-/informatiseringsmedewerker aan de slag gegaan op het Rijksinstituut voor Volksgezondheid en het Milieu (RIVM) op het toenmalige Laboratorium voor Water- en Levensmiddelenmicrobiologie (LWL). Voor ongeveer 60% zette hij zich in op watermicrobiologisch onderzoek, met name op het gebied van de microbiologische kwaliteit van zwemwater en kwaliteitscontrole van watermicrobiologisch onderzoek. Voor de overige 40% droeg hij de zorg voor het informatiserings-/automatiseringsbeleid van LWL.

Bij de oprichting van het Microbiologisch Laboratorium voor Gezondheidsbescherming (MGB) in 1995 koos hij geheel voor het onderzoek als modelleur op het gebied van watermicrobiologie. Naast het voorliggende promotieonderzoek over virusverwijdering door bodempassage voerde hij ook onderzoek uit naar de microbiologische kwaliteit van oppervlaktewater in Nederland door middel van emissie- en verspreidingsmodellering op nationale schaal.

---

# Appendix

## EQ2KIN code

Appendix –FORTRAN77 code of EQ2KIN.FOR

```

C EQ2KIN.FOR 03/02/2000
C
C *****
C *
C *   EQ2KIN VERSION 1.0
C *
C *   LAST MODIFIED:      August 16, 2000
C *
C *   NUMERICAL SOLUTION OF ONE-DIMENSIONAL DETERMINISTIC
C *   ONE-SITE EQUILIBRIUM AND TWO-SITE NONEQUILIBRIUM
C *   ADVECTION DISPERSION EQUATION
C *
C *   FOR DEVELOPMENT OF EXPLICIT SCHEME SEE:
C *   NE-ZHENG SUN,
C *   MATHEMATICAL MODELING OF GROUNDWATER POLLUTION,
C *   SPRINGER-VERLAG NY, 1995, CHAPTER 4,
C *   ISBN 3-540-94212-2
C *
C *
C *   JACK SCHIJVEN
C *   NATIONAL INSTITUTE FOR PUBLIC HEALTH AND THE ENVIRONMENT
C *   MICROBIOLOGICAL LABORATORY FOR HEALTH PROTECTION
C *   P.O. BOX 1, 3720 BA BILTHOVEN, THE NETHERLANDS
C *   TEL. +31 30 274 2994
C *   FAX. +31 30 274 4434
C *   E-MAIL JACK.SCHIJVEN@RIVM.NL
C *****
C
C   PROGRAM EQ2KIN
C
C   INTEGER i,j,ndx,ndt, stabilityfactor, mode, inputmode, nobs, t, n
C   REAL disp, v, c0, pulse_duration, xend, tfinal, dx, dt,
C   & att1, det1, att2, det2, muc, museq, mus1, mus2, Req,
C   & k1, k2, k3, k4, k5, k6, k7, k8, k9, k10, k11, k12, k13, k14,
C   & output_timestep
C   PARAMETER(maxdim=100000)
C   CHARACTER problem*80, FILEIN*40, FILEOUT*40
C   DIMENSION t0(maxdim), cin(maxdim),
C   & time(maxdim), obs(maxdim),
C   & cp(maxdim), cn(maxdim), cout(maxdim),
C   & slp(maxdim), sln(maxdim),
C   & s2p(maxdim), s2n(maxdim)
C
C   PARAMETERS
C   disp= dipersion coefficient [L2.T-1]
C   v= porewater velocity [L.T-1]
C   pulse_duration= duration of block-pulse of tracer [T]
C   c0= initial concentration of tracer [L-3]
C   xend= length of column or travel distance [L]
C   tfinal= final time of experiment [T]
C   att1= attachment rate coefficient to kinetic site s1
C   det1= detachment rate coefficient to kinetic site s1
C   att2= attachment rate coefficient to kinetic site s2
C   det2= detachment rate coefficient to kinetic site s2
C   muc= inactivation (or decay) rate coefficient of free tracer
C   museq= inactivaton (or decay) rate coefficient of tracer
C   attached to equilibrium sites
C   mus1= inactivaton rate coefficient of tracer
C   attached to kinetic sites s1

```

```

C      mus2= inactivation rate coefficient of tracer
C            attached to kinetic sites s2
C      Req= Retardation due to equilibrium adsorption
C      time= the observed time
C      obs= the observed concentration or C/C0
C      mode= '0' for inverse problem (fit)
C            and '1' for direct problem (simulation)
C      nob= number of observations
C
C      MODEL EQUATIONS:
C
C      Req*dc/dt=D*d^2c/dx^2-v*dc/dx-(att1+att2+muc)*c+det1*s1+det2*s2
C      ds1/dt=att1*c-(det1+mus1)*s1
C      ds2/dt=att2*c-(det2+mus2)*s2
C
C      ----- OPEN I/O FILES -----
C      CALL DOSPARAM('FILEIN',FILEIN)
C      IF(FILEIN.NE.' ') GO TO 10
C      WRITE(*,1000)
C      READ(*,1001) FILEIN
C      IF(FILEIN.EQ.' ') FILEIN='EQ2KIN.IN'
10 OPEN(5, FILE = FILEIN, STATUS = 'OLD')
C
C      ***Problem Description***
C      READ(5,*)
C      READ(5,1002) problem
C      ***column parameters
C      READ(5,*)
C      READ(5,*)
C      READ(5,*) xend,tfinal,v,disp
C      *** inputmode (0) c0 or (1) c0(t) ***
C      READ(5,*)
C      READ(5,*) inputmode
C      *** initial concentration
C      READ(5,*)
C      READ(5,*)
C      IF(inputmode.EQ. 0) THEN
C          READ(5,*) pulse_duration,c0
C      ELSE
C      Read t0 and cin
C          n=1
12      READ(5,*) t0(n),cin(n)
C          IF (t0(n).LE.0.AND.cin(n).LE.0) GO TO 15
C          n=n+1
C          GO TO 12
15      CONTINUE
C          pulse_duration=t0(n-1)
C      ENDIF
C      ***adsorption parameters***
C      READ(5,*)
C      READ(5,*)
C      READ(5,*) att1,det1,att2,det2,Req
C      ***inactivation parameters
C      READ(5,*)
C      READ(5,*)
C      READ(5,*) muc,museq,mus1,mus2
C      *** mode: inverse (0) or direct (1) + output_timestep***
C      READ(5,*)
C      READ(5,*)
C      READ(5,*) mode,output_timestep
C      ***observations (end with 0 0) ***
C      READ(5,*)

```

## Appendix

```
      READ(5,*)
      IF(mode.EQ. 1) GO TO 30
C     Read observed time and concentrations
      nobs=1
20    READ(5,*) time(nobs),obs(nobs)
      IF (time(nobs).LE.0.AND.obs(nobs).LE.0) GO TO 30
      nobs=nobs+1
      GO TO 20
30    CONTINUE
C
C     Close FILEIN
      CLOSE(5)
C
      CALL DOSPARAM('FILEOUT',FILEOUT)
      IF(FILEOUT.NE.' ') GO TO 40
      WRITE(*, 1003)
      READ(*, 1001) FILEOUT
      IF(FILEOUT.EQ.' ')FILEOUT='EQ2KIN.OUT'
40    OPEN(7, FILE = FILEOUT, STATUS = 'UNKNOWN')
C
C     Calculation of dx and dt
C     stabilityfactor is a factor larger than 1 for a stable solution
      stabilityfactor=2
      dx=2*disp/v/stabilityfactor
      dt=dx**2/2/disp/stabilityfactor
      ndt=tfinal/dt
      ndx=xend/dx
C
C     Linear coefficients in explicit scheme
      k1=(disp/dx**2-v/2/dx)*dt
      k2=Req-2*disp*dt/dx**2
      k3=(disp/dx**2+v/2/dx)*dt
      k4=att1*dt
      k5=det1*dt
      k6=att2*dt
      k7=det2*dt
      k8=muc*dt
      k9=museq*(Req-1)*dt
      k10=mus1*dt
      k11=mus2*dt
      k12=k2-(k4+k6+k8+k9)
      k13=1-(k5+k10)
      k14=1-(k7+k11)
C
C     Set initial concentrations to zero
      DO 50 i=1, ndx+1
          cp(i)=0.0
          slp(i)=0.0
          s2p(i)=0.0
50    CONTINUE
C
C     Calculate breakthrough concentrations
      n=1
      DO 60 j=1, ndt+dt
C
C     Upper boundary condition:
      IF ((j-1)*dt.LE.pulse_duration) THEN
          IF(inputmode.EQ.0) THEN
              cp(1)=c0
          ELSE
              IF((j-1)*dt.GE.t0(n)) n=n+1
              cp(1)=cin(n)
          
```

```

        ENDIF
    ELSE
        cp(1)=0.0
    ENDIF
C
C   Explicit scheme: calculate next from previous concentrations
DO 70 i=2, ndx
C
    cn(i)=(k1*cp(i+1)+k12*cp(i)+k3*cp(i-1)+k5*s1p(i)+k7*s2p(i))/Req
    s1n(i)=k4*cp(i)+k13*s1p(i)
    s2n(i)=k6*cp(i)+k14*s2p(i)
C
70 CONTINUE
C
C   Save last cn(ndx) in output concentration cout(j)
cout(j)=cn(ndx)
C
C   Lower boundary condition:
cn(ndx+1)=cn(ndx)
C
C   Shift next to previous concentrations
DO 80 i=2, ndx+1
    cp(i)=cn(i)
    s1p(i)=s1n(i)
    s2p(i)=s2n(i)
80 CONTINUE
60 CONTINUE
C
C   Write problem description
WRITE(7,1001) problem
C   Write parameters
WRITE(7,1004) c0
WRITE(7,1005) pulse_duration
WRITE(7,1006) xend
WRITE(7,1007) tfinal
WRITE(7,1008) v
WRITE(7,1009) disp
WRITE(7,1010) att1
WRITE(7,1011) det1
WRITE(7,1012) att2
WRITE(7,1013) det2
WRITE(7,1014) Req
WRITE(7,1015) muc
WRITE(7,1016) mus1
WRITE(7,1017) mus2
WRITE(7,1018) dx
WRITE(7,1019) ndx
WRITE(7,1020) dt
WRITE(7,1021) ndt
C
    IF(mode.EQ.1) THEN
C   Write time and cout(n) to file FILEOUT in increments of
t=output_timestep/dt
        t=output_timestep/dt
        IF(t.EQ.0) t=1
        WRITE(7,1022)
        DO 90 n=1, ndt+1, t
            WRITE(7,1023) n*dt, cout(n)
90 CONTINUE
        ELSE
C   Write time(n), obs(n), cout(t)
WRITE(7,1024)

```

## Appendix

---

```
        DO 100 n=1, nobs-1
          t=time(n)/dt
          WRITE(7,1025) time(n),obs(n),cout(t),LOG(obs(n)),LOG(cout(t))
100    CONTINUE
      END IF
C
C    Close FILEOUT
      CLOSE(7)
C
C    Read and Write formats
1000 FORMAT(' Enter input file name (default = EQ2KIN.IN)')
1001 FORMAT(A40)
1002 FORMAT(A80)
1003 FORMAT(' Enter output file name (default = EQ2KIN.OUT)')
1004 FORMAT(' c0',E12.3)
1005 FORMAT(' pulse_duration',F7.2)
1006 FORMAT(' xend',F7.2)
1007 FORMAT(' tfinal',F7.2)
1008 FORMAT(' v',E12.3)
1009 FORMAT(' disp',E12.3)
1010 FORMAT(' att1',E12.3)
1011 FORMAT(' det1',E12.3)
1012 FORMAT(' att2',E12.3)
1013 FORMAT(' det2',E12.3)
1014 FORMAT(' Req',F7.2)
1015 FORMAT(' muc',E12.3)
1016 FORMAT(' mus1',E12.3)
1017 FORMAT(' mus2',E12.3)
1018 FORMAT(' dx',F12.7)
1019 FORMAT(' ndx',I7)
1020 FORMAT(' dt',F12.7)
1021 FORMAT(' ndt',I7)
1022 FORMAT(' Time', ' Conc')
1023 FORMAT(F7.2,E12.3)
1024 FORMAT(' Time', ' Obs', ' Sim', ' lnObs', ' lnSim')
1025 FORMAT(F7.2,4E12.3)
C
C    END OF PROGRAM
      END
```





# Uitnodiging

tot het bijwonen  
van de verdediging  
van mijn proefschrift

op maandag 2 April 2001  
om 13.00 uur precies

in de

Senaatszaal van de Academie

van de

Technische Universiteit

Mekelweg 2, 6021 SX Delft

Recht na

na afloop van de proef

in de Frans van de Klasse

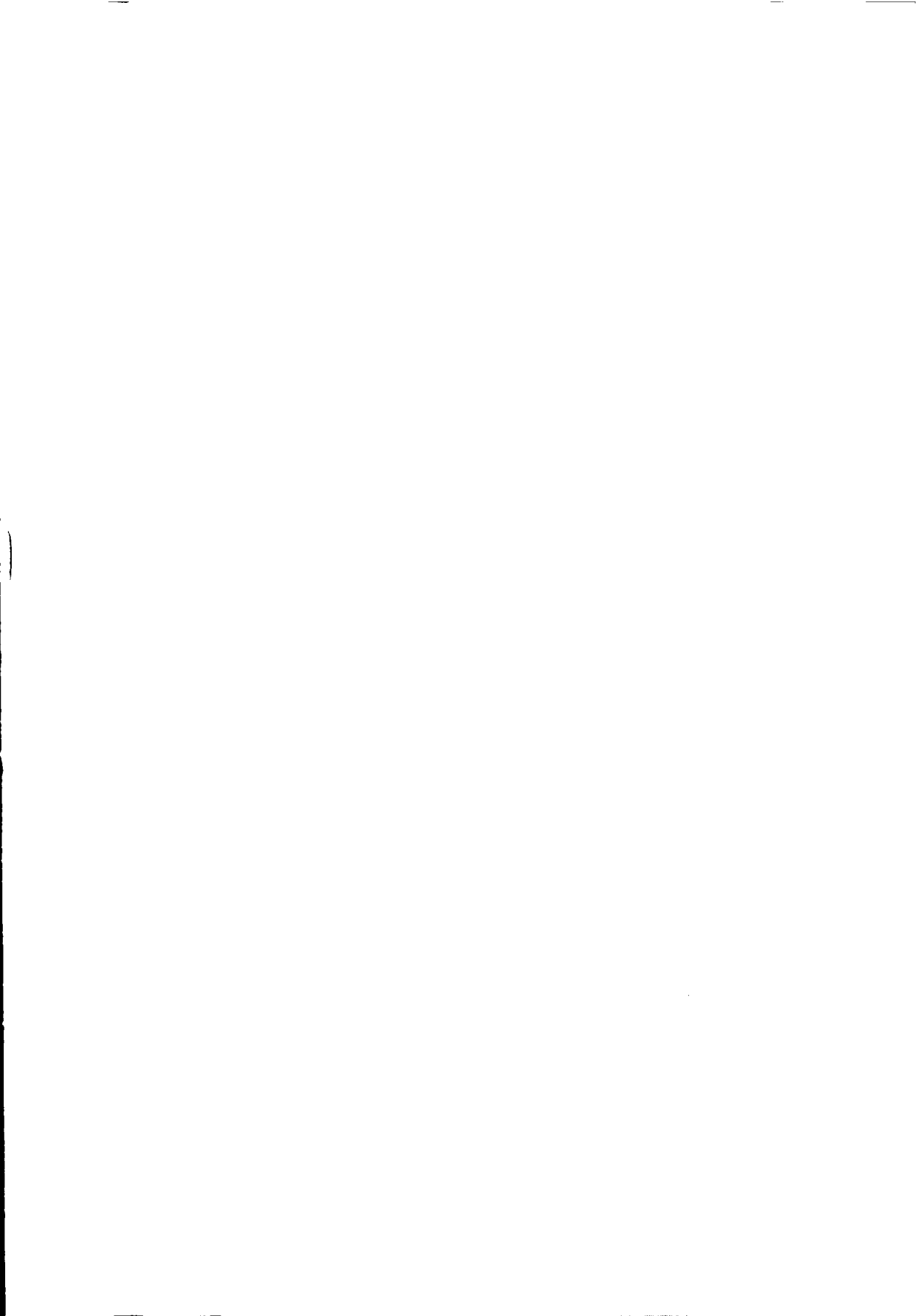
**Jack Smit**

Parasiten

Ria de Bruin

(030 265 4111)





**ISBN 90-646-4046-7**